The University Of Sheffield.

SNARE proteins in human mast cells

Reuben James Friend

A thesis submitted for the degree of PhD

Department of Biomedical Science

University of Sheffield

September 2013

Author's declaration

I hereby certify that all other writing and scientific figures presented in this thesis are original works by the author, unless otherwise stated in figure legends. All research displayed was carried out and processed by the author unless directly specified. All research findings, concepts and diagrams obtained from other sources have been clearly referenced with no known infringement of copyright. This statement is true at the date of submission.

Reuben James Friend

Acknowledgements

I would like to firstly thank my supervisor Dr Liz Seward who has given me great support and guidance throughout the last four years and whose novel ideas and insight have driven the project on. I would also like to thank my industrial supervisor Dr Elaine Harper for helping me settle into life at Syntaxin Ltd and for adding really useful insights from a different point of view throughout my project. Thank you to everyone in BMS and Syntaxin who have helped me along the way including Guillaume Hautberg, Paul Heath, Bob and John, Andrew Peden, Ian Birch-Machin and everybody in the Grundy lab.

Thank you to every member of the Seward lab, who have made my time here enjoyable and helped me throughout my PhD. Thank you to Kathryn, Claire and Jasmine for your patience and time at the start of my project teaching me the ropes and your continued help and support. Also to Hannah and Claudia who have helped me along the way! It's been a real pleasure working with everyone.

Thank you to my family for your support and belief in me in everything I do. Finally a special thank you to Emily for supporting and always being there for me, I'll finally get a 'proper job' now!

Abstract

Mast cells form an integral part of both innate and adaptive immunity; they help to orchestrate the inflammatory immune response through the release of a variety of inflammatory mediators [1]. Adverse reaction to allergens can lead to activation of mast cells, causing degranulation and release of a range of pro-inflammatory mediators contributing to the onset of allergy [2]. The most studied activation pathway in the adaptive immune response of mast cells is through the Immunoglobulin E (IgE) cell surface receptor FcεRI. Crosslinking of FcεRI leads to degranulation and *de novo* synthesis of mediators [3].

Every eukaryotic cell undergoes constitutive secretion. Alongside this general process, cells such as neuronal endocrine and immune cells, including mast cells, perform regulated secretion. This enables the cell to rapidly release mediators stored in secretory granules upon stimulation by a particular extracellular ligand. Mediators released fall into two categories; pre-formed, contained within these secretory granules; monoamines such as histamine as well as many proteases [4, 5], and de novo synthesized that are released through the constitutive secretory pathway, including prostaglandins, leukotrienes, cytokines and chemokines [6, 7]. Elucidating the mechanisms of mast cell mediator release is imperative for understanding many disease processes; however, knowledge of the precise mechanisms by which mast cell exocytosis is controlled remains elusive.

The aim of this study was to identify and characterise Soluble NSF attachment protein receptor (SNARE) proteins involved in the release of inflammatory mediators in human mast cells. Using LAD 2 human mast cells and primary human lung mast cells (HLMCS), expression of a variety of syntaxins and Vesicle associated membrane proteins (VAMPs), as well as the ubiquitously expressed SNAP-23 were found. To study the roles of individual VAMPs in exocytosis a novel technique utilising pH sensitive pHluorins was developed. Using VAMPs tagged with pHluorins, the cellular distribution of VAMP-3 and VAMP-8 containing vesicles and their behaviour upon IgE stimulation in live cells was monitored. In unstimulated cells, VAMP- 3 and 8 were found to have distinct cellular distributions. Upon IgE stimulation both VAMP-3 and VAMP-8 containing vesicles translocated to the

membrane and underwent membrane fusion, consistent with roles in exocytosis. However, their responses showed distinct time courses and calcium dependences. Importantly the VAMP-3 vesicle pool could be selectively targeted with a botulinum neurotoxin serotype B (BoNT)/B LC construct and in doing so inhibited the release of IL-6. The findings in this study support the notion that distinct vesicle pools, defined in part by expression of VAMP-3 and VAMP-8, regulate the release of inflammatory mediators from mast cells and that BoNTs might provide a novel means of targeting the release of chronic inflammatory mediators from mast cells for treatment of chronic inflammatory diseases.

Table of Contents

Chapter 1: Introduction 1
1.1 The Mast cell 1
1.1.1 Mast cell development 1
1.1.2 Mast cell mediators 5
1.1.3 Mast cell models 10
1.1.4 Mast cells in health and disease 13
1.2 Mast Cell activation 17
1.2.1 FcεRI activation 17
1.2.2 IgE independent receptor activation pathways 19
1.3 Mast cell Secretory pathway 22
1.3.1 Secretory granule biogenesis 22
1.3.2 Cytokine trafficking 24
1.3.3 SNARES- mediators of fusion 28
1.3.4 SNARE proteins and mast cells 32
1.3.5 SNARE interacting proteins 36
1.4 Tools for monitoring exocytosis 41
1.4.1 FM dyes 41
1.4.2 Acridine Orange 41
1.4.3 pH sensitive fluorescent proteins 42
1.4.4 Fluorescent false neurotransmitters 43
1.5 Botulinum neurotoxins 43
1.5.1 Structure and mechanism of action 43
1.5.2 BoNT modification – avenues for novel therapeutics 46
Thesis aims: 48

Chapter 2: Materials and Methods 49
2.1 HEK293 cell line 49
2.2 LAD 2 mast cell line 49
2.2.1 LAD 2 cell culture 49
2.3 HLMC 50
2.3.1 HLMC Isolation and Purification 50
2.3.2 Antibody Coating of Dynabeads 52
2.3.3 HLMC culture 53
2.4 Polymerase Chain reaction (PCR) 54
2.4.1 PCR reaction 55
2.4.2 Gel electrophoresis 55
2.5 Quantitative (Q) PCR 56
2.5.1 QPCR primer design and testing 56
2.5.2 QPCR reaction mix 57
2.6 Microarray 59
2.7 Antibodies table 60
2.8 Western Blot 60
2.8.1 Bradford assay 60
2.8.2 Western blot protocol 60
2.8.3 SDS Gels 62
2.9 Coverslip preparation 62
2.10 Immunostaining 62
2.11 Confocal imaging 63
2.12 β-hexosaminidase assay 63
2.13 Calcium imaging 64
2.13.1 Loading of cells with Fura-2 AM 66
2.13.2 Experimental set up and image acquisition 66
2.13.3 Imaging solution 68
2.13.4 HLMC purity 68

2.14 FFN511 assay ... **68**
2.14.1 Loading of FFN511 ... 69
2.14.2 Image acquisition ... 70
2.15 Bacterial Transformations and DNA extraction ... **70**
2.15.1 Solutions ... 71
2.15.2 Sequencing ... 71
2.16 Transfecting human mast cells ... **71**
2.16.1 Reagent transfection ... 72
2.16.2 Neon transfection ... 75
2.16.3 Neon transfection final protocol ... 76
2.17 Dual pHluorin and Calcium imaging ... **77**
2.17.1 Experimental set up and image acquisition ... 78
2.17.2 Data analysis ... 80
2.18 VAMP-8 shRNA ... **80**
2.19 IL-6 GFP construct ... **83**
2.19.1 IL-6 GFP release assay ... 83
2.20 BoNT LC constructs ... **83**

Chapter 3.Defining LAD 2 cells as a mast cell model ... **84**
3.1 Introduction ... **84**
3.02 Results ... **85**
3.2.1 Expression of mast cell associated receptors and mediators in LAD 2 cells ... 85
3.2.2 Calcium response of LAD 2 cells to FCεRI crosslinking ... 87
3.2.3 Loading of FFN511 in human mast cells ... 90
3.2.4 Pharmacological inhibition of FFN511 uptake and expression of VMATS ... 93
3.2.5 Stimulation dependent release of FFN511 and characterisation of human mast cell activation ... 95
3.03 Discussion ... **100**

Chapter 4: Identification of SNARE proteins in human mast cells ... **106**
4.1 Introduction ... **106**
4.2 Results ... **107**
4.2.1 Assessment of SNARE protein expression in HEK and LAD 2 mast cells through RT-PCR ... 107
4.2.2 Microarray identification and comparison of SNARE protein expression in human mast cells. ... 110
4.2.3 QPCR characterization of VAMP-2, 3, 7 and 8 ... 113
4.2.4 Protein expression of VAMPS-2, -3, -7 and -8 ... 116
4.2.5 Localisation and trafficking of VAMPS ... 117
4.2.6 Expression of plasma membrane Qbc SNARES ... 125
4.2.7 SNARE regulator expression ... 127
4.3 Discussion ... **132**

Chapter 5: Functional characterisation of VAMP-3 and VAMP-8 in human mast cells ... **143**
5.1 Introduction ... **143**
5.2 Results ... **143**
5.2.1 VAMP-pHluorins as tools to monitor exocytosis ... 143
5.2.5 Retargeted BoNT/E to target mast cell degranulation ... 157
5.2.2 Selective targeting of VAMP-3 vesicles by BoNT/B ... 162
5.2.3 VAMP-8-shRNA knockdown ... 162
5.2.4 Targeting VAMP-3 and VAMP-8 mediated exocytosis ... 163
5.3 Discussion ... **172**

Chapter 6: Discussion and future directions ... **180**

Bibliography ... **187**

Appendix ... **220**

Figure Index

Chapter 1: Introduction

Figure 1.1 The two suggested developmental pathways of mast cells 2
Figure 1.2 Mast cell mediators 5
Figure 1.3 Prostaglandin and leukotrine synthesis 9
Figure 1.4 FcεRI signalling in mast cells 19
Figure 1.5 Possible mechanisms of cytokine release 27
Figure 1.6 Intracellular organisation of SNARE proteins in mammalian cells 28
Figure 1.7 SNARE mediated membrane fusion 30
Figure 1.8 The complexin clamp 38
Figure 1.9 The structure of BoNTs 44
Figure 1.10 Cleavage sites of the BoNT serotypes 45

Chapter 2: Materials and Methods

Figure 2.1 Purification procedure for HLMCS 53
Figure 2.2 Primers used for RT-PCR 54
Figure 2.3 Primers used for QPCR experiments 56
Figure 2.4 VAMP-3 primers cycle and melt curves 57
Figure 2.5 QPCR cycling protocol 58
Figure 2.6 Diagram depicting the calcium sensitive nature of Fura-2AM 65
Figure 2.7 Experimental set of superfusion system 67
Figure 2.8 HLMC population defined by CD117 staining for imaging experiments 68
Figure 2.9 Structure of FFN511 69
Figure 2.10 Optimisation of transfection in human mast cells using non-liposomal based transfection reagents 73
Figure 2.11 Optimisation of X-tremegene HP transfection 74
Figure 2.12 Promotor expression in LAD 2 cells 75
Figure 2.13 Optimisation of Neon transfection in LAD 2 cells 76
Figure 2.14 Excitation wavelengths of Fura-2AM and GFP 77
Figure 2.15 pHluorin signal does not interfere with 380nm recording of Fura-2AM 78
Figure 2.16 pGFP-V-RS used for shRNA knockdown studies 81
Figure 2.17 VAMP-8 shRNA sequences 82

Figure 2.18 shRNA 4 produces greatest level of knockdown 82

Chapter 3: Defining LAD 2 cells as a mast cell model

Figure 3.1 LAD 2 cells express mast cell associated genes 84
Figure 3.2 Mast cell expression of src family kinases 87
Figure 3.3 IgE-induced calcium signals in LAD 2 cells and HMLCs 89
Figure 3.4 FFN511 is loaded into mast cells 90
Figure 3.5 FFN511 dye loss in LAD 2 cells 91
Figure 3.6.FFN511 is taken up into vesicular structures in LAD 2 cells 92
Figure 3.7 FFN511 does not induce degranulation in LAD 2 cells 93
Figure 3.8 Chloroquine abolishes vesicular staining in FFN511 in lad2 cells 94
Figure 3.9 FFN511 is loaded into human mast cells granules through VMAT2 95
Figure 3.10 Mast cell activators induce FFN511 release from LAD 2 cells 97
Figure 3.11 HLMC release FFN511 upon FCεRI stimulation 98
Figure 3.12 Comparison of LAD 2 and HLMC responses to IgE mediated FFN511 release 99

Chapter 4: Identification of SNARE proteins in human mast cells

Figure 4.1 SNARE protein mRNA expression in LAD 2 human mast cell line 108
Figure 4.2 SNARE protein mRNA expression in HEK293 cells 109
Figure 4.3 SNARE protein mRNA expression in HLMCS 109
Figure 4.4 Human mast cells express multiple syntaxins 112
Figure 4.5 Qb and bc SNARE expression in LAD 2 cells 112
Figure 4.6 VAMP protein expression 113
Figure 4.7 Relative QPCR of VAMPs in LAD 2 and HEK cells 114
Figure 4.8 mRNA expression of VAMPs increases after stimulation through IgE receptor crosslinking 115
Figure 4.9 Western blot of VAMPs-2, 3 and 8 in LAD 2 cells and HLMCS 117
Figure 4.10 VAMP-8 and VAMP-7colocalise to the mast cell granule marker tryptase 118
Figure 4.11 VAMP-3 and VAMP-8 traffic to the membrane upon stimulation in LAD 2 cells 120
Figure 4.12 VAMP-8 colocalises to the mast cell granule marker tryptase in HLMCs 121

Figure 4.13 VAMP-3 and VAMP-8 traffic to the membrane upon stimulation in HLMCS 122
Figure 4.14 VAMP-3 colocalises to recycling endosomes in LAD 2 cells 124
Figure 4.15 Il-6 GFP colocalises to recycling endosomes 125
Figure 4.16 LAD 2 and HLMCS express SNAP-23 but not SNAP-25 126
Figure 4.17 SNAP-23 resides on the membrane of human mast cells 127
Figure 4.18 LAD 2 and HLMCS express high levels of non-neuronal Munc13 and Munc18 isoforms and low expression of complexin II 128
Figure 4.19 LAD 2 and HLMC calcium sensor expression 130
Figure 4.20 FceRI crosslinking induces changes in syt expression 131

Chapter 5: Functional characterisation of VAMP-3 and VAMP-8 in human mast cells

Figure 5.1 VAMP pHluorin constructs 144
Figure 5.2. VAMP-8 pHluorin and VAMP-3 pHluorin localise to different cellular compartments 146
Figure 5.3 VAMP-3 and VAMP-8 pHluorins have distinct cell surface and intracellular distributions 147
Figure 5.4 VAMP-3 and VAMP-8 pHluorin cells undergo membrane fusion upon FcεRI cross-linking 150
Figure 5.5 Level of pHluorin expression does not determine the response size 151
Figure 5.6 VAMP-3 vesicles have greater calcium sensitivity than VAMP-8 vesicles 151
Figure 5.7 pHuorin response sizes in VAMP-3-pHluorin transfected cells are more evenly distributed than VAMP 154
Figure 5.8 VAMP-3-pHluorin cells have a faster calcium rise in response to FCεRI crosslinking than VAMP-8-pHluorin cells 155
Figure 5.9 VAMP-8 and VAMP-3 vesicles show distinct calcium sensitivities 156
Figure 5.10 BoNT/E(K224D) cleavage of SNAP-23 in LAD 2 cells 157
Figure 5.11 BoNT/E(K224D) LC has no effect on ionomycin induced exocytosis of VAMP-8-pHluorin 158
Figure 5.12 BoNT/E(K224D) LC inhibits FCεRI induced exocytosis of VAMP-8-pHluorin 159
Figure 5.13 BoNT/B cleaves VAMP-3 in LAD 2 cells 162

Figure 5.14 VAMP-8 shRNA knocks down the expression of VAMP-8 protein in LAD 2 cells 163
Figure 5.15 Knockdown of VAMP-8 in LAD 2 cells inhibits mast cell degranulation 164
Figure 5.16 BoNT/B LC does not significantly inhibit ionomycin-induced exocytosis of VAMP-8-pHluorin 165
Figure 5.17 BoNT/B LC inhibits exocytosis of ionomycin stimulated VAMP-3-pHluroin vesicles 166
Figure 5.18 BoNT/B LC does not significantly inhibit exocytosis of FCεRI VAMP-8-pHluorin vesicles 168
Figure 5.19 BoNT/B LC inhibits exocytosis of FCεRI stimulated VAMP-3-pHluroin vesicles 169
Figure 5.20 BoNT/B reverses VAMP-3-pHluorin induced fast calcium response to FCεRI crosslinking 170
Figure 5.21 BoNT/B inhibits IL-6 GFP release 171

Chapter 6: Discussion and future directions

Figure 6.1 Targeting of mast cell cytokine release using modified BoNTs 186

Table Index

Chapter 1

Table 1.1 Factors that affect mast cell development 3
Table 1.2 Mast cell subtype heterogeneity 4

Chapter 2

Table 2.1 Antibodies used for western blot and immunostaining 60

Abbreviations:

AMPAR

BDNF Brain derived neurotrophic factor

BMMC Bone marrow derived mast cell

BoNT Botulinum neurotoxin

BSA Bovine serum albumin

cAMP Cyclic adenosine monophosphate

CDS Cell dissociation solution

CD Cluster of Differentiation

CGRP Calcitonin gene-related peptide

CHR Corticotropin relasing hormone

CRAC Calcium release activated current

DAG Diaglycerol

DMEM Dulbecco's modified eagle medium

DMSO Dimethyl sulphoxide

EGF Epidermal growth factor

ER Endoplasmic reticulum

ERC Endocytic recycling compartment

ERK Extracellular signal regulated kinases

FCS Foetal calf serum

FcεRI High affinity IgE receptor

FFN Fluorescent false neurotransmitter

FGF Fibroblast growth factor

GFP Green fluorescent protein

GLUT Glucose transporter

GMP granulocyte/monocyte progenitor

GPCR G protein-coupled receptor

GST Glutathione s-transferase

HBSS Hank's balanced salt solution

HC Heavy chain

HEK-293 Human embryonic kidney cell line

hCBMC Human cord blood mast cell

HGMC Human gut mast cell

HLMC Human lung mast cell

HMC-1 Human mast cell line-1

IBD Irritable bowel disease

IBS Irritable bowel syndrome

IgE Immunoglobulin E

IL Interleukin

ITAM Immunoreceptor tyrosine-based activation motif

LAD Laboratory of allergic diseases

LC Light chain

MC-CPA Mast cell carboxypeptidase A

MCP Macrophage cationic peptide

MHC Major histocompatibility complex

miRNA Micro RNA

MPP multipotent progenitors

Munc Mammalian uncoordinated

NEAA Non-essential amino acids

NGF Nerve growth factor

NSF N-ethyl maleimide sensitive factor

PBS Phosphate buffered saline solution

PCR Polymerase chain reaction

PDGF Platelet derived growth factor

PI3K Phosphatidyl 3-OH kinase

PKC Protein kinase C

PLC Phospholipase C

PMA Phorbol myristate acetate

RANTES Regulated on activation, normal T cell expressed and secreted

RBL-2H3 Rat basophilic leukemia cell line

rhSCF Recombinant human SCF

ROI Region of interest

RT-PCR Reverse transcription-PCR

SCF Stem cell factor

SDS Sodium dodecyl sulphate

SG Secretory granule

shRNA Short hairpin RNA

siRNA Small interfering RNA

SLP Synaptotagmin-like protein

SM Sec1/Munc18-like

SNAP Soluble NSF attachment protein

SNARE Soluble N-ethyl-aleimide sensitive factor attachment protein receptor

SP Substance P

STIM Stromal interaction molecule

SV Synaptic vesicle

Syt Synaptotagmin

TGN Trans Golgi network

TLR Toll-like receptor

TNF Tumor necrosis factor

TRP Transient receptor potential channel

VAMP Vesicle associated membrane protein

VMAT Vesicle monoamine transporter

VIP Vasoactive intestinal peptide

Chapter 1: Introduction

Mast cells form an integral part of both innate and adaptive immunity, playing an important role in the inflammatory response. Adverse reaction to allergens can lead to activation of mast cells, causing degranulation and release of a range of pro-inflammatory mediators contributing to the onset of pathology. Mast cells have been further implicated in many other diseases associated with aberrant mediator release including irritable bowl disease (IBD) [8]. SNARE proteins have been identified as essential proteins for the exocytosis of all non-lipid derived mediators. Inhibiting secretion though disruption of SNARE-mediated vesicle fusion could provide a novel therapeutic approach for the treatment of a variety of mast cell mediated inflammatory diseases.

1.1 The Mast cell

1.1.1 Mast cell development

Paul Ehrlich first described mast cells over one hundred years ago. He observed unique staining of “protoplasmic deposits” by aniline dyes and named the cells “mastzellen” for fat, well-fed cells [9]. Having identified the cells in connective tissue, Ehrilch wrongly proposed the cells differentiated from fibroblasts. It is now known mast cells are derived from haematopoietic progenitors in the bone marrow and, unlike other blood cells, complete differentiation within their target tissue [10]. There is still conjecture as to their exact origin; work performed in murine models suggests potentially two alternate pathways for development (Figure. 1.1).

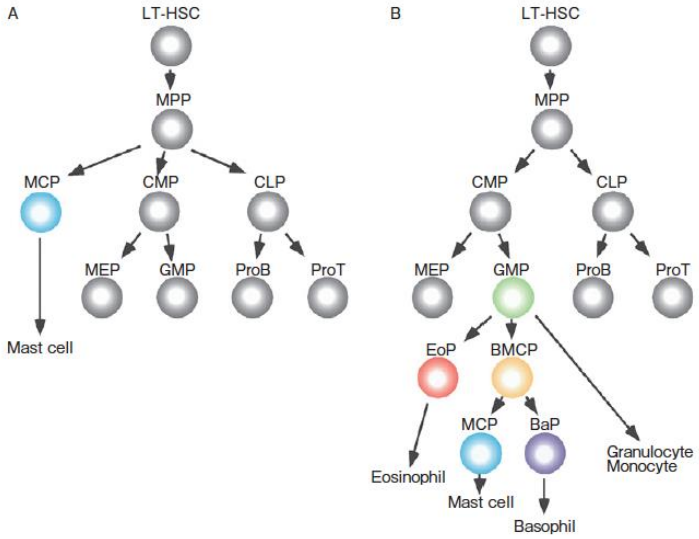

Figure 1.1

The two suggested developmental pathways of mast cells[11].

A. Chen et al [12] suggested mast cell progenitors are derived directly from multipotent progenitors (MPP), **B**. [13] showed that MCs can develop from committed myeloid progenitors notably from granulocyte/monocyte progenitors (GMPs) producing a common mast cell and basophil progenitor. Image taken from Arinobu et al 2009. Long-term Hematopoietic stem cells (LT-HSCs), common myeloid progenitor (CMP), megakaryocyte/erythrocyte progenitors (MEPs), common lymphoid progenitors (CLPs), basophil/mast cell progenitor (BMCP), basophil progenitor (BaP), mast cell commited progenitor (MCP), eosinophil commited progenitor (EoP).

Once in the blood, mast cell precursors can be identified through their expression profile of cluster of differentiation (CD) proteins. These are proteins that are present on the cell surface of leukocytes and are used for identification and classification of specific cell types [14]. For mast cell precursors these include: CD34+ a cell surface antigen that is present on human hematopoietic progenitor cells, CD13+ also termed aminopeptidase N, a zinc dependent exopeptidase that can cleave neuropeptides and cytokines, and C-kit+/CD117 a receptor for Stem cell factor (SCF).

Tissues mast cells are targeted to include those where there is a considerable host-environment interaction, for example in the skin and mucosas of the respiratory and gastrointestinal tracks [15]. Their homing to target tissues requires a mixture of chemokines, integrins and SCF [16]. Maturation and survival of both human and murine mast cells are dependent on SCF; mice with mutations to either KIT or SCF have greatly reduced numbers of tissue mast cells [17, 18]. There are numerous

other factors that regulate SCF-mediated mast cell development, some of these are summarised in Table 1.1.

Factors that affect mast cell development			
Cytokine	**Receptor**	**Effects on mouse mast cells**	**Effects on human mast cells**
SCF	C-kit	Proliferation, induces granulation and CT proteases	Proliferation, induces granulation and CT proteases
IL-3	IL-3R	Proliferation, promotes granule assembly	Proliferation not granule assembly
IL-4	IL-4R	Cofactor for proliferation	Depends on subtype and cytokine milieu
IL-5	IL-5R	ND	Cofactor for proliferation
IL-6	IL-6R	Induces mast cell development with TNF-a	Cofactor for proliferation or inhibition
IL-9	IL_9R	Cofactor for proliferation, may induce mucosal proteases	Cofactor for proliferation
IL-10	IL-10R	Cofactor for proliferation, may induce mucosal proteases	ND
IFN-g	IFN-g R	Inhibits proliferation	Inhibits proliferation
NGF	NGFR	Cofactor for proliferation, promotes CT type granule	
TGF-b	TGF-bR	Inhibits proliferation	Inhibits proliferation
GM-CSF	GM-CSFR	Inhibits proliferation	Inhibits proliferation
TPO	TPOR	ND	Induces mast cell development

Table 1.1

Factors that affect mast cell development [16] |
Adapted from Yoshimichi Okayama and Toshiaki Kawakami 2006. CT stands for connective tissue.

Exposure to specific cytokines and chemokines within the target tissues triggers maturation, and most probably accounts for the heterogeneity between mast cell populations. This heterogeneity enables the mast cell to produce distinct secretory responses to a diverse number of stimuli in different tissue locations. The tissue specific nature of mast cells can be defined in many ways. Murine mast cells are classed by their tissue specific location, as either mucosal or connective tissue type mast cells. In humans the main criterion used to distinguish mast cell types is through their mast cell specific protease content. MC^{TC} are those that express tryptase and chymase in secretory granules, while MC^{T} express tryptase but little or no chymase. There is even evidence that there are sub-populations of mast cells within specific tissues. HLMCs, for example vary depending on the particular region of the lung they reside. Using immunohistochemistry it was found that MC^{TC} mast cells present in pulmonary vessels were larger than those in small airway walls. Furthermore, there were significant differences in FcεRI expression, so much so that it is almost absent from mast cells present in alveolar parenchyma [19]. Table 1.2 summarises some of the heterogeneity in receptors and medaitors found in mast cell subtypes. These are discussed in greater detail thoughout this chapter.

	Human mast cells	
Subtype	**MCT**	**MCTC**
Mast cell location	Intestinal mucosa, Lung	Skin
Granule content	Histamine, Typtase	Histamine, Tryptase, Chymase, CPA
Nueropeptide activation	none reported	Substance P, CGRP, VIP
TLR expression	TLR 2,3,4,7,10	TLR 2,3,4,9
Complement receptor expression	none reported	C5a, C3a
Known difference in Cytokine profile	IL-5 and IL-6 high	IL-4 high
LTC4 release	High	No
PGD2 release	High	High

Table 1.2

Mast cell subtype heterogeneity

The table highlights how the two mast cell subtypes differ in mediator content and receptor expression. Leukotriene C4 (LTC4), Prostaglandin D2 (PGD2), Toll like receptor (TLR), Carboxypeptidase A (CPA), Calcitonin gene related peptide (CGRP), [20-26]

1.1.2 Mast cell mediators

Mast cell function relies on the release of a plethora of mediators following activation; these mediators allow mast cells to signal to and regulate the function of many other types of cells in the body. Mediators released can be broadly classed into three categories; (1) pre-formed and contained within secretory granules such as histamine and proteases [4, 5], (2) *de novo* synthesized cytokines and chemokines [6, 7] and (3) *de novo* synthesized lipid mediators including prostaglandins and leukotrienes. Some mediators, such as tumour necrosis factor alpha (TNF-α) are contained within pre-stored vesicle populations, and are newly synthesised upon activation [6, 27]. Figure 1.2 shows the numerous mediators released from mast cells. The combination of mediators secreted by a mast cell will depend on both the tissue in which it is resident as well as the receptors that are activated in any one situation.

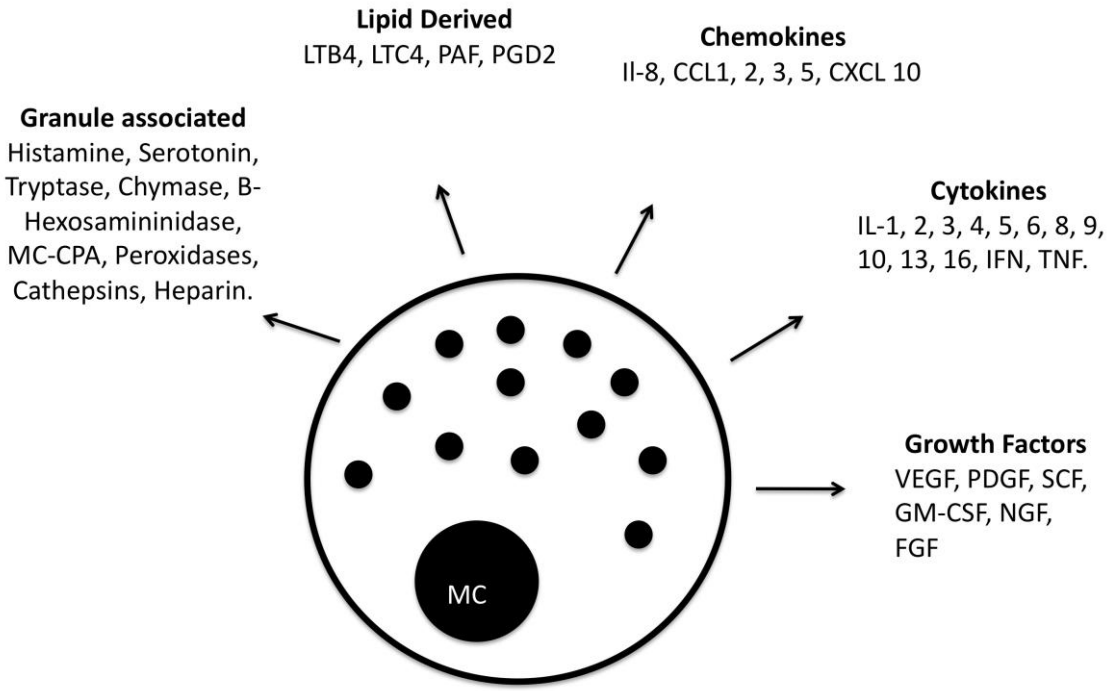

Figure. 1.2

Mast cell mediators

Diagram depicts mediators released by mast cells. Granule associated mediators are released within minutes of stimulation, while many growth factors and cytokines are *de novo* synthesised and can be released hours after stimulation.

Histamine

Preformed mediators present in secretory granules (SGs) are released within minutes of activation through a reaction termed degranulation [28]. The biogenic amine histamine is one of the most well-known and studied preformed mediators present in mast cell SGs. It is formed from L-histidine by the enzyme histidine decarboxylase [29]. Storage of positively charged histamine in SGs requires negatively charged serglycan proteoglycans [30], these are discussed in greater detail below. Histamine exerts a number of effects, including vasodilation and bronchoconstriction.

Serotonin

Serotonin was identified in murine mast cell granules in the 50s [31]. It was originally thought that it wasn't expressed in human mast cells until recently, when limited evidence suggests it might be present in small quantities [32]. Due to the more ubiquitous expression of serotonin deciphering the function of mast cell derived serotonin has proven difficult and given the little evidence of the presence of human mast cell serotonin, serotonin released from mast cells in humans might be limited.

Vesicle Monoamine Transporters (VMAT) 1 and 2 mediate monoamine transport into secretory vesicles from the cytoplasm. They act through an ATPase generated proton gradient [33, 34], where the inward transport of monoamines is coupled with the efflux of two protons per amine molecule [35, 36]. VMATS and their importance in serotonin transport have been described in RBL-2H3 cells [37]. However, only one study has described expression of these transporters in human cells[38]. Both studies identified the expression of VMAT 2 and not 1.

Proteases

Proteases are stored at very high levels in SGs in their active forms. Three proteases are specifically expressed in mast cells; Tryptase, Chymase and Mast cell carboxypeptidase A (MC-CPA), although there are proteases present in mast cells that are expressed in other cell types as well, such as cathepsins and granzymes [39, 40]. Mast cell proteases are synthesised as prepropeptides, which are subsequently cleaved intracellularly, therefore active forms of these proteases are stored within

granules. Storage of these proteases, as with histamine, requires Serglycan proteoglycans. These consist of a protein core to which sulphated negatively charged glycosaminoglycans bind, for mast cells this is sulphated heparin [41, 42]. Alongside storage of proteases, serglycan proteoglycans are also required for tryptase activation and modulate activity of chymase and MC-CPA. The requirement of serglycan proteoglycans in tryptase activation is thought to be through the fact that tryptase consists as tetrameric structure [43] and serglycan proteoglycans mediate the formation of this, while SGs help to mediate the cleavage of proMC-CPA to its active form [44] and allow more efficient presentation of substrates to chymase [45]. After mast cell proteases are released into the extracellular environment, the higher pH results in tryptase becoming dissociated from serglycan proteoglycans while MC-CPA and chymase remain in complex. This complex has been reported to hinder their diffusion and so keep protease induced inflammation and protease action near their site of release [46].

Tryptase is a serine class peptidase and cleaves peptides after lysine and arginine. There are four groups of tryptases present in human mast cells α, β, γ and δ. γ tryptase is membrane anchored and could resemble the ancestral form from which the soluble forms are derived [47]. Of the soluble tryptases only β seems to have an important role outside the cell, where the catalytic domains of α and delta have greatly reduced catalytic activity [48]. β Tryptase is the best studied of the tryptases and can activate PAR-2 receptors in nerves [49, 50], suggesting a role in hypersensitivity. Other actions of tryptase include acting as a mitogen to fibroblasts, again through PAR-2 [51, 52], acting as an anticoagulant through degradation of fibrinogen [53, 54] and even to act on other immune cells including mast cells inducing degranulation.

Chymase is a chymotrypsin-like serine proteinase. In humans there is only one gene, while in rodents these have expanded into five [55]. One possible explanation to this is that chymases have been shown to confer defence against venoms [56] that are non-lethal in humans but lethal in rodents. This proliferation of proteases might be the result of acquired defence against a range of venoms. Due to the inter-species differences of rodent and human chymases, translating work from rodents into human has proven hard. However they have provided useful insights.

Chymases have wider protease activity than the tryptases and can degrade matrix proteins, evidence suggests a role in tissue remodelling and homeostasis [57].
MC-CPA is a metallocarboxypeptidase. Only one gene has been found for MC-CPA in either humans or murine models. Knockout of MC-CPA results in impaired granule storage of chymase and is suggestive of a role of MC-PCA in granule homeostasis possibly through effects on compounds stored within the granules [58]. MC-CPA has also been shown to be important in degrading the snake venom sarafotoxin [59].

Lysosomal enzymes

Mast cell granules contain many lysosomal associated enzymes. These include β-hexosaminidase, which is thought to be involved in carbohydrate processing [60]. It is expressed ubiquitously in all subtypes of mast cells [61]. Cathepsins, are lysosomal associated proteases [62] that can be released upon immunoglobulin E (IgE) mediated stimulation. Although thought to be only active in the low pH of the granules, some evidence suggests that these enzymes might be functional after release [63]. β-hexosaminidase release is often used to monitor mast cell degranulation through its ability to catalyse the hydrolysis of -glycosidically linked N-acetylglucosamine and N-acetylgalactosamine residues from a number of glycoconjugates [64]. 4-Nitrophenyl N-acetyl-β-D-glucosaminide can be used as a substrate to monitor release, where it is converted to 4-nitrophenol by β-hexosaminidase and absorbance can be measured at 405nm to determine enzyme activity using spectroscopy.

Pre-formed cytokines and chemokines

Mast cells can pre-store cytokines within their granules or in small vesicles [27]. This has been well defined for TNF-α and even functional roles for this have been described, including the induction of lymph node hypertrophy seen in bacterial infection [65]. Other cytokines and growth factors identified in mast cell granules include Vascular endothelial growth factor (VEGF) [66, 67] and Il-4 [68]. The evidence for this and the possible trafficking pathways are discussed in detail in section 1.3.2

Lipid Mediators

Cysteinyl leukotriene and prostaglandins are eicosanoids derived from arachidonic acid metabolism, as illustrated in Figure 1.3. Mast cells can synthesize and release PGE_2 and PGD_2 as well as the leukotriene LTB_4, and LTC_4. These mediators are pro-inflammatory and lead to leukocyte chemotaxis, bronchoconstriction, vasodilation and platelet activation. Eicosanoid production is thought be carried out in part within lipid bodies [69]. These cytoplasmic organelles are present in mast cells. Arachidonic acid is incorporated into lipid bodies and could act as a store for eicosanoid production. Furthermore eicosanoid-forming enzymes localise to lipid bodies and eicosanoid formation occurs within them [70].

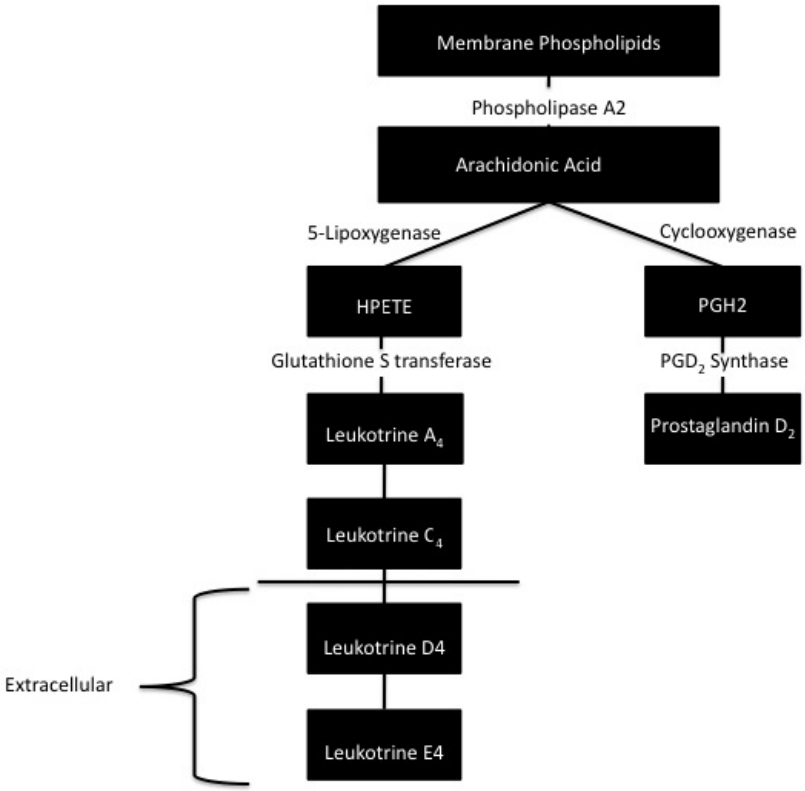

Figure 1.3
Prostaglandin and leukotriene synthesis [71]

Cytokines, chemokines and Growth factors

Alongside degranulation mast cells synthesise and subsequently release many cytokines, chemokines and growth factors over the course of a number of hours post stimulation. The list of factors released can be seen in Figure 1.2. The large numbers of cytokine and chemokines released by mast cells have many functions.

Cytokines are classed by their function; initially many were termed interleukins based on the assumption that they were produced by and targeted leukocytes. However it has become clear that interleukins are produce by a wide number of cells. The interleukin nomenclature represents the biological activities of individual cytokines although there are overlapping functions [72]. Cytokines can promote angiogenesis and act as growth factors, survival factors and mitogens.

Chemokines are cytokines that mediate chemoattraction directing the traffic of leukocytes to the sites of inflammation [73, 74]. They can be classed into four groups based on structure and function. The CC chemokines are the largest group and are so called due to the first two of the first four cysteine residues being adjacent to one another, these attract mononuclear cells to sites of chronic inflammation[75]. CXC chemokines contain a single amino acid between the cysteine molecules and attract leukocytes during acute inflammation[75]. The last two groups (XCL and CX_3C) only have one member each [74]. The possible pathways that govern cytokine release in mast cells are discussed in detail in section 1.3.2

1.1.3 Mast cell models

The large degree of heterogeneity between mast cell populations means utilising primary mast cells for *in vitro* work can provide novel insights into differences and similarities between these populations. For example HLMCs are widely used, as well as mast cells derived from skin and the intestines. There are however, some notable issues related to using primary mast cells, including the expense of their isolation from resected tissue, limitations in performing many experiments due to low cell number and the various sub-populations within native tissues. Coupled to the difficulty of genetically manipulating primary mast cells, model mast cell lines have provided a useful tool in deciphering the workings of these multifaceted cells.

RBL 2H3

The first cell line most commonly used as a mast cell model was the RBL-2H3 cell. These were in fact derived from cells isolated from a basophilic tumor in the 1970s from rats treated with a potent carcinogen [76] and therefore are basophil in origin. RBL-2H3 cells were developed from further cloning of these cells [77, 78]. RBL-2H3

cells are an easily cultivated line, relatively cheap to maintain and are fast dividing as a result of a mutation in KIT that results in constitutive activation of the receptor [79, 80]. Consequently they have become widely used as models for mast cells despite their basophilic origins. These cells can be stimulated through cross-linking of FcεRI in response to antigen-bound IgE and release mediators such as histamine and serotonin. Their phenotype is thought to be most similar to mucosal mast cells, however, there are differences; for example they differ in their responses to lipopolysaccarides (LPS) and in their expression of certain receptors [81, 82]. It has also been shown that there is a degree of heterogeneity between RBL cell lines [83]. Therefore, despite the wide use of these cells within the mast cell community they are not an ideal model in studying mast cell biology as they lie phenotypically somewhere in between a mast cell and basophil, and do not consistently express many mast cell associated factors and receptors. Furthermore, considering murine and human mast cells differ considerably in mediator content, tissue specificity and receptor expression care must be taken when extrapolating knowledge gained through the use of these models into humans.

HMC-1

HMC-1 cells are a human mast cell line, established from a patient with mast cell leukaemia [79]. These cells express a constitutively phosphorylated tyrosine residue on KIT and therefore do not require the growth factor SCF for survival in culture and have a comparable doubling time to RBL-2H3 cells. They lack consistent expression of FcεRI [84] and as a result don't readily respond to IgE stimulation. This has meant that non-physiological stimuli such as the calcium ionophore, ionomycin are often used to monitor activity in these cells, which are of limited use when modelling allergic responses. HMC-1 cells only contain small amounts of preformed granule mediators such as histamine, tryptase and ß-hexosaminase and no chymase. HMC-1 cells can produce and release cytokines upon stimulation, including TNF-α and Il-8 [85]. However, their profile of release is much smaller than that of primary mast cells [86], for example they do not release IL-5 or Il-4 and the amount of preformed mediators released are much lower [87]. With HMC-1 cells inability to respond to normal physiological stimuli, and containing and releasing minimal amounts of mast cell associated mediators, they can be considered an

immature cell line; not possessing all of the attributes of fully differentiated mast cells.

LAD 2

As with HMC-1 cells, LAD 2 cells were isolated from a patient with mast cell leukaemia [88]. They express a functional FcεR receptor and contain and release granule contained mast cell mediators such as histamine, tryptase and chymase. Unlike HMC-1 and RBL-2H3 cells, LAD 2 cells respond to SCF and are dependent of SCF for proliferation and survival. LAD 2 cells also have a doubling time of weeks rather than days. They can release a number of cytokines and chemokines including a number of interleukins, TNF-α, Regulated on activation normal T cell expressed and secreted (RANTES) and MCP-1, in particular in response to non-immulogical stimuli such as neuropeptides [89]. These characteristics are suggestive of a more differentiated cell than the lines described above. Despite these characteristics, LAD 2 cells do not represent a fully differentiated model; although containing and releasing greater amounts of preformed mediators than HMC-1 cells, their release is still small when compared to primary skin mast cells amounts of proteases such as tryptase [90]. Furthermore stimulation of FcεRI results in limited cytokine release. This might be due to reduced FcεRI subunit expression or a lack of fully mature signaling or cytokine production pathways. LAD 2 cells can therefore be regarded as an intermediately differentiated mast cell model providing a more robust tool than previously used models but still not fully representing a mature mast cell.

LUVA

LUVA cells are a recently described mast cell line [91]. They arose spontaneously from a culture of non-transformed hematopoietic progenitor cells. They possess numerous granule-associated mediators, such as histamine, tryptase and ß-hexosaminidase and express a functional FcεR receptor, activation of which induces degranulation, synthesis of prostaglandins and stimulates production and release of cytokines at much greater levels than LAD 2 cells. Like LAD 2 cells they also respond to SCF, although this is not needed for survival, and again are thought to represent an intermediately differentiated mast cell model. Being a newly development model many questions remain; such as their ability to maintain their phenotype in culture over time, and how they are able to respond to SCF but not require it for

proliferation or survival. No mutation in Kit is present and it is not autophosphoylated so the how they are able to survive without SCF is unknown. With probable mutations occurring elsewhere-conferring survival and propagation- it is impossible to determine the functional consequences of these mutations and how they affect their usefulness as a mast cell model.

In conclusion all mast cell models have their advantages and disadvantages. The most common problems with them are the amounts and variety of mast cell associated mediators released and the variable expression of mast cell associated receptors. The best models currently available to study mast cell biology are LAD 2 and LUVA cells, although the latter remain to be fully defined.

1.1.4 Mast cells in health and disease

The multitude of factors released by mast cells allow them to perform a diverse array of functions, some of these functions are described in the next section.

Innate and adaptive immune response to pathogens

Mast cells are best known for their involvement in the allergic response. However, it has become evident that they have important roles in both immune and non-immune processes. The innate immune system acts as the first line of defence to infections. The mucosal location of mast cells places them at an ideal position to respond to bacteria, virus and parasitic infection [92, 93]. Mast cell deficient mice show decreased survival to infections from numerous species of bacteria, which can be reversed upon reconstitution with bone marrow derived mast cells [94, 95]. Mast cells exert their protection only after activation through pathogen or host derived signals, such as compliment components. Release of mediators such as TNF-α results in the recruitment of other inflammatory cells, including neutrophils, that target the pathogens [96]. Mast cells might play a direct role in the clearance of pathogens themselves; *in vitro* they have been shown to phagocytose bacteria and release antimicrobial peptides [97, 98]. However, their low mobility and low numbers in tissues puts the *in vivo* relevance of this in question. Nevertheless these findings suggest the mast cell plays at least a supporting role in the clearance of bacterial infections. Mast cells have been postulated to have a role in the protective

immunity of parasitic infections. Mast cells are functionally active during immune elimination of nematodes [99] and mice lacking mast cell chymase show delayed removal of the nematode *Trichinella Spiralis [100].* Mast cells can also release a number of chemokines and cytokines in response to virus associated stimuli [101, 102] and mast cell numbers increase around the site of viral infection [103].

Mast cells are also important in the adaptive immune responses to pathogens. Mast cell derrived TNF-α enhances the recuitement of T-cells [65] to lymph nodes. Furthermore, mast cells express major histocompatablilty complex (MHC) molecules and can act as antigen presenting cells [104, 105]. They have been shown to process and present bacterial antigens to T cells [97].

It is clear that mast cells contribute to the immune response to pathogens, whether directly through release of proteases and phagocytosis or indirectly, through the release of chemokines and cytokines that recuit other immune cells to the sites of infection.

Wound healing

Mast cells can release numerous growth factors, such as VEGF, nerve growth factor (NGF), fibroblast growth factor (FGF) as well as tryptase and histamine [106-108]. These factors can induce the proliferation of epithelial cells and fibroblasts, suggesting a role for the mast cell in wound healing through re-epithelialisation and re-vascularization, acting alongside the function of the mast cell in the initial inflammatory response in response to wounds [109]. Further evidence of the wound healing function of mast cells comes from the observation that mice deficient in mast cells show impaired wound healing [110].

The knockout mice strain used in the study, (kit $^{w/wv}$), have impaired melanogenesis and are anaemic and sterile [111]. It is not fully clear how much these deficiencies in the model affect wound healing, although reconstitution with mast cells did restore much of the wound healing function. Another strain Kit $^{w\text{-}sh}$, which have an inversion mutation upstream of c-kit are thought to have less 'off target' effects that the kit $^{w/wv}$ mice. They have still been found to show some hematopoietic abnormalities [112] and highlight the pitfalls of using knockout models.

Reconstitution experiments, where a functional defect can be rescued by the engraftment of mast cells, are a must when using these models.

Mast cells and allergy

The first documented allergic response was Pharaoh Menes in 2640 BC, who according to hieroglyphic records, died from a wasp sting [113]. The first scientific observation came from Charles Blakey in 1864. He performed the first skin test on himself, testing and confirming that pollen caused his hay fever [114]. Anaphylaxis was described by Richet and Portir in 1902, while the term allergy was coined by Clemens von Pirquet in 1906, where he described the immune response itself causing disease through the formation of a pathogen-interacting "antibody" [115]. The "antibody" in question was IgE, although this wasn't identified until 1967 by Ishizaka and Ishizaka [116]. Histamine was identified in 1907 and was initially called β-iminazolyethylamine [117], three years later it was proven to induce a shock-like syndrome when injected into mammals [118]. Histamine was shown to reside in mast cells through studies in the 1950s by Riley and West [119] and subsequently shown to lead to wheal and flare reactions, connecting it to anaphylaxis. Allergic reactions are multiphasic, consisting of this acute response and also a late phase response. The early phase is caused by FcεRI activation; this is produced by sensitisation of the immune system with allergen leading to the production of large amounts of IgE [120]. Upon a second challenge the IgE-bound FcεRIs become cross-linked, leading to activation of the mast cell. This allergic response mediated through IgE is termed type 1 hypersensitivity. The early phase response consists of degranulation and the release of pro-inflammatory, granule-associated mediators, such as histamine and proteases, and lipid mediators, together leading to the wheal and flare response within minutes. After this first phase the mast cells start to synthesise mediators such as cytokines and chemokines that recruit and lead to the infiltration of other immune cells, such as neutrophils and eosinophils, to the site of inflammation, resulting in the late phase response that can last for hours after the initial response [2].

Chronic allergic inflammation occurs when this response repeats over time. The most studied of these allergic diseases is asthma. Asthma is associated with excessive production of mucus, hyper-responsiveness of the airways, bronchoconstriction and infiltration of other immune cells into the lungs. Large

numbers of mast cells are seen associated with airway smooth muscle in asthmatic patients and secreted preformed mediators such as histamine and tryptase induce contraction of these muscle cells, thereby contributing to hyper-responsiveness. Mast cells are also present around mucous glands and mast cell mediators can induce secretion from these [120, 121].

In the GI tract mast cells are responsible for many of the symptoms seen in food allergy. Patients have increased levels of mast cell mediators such as histamine and tryptase in stool and gut lavage fluid [8]. In the gut, mast cell mediators lead to changes in gut function, inflammation and contribute to intestinal pain [8]. Mast cells are thought to be key players in irritable bowel disease and irritable bowel syndrome (IBD and IBS, respectively). Although the exact role that histamine, proteases and neuropeptides released by mast cells play in these diseases is not fully understood [8]

Tumour development

There is a growing body of evidence that mast cells are associated with and have an active role in the growth and development of tumors; large numbers of mast cells accumulate around the sites of tumors [122, 123]. Considering mast cells are capable of releasing both pro- and anti-tumor factors, the question arises as to whether the mast cell aids tumor development or is detrimental to the tumor. Mast cells are attracted to the site of tumors through the release of chemo-attractants such as RANTES and SCF [124]; large mast cell numbers correlate to poor prognosis [125]. Activation of Myc, a transcription factor that is overexpressed in many tumours, leads to recruitment of mast cells to the tumour site and this is required for tumour expansion in pancreatic islet tumours [126].

As mentioned briefly above, mast cells can release many factors that could both aid and hinder tumour development. Mediators such as VEGF, II-8, MCP-1, Platelet derived growth factor (PDGF) and Il-6 are pro-tumour factors released by mast cells that can stimulate angiogenesis and tumour growth[127, 128]. Differential release of mast cell mediators through activation of different receptors could lead to selective release of these pro-tumour factors by mast cells over anti-tumour factors. In hypoxic conditions, such as those encountered within the tumour

microenvironment, mast cells are selectively stimulated to release pro-tumour factors, including VEGF and IL-6 [129-131]. Furthermore, factors released from damaged tumour cells, such as SCF and toll like receptor (TLR) 4 ligands, inhibit degranulation and induce production of pro-tumour factors such as VEGF and PDGF [132]. Mast cell often accumulate at the periphery of tumours, near to the vasculature [133] and there is a correlation between mast cells and angiogenesis in breast, colorectal, lung and uterine cancers [134, 135]. VEGF and FGF over expression in mast cells often results in poor prognosis [136, 137]. Mast cells are also a source of many proteases and tissue-remodelling factors that serve an important function in wound healing; these factors lead to remodelling of the extracellular matrix (ECM) and increase vascular permeability. Within the context of tumour development, these factors could aid tumour metastasis and progression [133, 138] particularly as mast cells lie at the interface of tumour and healthy tissue.

Clearly mast cells can also release factors that will lead to an immune response detrimental to the tumour, such as chymase and many cytokines. Mast cells can recruit eosinophils and neutrophils as well as activate adaptive B and T cell responses [133]. However, once in the tumour microenvironment mast cells might become agents for tumour growth and invasion through exposure to factors described above and these findings provide a possible means by which the tumour microenvironment modifies mast cell function, aiding tumour growth through release of pro-tumour factors while inhibiting anti-tumour factor release.

1.2 Mast Cell activation

The functions of mast cells described above require the mast cell to detect environmental signals. Mast cells possess a number of receptors that through differing signalling pathways lead to the differential release of mast cell factors.

1.2.1 FcεRI activation

The most studied activation pathway in mast cells is activation through the IgE cell surface receptor FcεRI. Cross-linking of FcεRI leads to degranulation and *de novo* synthesis of mediators [3]. The FcεRI receptor consists of three subunits; α, β and

disulphide linked γ units. The α subunit binds IgE but doesn't participate in downstream signalling. The γ subunits contain a cytoplasmic immuno-receptor tyrosine-based activation motif (ITAM) that initiates downstream signalling, the β subunit also contains this motif and is thought to act to amplify the signal [139]. Aggregation of the receptor results in trans-phosphorylation of the ITAMS by Lyn and Syc family kinases [140]. The phosphorylated ITAM then acts as a scaffold, allowing the binding of enzymes and adaptors including phosphatidyl 3-OH kinase (PI3K)[141]. A parallel pathway involves Fyn and leads to activation of PI3K by phosphorylation of Gab2. The Fyn signalling cascade eventually leads to the activation of Phospholipase C (PLC)-γ and subsequent production of Inositol trisphosphate (IP_3) and diaglycerol (DAG) [142]. DAG activates protein kinase C (PKC), while IP_3 induces release of calcium from the endoplasmic reticulum (ER) through activation of IP_3R. STIM1, acting as a calcium sensor of ER calcium levels, then redistributes to parts of the ER proximal to the plasma membrane [143]. STIM1 acts to activate the highly selective calcium release activated channel (CRAC) ORAI1, opening the channel pore through the interaction of a positively charged sequence on STIM1 with the acidic coiled-coil of ORAI1 [144]. The activation of ORAI1 leads to a large influx of extracellular calcium into the cell and subsequent degranulation. ORAI 2 and 3 have been shown to be expressed in mast cells [145] but their functional roles have not yet been determined; ORAI1-/- liver derived mast cells lack calcium release activated current (CRAC) currents suggesting there is no redundancy.

The fact that some calcium entry remains in ORAI1 -/- mast cells and other divalent ions can permeate and support degranulation suggests other channels are acting alongside ORAI1, most likely the TRP channels. In RBL-2H3 cells TRPC5 has been shown to contribute to calcium entry by acting alongside ORAI 1 [146] and mast cells express a number of TRP channels [147]. These channels could act to modify CRAC channel calcium entry in cells when expressed in a 'mix and match' manner, forming channels with different properties allowing differential responses to different stimuli.

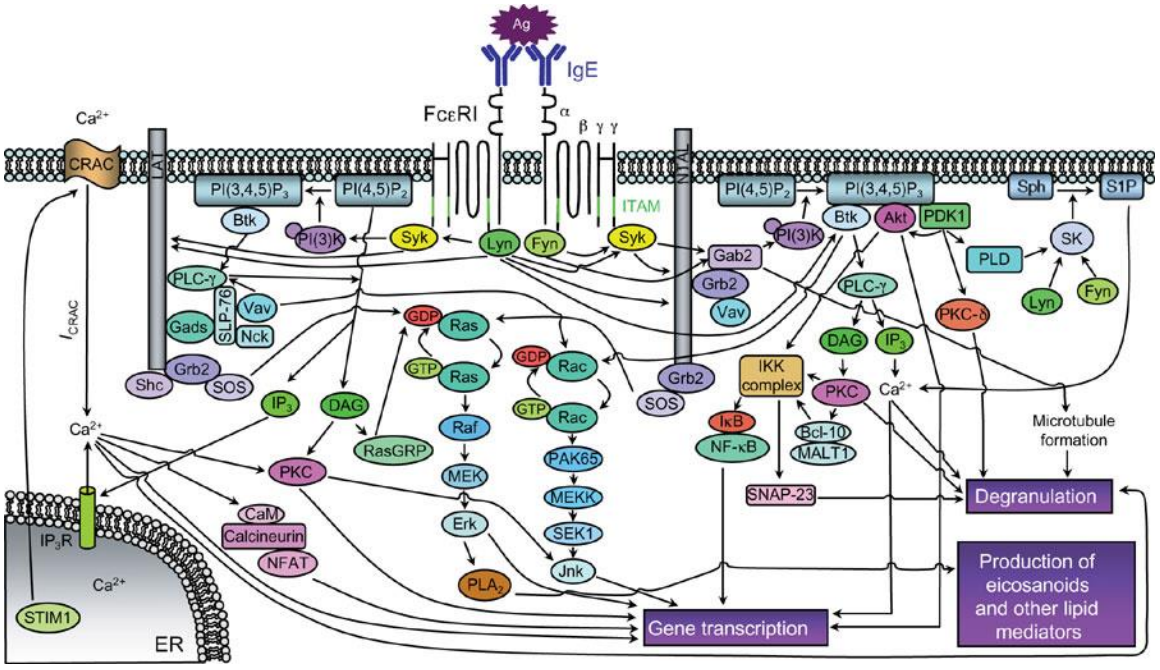

Figure. 1.4

FcεRI signalling in mast cells

Upon cross linking of FcεRI by IgE the src-family kinases Syk, Fyn and Lyn become activated, leading to a signalling cascade that ultimately gives rise to large increases in cytosolic Ca^{2+} [142] through production of IP3 and the resulting release of Ca^{2+} from the ER. This in turn leads to the influx of external Ca^{2+} through CRAC channels and results in mediator release. Figure from Kalesnikoff et al (2008)

1.2.2 IgE independent receptor activation pathways

Alongside the IgE receptor, mast cells possess numerous receptors that contribute to the ability of mast cells to respond to diverse stimuli. Some of which are discussed below

C-kit

The c-kit receptor has been shown to be vital to mast cell development and survival; mice with impaired SCF and C-kit have greatly reduced numbers of tissue mast cells [16]. In other cell types the expression is down regulated as they mature, mast cells are the exception to this and express high levels of the receptor after maturity. The receptor has intrinsic tyrosine kinase activity that is activated upon ligand binding and subsequent receptor dimerisation. Autophosphorylation creates binding sites for molecules such as the src family kinases and PLC γ [148]. The resulting downstream signalling cascade leads to the production of transcription factors

important for mast cell migration, survival, growth and cytokine production [16, 149, 150].

Complement receptors

Complement receptors are G-protein coupled receptors, activated by the potent inflammatory mediators, anaphylatoxins C3a and C5a. Mast cells have been shown to express both C3aR and C5aR but there is significant tissue specific heterogeneity; for example human skin mast cells respond to C5a [151] while human lung and tonsilar cells do not [152, 153]. C3aR are expressed in both primary mast cells and the mast cell line LAD 2 [154, 155] and can induce calcium mobilisation and subsequent degranulation, chemotaxis and production and release of chemokines [154]; in the same study C5a induced only a small rise in intracellular calcium and didn't induce degranulation but did lead to a small rise in MCP-1 production. Both C3aR and C5aR couple to the Gαi family of heterotrimeric G proteins and their effects can be inhibited with pertussis toxin [156]. Interestingly there seems to be separate signalling pathways for release of chemokines and degranulation through complement activation. Addition of a PI3K inhibitor blocks C3a mediated MCP-1 generation while leaving RANTES production intact, while inhibiting Extracellular signal Regulated Kinase (ERK) phosphorylation blocks release of both [154]. No further evidence exists as yet but given mast cells exhibit differential release it is plausible that activation of certain receptors, such as C3a, leads to activation of numerous downstream pathways resulting in release of a wide number of mediators. While other receptors, known to induce selective release of mediators, only activate the particular pathway for certain mediators for example a PI3K pathway leading to MCP-1 release but not RANTES. IgE or LPS stimulated Il-6 release is not inhibited by wortmannin, the PI3K inhibitor, but degranulation is [157, 158]. The effect on other cytokines was not tested but this still highlights the different downstream signalling pathways used by the same receptor in releasing certain mediators.

Toll like receptors (TLRs)

Response to bacteria and viruses are mediated through pathogen recognition receptors, the best studied are TLRs. TLRs recognise a large number of pattern associated membrane proteins. There are 10 human TLRs [159] each one

recognises one of a number of PAMPs. Some are expressed on the cell surface, such as TLR 2, 4 and 5 and often recognise bacterial components such as lipopolysaccharide (LPS) and flagellin. Others are present on endocytic compartments and detect nucleic acids, for example TLR 3 responds to double stranded RNA [160]. Mast cells have been shown to express the majority of TLRs [161]. Different TLRs induce different responses in mast cells [24, 162] and suggests activation of different TLRs activates different signalling pathways. For example in Bone marrow derived mast cells (BMMC) TLR 2 activation induces the release of IL-4 and 5 but not IL-1 whilst TLR 4 activation leads to production of IL-1 but not IL-4 or 5[163]. One signalling pathway of TLRs in mast cells is through a MyD88-dependant pathway [164]. The MyD88 leads to production of pro-inflammatory cytokines through transcription factors NF-KB and AP-1. How activation of particular TLRs leads to differential release is still not known. The expression of TLRs in mast cells means care has to be taken when looking at performing genetic modifications. Viral and siRNA mediated gene knockdown are common ways of monitoring gene function, but given mast cells have been shown to express TLR 3 and 9, which recognise viral PAMPS, there is a possibility of unwanted activation [26]. Antagonists to TLRs exist which could reduce any the effects of shRNA or siRNA but if assessing innate immune responses in mast cells then these would be counter productive. This highlights the importance of using scramble controls as a means of testing any potential affects not directly associated with gene knockdown.

Peptide receptors

Mast cells are often positioned near to neurons and are capable of responding to factors they release [165]. Substance P, vasoactive intestinal peptide (VIP) and somatostatin induce human skin mast cells to degranulate [166]. It must be noted that there are large differences in the expression of these receptors depending on the tissue location of the mast cell. For example, neuropeptides do not cause histamine release from human gut mast cells (HGMC) [167]. However, HGMCs do express neurokinin-1 receptor, a target of neuropeptide substance P, upon stimulation with IgE crosslinking, indicating that mast cells may become primed to respond to neuropeptides during allergic inflammation. *In vitro* differentiated primary mast cells and LAD 2 cells have been shown to express neurokinin receptors 1, 2 and 3 as well as VPAC2, and these cells release cytokines different to

those of cells stimulated through FcεRI and degranulate when stimulated with substance P or VIP[89]. Activation through these peptides is sensitive to pertussis toxin and wortmannin, identifying a G-protein/PI3K pathway but is insensitive to PKC inhibition. The receptor activation pathways for both Substance P and VIP do differ; forskolin inhibits VIP-induced but not Substance P-induced activation suggesting VIP is more sensitive to high levels of cAMP [89].

Stimulation of other receptors can induce selective release of mediators: Corticotrophin release hormone (CRH) can induce the selective release of VEGF. PGE_2, is also able to induce selective release, which also inhibits FcεRI induced histamine release [60]. Activation through the PKC activator Phorbol myristate acetate (PMA) alone in mast cells induces selective release of mediators such as MCP-1 and VEGF [168, 169]. Il-6 can be selectively released through stimulation of cord blood derived mast cells with Il-1 [170]. What these experiments highlight is the multitude of ways mast cells can respond to different stimuli that enable them to modulate their responses according changes in their local microenvironment.

1.3 Mast cell Secretory pathway

1.3.1 Secretory granule biogenesis

Every eukaryotic cell has a constitutive secretory pathway. Alongside this general process, cells such as neuronal, endocrine and immune cells, including mast cells, perform regulated secretion. This enables the cell to rapidly release mediators stored in secretory granules upon stimulation by a particular extracellular ligand. The endocytic pathway can be regarded as the opposite, through which material is removed from the cell surface to be recycled or degraded. Regulated secretion and endocytosis in most cells can be generally regarded as separate processes but in certain cell types, including mast cells, the two processes overlap. The resulting secretory granules formed by this interaction of the endocytic and exocytotic pathways, are often termed secretory lysosomes [171]. These secretory lysosomes have an acidic pH and contain lysosomal proteins, as found in regular lysosomes [172-174] and degranulation of mast cells is often measured using the lysosomal

associated ß-hexosaminidase. Lysosomes in non-specialised secretory cells can also undergo exocytosis [175]. In non-secretory cells, lysosomal exocytosis is important for plasma membrane repair, enabling the resealing of damaged sites [176]. Secretory lysosomes differ by their ability to undergo regulated secretion [177]. The evidence that these processes require different machinery comes from genetic diseases that affect secretory lysosomes, without affecting membrane repair. This includes Griselli's syndrome, caused by mutations in RAB 27a [177].

In BMMC, three distinct SGs have been defined [178]. Type I granules contain MHC class II molecules as well as lysosomal markers but not serotonin, type II granules contain MHC class II molecules, lysosomal markers and serotonin. Type III granules do not contain lysosomal markers but contain serotonin suggesting that type II granules are formed by fusion of type I and type III granules. It is not clear whether these represent different granule subtypes or immature non-functional intermediates. Other cell types containing secretory lysosomes, such as platelets, also contain conventional lysosomes. They contain three granules: Dense granules, alpha granules and lysosomal granules. These three are well defined and contain distinct contents from one another [179]. The fact that type I and III granules described above contain a mix of contents that are then combined in type II granules is more suggestive of non-functional intermediates fusing to produce a mature granule. An important point to note is that human mast cells contain very little if any serotonin [32] and so this type of granule, or granule intermediate, might not be relevant in describing human mast cell SGs.

Very little is known about the sorting mechanisms that lead to granule targeting in mast cells. Possible mechanisms might include the mannose-6-phosphate system whereby proteins are "tagged" with a mannose-6-phosphate moiety that is recognised by mannose-6-phosphate receptors. These cycle between late endosomes and the trans-Golgi network (TGN) carrying proteins to lysosomes [177]. Another possible mechanism is through serglycin, that could act as an intracellular carrier [61]. Another feasible mechanism is P-selectin meditated targeting. This is a type I membrane protein and adhesion receptor for leukocytes. It contains targeting signals for secretory granules and lysosomes; expression of an HRP-P-selectin results in targeting to secretory granules in RBL-2H3 cells [180].

Finally, proteins bound for secretory granules might be trafficked directly from the Golgi to the granules. One protein has been identified to do this is the Fas Ligand. In T-lymphocytes and natural killer cells Fas ligand is sorted directly to secretory granules through a proline-rich domain [181].

1.3.2 Cytokine trafficking

In other immune cells such as macrophages, the adaptation of the endosomal/lysosomal pathway is not limited to the release of preformed mediators, but to newly synthesised mediators such as cytokines. TNF-α and Il-6 are delivered to the plasma membrane from the TGN through the recycling endosome [182, 183], furthermore, Il-6 and TNF-α are released in a different temporal and special pattern from the recycling endosome, suggesting the recycling endosome is used as a key sorting mechanism for cytokine release. The recycling endosome is also utilised in GLUT4 transport. GLUT4 is found in the recycling endosomes of unstimulated adipocytes acting as a pre-stored pool to be released through insulin stimulation [184-186]. It is possible that in mast cells a similar pathway could exist. In mast cells the cytokine trafficking pathways are not well defined, and studies are few and lacking sufficient detail. Il-6 can be differentially released by mast cells through stimulation by IL-1 [87]. Ultra structural studies in HMC-1 and hCBMCS found pools of IL-6 present in vesicles 40 to 80 nm in size, distinct from SGs. Interestingly some of these pools were present in resting cells. It is not clear from this study whether mast cells are constitutively trafficking and releasing IL-6 in resting conditions or represent a resting store, distinct from SGs. Release of Il-6 is brefeldin A sensitive [187] and so most probably involves vesicles budding from the Golgi but, as with macrophage release, it might be a two-step process by which vesicles are trafficked to the plasma membrane via the TGN and the endosomal pathway. Perhaps the pools seen in resting cells is Il-6 residing in an endosomal compartment in a manner similar to GLUT4.

TNF-α is a cytokine where there is strong evidence showing it is both de novo synthesised and pre-stored. Evidence for pre-stored release is based on the fact that small amounts are released within minutes of stimulation, too shorter a time for de-novo synthesised release [27]. TNF-α is present in SGs and overexpressed TNF-

α colocalises to SGs when transfected into RBL-2H3 and LAD 2 cells [247]. After this initial release, TNF-α mRNA expression increases and newly produced TNF-α is trafficking through a brefeldin A sensitive pathway hours after initial stimulation.

VEGF is also reported to be present in pre-stored pools; immuno-gold labelling identified VEGF in resting cells in SG like structures in human skin mast cells [107]. VEGF can also be selectively released without full degranulation [69,114,181] but whether this release is confined to only de novo synthesized or also involves selective release of preformed pools has not been determined. Given the limited evidence (a single ultra-structural image) no complete conclusions can be drawn. However, not all granules seemed to contain VEGF and so subsets of SGs, containing both preformed traditional granule mediators, such as histamine, might co-exist with another form containing additional cytokines and growth factors. An alternative, described above, is that these cytokines are not actually present in SGs at all and exist in pools residing in a recycling endosomal compartment that can be differentially released to SGs.
Many other de-novo secreted cytokines are thought to be release through a more direct pathway, through small vesicles budding from the TGN and passing directly to the cell surface [188].

Mast cell granule contents can be released by piecemeal degranulation. In this process small vesicles bud off from larger granules and fuse with the plasma membrane [189]. This mechanism might permit the release of selected mediators from granules without the need for full fusion. It must be noted that the only evidence for this in mast cells is through ultrastructural studies where mast cell granules appear partially empty. In other immune cells, such as eosinophils, this mechanism is accepted as a means of selective release of cytokines. For example, pre-stored cytokines, such as RANTES and Il-4 stored in granules can be selectively released in this process through small vesicles [190, 191]. Evidence for how this is achieved comes from EM studies where vesiculotubular structures could be seen within emptying granules and immuno-gold labelling identified RANTES present within granule sub-compartments, another study identified Il-4 in distinct granule vesicular compartments [192],[193]. As has been described in detail above, mast cells contain numerous pre-stored cytokines. Piecemeal degranulation might

provide the means by which mast cells can selectively release mediators, such as VEGF, in a process similar to eosinophils, alongside or as an alternative mechanism to the pathways described above.

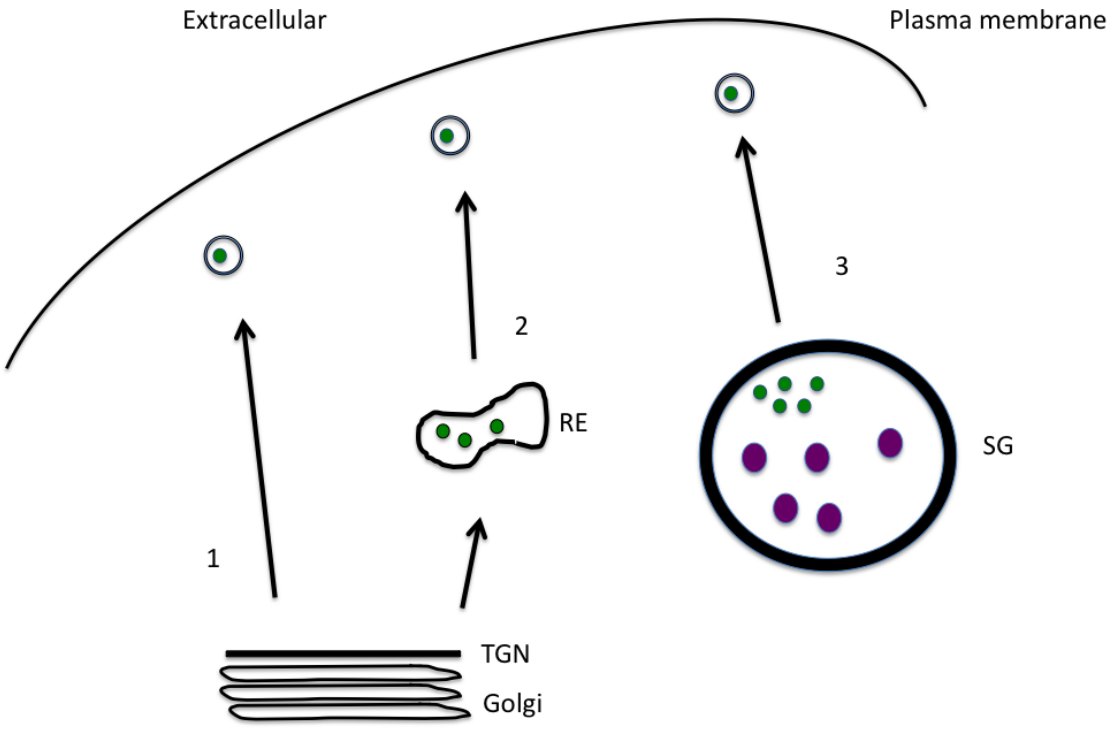

Figure 1.5

Possible mechanisms of cytokine release

1: Direct trafficking from the TGN to the plasma membrane. 2: Vesicles containing cytokines budding off from a recycling endosomal store. 3: Release of cytokines by piecemeal degranulation, with cytokines stored and sequestered in granules.

In mast cells a large proportion of secretory granules fuse to one another, as well as with the plasma membrane, in a process termed compound exocytosis [194]. Mast cell granules have been shown to fuse sequentially; whereby firstly a granule fuses to the plasma membrane and then other granules subsequently fuse to it, and fuse homeotypically; where vesicles fuse together and then undergo plasma membrane fusion [195, 196]. Compound exocytosis was first identified in mast cells by electron microscopy [107]. Evidence for homeotypic fusion relies on capacitance recordings [195]. Homeotypic fusions were stated to occur where large increases in capacitance were seen that were too large to be explained by sequential fusion of granules. There is currently no microscopic evidence for homeotypic fusion, one would expect to see fused SGs that are not fused with the plasma membrane and possibly exist in resting cells. Compound exocytosis allows for quick and complete release of granule contents within a relatively short period of time.

Finally, there is also some putative evidence of mast cell granules undergoing kiss and run fusion, in this process the granule contents are partially released and recloses not completing full fusion [197]. Assessed using fluorescent dextrans loaded into RBL-2H3 cells kiss and run fusion was determined to occur when a prolonged period of secretion of dextran was seen after an initial peak as the dextran loaded SGs passed up to the membrane and partially released contents. A full fusion event was defined as a large spike in fluorescence that was rapidly released. This is not convincing as the prolonged period of release might represent a larger granule containing more dextran or a granule loaded with more dextran leading to a longer release period. Furthermore determining the differences between piecemeal and kiss and run fusion of mast cell granules is difficult; the partially empty granules described above, seemingly showing SGs after piecemeal degranulation, might have emptied as a result of kiss and run.

1.3.3 SNAREs- mediators of fusion

Release of amine, peptide or non-lipid mediators from mast cells requires the fusion of secretory vesicles with the plasma membrane. SNAREs are fundamental to membrane fusion and exocytotic mediator release. SNARE proteins were first purified and described in the late eighties. Synaptobrevin, or vesicle associated membrane protein 2 (VAMP-2), named after the Latin *brevis* (short) was identified in synaptic vesicles (SV) in rat brains [198], while VAMP-1 was purified from *Torpedo californica* [199]. Around the same time two other proteins present on the neuronal plasma membrane were identified, these were termed p35 or syntaxin [200, 201] and synapse associated protein of 25 kDa (SNAP-25)[202]. It quickly became apparent that these proteins were highly conserved across species [203-205] and therefore thought to be of high importance in neurotransmitter release. This functional importance was confirmed through the discovery that SNARE proteins are the targets of Clostridial neurotoxins [206-210], which inhibit synaptic neurotransmitter release and are discussed in greater detail below. Furthermore, it was shown that these proteins could form a protein complex [211]. Over the next few years more SNAREs were identified and were subsequently shown to be ubiquitously expressed in many cell types, their expression not just confined to

neuronal cells [212-214]. It is now clear that SNARE are important sfor all forms of membrane fusion within the cell, there are 36 identified mammalian SNAREs to date Figure 1.6 shows the localisation of SNAREs to particular trafficking pathways.

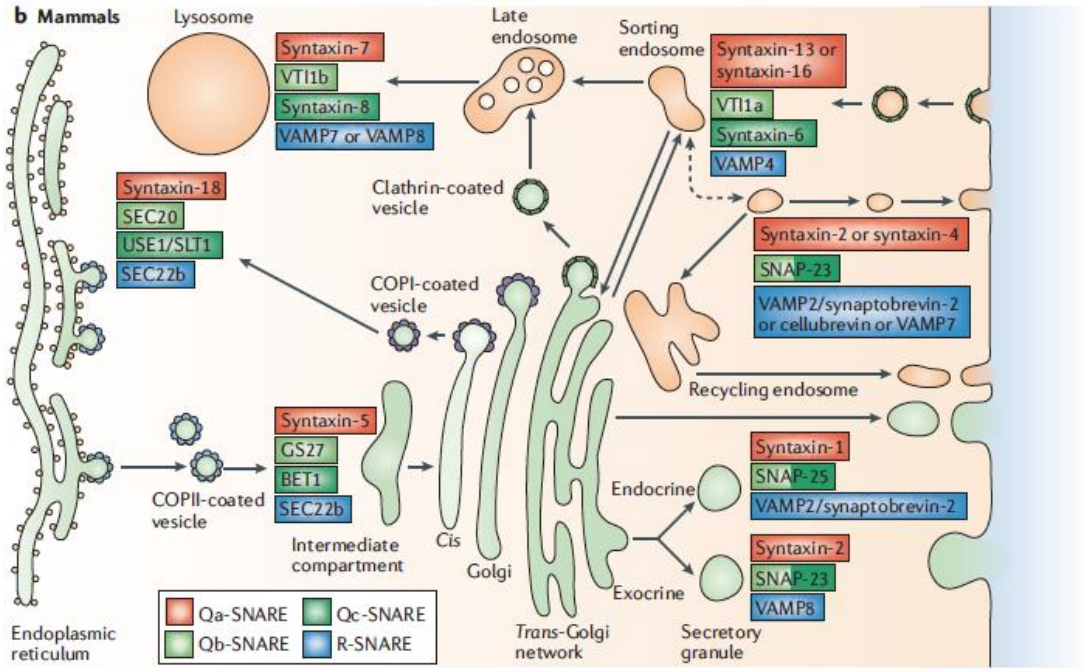

Figure 1.6.

Intracellular organisation of SNARE proteins in mammalian cells. [215]

Figure from Jahn and Scheller 2006

SNARE proteins are classically grouped according to the membrane at which they are localised; t-SNAREs on target membranes and v-SNAREs when present on vesicle membranes. The syntaxins and SNAPS are generally regarded as t-SNARES while VAMPs are categorised as v-SNAREs. SNARE mediated membrane fusion occurs through the formation of a four α -helix bundle [216], three of these helices are supplied through t-SNAREs and one from the opposing v-SNARE. The majority of SNARE proteins contain a trans-membrane domain within their C-termini that is connected to the SNARE domain by a short linker. Some exceptions to this include synapse associated protein of 23 kDa (SNAP-23) and SNAP-25 that lack trans-membrane domains. These SNAREs are tethered to the plasma membrane through palmitoylated cysteine residues.

Each SNARE protein contains a conserved SNARE domain of 60 to 70 amino acids that mediates complex formation. Within the SNARE motif there is a highly conserved central area containing either one of three glutamine (Q) residues or an

arginine (R) residue. Mutations in these amino acids cause trafficking defects [217]. A more complete grouping of SNAREs is achieved through classification based on Q/R SNARE classification. Where SNARE motifs can be classified as Qa, Qb, Qc and R depending on the particular amino acid present in this highly conserved region. The 4 helical complex formed by these motifs requires each one of these subfamilies. There are exceptions, however, those complexes formed from different combinations are less stable and might not be able to facilitate membrane fusion. [215]. Most SNARE proteins contain one SNARE domain, although some including SNAP-23 and SNAP-25 have two. These SNAREs are classed as Qbc SNAREs which flank the palmitoylated residues anchoring the SNAREs to the membrane.

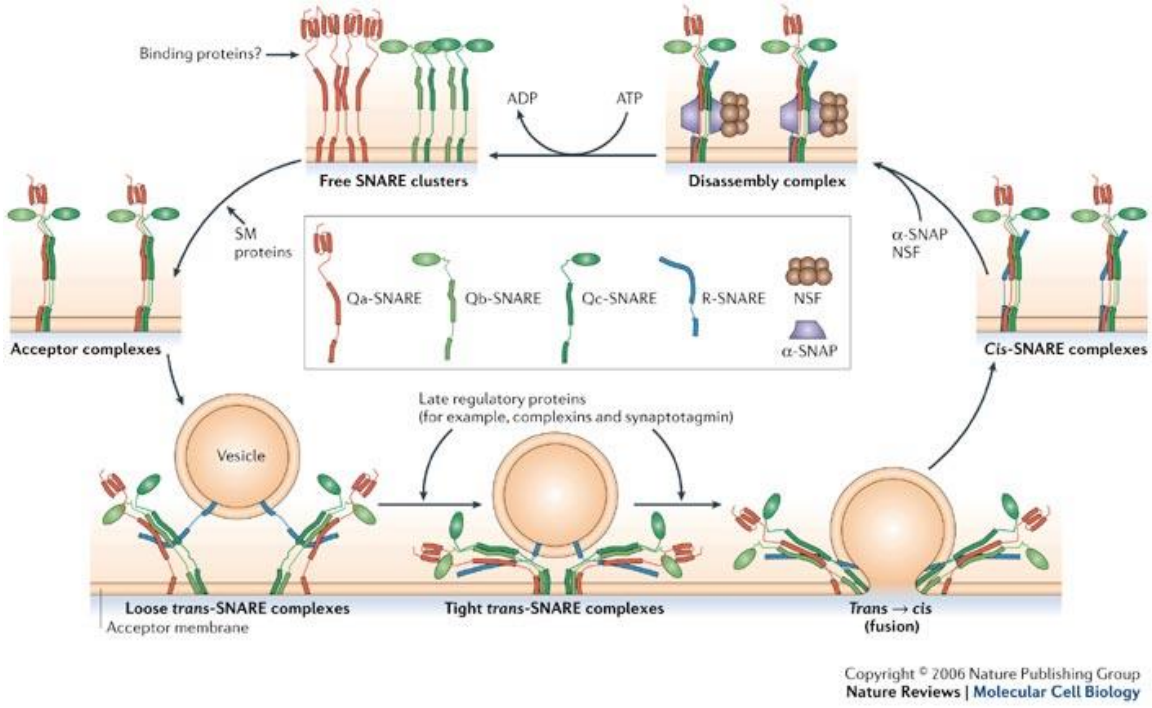

Figure. 1.7.

SNARE mediated membrane fusion. [215]

Figure from Jahn and Scheller 2006

To drive membrane fusion the SNARE bundle containing the four SNARE helices forms a 'trans' SNARE complex spanning both membranes. This so called 'SNAREpin' consequently zips together from the N-terminal through to the C-terminal leading to fusion of the two opposed membranes. Once this fusion has occurred and a fusion pore formed, the SNAREs are no longer exerting a driving force and the complex is now present on the same membrane, it is said to be in a stable cis-conformation. The SNAREpin is the minimal requirement for fusion of two

lipid membranes [218]. This process requires many supporting regulators that enable the cell to exert control of the fusion process, some of which will be discussed later. Disassembly of the SNARE complex requires considerable energy; the AAA ATPase N-ethylmaleimide-sensitive factor (NSF) catalyses this disassembly [219]. Structural studies [220, 221] have shown that NSF doesn't bind to the SNARE complex directly but requires adaptor molecules; these are termed Soluble NSF attachment proteins (SNAPS). SNAPS bind directly to SNARE proteins and mediate the unwinding of the SNARE complex by NSF [222]. The SNARE cycle is shown in Figure. 1.7.

The N-terminal domains of SNARE proteins, unlike SNARE domains, are highly variable and are thought to confer functional differences between SNARE isoforms. Syntaxin possesses an N-terminal extension that is independently folded, termed the Habc domain; an antiparallel three helix bundle [223, 224]. In neuronal cells a model has been proposed, where the Habc domain folds back on the SNARE motif resulting in the "closed conformation" of syntaxin, whereby it cannot interact with other SNARE proteins. In this closed formation the Habc domain exhibits a high affinity to Mammalian uncoordinated-18-1 (Munc18-1) [225]. Munc18-1 can displace SNAP-25 from syntaxin 1 with the help of NSF-SNAPS [226] and holds syntaxin in a closed conformation. Then Munc13-1 binds to the syntaxin/Munc18-1 complex to "open" syntaxin and along with Munc18-1 mediates trans-SNARE complex assembly. These observations were made in reconstitution experiments using liposomes and eight key components of the neuronal secretory machinery to try and give physiologically relevant results. This highlights the issues with monitoring these interactions and being able to obtain physiologically relevant data. For example; neurotransmission is abolished in the absence of Munc18-1 or Munc13-1 [227] but in vitro SNAP-25-syntaxin 1-lipsosomes can fuse with VAMP-2-liposomes in the presence of synaptotagmin (syt) I and calcium without Muncs. Therefore a lot more work needs to be done to bring together the in vitro and in vivo data for membrane fusion. Munc proteins are described in more in section 1.3.5.

VAMP-7 is one of the largest R-SNAREs, it's size due to a large N-terminal longin domain [228]. This domain is important for localisation of the protein and it's

function. For example the interaction of the VAMP-7 longin domain with the AP3 adaptor complex is important for sorting to endosomal compartments. The longin domain binds to the δ-adaptin subunit of AP3 and VAMP-7 is the only VAMP that co-precipitates with δ-adaptin, secondly it regulates the ability of VAMP-7 to participate in SNARE complexes [229-231].

The role of the longin domain highlights the way in which the structure of individual SNAREs can lead to their distinct intracellular targeting, and ultimately give rise to the function each SNARE has in membrane fusion events within a cell.

1.3.4 SNARE proteins and mast cells

Despite the wealth of knowledge and understanding of the function of SNARE proteins in neuronal exocytosis, less is understood of their functions in immune cells. Much of the work of identifying SNARE proteins present in mast cells, and their importance for mediator release, has been performed in murine mast cell models.

Experiments in RBL-2H3 cells at the beginning of 2000 started to define SNAREs present on mast cell granules. VAMP-7 and syntaxin 3 were shown to be expressed by reverse transcription-polymerase chain reaction (RT-PCR) and fluorescently tagged forms of these proteins translocated towards the membrane upon stimulation [232]. However, the images of this translocation are not clear and there was no assessment of endogenous levels so the validity of this experiment is dubious. Another group identified syntaxin 4, SNAP-23 and VAMP-8 involvement in mast cell degranulation [233]. Localisation of VAMP-8 with serotonin was shown by immunostaining in RBL-2H3 cells. In the same study overexpression of syntaxin 4 by transient transfection caused inhibition of degranulation, measured by flow cytometry. Syntaxin 2 and 3 over expression had no effect. There was evidence of SNAREs localizing to distinct secretory vesicles in the same study, VAMP-2 and VAMP-7 partially localised with secretory granules that were dissimilar to VAMP-8 in size. This highlights the possibility of distinct subsets of SGs, possibly differentially released. It must be stated that these results are not conclusive; immunostaining alone cannot be used to define the SNARE involved in a particular

pathway and for a more complete assessment overexpression studies should be supplemented with knockdown experiments to look for contrasting affects. What these initial studies did do though was to pave the way for more detailed analysis of the SNAREs involved in mast cell exocytosis.

Further evidence for VAMP-8 involvement in SG exocytosis does come from knockdown experiments. Knocking out VAMP-8 in murine bone marrow derived mast cells reduces serotonin and cathepsin D release, while histamine and TNF-α release are unaffected [234]. [235] Tiwari et al have also shown VAMP-8 deficient bone marrow derived mast cells do not have reduced release of cytokines, whereby TNF-α and IL-6 release remained intact, however, they saw reduced histamine release in the same cell line producing conflicting results. Both studies used FcεRI stimulation on BMMC that were treated in a similar manner. FcεRI mediated histamine release in Puri et al was only 10% in control cells, lower than serotonin (40%) and much lower than FcεRI mediated release in Tiwari et al (50%). Furthermore, Tiwari et al performed additional in vivo experiments whereby they found reduced plasma histamine after anaphylactic challenge. The reasons for such low histamine release are not clear but with histamine release being so low it is not surprising no significant decrease was seen in VAMP-8 knockdown if histamine release was already compromised. Also, how the differential control of serotonin release relates to human mast cells is open to conjecture, as they express very little if any serotonin [32].

The results identifying the key SNAREs involved in preformed mediator release have been augmented with recent work utilising a siRNA approach to knockdown SNAREs in RBL-2H3 cells, identifying VAMP-7 and -8 as well as SNAP-23 and syntaxin 4 as key SNAREs in pre-formed mediator release [236]. Knockdown of these SNAREs inhibited release of antigen-induced histamine and β-hexosaminidase release. They did not determine any compensatory expression of other SNAREs upon knockdown, which might explain why a full inhibition of degranulation was not seen. VAMP-8 and syntaxin 4 co-precipitated with SNAP-23, which was expressed at high levels determined by qPCR, while VAMP-7 could not.
The findings from all these studies in murine mast cells together suggest a model whereby SG release is mediated through the actions of SNAP-23, syntaxin 4 and

VAMP-8. In other non-immune cell types, such as HeLa cells, VAMP-7 has been shown to mediate the trafficking from the late endosome to the lysosome [237] and although VAMP-7 knockdown inhibits degranulation and partially colocaslises with SGs, the fact that it does not co-precipitate with other SNARE heavily implicated in SG exocytosis suggests that it is not directly mediating the fusion of SGs to the plasma membrane. VAMP-7 might represent a trafficking compartment that is important for maturation of granules or trafficking granule components to granules, in this instance release of preformed mediators would still be compromised upon knockdown.

What is clear from the experiments above is that VAMP-8 knockdown has no effect on TNF-α and IL-6 release [235], therefore another SNARE must be important for the trafficking of these mediators. Knockout of VAMP-2 and VAMP-3 has no effect on β-hexosaminase release [234]. Whether or not knockdown of these SNAREs affects the release of other mediators has not been determined, however, VAMP-3 was shown to localise with TNF-α upon stimulation with IL-1B by immunostaining. This observation suggests a possible role for VAMP-3 in TNF trafficking. IL-1B doesn't induce degranulation, so the role of VAMP-3 in mast cell exocytosis might just extend to trafficking of newly synthesized TNF rather than pre-stored pools, or it could be present on a subset of differentially released preformed vesicles. VAMP-3 increases association with SNAP-23 when VAMP-8 is knocked down, determined by immunoprecipitation [238]. This highlights issues with knockdown experiments, where compensation is known to occur through overexpression of other SNAREs. It is therefore important to take a combinatorial approach to assessing SNARE function and care must be taken when interpreting these studies. This might explain how in the above experiments using knockdown of SNAREs no complete inhibition of mediator release was seen. It is possible that other SNARE were asble to compensate in part for the loss of a particular SNARE.

Many of the SNAREs utilised for exocytosis in murine mast cells have a conserved function in human mast cells. VAMP-7 and VAMP-8 translocate to the membrane upon stimulation and inhibition of these two SNAREs, as well as SNAP-23 and syntaxin 4, through inhibitory antibodies inhibit pre-formed histamine release [239]. This effect is not seen with inhibition of VAMP-3 or VAMP-2. A more recent

study has shown the release of many chemokines, including IL-8, CCL2 and CCL4 [240], is mediated through SNAP-23 and syntaxin 3, while a small proportion is mediated by syntaxin 6 and another by the SNAREs important for pre-formed mediator release VAMP-8 and syntaxin 4. The method of inhibition used (inhibitory antibodies) is not ideal. The membrane needs to be permeablised and the specificity of the antibodies once inside the cell could be questioned. Even so these results would imply that many factors in mast cells are released through a diverse set of pathways under the control of multiple SNARE complexes. The eventual release of all mediators from the plasma membrane requires the Qbc SNARE SNAP-23, neuronal SNAREs do not seem to be utilised by mast cells and SNAP-25 is not expressed [239, 240]. One caveat to the notion of SNAP-23 mediating these events is the relatively recent discovery of multiple SNAP proteins, including SNAP-29 and SNAP-47 [241-243]. SNAP-29 localises to the endosomal membrane [244], has been implicated in FcεRI mediated exocytosis [245] and has been suggested to function in mast cell phagocytosis [246]. SNAP-47 has high levels of expression in nervous tissue and is enriched in SV fractions [241]. Both these SNAPS don't have palmitolyated cysteine clusters and seemly lack a membrane anchor, although it is not known for sure whether there are post-translational modifications that lead to membrane association as SNAP-47 is membrane bound. Rather than being present at the plasma membrane they are most probably important for intracellular trafficking, where both seem to have a broad intracellular distribution [243, 247].

VAMP-3 is known to be important in cytokine release in LPS activated macrophages. As has been discussed above, macrophages release TNF-α and Il-6 through a pathway that utilises the recycling endosome. VAMP-3 localises to this and mediates the trafficking of these cytokines to the cell surface [182]. GarcÌa-Roman et al [248] have shown that VEGF secretion is sensitive to tetanus toxin in mast cells, while degranulation remains unaffected. This would imply that one of the tetanus sensitive VAMPs (VAMP-1 2 or 3) is important for VEGF release. Considering human mast cells express little or no VAMP-1 and 2 and the fact that VAMP-3 is prominent in cytokine release in other immune cells, VAMP-3 is a likely candidate for release of certain growth factors and cytokines and could potentially be added to the plethora of SNAREs important for mast cell mediator release.

The variety of SNAREs residing on secretory vesicles, and their numerous regulatory proteins, might form the basis for their differential trafficking and release. Many of these regulatory proteins help to confer selectivity of vesicles to respond differentially to cytosolic cues, such as syts, which act as calcium sensors and allow the cell to impart a greater control on the release of mediators. Some of these regulatory proteins are discussed below.

1.3.5 SNARE interacting proteins

Synaptotagmins

Synaptotagmins (Syts), as with much of the exocytotic fusion machinery, were first identified in neurons [217]. They are integral membrane proteins containing two C2 domains C2a and C2b within their C termini, important for calcium dependent and independent protein-protein interactions [249]. The C2a domain of a number of Syt iosoforms can bind syntaxin I and phospholipids in the presence of calcium, as well as the adaptor complex AP-2 [174].

So far 17 mammalian isoforms of syt have been identified [250]. Different isoforms of syts have differing calcium sensitivities and can be classed into groups accordingly [251, 252]. Syts I II and III have low affinities to calcium and are important in fast release in the presence of high calcium concentrations in neurons. Syts V VI IX and X are intermediate in their affinities while Syt VII shows high affinity and mediates slow release. These differing calcium sensitivities have been shown to facilitate differential responses in neuronal exocytosis [253]. A study in PC12 cells has shown that different sized dense core vesicles (DVCs) harbor different syt isoforms [254]. For example small DCVs contain large amounts of syt I, which has a low calcium affinity, it confers onto them a greater propensity to undergo kiss and run fusion rather than full fusion, while vesicles expressing IX or VII isoforms show intermediate or low propensity to undergo kiss and run, respectively. These results would be expected when considering the relative affinities to calcium of these three isoforms and highlight the mechanisms by which cells can control differential release of vesicle populations based on differing calcium signals.

In murine mast cells four isoforms of syt are known to be expressed: syt II, III, V and IX [255-258]. Different isoforms have been shown to have unique localizations and exert diverse effects within the mast cell; over-expression of the neuronal syt I was shown to localize to secretory granules containing histamine and result in a potentiation of calcium triggered exocytosis [259], although syt 1 is not expressed at any great level in mast cells and so these results do not give any great insight into endogenous syt control of exocytosis.

Syt II was found to negatively regulate calcium regulated exocytosis upon overexpression [255] , while histamine release was reduced in knockout mice (Baram,Adachi et al. 1999). In more recent studies the role syt II plays in mast cell exocytosis has become even more apparent; Syt II has been found to negatively regulate MHC class II presentation [174] and another recent study found Syt II to control, exclusively, regulated exocytosis in BMMCS [260]. Whereby, using syt II knockout mice, release of SG mediators such as histamine were reduced while prostaglandin and TNF-α release was unaffected. Mast cells appeared normal in morphology and tissue location and stimulated calcium rises were not affected.

Syt III co-localizes to early endosomal markers including syntaxin 7, and also to early SG markers including histamine [261]. Knock down of syt III causes recycling of transferrin to the ERC to be impaired (internalisation and trafficking into early endosomes was unaffected) and enlargement of SG, suggesting a role in recycling from early SG. Syt IX in murine mast cells also has a role in the endocytic pathway. It is thought to be important in the correct sorting of SG proteins; knock down results in mis-targeting of TGN38, which normally cycles between the plasma membrane, endocytic recycling compartment (ERC)and TGN, to SG (Haberman, Ziv et al. 2005; Haberman, Ziv et al. 2007). The complex interplay of the endocytic pathway and release of cytokines in other immune cells, such as TNF-α in macrophages, suggests that many of these syntaptotagmin isoforms might form part of the complex system that controls the release of cytokines.

Given the roles different isoforms of syts have in regulating differential release in neurons, and the fact that mast cells express numerous isoforms with differing calcium sensitivities, differential syt and SNARE expression might be of key

importance in conferring the release of a particular subset of vesicles in response to different external stimuli.

Complexins

Complexins are small proteins that contain an α helical region that is important for high affinity SNARE binding [262]. Complexin was initially thought to mediate SNARE complex zippering through binding of its central region as an anti-parallel α helix to the SNARE N-terminal coil-coil [263]. The N-terminal portions of the SNARE complex are 'zippered' but the complex is then clamped, whereby the C-terminal portions are stopped from zippering by a part of the complexin molecule called the accessory helix which competes with the VAMP-2 C-terminus for binding to the t-SNARE [264, 265]. A further level of inhibition might also occur through the cross-linking of SNARE complexes; the accessory helix extends from the SNAREpin and can bind to other SNARE complexes. This crosslinking might allow additional inhibition through the formation of a 'zigzag' array (figure 1.8) [266]. Upon calcium influx after stimulation, this clamp is then released as calcium binds to syt which competes with complexin, displaces it and allows for full fusion to occur [267].

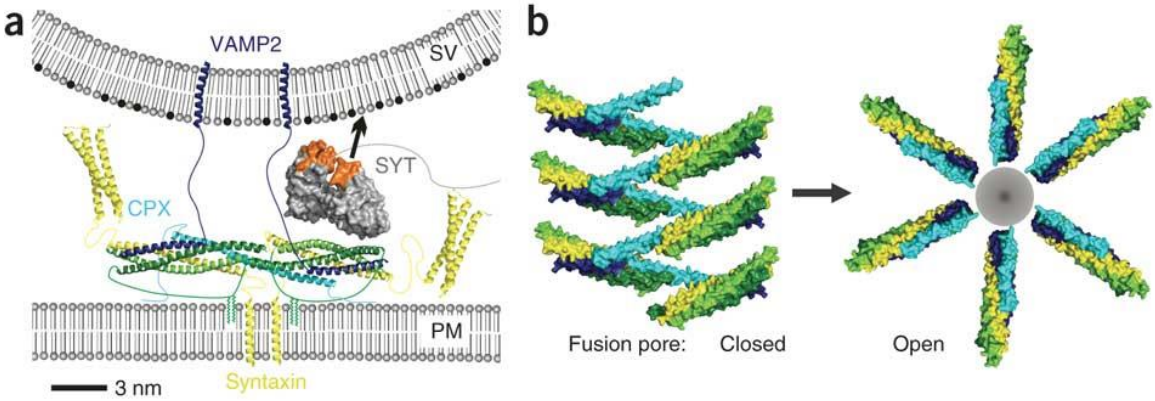

Figure 1.8

The complexin clamp

A. Complexin clamps the half zippered SNARE complex. **B**. Shows the model for the 'zigzag' array whereby the accessory helix of complexin molecules can bind to other SNARE complexes and crosslink adding an additional layer of control. Figure from Kummel et al 2011.

There are four complexin isoforms, with complexin III and IV exclusively expressed in retinal ribbon synapses [268]. Complexin studies in mast cells have only been carried out in RBL cells. Knockdown of complexin II reduces degranulation and complexin II translocates to the membrane after stimulation through FcεRI [269]. Complexin II has been postulated to regulate degranulation through interaction of

the site near the central a-helix region with syntaxin 3, SNAP-23 and VAMP-8, determined by GST pull down and the use of mutagenesis of the complexin II molecule [270]. Interestingly no interaction was seen with syntaxin 4 despite it being a SNARE heavily implicated in mast cell exocytosis. This might be explained by exocytosis through syntaxin 4 being dependent on other regulatory proteins, not complexin II. Complexin in neurons is known to facilitate rapid fusion of docked vesicles [271]. The mast cell doesn't undergo such rapid exocytosis and so this might explain the apparent lack of interaction with syntaxin 4. Complexin might have differing roles in the mast cell as to that in neurons. Syntaxin 3 is reported to be present on SGs as well as the plasma membrane, it is possible that the role of complexin II in the mast cell lies predominantly in granule to granule fusion. This would occur during compound exocytosis and most probably only under large sustained increases in calcium. Compound exocytosis can occur rapidly (seconds) after stimulation in mast cells [195]. The authors explained the rapid time course by suggesting granules are fused before simulation. Perhaps complexin II, present on mast cell granules, actually allows rapid granule-to-granule fusion to occur after stimulation to enable the mast cell to release SG contents at a much greater rate.

Mammalian Uncoordinated proteins

Munc 18 proteins have been briefly described in section 1.3. There are three Munc 18 members, members of the SM family that are exclusively implicated in exocytosis. Munc 18-1 is thought of as a neuronal specific isoform while Munc 18-2 and Munc 18-3 show more ubiquitous expression. They have different specificities for different syntaxins, Munc18-1 interacts with syntaxins 1, 2 and 3, 18-2 with 1 and 3 and 18-3 with 2 and 4 [272]. Knockout mice for Munc 18s have severe defects in exocytosis and are born live but die [273]. Munc18 proteins have a horseshoe like structure that can hold syntaxin in its closed conformation and exert actions described in section 1.3.3. The end terminal peptide motif of syntaxin recuits Munc18 into the SNARE bundle through physical tethering, thus acting as an initiating factor for the SNARE-SM membrane fusion complex [274]. This N-peptide has a distinct role from the Habc domain whereby the N-pepide is postulated to be essential for vesicle fusion, whilst the Habc domain regulates fusion. Furthermore, only loss of the Habc domain reduces the amount of Munc18 present suggesting a role in stabilising Munc18[275]. Mast cells express all three isoforms of Munc 18 at

the mRNA level [276]. However, Munc18-1 protein, determined by western blot isn't present in any great amount [277]. Munc18-2 seems to be the most predominant Munc in mast cells [276, 277]. It localises to granules, interacts with syntaxin 3 and knockdown of the protein inhibits degranulation [277, 278]. Interestingly Munc18-2 doesn't interact with syntaxin 4, which has been heavily implicated in mast cell granule exocytosis. Munc18-3 does interact with syntaxin 4 and is found on the plasma membrane in mast cells [277]. Therefore, the most likely set up is Munc 18-2 on mast cell granules and Munc18-3 on the plasma membrane, mediating granule-to-granule fusion and granule-to-plasma membrane fusion, respectively. A more recent study in RBL-2H3 cells showed Munc18-2 interaction with syntaxin 11; knocking down Munc18-1 and 2 reduced syntaxin 11 expression but not its localisation and inhibited degranulation. The expression of other syntaxins was unaltered but what this study highlights is that altering one protein of the secretory machinery can have significant effects on the expression of others [279].

Munc13s are also of key importance to vesicle fusion. They are important for opening the syntaxin molecule from its closed to its open conformation and interact with a host of other factors that are important for calcium-dependent exocytosis. There are four isoforms; -1, -2 and -3 are neuronal while 13-4 is more ubiquitously expressed. They contain multiple domains including calcium-sensing C2 domains and a DAG-sensing C1 domain [272]. Munc13-4 is highly expressed in mast cells, co-localises with secretory granules and overexpression increases β-hexosaminidase release [280, 281]. Munc13s can interact with rabs; interactions with rab27a in T-lymphocytes is required for tethering of vesicles to the plasma membrane[282]. In mast cells, Munc13-4 is a direct partner of rab27a and b [283], it also co-localises and interacts with Doc2α . Mutants lacking the Munc13-4 binding domain in Doc2a have inhibited exocytosis [284]. Mast cells derived from rab27a knockout mice have abnormal cortical F-actin distribution and the rab27b and rab27a/b knockout phenotypes mimic that of the Munc13-4 knockout [285]. These results suggest Munc13-4, with Doc2α and rab27 proteins might act to help dock and tether mast cell granules to the plasma membrane.

Rabs

Rab proteins are a group of more than 60 that regulate vesicle trafficking. As with SNAREs, they are localised to distinct regions within the cell and help to organise and co-ordinate membrane traffic. They are GTPases that alternate between GTP-bound or 'on' and GDP-bound or 'off'' [286]. Rabs are important for recruiting effectors that allow for vesicle movement along the cytoskeleton, vesicle tethering and vesicle un-coating [287]. The potential function of rab27 proteins in mast cells has already been discussed and is of key importance in mast cell granule exocytosis [288], Rab 5a, an endosomal rab, has been implicated in regulation of FcεRI cell surface expression in BMMCs [289]

1.4 Tools for monitoring exocytosis

1.4.1 FM dyes

Many optical methods exist to monitor exocytosis, they have proven key in developing understanding of this process. FM dyes have been used to monitor exocytosis and endocytosis for almost twenty years. FM dyes are styryl dyes that have a lipophilic tail and a cationically charged head, linked via a double or triple bond bridge, termed the nucleus [290]. The head is an important determinant of the dyes ability to penetrate membranes, cationic dyes are the most useful for studies of exocytosis as these render the dye membrane impermeable [291]. The nucleus region determines the fluorescent properties of the dye. One of the most widely used styryl dyes is FM1-43. Cell membranes can be loaded with the dye and the cells stimulated, upon compensatory endocytosis the dye is internalized and new secretory vesicles become stained with the dye. Then upon stimulation, dye loss can be used to monitor exocytosis[292].

1.4.2 Acridine Orange

Acridine orange is a fluorescent cationic dye. The molecule exhibits pH sensitivity such that it can become trapped in the acidic compartments of secretory granules due to protonation. When the dye becomes de-protonated it becomes membrane permeable and so upon granule pH increases it would subsequently leave the

granule. Acridine orange also shows a concentration-dependant red shift [293] in fluorescence. These two properties can be used to monitor activation. Acridine orange can be loaded into secretory granules where it will accumulate and fluoresce red. Upon stimulation, the granule will alkalize, the dye leak out and there will be a burst of green fluorescence as the dye diffuses out[294]. The problem with this technique is targeting of the dye to other acidic compartments resulting in no selectivity for SGs.

1.4.3 pH sensitive fluorescent proteins

An alternative way of studying exocytosis is to use cells transfected with a pH-sensitive fluorescent construct. Termed pHluorins, these proteins were formed through the mutation of the green fluorescent protein (GFP) molecule rendering them sensitive to pH [295]. There are two forms, ratiometric and ecliptic. In ratiometric pHluorin, the fluorescence intensity at one excitation wavelength (395nm) decreases with acidic pH changes while excitation at 475nm increases, both have an emission maximum of 509nm. The ratiometric form has been a useful tool in monitoring the pH of cellular compartments and for studying endocytosis. Using the ecliptic form it becomes difficult to ascertain whether loss of signal is due to the tagged proteins being taken up into acidic vesicles or if the protein is being degraded [296]. The ecliptic form is however, ideal for visualising exocytosis. Its fluorescence is quenched in acidic pH environments, such as those encountered in resting vesicles (pH 5.6). These proteins can be tagged to the intravesicular domains of vesicle proteins, such as VAMPs. Upon fusion of these vesicles with the plasma membrane the extracellular solution mixes with the vesicular solution, this results in the pHluorin becoming exposed to more alkaline pH. This leads to de-quenching of the molecule and the resulting increase in fluorescence can be measured. More recently a new pH sensitive protein has been developed; a variant of dsRED termed mORANGE [297]. This has been used to perform dual-colour imaging and allows for the study of trafficking behaviours of multiple vesicle pools. For example one group has identified a distinct pool of vesicles defined by Vti1a that maintains spontaneous neurotransmitter release, using dual colour confocal imaging of pHluorin and mORANGE [298].

1.4.4 Fluorescent false neurotransmitters

Overexpression can often lead to miss targeting of proteins and these experiments are impossible to perform in cells refractory to transfection. Recently production of a novel dyes, termed fluorescent false neurotransmitters have led to an alternative means of effectively monitoring exocytosis in many cell types using fluorescent based assays. Fluorescent false neurotransmitter 511 (FFN511) and mini 202 are two optical probes that have recently been developed [299, 300]. These molecules are similar in structure to monoamines such as dopamine but have an additional aromatic moiety that gives the molecule enhanced fluorescent properties. They take advantage of the fact that VMATS are only fairly selective, less so than plasma membrane transporters. FFN511 is lipophilic enough to be passively transported across the plasma membrane, whereby it can then be loaded into secretory vesicles through the action of VMATS. FFN511 can be loaded into primary chromaffin cell dense core vesicles and upon stimulation of exocytosis the release of the dye measured through total external reflection fluorescence microscopy [299].

1.5 Botulinum neurotoxins

1.5.1 Structure and mechanism of action

BoNTs are clostridial neurotoxins produced by Clostridium botulinum. There are seven serotypes termed A–G. BoNT's inhibit acetylcholine release at the neuromuscular junction causing paralysis [301, 302]. The structure of BoNT is illustrated in (Figure 1.9). BoNT consist of a heavy chain and a light chain bound together through disulphide bonds. The heavy chain can be subdivided into the Hc and Hn domains that are responsible for the two functions of the heavy chain [303]. The Hc is responsible for the binding to neuronal receptors through a double receptor mechanism; the toxins initially bind to gangliosides present on nerve cell membranes that allow accumulation of the toxin on the plasma membrane. Then, through binding to a protein receptor, the toxin is taken up into the cell through receptor-mediated endocytosis. Different serotypes bind different protein receptors. The specific receptors for four serotypes have been identified so far; BoNT/A binds SV protein 2 (SV2), BoNT/E binds to glycosylated forms of SV2 A and

B, while the binding proteins for BoNT/B and BoNT/G serotypes are syt I and syt II [304, 305]. Stimulation of neurons leads to increased activity of BoNT/A [304] suggesting increases of SV exocytosis leads to exposure of a greater number of receptors available for BoNT to bind to and subsequently be taken up into the cell.

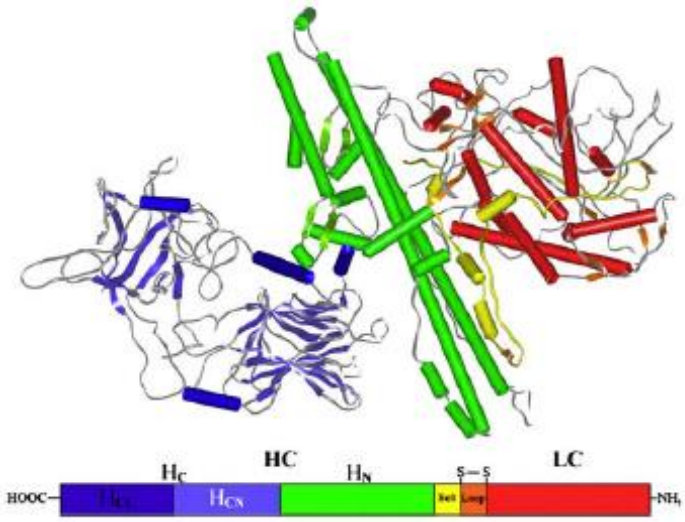

Figure 1.9

The structure of BoNTs

BoNTs are produced as a single peptide that is proteolyticaly cleaved producing a heavy (HC) and a light (LC) chain. The two chains remain associated to each other through a disulphide bridge and non-covalent interactions. The HC is responsible for the binding to surface receptors and translocation of the toxin into a cells cytosol. The HC can be subdivided into the Hc and Hn domains that are responsible for the two functions of the heavy chain [303]. The blue/purple corresponds to the Hc domain of the HC important for neuronal binding. The Hn domain forms a channel in the acid environment of a vesicle to allow the translation of the catalytic domain (red) into the cytosol. [303] Figure adapted from Brunger and Rummel 2009.

Once the toxin has been endocytosed, in the low pH environment of a vesicle, the toxin undergoes a conformational change that allows membrane insertion. The Hn domain forms a channel on the vesicle membrane that allows the light chain, LC to pass into the cytosol and there it cleaves its target, the SNARE proteins. The LCs of BoNTs are Zn^{2+} requiring endopeptidases that cleave neuronal SNAREs with high specificity to inhibit acetylcholine release. Different serotypes cleave different neuronal SNARE proteins (Figure 1.10). Subtypes B, D F and G can cleave VAMPs 1, 2 and 3 with varying affinities. BoNT B, D and F surprisingly have been found to have a higher affinity to the non-neuronal VAMP-3 than VAMP-1 or 2, in fact BoNT D has a much lower affinity to VAMP-1 due to a single substitution of a Met with Ile at

residue 48 [306]. BoNT/A and /E cleave SNAP-25 whereas BoNT/C can cleave both SNAP-25 and syntaxin 1[307].

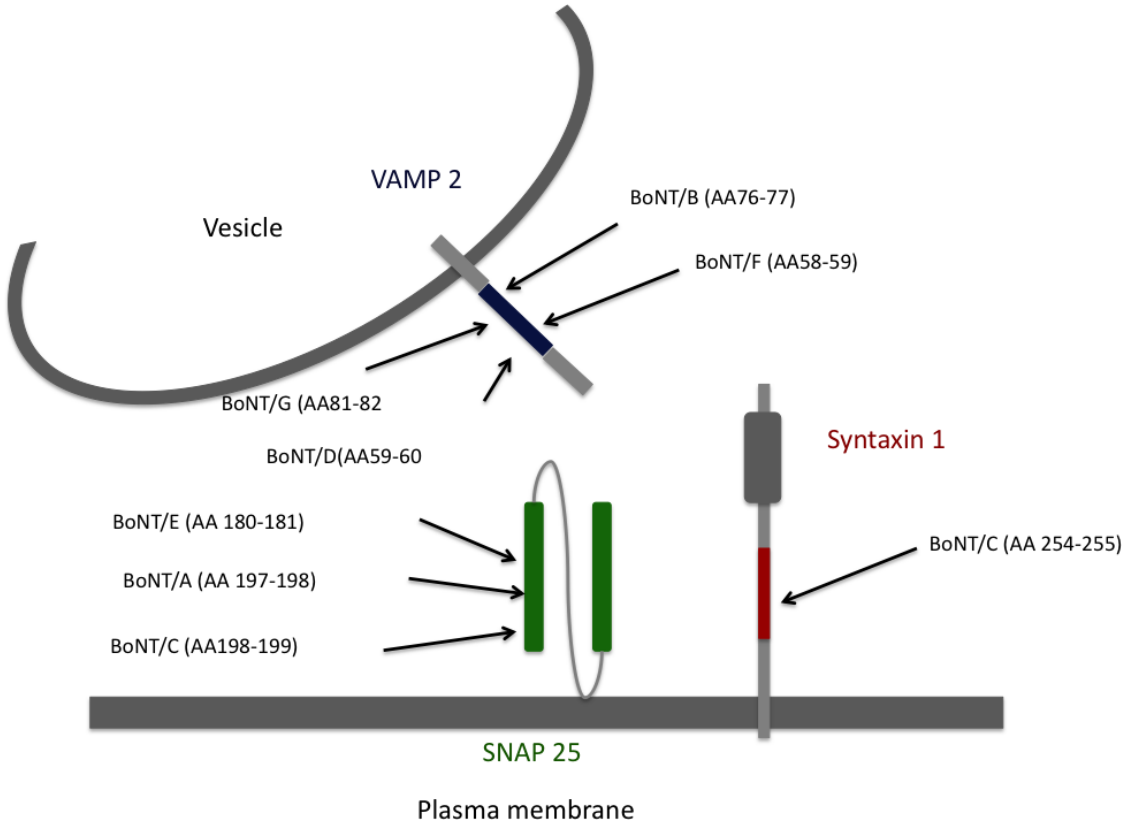

Figure 1.10
Cleavage sites of the BoNT serotypes

BoNT/A and BoNT/E cleave SNAP25 at different sites, both cleave at the C-terminal but BoNT/A cleaves 9 amino acids of SNAP-25 while BoNT/E cleaves off 17[308]. This leads to differences in the duration of action; BoNT/A has a longer duration of action because it can still form a SNARE complex and so is stabilized despite it being nonfunctional. BoNT/E cleaved SNAP-25 cannot form the SNARE complex and so becomes removed much more rapidly leading to a shorter duration of action [309]. Expression of GFP tagged LCs in PC12 cells has shown BoNT/E has a more cytoplasmic localisation as opposed to BoNT/A LC, which was present in puncta on the PM. This might mean BoNT/E is more accessible to degradation pathways than BoNT/A and might contribute to the shorter duration of action [310].

BoNT subtypes can be further differentiated into toxin variants; variability within subtypes can be as much as 31.6% [311]. There are four known BoNT/A variants, A1-4, and although all have highly conserved structures there are some notable differences. For example there is only 76% conservation between the LC of

subtypes 3 and 4 [312]. BoNT/E has 6 subtypes described [313], but despite most variations in the subtypes occurring in the catalytic and binding domains, the Zinc domain required for protease activity and the receptor-binding motif are conserved across the subtypes [313]. As with BoNT/A and BoNT/E, BoNT/B and /F have many subtypes described [314, 315] BoNT/F5 has a highly divergent LC but can still cause botulism and so is most probably active [314]. The functional implications of all these variants have yet to be fully determined, but the large number and surprising diversity within serotypes suggest some might be found.

1.5.2 BoNT modification – avenues for novel therapeutics

The high specificity of the BoNT receptor binding and SNARE cleavage limits their use therapeutically. Recent work has been focused on modifying the targeting and substrate specificity of these toxins to widen their therapeutic potential. A fragment of BoNT/A containing just the LC/Hn still has the ability to form permeable channels and has catalytic activity, but cannot bind neurons as it lacks the Hc domain. [316, 317]. Duggan et al [318] utilised a modified form of this construct conjugated to a lectin to switch the neuronal specificity to nociceptive spinal neurons [318]. Reduced sensory transmission was measured confirming the potential of retargeting BoNT for treatment of chronic pain. Further work identified calcitonin gene-related peptide (CGRP) release in trigeminal ganglionic neurons, a key mediator of inflammatory pain, being mediated by a cleavable SNARE protein [319], VAMP-2. Treatment with BoNT/D reduced calcitonin gene related peptide (CGRP) release. BoNT/A also inhibited release of CGRP but only upon release evoked by K+ depolarization not TRPV1; this is due to TRPV1 causing a more prolonged increase in calcium influx, whereby pre-fusion complexes of syntaxin/SNAP-25 and VAMP are destabilised by BoNT/A and as a result the probability of full fusion is reduced so that only a prolonged calcium influx can stimulate exocytosis. BoNT/E had no effect on release as it can't bind; they express SV2C rather than A or B but it allows binding of BoNT/A. BoNT/E cleaves a larger number of residues from SNAP-25 than BoNT/A [320]. Combining the catalytic domain of serotype E with the binding domain of type A was postulated to allow entry of the BoNT/E LC into trigeminal ganglionic neurons and block CGRP release by all stimuli. A chimera termed chimera E/A containing BoNT/A HC with BoNT/E

LC was able to enter trigeminal ganglionic neurons and block TRPV1-mediated CGRP release [321]. This gave proof of principle that the serotype E toxin, as with serotype A, can be re-targeted to other neuronal targets.

The results so far have shown the potential for the toxins to be retargeted to different neuron subtypes. Foster et al were able to re-engineer the specificity of BoNT to a non-neuronal target [322]. Here the LC/Hn domain of BoNT/C was coupled with epidermal growth factor to create a novel chimera. This construct was able to inhibit mucin secretion from A549 cells in a concentration-dependent manner through cleavage of syntaxin1. One key limitation still apparent with all these modified forms; they could only target neurons, or non neuronal cells utilizing the neuronal SNARE proteins SNAP-25, VAMP-1/2/3 or syntaxin 1.

To extend the therapeutic potential of the toxins beyond a limited number of targets, modification of the LC is required to switch substrate specificity to non-neuronal SNAREs. This has recently been achieved by a group using a modified form of the LC of BoNT/E [323]. Introduction of a single point mutation in LC/E was able to alter its substrate specificity to enable the modified toxin to cleave both its endogenous SNARE substrate SNAP-25 and SNAP-23. This modified toxin was shown to inhibit TNF-α induced mucin and IL-8 secretion when transfected or permeablised into HeLa cells. It has also been suggested that serotype F might be re-targeted to VAMP-7 through the removal of negative charged amino acids 315 and 310 and exchanging Arg133 [324].

These sets of experiments have allowed for a greater understanding of the workings of the BoNT. Altering BoNTs' cell targeting and substrate specificity to inhibit secretion in non-neuronal cell types provides a novel therapeutic potential. SNAP-23 is likely to be ubiquitously expressed in non-neuronal cells, therefore using a modified form of BoNT/E LC could have potential toxic effects. With SNAP-23 being a major constituent of membrane trafficking in non-immune cells, targeting this SNARE with a BoNT will no doubt show numerous off target effects and so care would have to be taken if pursuing this route. Targeting to specific cells types may circumvent this problem. The studies discussed above have proved that chimeras of BoNT containing modified HCs can be retargeted to non-neuronal cells. Combined

with altered substrate specificity, this could provide a powerful therapeutic tool. The hyper secretion seen in mast cells in chronic inflammatory disease would place these cells as optimal targets for a modified toxin. Their expression of peptide receptors could be utilised as an entry point for a modified toxin while a modified LC could be used to cleave the potential SNAREs involved with mediator release.

Thesis aims:

The aim of this study is to identify and characterise the SNARE proteins expressed in human mast cells using the LAD 2 mast cell model and primary HLMCs. New assays will be developed to do this and used to assess the potential for therapeutically targeting the release of chronic inflammatory disease by targeting SNARE proteins with BoNTs.

Chapter 2: Materials and Methods

2.1 HEK293 cell line

Human embryonic kidney (HEK) 293 cells are a commonly used cell line derived from transformed human embryonic kidney cells in Alex van der Eb's laboratory. Cells were cultured in DMEM/F12 media (Gibco Cat: 31331-028) supplemented with 10% foetal calf serum (FCS) and maintained at 37ºC in a humidified atmosphere of 5% CO_2 incubator. Cells were split upon reaching confluency (twice weekly) using cell dissociation solution (CDS) (Sigma Cat: C5914) followed by centrifugation at 110g for 4 minutes. Cells were resuspended in new media and 1/5 of the total cell number seeded onto a new 25cm^2 Nunclon^{tm} surface tissue culture flask.

2.2 LAD 2 mast cell line

LAD 2 mast cells, derived from a patient with mast cell leukemia, were a kind gift from Dr. D Metcalfe (National Institute of Allergy and Infectious Diseases, National Institutes of Health, Bethesda, MD). The cell line is described in more detail in section 1.1.2

2.2.1 LAD 2 cell culture

Cells were cultured in StemPro-34 SFM serum-free complete medium (Invitrogen Life Technologies), supplemented with StemPro-34 nutrient supplement (supplied as 40X solution) and 2mM L-glutamine (Gibco Cat: 25030-032), making up "Total media". 100ng/ml rhSCF. (R&D, Abingdon, UK) was added at weekly intervals from frozen aliquots of a 100µg/ml PBS with 0.1% Bovine Serum Albumin (BSA) (Sigma cat: A7906) solution. Cells were maintained at a density of 200,000 to 500,000 cells/ml and were diluted with the appropriate amount of full media. Cells were maintained at 37^{0}C in a humidified atmosphere of 5% CO_2 incubator.

To obtain frozen stocks of LAD 2 cells, 10 million cells were centrifuged at 100g and resuspended into 1.5ml of PZerve cryopreservative (Protide pharmaceuticals) supplemented with 200ng/ml rhSCF as described in [88]. Vials were place into a cryocontainer for 30 minutes at room temperature, 1 hour at -20^{0}C and 1 hour at -80^{0}C before being placed into liquid nitrogen for long-term storage. For thawing, cells were removed from liquid nitrogen and 1.5ml total media was added containing 100ng/ml rhSCF at room temperature. Cells were transferred to a 6 well plate and rocked at room temperature for 6 hours, with large clumps of cell debris being removed by pipette. After this period cells were transferred to 75cm^2 tissue culture flasks and placed at 37^{0}C in a humidified atmosphere of 5% CO_2 incubator.

2.3 HLMC

HLMCS were obtained from non-lesional tissue from lung resections of lung cancer patients following surgery, in collaboration with Dr Peter Peachell, Department of Infection and Immunity, University of Sheffield. The provision of lung tissue and the use of the tissue in this study were approved by the National Research Ethics' Committee.

2.3.1 HLMC Isolation and Purification

All steps were carried out in aseptic conditions. Lung tissue was cut into small pieces using scissors and tweezers and placed onto 100µm nylon gauze placed over a beaker. The tissue was washed with Dulbecco's modified eagle medium (DMEM) (Gibco Cat: 32430-027 this type of DMEM was used for all HLMC work using DMEM) + 2% heat inactivated FCS (Gibco cat: 10108) before being placed into a new beaker and chopped into a pulp using scissors, when the tissue was sufficiently chopped it was placed into fresh 100µM gauze and washed twice in DMEM + 2% FCS. The tissue was subsequently stored overnight at 4^{o}C in a sterile screw top container containing 4ml of DMEM + 10% FCS + 1% antibiotic/antimycotic solution (containing 10 units/ml penicillin, 10 units/ml streptomycin and 25µg/ml amphotericin B) + 1% MEM non-essential amino acids (NEAA) (Gibco Cat: 11140-035) per 1g of tissue.

The next day tissue was equilibrated to room temperature and lung tissue digested using 37.5mg hyaluronidase (Sigma) and 50mg collagenase type 1A (Sigma) per 10g tissue for 90 minutes at 37^{o}C with stirring. After this time point the tissue was forced through a 50ml syringe at least 30 times to liberate cells. The pulp was then filtered three times through 100µM gauze with DMEM + 2% FCS and the filtrate collected in 50ml falcon tubes. The filtrate was washed three times by spinning cells at 160g, 4^{o}C for 8 minutes, the supernatant being removed after each spin and cell being resuspended with fresh DMEM + 2% FCS. At this stage 5µl of cells were taken out and placed with 45µl Kimura stain to count the number of mast cells present. Kimura stain consisting of 0.05% Toluidine blue solution, 0.03% Light green, Saponin saturated in 50% ethanol, 0.067M/6.4pH Phosphate buffer. After the last wash the mixed population of cells were resuspended into 2ml cold Hanks balanced salt solution (HBSS) (Gibco Cat: 14170)/FCS placed into a screw top 2ml eppendorf and incubated at 4^{o}C on a roller for 30 minutes to block cells to ensure minimal non-specific binding of mouse anti-c-kit antibody (mAb YB5.B8).

The remaining procedures were carried out with solutions at 4^{o}C. HLMCS were purified using immunoaffinity magnetic selection. Anti-mouse IgG1 Dynabeads® coated with mouse anti-c-kit antibody (mAb YB5.B8) were used to positively select CD117-expressing HLMCS.

After blocking, 20ml HBSS +2% FCS was added to cells and cells filtered through 70µm bottle top filter into a 50ml falcon tube. The filter was subsequently washed to retain as many cells as possible up to the volume of 50ml. Cells were pelleted by centrifugation (160g 4^{o}C for 8 minutes). Cells were resuspended into 1ml HBSS/FCS, transferred to a screw top 2ml eppendorf and dynabeads added at the appropriate concentration (5:1 ratio beads to mast cells). Cells were incubated with the coated beads for 1h 30 minutes at 4^{o}C with rolling. After incubation cells were transferred to a 15ml falcon tube containing 10ml HBSS + 2% FCS and placed into a magnetic field for 3 mins to allow beads, with mast cell attached, to collect at the side of the tube. Supernatant containing other cell populations was removed by pipetting and mast cells attached to side of tube were subsequently resuspended into fresh HBSS +2% FCS. The process was repeated two more times. After the final

wash cells were suspended into culture media (see HLMC culture) and counted for a second time and placed into a Nunclon^{tm} surface tissue culture flask with the concentration of mast cells adjusted to 10^6/ml. Figure 2.1 gives an overview of the mast cell purification process.

2.3.2 Antibody Coating of Dynabeads

100µl of beads were placed into 10ml HBSS + 2% FCS and washed twice in a magnetic field using the same process as for mast cell washing in 2.3.1. Beads were resuspended into 400µl HBSS/FCS and transferred to a screw top 2ml eppendorf, 8µl (10µg/ml) of mouse anti-c-kit antibody was added to mix. The beads were left to incubate with the antibody for 2 hours on a roller at 4^{o}C. After this time the beads were washed three times in HBSS + 2% FCS and resupended into 100µl HBSS/Protein and stored 4^{o}C until use, typically 24hours or they were coated on the day.

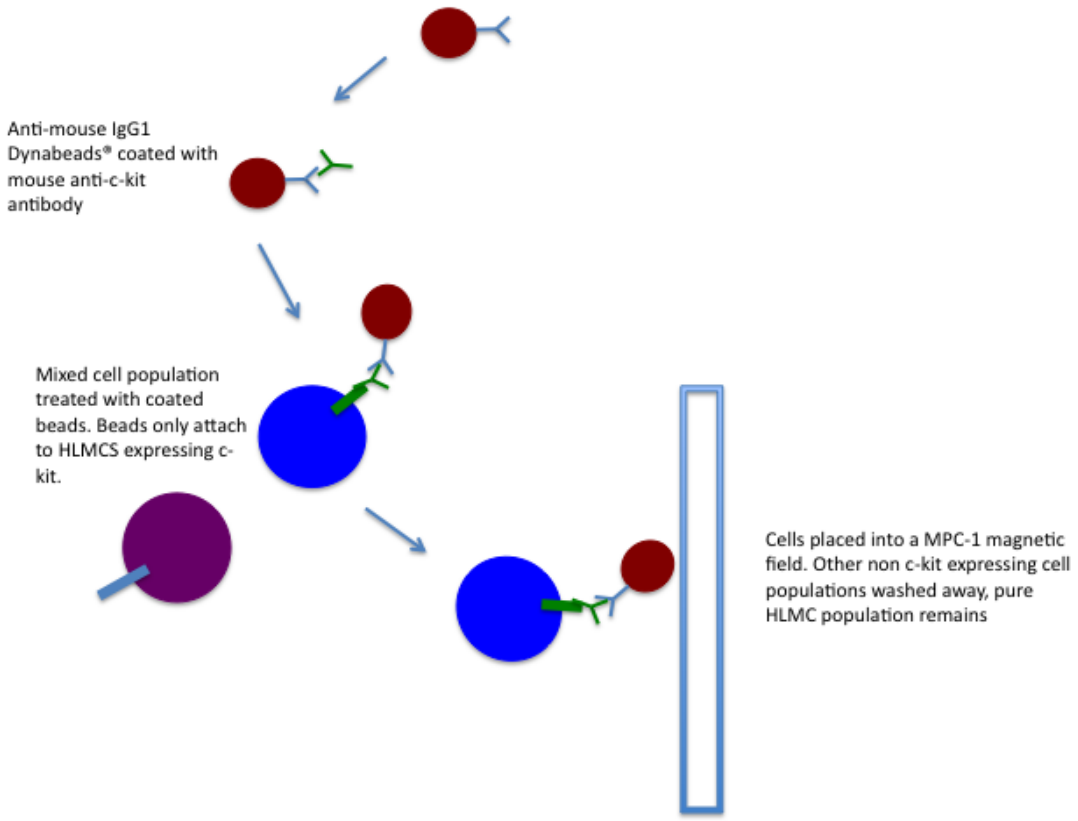

Figure. 2.1

Purification procedure for HLMCS

Anti-Mouse IgG1 Dynabeads (red) are coated with mouse anti-c-kit antibody (green) and subsequently incubated with a mixed population of cells, containing HLMCS (blue). Beads bind to the c-kit expressing HLMCS and a magnetic field is applied by placing a tube containing the cells next to a magnet. HLMCS are purified from the mixed population of cells by being held by the magnetic field as other cells are washed away.

2.3.3 HLMC culture

HLMC were cultured in DMEM containing 1% antibiotic/antimycotic solution (Gibco), 1% NEAA and 10% FCS. Cytokines in a PBS 0.1% BSA solution were added on a weekly basis at the following final concentrations: 100 ng/ml SCF, 50 ng/ml IL-6, and 10 ng/ml IL-10 (all from R&D systems). Cells were maintained at 37^0C in a humidified atmosphere of 5% CO_2 incubator.

2.4 Polymerase Chain reaction (PCR)

Primer Sequence	Product Size	Gene
TGCCTCTGGGATCATCATGG	239	Syntaxin 1a F
ACTTGACGGCCTTCTTGGTG		Syntaxin 1a R
TTGAGACGAGGCACAATGAG	115	Syntaxin 1b F
ATGCGGTCAATCATCTCTCC		Syntaxin 1b R
TGCTGTCTCGGAAGTTTGTG	120	Syntaxin 2 F
CTGTGGTGGTTCTCCCAGTT		Syntaxin 2 R
GAGCCAAAAACCAAGGATGA	191	Syntaxin 3 F
TTG GTCATCACCTCCACAAA		Syntaxin 3 R
CAGAAGGAGGAAGCTGATGA	263	Syntaxin 4 F
TGCGTGTCCTTCAGGATATT		Syntaxin 4 R
TCATCTGTGCAGGCATTAGC	152	Syntaxin 6 F
TGCTGCTCCTCAATGAAATG		Syntaxin 6 R
GTACGAGGAGAATCCTGGGT	187	SNAP-23 F
CAGACACAAAGGCCACAGCA		SNAP-23 R
TCAGGACTTTGGATGTTGGA	479	SNAP-25 F
CAGCATCTTTGTTGCACGTT		SNAP-25 R
GTAACAGGAGACTGCAGCAG	179	Vamp 2 F
TTTGCGCTTGAGCTTGGCTG		Vamp 2 R
GAAGCTCTCTGAGTTAGACG	174	Vamp 3 F
GAGACAACCCACACGATGAT		Vamp 3 R
CTTCCTGGAGGTGACAGAGC	150	Vamp 7 F
CGGGAACGTTCAAAATCATC		Vamp 7 R
GTGCGGAACCTGCAAAGTGA	261	Vamp 8 F
GAAGGCACCAGTGGCAAAGA		Vamp 8 R
CTTTGGAGTTGGTTTTGC	301	VMAT 2 F
GCAGTTGTGATCCATGAG		VMAT 2 R
CTGAAGGAGGGGAGAGC	553	VMAT 1 F
GGGCCACAAAGAGTAGAGT		VMAT 1R
ATATCGCCGCGCTCGTCGTC	583	Beta Actin F
TAGCCGCGCTCGGTGAGGAT		Beta Actin R

Figure. 2.2

Primers used for RT-PCR

Primer sequences of SNAREs from human syntaxin 1a through to SNAP-23 were taken from [239]. Syntaxin limited supplied SNAP-25 primers. VMAT primers are described in [325]. All primers were tested using Basic Local Alignment Search Tool (BLAST) to ensure the correct gene product was detected before use. Primers were dissolved into nuclease free H_2O to 100µM and stored at -20^{0}C. Working stocks were made by adding 10µl of primers to 490µl nuclease free H_2O.

500,000 LAD 2 cells were centrifuged at 100g, 4mins at room temperature. Pelleted cells were washed once in PBS and centrifuged again using the same parameters.

Total RNA was extracted from cultured LAD 2 cells using a RNeasy Kit (Qiagen) according to manufacturers' instructions and after extraction into RNase free H_2O, RNA was stored at -80^{0}C. 1µg RNA was subsequently transcribed into cDNA using iScript™ cDNA synthesis kit (Bio-Rad). As a negative control H_2O was added in equivalent volumes to reverse transcriptase (-RT). RNA quantity and quality was measured using a nanodrop (Thermo-scientific). The ratio of 260nm/280nm absorption was monitored to assess RNA quality and only RNA with ratios between 1.8-2.0 was used.

The reaction was carried out using a Mycycler thermo cycler (BioRAD) with the following protocol: 25^{0}C for 5mins, 42^{0}C for 30mins, 85^{0}C for 5 mins and then a holding temperature of 10^{0}C. The reverse transcription product was used for PCR.

2.4.1 PCR reaction

PCR reaction mix consisted of: 10X Taq polymersase buffer 2.5µl, 2mM dNPT, 2.5mM $MgCl_2$ 1µl, H_2O 12.5µl, Taq Polymerase (New England Biolabs) 0.5µl, cDNA 1µl, Forward Primer 2 pmol/ml, Reverse Primer 2pmol/ml

For SNARE primers, 35 cycles of (94^{0}C 30s, 60^{0}C 45s and 72^{0}C 35s) were performed and a final hold of 10^{0}C.

For VMAT 1 and 2 primers, 40 PCR cycles after initial denaturing at 94^{0}C 2mins of (300C s 54, 72^{0}C 1 min and 94^{0}C 30 s).

2.4.2 Gel electrophoresis

For analysis, all PCR products were run on a 1% agarose gel containing 0.5µg/ml ethidium bromide. Bands were visualized using a UV transilluminator (UVP).

2.5 Quantitative (Q) PCR

2.5.1 QPCR primer design and testing

Primer Sequence	,	Primer Name
GCGCAAATACTGGTGGAAAA	,	Vamp 2 F
CTCCTCGGGGATTTAAGAGC	,	Vamp 2 R
GCCACTGGCAGTAATCGAAG	,	Vamp 3 F
TGCACGGTCGTCTAACTCAG	,	Vamp 3 R
CAAACATGCTTGGTGTGGAG	,	Vamp 7 F
AAATTAAAGGCTCGGGAACG	,	Vamp 7 R
ACTTGGAACATCTCCGCAAC	,	Vamp 8 F
CTTCCACCAGAATTTCCGAG	,	Vamp 8 R
CTGAAATCTCTGGCCTCACC	,	Vamp 2 F p3
CCAGCAAGTCCCATACACAC	,	Vamp 2 R p3
GAGGCACTGAGGGAGAAAGA	,	Vamp 3 F p3
AATGGAAGCTGTGTCCTGGT	,	Vamp 3 R p3
GGCCAAGCTGTGTGAAGAA	,	Vamp 7 F p3
TAAACCTGGAGGCATGGAAC	,	Vamp 7 R p3
CATCTCCGCAACAAGACAGA	,	Vamp 8 F p3
TGGGAGAGGTTCCCTGTTACT	,	Vamp 8 R p3

Figure. 2.3

Primers used for QPCR experiments.

Primers testing was performed to select optimal conditions for the QPCR reaction, 2 primer pairs for each gene were tested. One set was designed using primer3plus tool (http://www.bioinformatics.nl/cgi-bin/primer3plus/primer3plus.cgi/) the other primer sets were used from previously designed sequences deposited in primerdepot (http://primerdepot.nci.nih.gov/). All primers were tested using Basic Local Alignment Search Tool (BLAST) to ensure the correct gene product was detected before use. Forward and reverse primers were designed to have similar melting temperatures (Tms), the maximum 3' self-complementarity was set to 1 in primers designed through primer 3 plus (Only one complementary base between the forward and reverse primers) to reduce the chance of primer dimers. The maximum allowed length of a mononucleotide repeat was 3.

Total RNA was extracted from cultured LAD 2 cells (500,000 cells) and cDNA produced in the same process as for section 2.4. 1µg of RNA was used for each cDNA reaction.

2.5.2 QPCR reaction mix

2XSensiMix SYBR reaction mix (Bioline) containing SYBR®Green 5µl, cDNA 1µl, Forward/reverse primer mix 1µl (100ng/µl), H_2O 2.6 µl.

The PCR reaction was run on a Rota-Gene 6000 real time PCR machine (Qiagen). Each primer set was tested at three different annealing temperatures (59^{0}C, 59.5^{0}C and 60^{0}C) with 6 repeats for each temperature and 2 non-template controls, replacing cDNA with H_2O to ensure no reagent contamination. The subsequent cycle and melt curves were used to determine reliability and specificity of the primers (Figure 2.4).

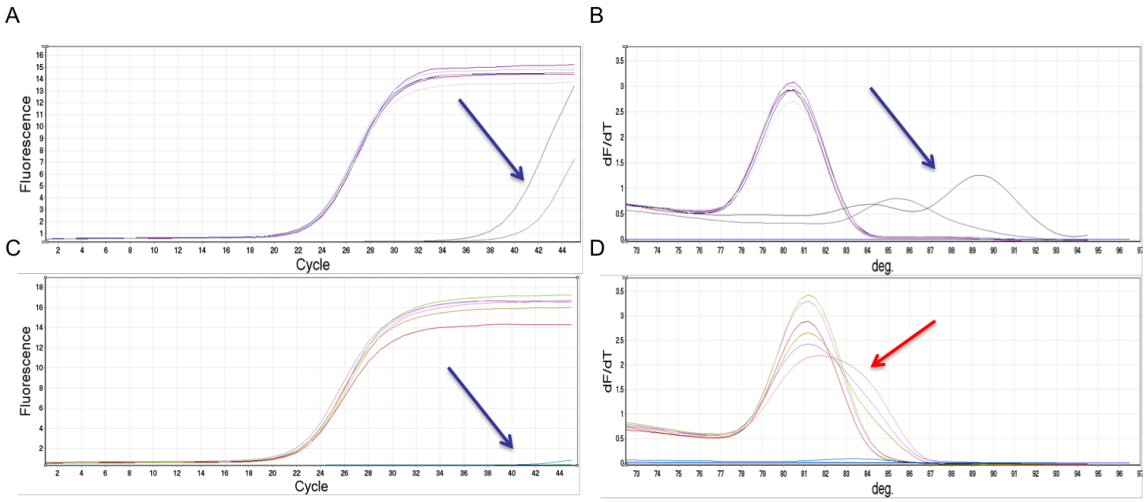

Figure. 2.4

VAMP-3 primers cycle and melt curves

Graphs show example results of qPCR primer testing, in this case for VAMP-3 primers at 60^{0}C. VAMP-3p3 showed greatest specificity and was used for QPCR experiments. VAMP-2, VAMP-7 and VAMP-8p3 primers at this annealing temperature were also used as they showed similar specificities. **A** and B. VAMP-3p3 primer cycle and melt curves respectively. C and D VAMP-3 primer cycle and melt curves respectively. Each line represent each repeat. Blue arrows point to non-template controls. Red arrow points to different sizes amplicon for the VAMP-3 primer.

The cycle curves (figure 2.4) show the increase of the PCR product through each PCR cycle by gain in fluorescence. SYBR® Green is a fluorescent dye that binds to

the minor groove of the DNA double helix and fluoresces strongly when bound to double stranded DNA. As the PCR product is produced the amount of double stranded DNA increase and so the fluorescence increases. This allows measurement of the amount of amplicon produced, which is exponential. In the control experiments ideally all the cycling curves would be very close together for all 6 repeats, giving a consistent readout for the amount of product. As the temperature is increased after the reaction, through the dissociation temperature, the dsDNA is broken down and the fluorescent signal decreases. The maximum point at which fluorescence is lost is the Tm (melting temperature), this is shown on the melt curves (figure 2.4). Different sized amplicons have different Tms and so the specificity of the primers, and the presence of dimers, can be determined by looking for only a single peak on the melt curve for all 6 repeats (multiple or misaligned peaks would imply multiple or different sized amplicons are being produced). An example of the process is show in Figure 2.4 for the VAMP-3 primers at 60^0C annealing temperature, this process was performed for all four VAMPs used. VAMP-2 and VAMP-7 primers from primer depot while VAMP-3 and VAMP-8 primers from primer3plus were found to have the highest specificity and consistency and so were used in future experiments. The optimal conditions that produced single products for all four primer sets used are shown in Figure 2.5. The primer sets chosen were: VAMP-2, Vamp3p3, VAMP-7, VAMP-8p3.

Cycle		Cycle Point
Hold @ 95°c, 10 min 0 secs		
Cycling (45 repeats)	Denaturation	Step 1 @ 95°c, hold 10 secs
	Annealing	Step 2 @ 60°c, hold 15 secs
	Extention	Step 3 @ 72°c, hold 25 secs, acquiring to Cycling A([Green][1][1])
Message	Melt (72-95°c) , hold secs on the 1st step, hold 5 secs on next steps, Melt A([Green][1][1])	

Figure. 2.5

QPCR cycling protocol.

Step one denotes denaturation step where double stranded bonds are broken to produce single stranded DNA. Step two is the annealing step where primers bind to specific DNA sequences. The extension step is where Taq polymerase adds DNA nucleotides making two double stranded molecules from each one double stranded molecule that was denatured.

To quantify the levels of expression of each gene, levels were normalized to U1 a sn(small nuclear)RNA. This has been shown to be more stable in its expression than other more widely used normalisers such as GAPDH [326]. For every reaction a non-template control was used to show there was no cross contamination. For experiments comparing LAD 2 with HEK SNARE expression levels, –RT controls were also used to rule out DNA contamination. Due to limits on the number of wells for the stimulation experiments –RT controls couldn't be used. However, primers designed from primer3plus were made so to span introns so any DNA contamination could be detected and RNA was treated with DNAse (Qiagen) to remove DNA.

For stimulation experiments 500,000 LAD 2 cells were placed into 12 well plates at 500,000/ml and incubated overnight with 300ng/ml Human-IgE Myeloma (Calbiochem) in full media. The next day cells were stimulated with 10μl Anti-Human IgE (Sigma) and 100ng/ml rhSCF for 2, 6 and 12 hours. Cells were collected at these time points and the samples processed as described in section 2.5.2.

2.6 Microarray

The microarray was performed in collaboration with Paul Heath (Sheffield Institute for Translational Neuroscience). Total RNA was extracted from 500,000-cultured LAD 2 and HLMCS using a RNeasy Kit (Qiagen) according to manufacturers' instructions. After extraction into RNase free H_2O, RNA was stored at -80^{0}C. The microarray chip used was an Agilent SurePrint G3 Gene Expression 8X60K one-colour microarray system. The system was chosen as it enables estimation of absolute levels of gene expression between arrays. Only a single dye is used to label RNA and so data collected represents absolute values.

Microarray experiments were performed by Paul Heath. Data was extracted through Agilent feature extraction software and the data processed further using excel. To compare values across arrays each data set were normalised to the 75th percentile intensity of all non-control probes, as per manufacturer's instructions.

2.7 Antibodies table

Name	Type	Species	WD immuno	WD Blotting	Company/Cat No
Secondary Antibodies					
Anti-Mouse IgG peroxidase	Polyclonal	Goat	-	1 in 1000	Sigma A4416
Anti-Rabbit IgG peroxidase	Polyclonal	Goat	-	1 in 1000	Sigma A6154
Anti-Rabbit Alexa Fluo 488	Polyclonal	Goat	1 in 1000	-	Invitrogen A111 034
Anti-Mouse Texas red	Polyclonal	Goat	1 in 300	-	Jackson
Primary Antibodies					
VAMP 2	Monoclonal	Mouse	-	1 in 1000	S.Systems A104 211
VAMP 3	Polyclonal	Rabbit	1 in 100	1 in 500	A.Peden
VAMP 7	Monoclonal	Mouse	-	1 in 1000	A.Peden
VAMP 7	Polyclonal	Rabbit	1 in 50	-	A.Peden
VAMP 8	Polylconal	Rabbit	1 in 100	1 in 500	A.Peden
SNAP 23	Polyclonal	Rabbit	1 in 100	1 in 500	S.Systems 111 202
SNAP 25	Monoclonal	Mouse	-		S.Systems
Tryptase	Monoclonal	Mouse	1 in 100	-	Dako M7057
VEGF	Monoclonal	Mouse	1 in 100	1 in 500	Abcam ab1316
GFP	Polyconal	Rabbit	1 in 500	1 in 5000	Invitrogen A111 22
Alpha-Tubulin	Monoclonal	Mouse	-	1 in 1000	Sigma T5168
C-myc	Monoclonal	Mouse	1 in 100	1 in 1000	Sigma M5546
Rab 11	Monoclonal	Mouse	1 in 50	-	BD Bioscience

Table 2.1

Antibodies used for western blot and immunostaining. (WD refers to working dilution).

2.8 Western Blot

2.8.1 Bradford assay

Cell lysate protein concentration was measured using Bradford assay. Briefly 5µl of protein standard of BSA (Sigma) at 0.1-1.4mg/ml were placed into 96 well plate wells other wells contained 5µl of sample. 250µl of bradford reagent (sigma) was added to each well mixed and incubated at room temperature for 10 minutes. Absorbance was measured at 595nm using an Expert Plus Microplate reader (Biochrom Ltd). Concentration of sample was derived from the standard curve produced from absorbance values of protein standard.

2.8.2 Western blot protocol

For western blot lysate preparation 1million HEK and PC12 cells were washed once in cold PBS and subsequently lysed by treatment with lysate buffer, consisting of RIPA buffer (Sigma) and Protease inhibitor cocktail III (Fisher). For LAD 2 cell lysate preparation, cells were centrifuged at 100g for 4 minutes, the supernatant was removed and lysate buffer added at 1ml per 10 million cells. After application of lysate buffer samples were freeze-thawed twice at -20^{0}C and then centrifuged at 20000g at 4^{0}C for 15minutes. Supernatants were removed and stored at either -20^{0}C or -80^{0}C for storage of longer than a week. On day of western blot, laemeli buffer (Sigma) was added to thawed cell lysates in a 1:1 ratio. Samples were then heated at 95^{0}C for 5 minutes and after this time were centrifuged briefly to clear any precipitate from the samples.

10μg of samples were pipetted into stacking gel alongside a pre-stained recombinant protein ladder (Fisher Cat: BP3603-500) inside a Gel tank (Biorad) filled with Running buffer consisting of 250mM Glycine (Sigma), 25mM Tris-base (Sigma) and 0.1% SDS (Composition of SDS gels are described in section 2.8.3). The gels were run at 100mV until a good level of protein separation was achieved determined by separation of protein ladder. Proteins were transferred onto nitrocellulose membranes (Biorad) through wet transfer at room temperature for 40 minutes in transfer buffer (25mM Tris base, 192mM Glycine, 15% methanol). Membranes were subsequently blocked in blocking buffer consisting of TBST (50mM Tris, 150mM NaCl and 0.05% Tween 20 (Sigma) containing 5% non-fat skimmed milk powder for 1 hour at room temperature. After this period membranes were incubated with primary antibodies (see antibody list above) in blocking buffer overnight at 4^{0}C on a rotating platform in heat-sealed plastic. The next day the membrane was removed and washed 3 times for 15 minutes in TBST before incubation with secondary antibodies in blocking buffer for 1 hour at room temperature in heat sealed plastic. Membranes were then washed 3 times for 15 minutes in TBTS and excess liquid removed before being place onto cling film and ELC plus detection reagent (GE Healthcare) was applied for 5 minutes. After this time excess liquid was removed and the membrane transferred to a film cassette. Chemiluminescence film (GE healthcare cat: RPN2132) was exposed to the membrane in the dark and developed using an X-ray developer.

2.8.3 SDS Gels

SDS-PAGE running gel (12%) was made using 2.5ml Tris 1.5M pH 8.8, 200µL 10% SDS, 4ml 30% Acrilamide solution (BioRAD), 50µL 10% ammonium persulphate (APS) solution (Sigma), 5µL TMED and 3.5ml H_2O.

Stacking Gel (5%): 2.5ml Tris 0.5M pH 6.8 (BioRAD), 100 µL 10%SDS, 1.0ml 30% Acrilamide solution, 50µL 10% APS, 10µL TMED, 6.4ml H_2O.

2.9 Coverslip preparation

16mm, thickness number 1 glass coverslips (VWR) were washed overnight in a 95% ethanol 5% acetic acid solution on a rocker before being washed copiously with dH_2O and left to dry on filter paper in glass Petri dishes. Coverslips were autoclaved before use.

HEK 293 cells were plated directly onto coverslips and allowed to adhere overnight before experiments were performed so at the time of fixing they would be 70% confluent. Non-adherent LAD 2 cells were plated onto 0.1% poly-l-lysine hydrobromide (Sigma) coated coverslips. To coat coverslips, Poly-l-lysine was dissolved in sterile H_2O and 150µl, applied to the coverslips in 12 well plates for 30 minutes at 37^0C and after this time were washed in H_2O and dried in sterile conditions. To attach cells to coated coverslips, between 20 to 40µl of cells were placed onto coverslips for 30 minutes prior to flooding with media.

2.10 Immunostaining

Adhered cells were washed in cold PBS and then fixed in PBS containing 4% Paraformaldehyde (PFA) and 4% sucrose by weight (pH 7.4) for 15 minutes. Cells were then washed once in PBS and permeablised in 0.1% triton-x (Sigma) in PBS with 50mM NH_4CL for 10 minutes. Cells were washed once in blocking buffer (0.2% Fish skin gelatine (FSG) (Sigma) and 0.02 % triton-x in PBS) before being blocked for at least 1 hour at room temperature. Primary antibodies were diluted in

blocking buffer and 50µL spotted onto parafilm in a humidified chamber and coverslips containing cells were transferred from 12 well plates face down onto the spots of antibody and left overnight at 4^0C. The next day the coverslips were transferred back to the 12 well plate wells and washed 3 times for 15 minutes in blocking buffer, subsequently cells were incubated with secondary antibodies diluted in blocking buffer again in the humidified chamber for 1 hour room temperature in the dark. Finally coverslips were washed 3 times for 15 minutes in PBS and were mounted onto microscope slides (Fisher) using DAPI-Fluoromount G (Southern Biotech) and sealed with nail polish. Coverslips were stored at 4^oC. Antibody concentrations are described in antibody table (section 2.7)

For stimulation experiments cells were incubated overnight with 300ng/ml Human-IgE Myeloma (Calbiochem) in full media. Cells were then adhered to coverslips and stimulated in 12 well plates with agonist present in 500µL external solution minus BSA for 20 minutes, agonists used are described in the appropriate results section. After this time cells were processed as described earlier in this section.

2.11 Confocal imaging

Coverslips were mounted onto an Olympus FV1000 confocal with SIM-scanner on a BX61 upright microscope and viewed using a 60X oil objective (N.A. 1.42). Samples were illuminated at the required wavelength using 405nm (laser power 2%), 488nm (2%) (argon), 561nm (20 %) lasers. Samples were acquired at a section thickness of 500nm using FV1000 software and analysed using Image J software. Any further analysis and graphing were performed using Prism (GraphPAD software).

2.12 β-hexosaminidase assay

β-hexosaminidase is a lysosomal enzyme present in mast cell granules and is regularly used to monitor mast cell degranulation. β-hexosaminidase catalyse the hydrolysis of -glycosidically linked N-acetylglucosamine and N-acetylgalactosamine residues from a number of glycoconjugates [64]. 4-Nitrophenyl N-acetyl-β-D-

glucosaminide can be used as a substrate to monitor release, where it is converted to 4-nitrophenol by β-hexosaminidase and absorbance can be measured at 405nm to determine enzyme activity using spectroscopy.

LAD 2 cells were incubated overnight with 300ng/ml Human myeloma IgE (Calbiochem). The following day 40,000 LAD-2 cells per well were plated in a 96 well V bottomed plate in 40µl external solution per well and incubated at 37^0C for 10 minutes. Cells were incubated at 37^0C for 5-10 minutes before the addition of agonists; Crosslinking of FcεRI receptor was induced with Anti-Human IgE (Sigma) and cells were then incubated at 37^0C for an additional 20 minutes before being centrifuged (550g, 10mins, 4^0C) and the supernatants removed. Supernatants were incubated with 40µl substrate (2mM final concentration of 4-Nitrophenyl N-acetyl-β-D-glucosaminide diluted in 0.2M citrate buffer for 2 hours at 37^0C (Citrate buffer consists of: 0.2M critic acid and 0.2M sodium citrate pH 4.5). The reaction was stopped by the addition of Tris-HCl buffer (1M Trizma-HCL, pH 9.0) and absorbance at 405nm measured (Expert Plus Microplate reader, Biochrom Ltd). Spontaneous β-hexosaminidase release was determined by the addition of imaging solution only. Total β-hexosaminidase content was determined by the addition of Triton X-100 (0.06%) to lyse the cells. Background readings were determined for later subtraction from wells containing only external solution and substrate. All test conditions were done in duplicate in a single experiment and each experiment repeated a minimum of three passages. Average background values and average spontaneous β-hexosaminidase release values were subtracted from the reading for each well. Release was then expressed as a percentage of the average total β-hexosaminidase content determined from the Triton-treated wells. Results are displayed as mean ±SEM. Significance was assessed using one-way ANOVA of log-transformed data with Tukey post-test.

2.13 Calcium imaging

To monitor intracellular calcium changes fluorescent calcium imaging was used. Fluorescent calcium dyes show a spectral response to calcium binding that allow for the monitoring of changes in intracellular calcium. The dyes can be grouped in a number of ways, one way is whether they are ratiometric or single wavelength [327]. One of the most commonly used ratiometric calcium indicators is Fura-2. AM

ester dyes, such as Fura-2AM, can be passively loaded into cells. Upon entry into the cell the ester is cleaved by esterases and the dye becomes membrane impermeable, this allows non-invasive measurement of intraceullar calcium activity. Fura-2 is ratiometric; this reduces the effects of leakage, and photobleaching. The dye is based on calcium chelators such as EGTA and were developed by Roger Y. Tsien [328]. Figure 2.6 shows the excitation profile of Fura-2 with varying calcium concentrations. Fura-2 has a single emission peak of 510nm but dual calcium dependant excitation peaks (340nm and 380nm). The 340nm signal increases with increasing concentrations of calcium while the 380 signal decreases. The two values can then be recorded as a ratio, which reduces the effects described above.

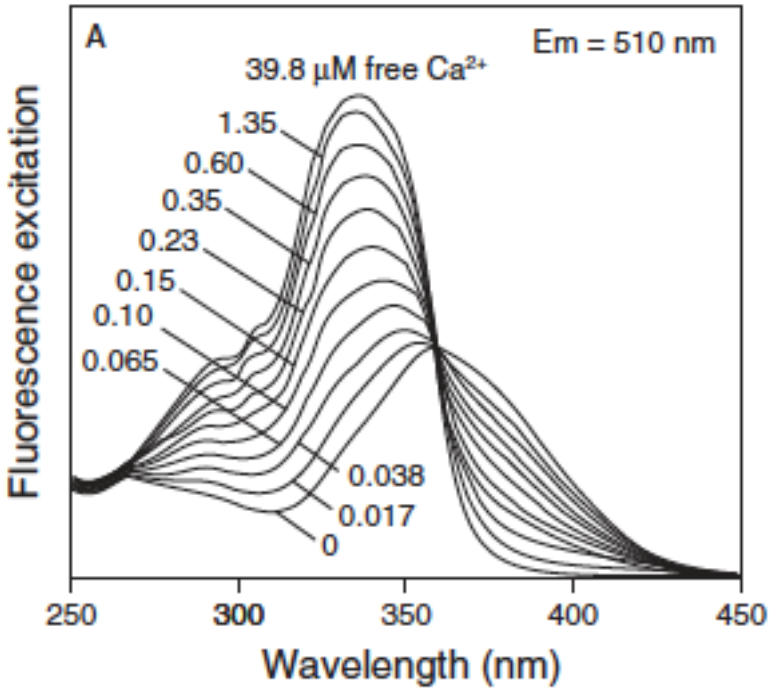

Figure. 2.6

Diagram depicting the calcium sensitive nature of Fura-2

A higher concentration of calcium results in an increase in the 340nm signal while inducing a decrease in the 380nm.

Figure reproduced from: http://www.invitrogen.com/site/us/en/home/References/Molecular-Probes-The-Handbook.html

2.13.1 Loading of cells with Fura-2 AM

Cells were plated onto coverslips as described in section 2.9. Coverslips were subsequently flooded with full media and left for 10 minutes to become detached from the plate. After this time coverslips were placed into loading media, consisting of culture medium with 0.1% BSA and 1μM Fura-2AM (frozen aliquotes of 1mM made up in DMSO) (Invitrogen Ltd, Paisley, UK) for 30 minutes in a 5% CO_2 humidified atmosphere at 37°C. Coverslips were then placed into loading media minus Fura-2AM for 15 minutes in a 5% CO_2 humidified atmosphere at 37°C. Cells were then transferred to external solution for a further 15 minutes at room temperature (24°C). Coverslips were protected from light at all stages.

2.13.2 Experimental set up and image acquisition

Coverslips were placed into a Warner recording chamber (bath dimensions (lxWxH) 24x13x4.1mm, volume by depth 133μl/mm) (RC-25F, Warner instruments) and superfused with external imaging solution from a reservoir bottle. The time taken for the solution to reach the recording chamber was 40s, determined by monitoring the flow of a dye into the recording chamber, the flow rate being 3ml/min. Figures have been adjusted accordingly. Syringes present on a perfusion rack were used to apply additional solutions when required. Syringes were aligned at the same height as the inflow tubing from the reservoir bottle and stoppers with tubing were placed into the syringes to ensure a constant flow rate. Tubing passed through a peltier heating element to warm solutions and bath temperature was monitored with a thermometer. The outflow of the recording chamber was a bevelled needle connected to a length of silicone tubing, with a suction pump (Watson Marlow SciQ 323) being used to draw the fluid into a waste bottle. Figure 2.7 shows a diagram of the recording set up used.

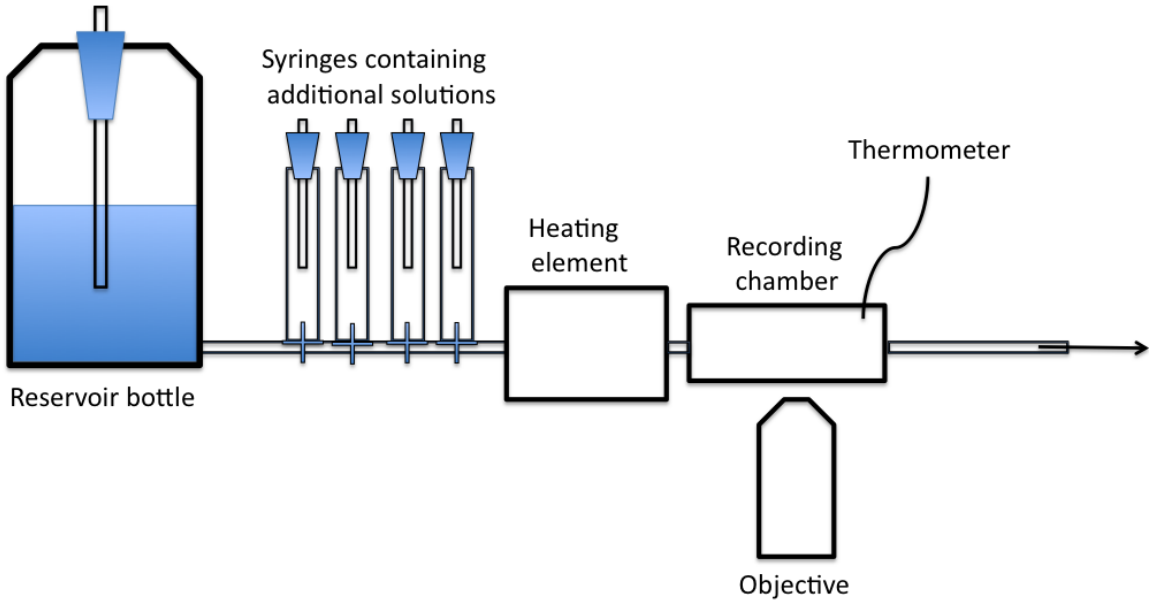

Figure 2.7
Experimental set of superfusion system

Coverslips were mounted onto a Zeiss Axiovert S100TV inverted microscope and viewed using a 40X oil immersion objective (NA1.3, Zeiss), which enabled visualisation of individual cells. Cells were subsequently illuminated at 340nm and 380nm and images taken at 2s intervals using a monochromator (Polychrome IV, TILL Photonice LPS-150). The emitted light was passed through a 510-540nm band-pass filter before detection and detected using a cascade 512B CCD camera (Roper scientific, Photometrics UK). Images were analysed by regions of interest being placed around individual cells and analysed using Metamorph® software (Meta Imaging) and further analysis and graphing were performed using Prism (GraphPAD software). All data is background subtracted, the background fluorescence corresponding to each frame was digitally subtracted from the fluorescence value for each cell at each wavelength.

2.13.3 Imaging solution

Imaging solution consisted of (in mM) 142 NaCl, 5 $NaHCO_3$ 10 HEPES, 16 Glucose, 2 KCl, 2 $CaCl_2$, 1 $MgCl_2$ and 0.1% BSA (pH 7.3, NaOH). For calcium free experiments the solution consisted of: 142 NaCl, 5 $NaHCO_3$ 10 HEPES, 16 Glucose, 2 KCl, 3 $MgCl_2$ and 0.1% BSA (pH 7.3, NaOH).

2.13.4 HLMC purity

Assessment of purity was determined during imaging experiments. Mouse Anti-CD117-PE IgG1 was applied to cells following experiments. HLMCS expressing C-kit (CD117) were stained enabling determination of mast cell purity by exciting cells at 488nm. Purity of all coverslips was >98% (Figure 2.8).

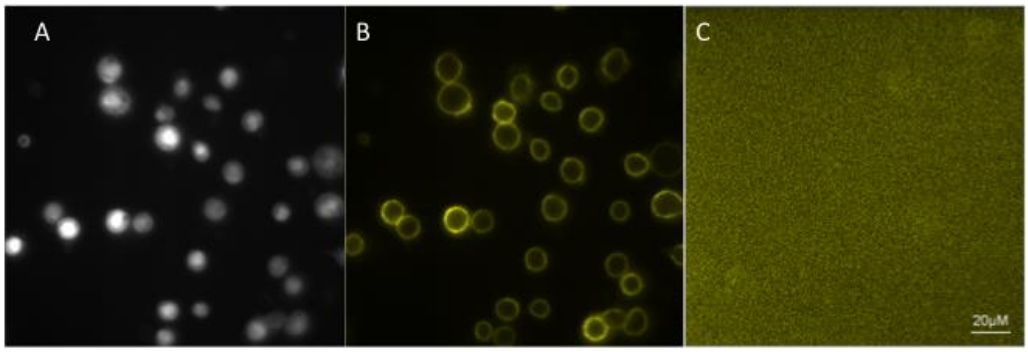

Figure. 2.8
HLMC population defined by CD117 staining for imaging experiments
A, Fura-2 fluorescence**. B.** HLMCS in A treated with CD117 show staining around the plasma membrane. **C**. Isotype control antibody.

2.14 FFN511 assay

FFN511 is a fluorescent false neurotransmitter. These are fluorescent compounds that closely resemble neurotransmitters. They can be loaded into SVs and released as neurotransmitters [329] enabling visualisation of exocytosis. FFN511 is similar in structure to monoamine neurotransmitter such as dopamine/serotonin and acts as a substrate for the VMAT that transport monoamines from the cytoplasm into secretory vesicles [299]. In a pH 7 solution the excitation MAX is 406nm and the emission MAX is 501nm.

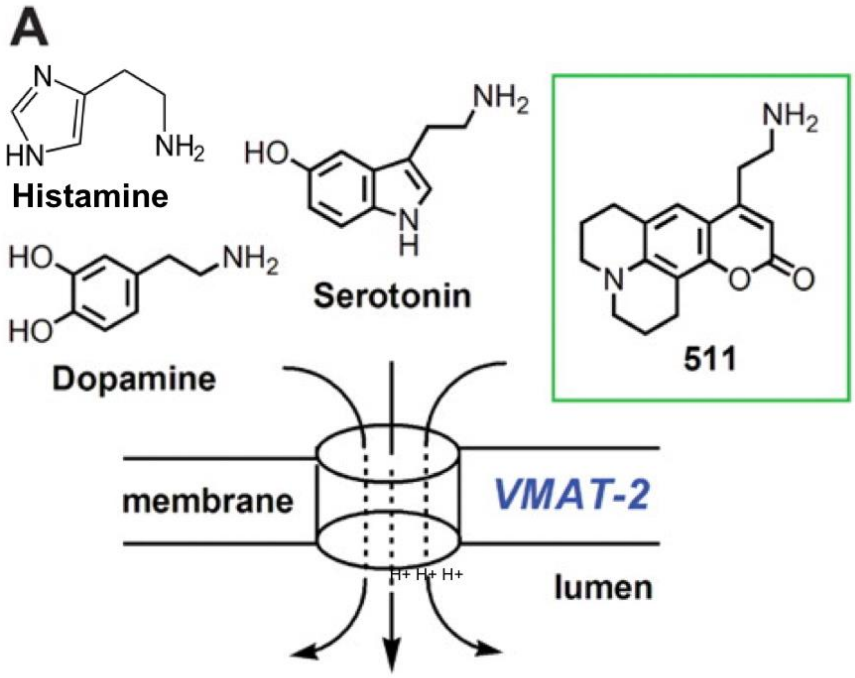

Figure. 2.9

Structure of FFN511

FFN511 is designed to be similar in structure to monoamines such as serotonin so it can be transported into vesicles through VMATS. Figure adapted from [299].

2.14.1 Loading of FFN511

For stimulation experiments, loading of HLMC and LAD 2 cells with FFN511 was achieved by incubating cells overnight with 1µM of the dye in total media + 100ng/ml rhSCF. After this time point coverslips were washed with a dye-free external solution for 10 minutes in a 5% CO_2 humidified atmosphere at 37°C.

For inhibition studies of FFN551 (Ascent Scientific) uptake with the vesicle monoamine transporter inhibitor reserpine, LAD 2 cells were treated overnight with either 1µM reserpine (Tocris) or dimethyl sulphoxide (DMSO) as a control. The following day cells were immobilised on Poly-L-Lysine (0.1%) coated 16mm glass coverslips (VWR) and incubated with 1µM FFN511 in total media for 10 minutes before undergoing two 15 minute wash steps with dye-free imaging solution. For experiments using chloroquine (Sigma), FFN511 loaded cells were treated for 10 minutes with 300µM chloroquine in imaging solution prior to imaging.

Coverslips were mounted onto the recording chamber and imaging solution was perfused onto the cells as described for calcium imaging. Imaging solution was

maintained at 32°C by passing the silicone tubing through a peltier heating element, bath temperature was recorded during experiments to ensure a constant temperature was maintained.

2.14.2 Image acquisition/ data processing

Coverslips were viewed either a40X oil immersion objective (NA1.3, Zeiss) or a 100X oil immersion objective (N.A. 1.6 Zeiss). Cells were illuminated at 400nm and images taken at 30s intervals. In FFN511 uptake experiments LAD 2 cells were perfused with 1μM FFN511 for the stated period and imaged at 2s intervals. The emitted light was passed through a 510-540nm band-pass filter before detection. All data is background subtracted, the background fluorescence corresponding to each frame was digitally subtracted from the fluorescence value for each cell. Cells were classified as 'responding' to a particular stimulus when FFN511 fluorescence, measured as a ROI placed over the whole cell, fell by more than 7 standard deviations over the baseline fluorescence Baseline fluorescence was measured as the average of the first five frames. Data is presented as a percentage of baseline fluorescence.

2.15 Bacterial Transformations and DNA extraction

DH5α cells (Sigma) were transformed with plasmid DNA (see table) using the following protocol: 1μl of DNA was added to 20μl DH5α cells and left on ice for 30mins. After this time point cells were heat shocked for 30s at 42°C. Cells were then placed on Ice for 2mins. 250μl of SOC media was added to cells and placed in a shaking incubator (220rpm) 37°C for 1hour. 100μl of cells were pippetted onto agar plates containing the appropriate antibiotic and left overnight at 37°C. The next day cells were sealed with parafilm™ and stored at 4°C.

Single colonies were picked and a starter culture made by placing tips containing colonies into LB media (for composition see 2.15.1) (5ml), containing appropriate antibiotic, overnight in a shaking incubator (220rpm) 37°C. The next day 100μl of starter culture was transferred to 50ml of fresh LB media containing appropriate

antibiotic and cultured overnight at 37°C with shaking (220rpm). DNA was extracted the following day using GenElute™ plasmid midiprep kit (Sigma) as per manufacturer's instructions.

2.15.1 Solutions

LB: 10g Tryptone, 5g Yeast extract, 10g Nacl. (pH 7.5 NaOH). Volume made up to 1l using ddH_2O.

SOC: 20g Tryptone, 5g Yeast extract, 10mM Nacl, 2,5mM KCL, 10mM $MgCl_2$, 20mM Glucose in 1l ddH_2O.

2.15.2 Sequencing

10µl of 100ng/µl of purified plasmid DNA in water was sent to The University of Sheffield Core Genomic Facility to sequence plasmid DNA, to confirm there were no mutations or variations in sequences.

2.16 Transfecting human mast cells

LAD 2 cells are notoriously refractory to transfection through traditional liposomal-based techniques. Recently, numerous new transfection reagents utilising biodegradable polymers have been developed. These encapsulate plasmid DNA forming a nanoparticle that is rapidly degraded once endocytosed by the cell, delivering cargo into the cell.

A number of these new non-liposomal transfection reagents were tested using a GFP reporter plasmid (GFP-V-RS) to identify a method of obtaining suitable levels of efficiency (Figure. 2.10). Transfection of LAD 2 cells using X-tremegene HP (Roche) showed promising levels of transfection in comparison to other reagents tested. Transfection was further optimised through varying cell concentrations and DNA: reagent ratios (Figure. 2.11). A cell concentration of 500,000 per ml and DNA: reagent ratio of 1:1 proved to provide the best levels of transfection. However, after initial success in transfecting LAD 2 cells, this method of transfection proved to be

highly variable and the same efficiency couldn't be obtained. This was independent of cell passage number, DNA quality or lot number of reagent.

2.16.1 Reagent transfection

For reagent based transfection testing, the four reagents used are described in Figure 2.9. LAD 2 cells were plated at 1 million per ml into 500µl total media and 100ng/ml rhSCF left for 30 minutes to settle. Transfections were performed as per each manufacturer's instruction with the following alterations: Reagents were added to cells and left to incubate for 5 hours. DNA/reagent combinations are described in Figure 2.11. The mixes were made up in Stem-pro media, apart from Xfect, which was made up in the buffer provided. After 5 hours fresh media was added to cells to take the total volume up to 1ml.

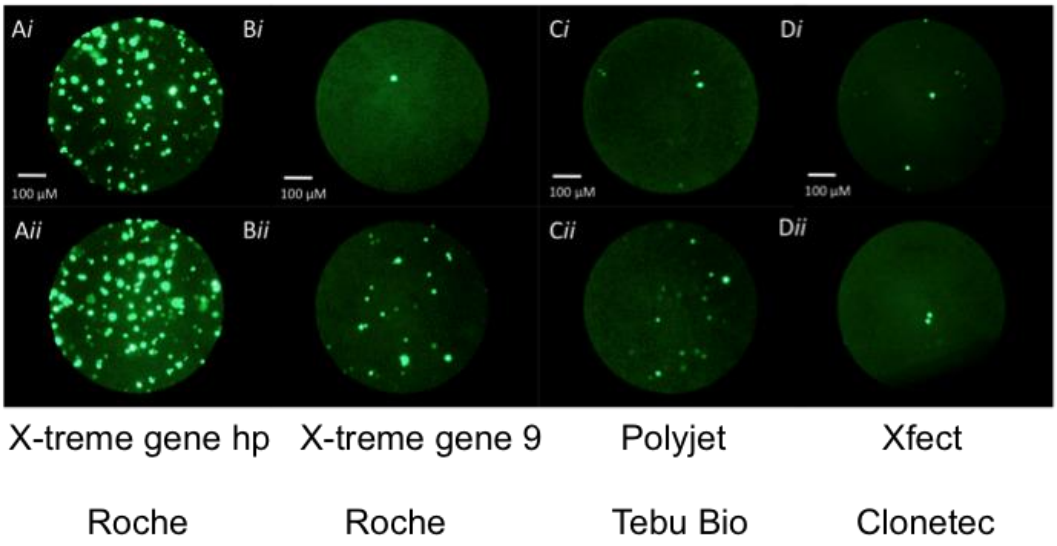

Figure. 2.10

Optimisation of transfection in human mast cells using non-liposomal based transfection reagents.

LAD 2 cells were transfected with a pGFP-V-RS vector using four transfection reagents and imaged for GFP expression 48 hours post transfection. **A.** LAD 2 cells transfected with X-tremegene HP (Roche) at a DNA to reagent ratio of 1:1 (**Ai**) and 1:3(**Aii**). B. LAD2 cells transfected with X-tremegene 9 (Roche) at a DNA to reagent ratio of 1:1 (**Bi**) and 1:3(**Bii**). C. LAD 2 cells transfected with Polyfect (Tebu-bio) at a DNA to reagent ratio of 1:2 (**Ci**) and 1:4(**Cii**). D. LAD 2 cells transfected with Xfect (Clontec) using 1µg DNA (**Di**) and 2µg DNA (**Dii**). Scale bars represent 100µm

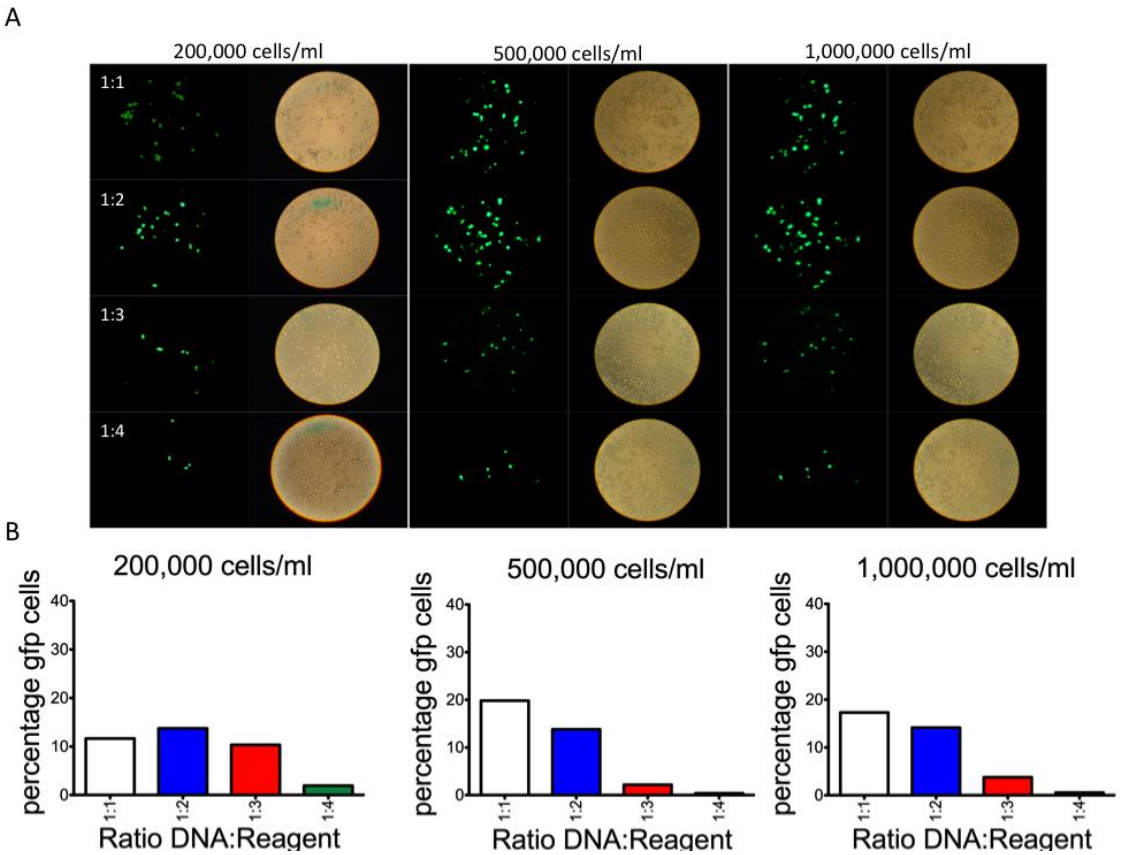

Figure. 2.11

Optimisation of X-tremegene HP transfection.

LAD 2 cells were seeded at either 200,000 500,00 or 1 million cells per ml and transfected with a GFP reporter construct with X-tremegene HP in ratios 1:1, 1:2,1:3 or 1:4 DNA:Reagent. **A.** LAD 2 cells transfected with a GFP reporter construct were imaged 24 hours post-transfection in both epifluorescence and bright field. **B**. Approximate transfection efficiencies were calculated by comparing both GFP and bright field images through image J cell counter.

It has been reported that efficiency of transfection can vary greatly depending on the promoter used [330], to assess whether using a different promoter could provide a more reliable transfection efficiency, vectors expressing GFP under various promoters were tested (Figure. 2.12). Vectors expressing GFP under pCMV or pCAG promoters produced the greatest levels of expression. Considering the majority of vectors that we had available utilise the pCMV promoter, it was decided to continue to use vectors that contained this promoter. Transfection efficiencies continued to vary greatly between experiments and so a new reliable transfection method was sought.

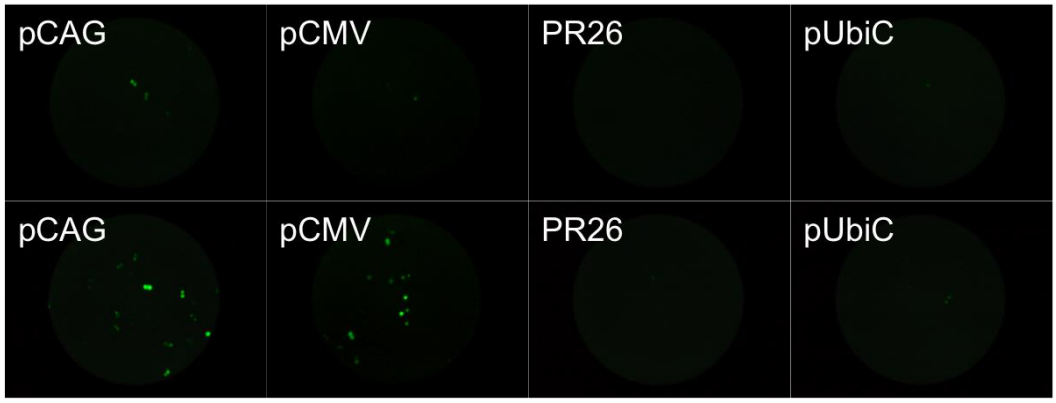

Figure. 2.12

Promotor expression in LAD 2 cells

LAD 2 cells were seeded at 500,000 cells per ml and transfected with GFP reporter constructs utilising one of four expression promotors. pCAG and pCMV produced the highest numbers of GFP positive cells.

2.16.2 Neon transfection

Electroporation has been shown to be successful in a number of hard to transfect cells including LAD 2 cells [331]. There are a number of issues with electroporation; often the technique can be very damaging to cells and can result in low viability. Furthermore, many protocols require many millions of cells, which is a particular issue using human mast cells. A relatively new electroporation system developed by Invitrogen, the neon transfection system, uses gold coated tips to electroporate cells in a pipette tip chamber. The advantages of this system is that as few as 50,000 cells can be used per transfection, the resulting viability is reported to be much greater [332]. The method requires low cell numbers and should show less variability compared to reagent-based techniques. LAD 2 cells were transfected using the GFP-V-RS GFP reporter plasmid used in previous experiments. A number of protocols were tested to assess the best conditions for transfection (Figure. 2.13). A pulse duration of 30ms and voltage of 1600mv provided 30% transfection efficiency and was used in future experiments. All further transfection experiments were performed using the neon transfecton system.

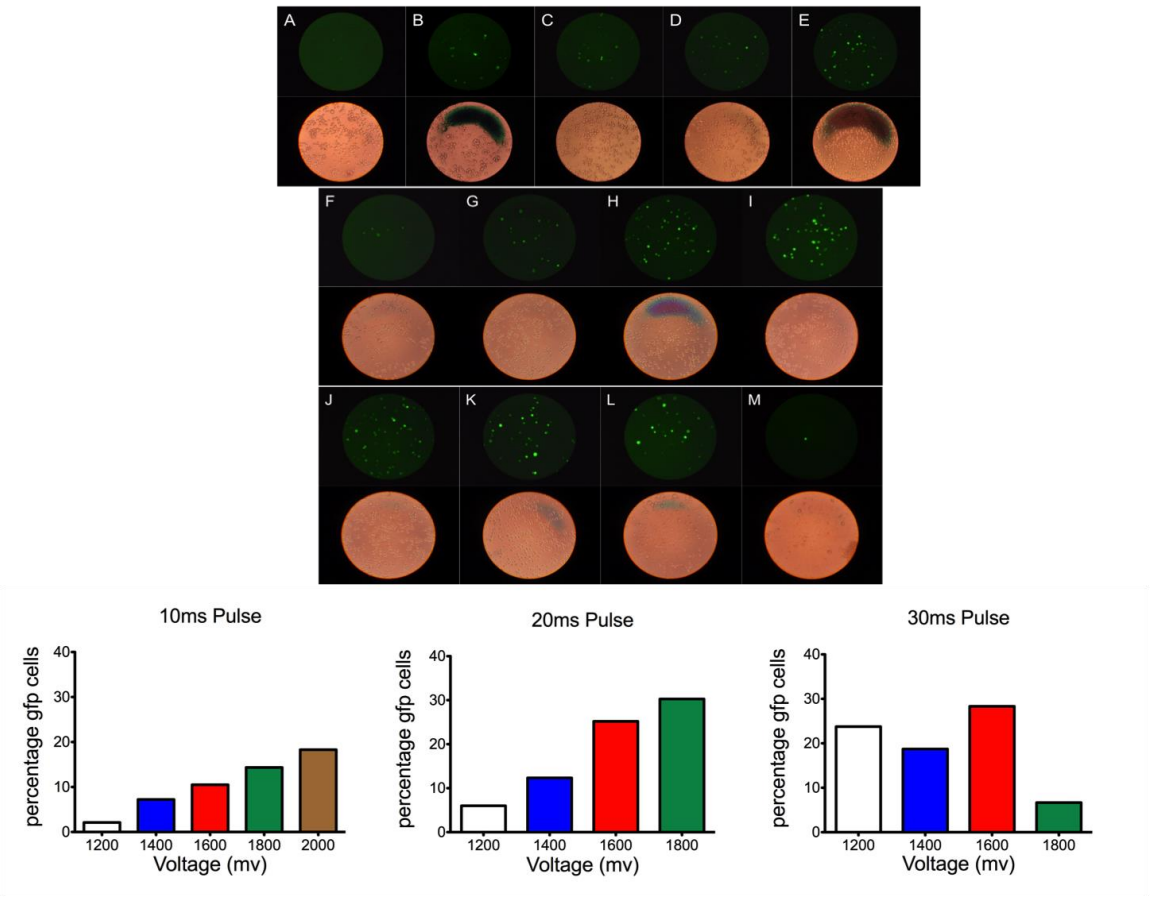

Figure. 2.13

Optimisation of Neon transfection in LAD 2 cells

LAD 2 cells were transfected using Neon transfection using the following conditions: **A-E** 10ms pulse of between 1200 to 2000mv, F-I 20ms pulse 1200-1800mv, J-M 30ms pulse 1200-1800mv. Graphs below show percentage of GFP positive cells from total cells.

2.16.3 Neon transfection final protocol

Neon transfection buffers E and R were warmed to room temperature. LAD 2 cells were counted before transfection and between 100,000 to 500,000 cells were used per transfection (no discernable differences could be seen in transfection efficiencies between these concentrations). Cells were centrifuged at 100g for 4 minutes, media removed, PBS added and cells washed by centrifugation using the same centrifugation settings. PBS was aspirated off and cells were suspended in buffer R, at least 12µL per transfection, and transferred to an eppendorf. Plasmid DNA was added at a concentration of 1µg/transfection ensuring the amount added was no greater than 10% of the total volume. The electroporation tube was placed into the neon station and 3ml of buffer E was pippetted into the tube. The cell

suspension was taken up into a 10µl reaction tip ensuring no bubbles were present and clicked into the electroporation tube. Cells were electroporated using a protocol of one pulse of 1600mv with 30ms pulse duration. Cells were dispensed into fresh total media containing 100ng/ml rhSFC. After transfection the tips were washed in 100% ethanol and left to air dry in a sterile environment. Tips were reused 4 times before being discarded. Experiments were carried out 48 hours post transfection.

2.17 Dual pHluorin and Calcium imaging

pHluorin is a pH sensitive variant of GFP. The ecliptic form carries substitutions at S147D, N149Q, T161I, S202F, Q204T and A206T, which renders the molecule pH sensitive; fluorescence becomes lower as the pH is lowered until <6.0 where the excitation peak disappears [295]. Fusion of acidic vesicles with the plasma membrane results in alkalisation of the intravesicular compartment as they become exposed to the more alkaline extracellular environment [333]. Tagging VAMPs C-terminally with pHluorin has allowed visualisation of vesicle fusion. Upon VAMP mediated membrane fusion, and subsequent alkalisation, the pHluorin tag becomes de-quenched. This increase in fluorescence can be used to monitor exocytosis [334].

These experiments were initially performed using SynaptopHluorin, a VAMP-2 tagged form [295]. In this study, VAMP-2 super ecliptic pHluorin present in the pCI neo mammalian expression vector was kindly provided by G.*Miesenböck*. VAMP-3 and VAMP-8 cDNA clones in Vector pOTB7 were purchased from Source Bioscience. Plasmids were sequenced upon arrival to ensure quality.

VAMP-3 and VAMP-8-pHluorin constructs were produced by Mutagenex. VAMP-2 was replaced within the pCI neo backbone with VAMP-3 and VAMP-8 coding sequences, through EcoRI 5'-end ligation and chimeragenesis/recombination for 3'-end ligation. Cells were transfected using the neon transfection system. For Dual pHluorin and BoNT LC experiments 1µg of BoNT LC and 500ng of pHluorin DNA was used and experiments carried out 48 hours post transfection.

2.17.1 Experimental set up and image acquisition

Coverslips were prepared, loaded and superfused with external solution in the same manner as for calcium imaging described in section 2.13.2. Cells were subsequently illuminated at 340nm and 380nm and 50ms at 480nm and images taken at 2s intervals using a monochromator (Polychrome IV, TILL Photonice LPS-150). Due to the possibility of excitation of pHluorin at 380nm (Figure 2.14) a short exposure time was used for Fura-2AM excitation (10ms). Images taken at 380nm in pHluorin-transfected cells show there was no crossover of signal (Figure 2.15). Un-transfected cells had a similar fluorescence value, both much lower than for Fura-2AM loaded cells.

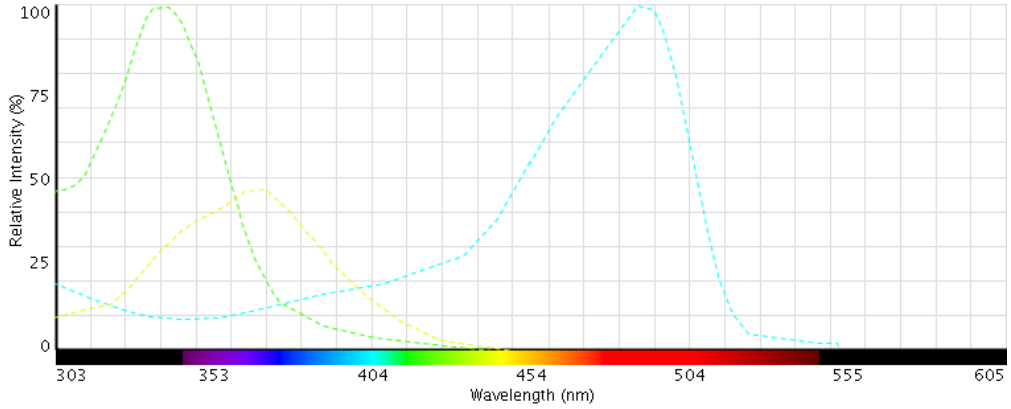

Figure. 2.14

Excitation wavelengths of Fura-2AM and GFP.

Diagram depicts the excitation wavelengths of both the calcium free (yellow) and bound (green) Fura-2AM and of GFP (Blue). Some excitation of GFP occurs at 380nm. Values and graph obtained from Invitrogen spectral viewer. http://www.invitrogen.com/site/us/en/home/Products-and-Services/Applications/Cell-Analysis/Labeling-Chemistry/Fluorescence-SpectraViewer.html

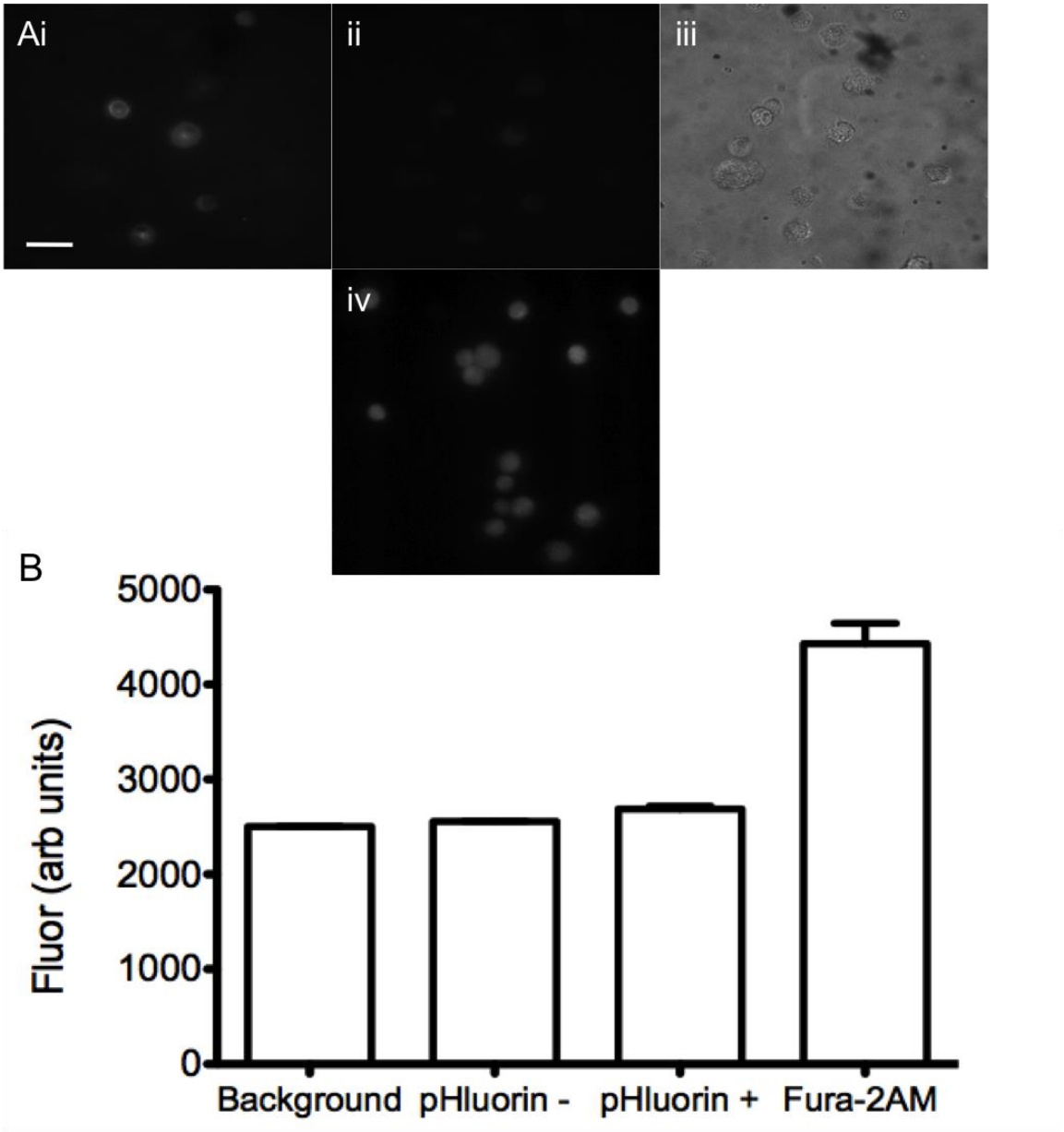

Figure. 2.15

pHluorin signal does not interfere with 380nm recording of Fura-2AM

LAD 2 cells transfected with pHluorin were illuminated at 380nm to assess possible interference with Fura-2AM signal. **Ai-iv**, representative coverslips from pHluorin transfected or Fura-2AM loaded cells, **Ai** excitation at 480nm, **ii** 380, **iii** bright field. **Aiv** representative coverslip of untransfected Fura-2AM loaded LAD 2 cells imaged at 380nm. **B**. Fluorescence intensity values at 380nm excitation wavelength of background (n=5), pHluorin negative (n=42) and pHluorin positive (n=18) cells compared to Fura-2AM loaded cells (n=45). Data represents mean±SEM of individual cell fluorescence. Scale bars represent 20μm.

The emitted light was passed through a GFP/mCherry dual-band polychroic mirror with extended reflection down to 340nm and GFP/Cherry emission filter (Chroma). Images were acquired by regions of interest being placed around transfected individual cells and analysed using Metamorph® software (Meta Imaging) and

further analysis and graphing were performed using Prism (GraphPAD software). The background fluorescence corresponding to each frame was digitally subtracted from the fluorescence value of each cell.

2.17.2 Data analysis

Cells were classified as 'responding' to a particular stimulus when fluorescence, measured as a ROI placed over the whole cell, increased by more than 10 standard deviations over the baseline fluorescence. Baseline fluorescence was measured as the average of the last 10 frames before application of drug. Data is presented as $\mathbf{(\Delta f/f_0)/f_T}$, where $\mathbf{\Delta f}$ is the change in fluorescence and $\mathbf{f_0}$ represents the baseline fluorescence. Data was then normalised to total fluorescence $\mathbf{f_T}$, derived from NH_4CL wash. This calculation was used to account for variations in the starting fluorescence and in the total amount of pHluorin present in individual cells.

For acid wash experiments all individual transfected cells were selected and the proportion of intracellular to cell surface pHluorin fluorescence was determined. Firstly by calculating the cell surface fluorescence by subtracting the minimum fluorescent value (average of five frames) resulting from quenching of cell surface pHluorin by a pH 5.6 acid (pH with HCL) wash from the baseline value. The intracellular fluorescence was determined by subtracting the baseline fluorescence from the maximum fluorescent value (average of 5 frames) resulting from de-quenching of intracellular pHluorin from an NH_4CL wash. Total fluorescence was calculated by subtracting the minimum fluorescent value from the maximum fluorescent value. Percentage values were subsequently calculated by dividing the cell surface or intracellular fluorescence by the total fluorescence and multiplying by 100.

2.18 VAMP-8 shRNA

Short Hairpin RNA (shRNA) is a RNA sequence containing a hairpin turn or "loop', mimicking micro RNA (miRNA). Once expressed through plasmid transfection or transduction into the cell, the shRNA molecule is transported out of the nucleus through the actions of Exportin 5. Dicer, a ribonuclease III (RNase III) family member, chops the shRNA into siRNA and it is incorporated into the RNA-induced

silencing complex (RISC). This complex then targets the mRNA that the siRNA is identical to, resulting in the degradation of the target mRNA [335].

VAMP-8 HuSH shRNA plasmids were purchased from OriGene for VAMP-8 knockdown. The pGFP-V-RS vector contains a pCMV driven tGFP gene to allow visualisation of transfected cells. The targeting shRNA sequence expression is driven under the human U6 promotor (Figure 2.16).

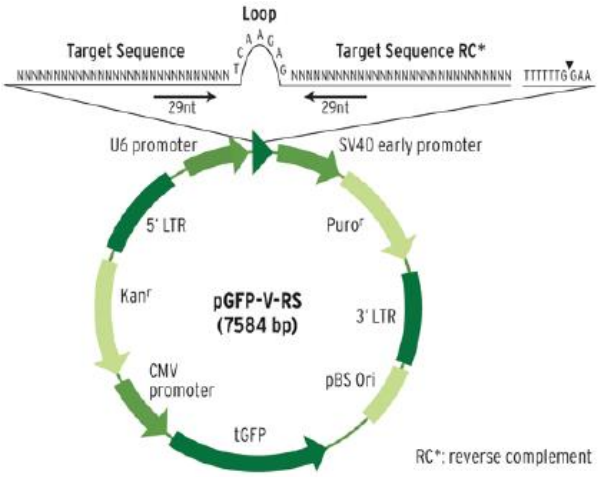

Figure. 2.16

pGFP-V-RS used for shRNA knockdown studies

The U6 promotor drives expression of shRNA, while CMV drives GFP expression. Figure taken from OriGene HuSH shRNA application guide:
http://www.origene.com/assets/Documents/HuSH/AppGuideHuSH29.pdf

Four unique shRNA constructs were supplied alongside a non-targeting scramble control. Each construct was numbered 1-4 from top to bottom as seen in Figure 2.17 and tested for knockdown using western blot (Figure. 2.18). Constructs were transfected using the neon transfection protocol outlined above. After transfection cells were left for 48 hours before experiments were performed.

This kit containing following constructs: (Two negative control plasmids are provided with each shipment.)

Sequences	Tube ID	Species Specificity (human, mouse, rat)
AATGATCGTGTGCGGAACCTGCAAAGTGA	GI362929	H
ATATTATGACCCAGAATGTGGAGCGGATC	GI362926	H
TTGGAACATCTCCGCAACAAGACAGAGGA	GI362928	H
AAGCCACATCTGAGCACTTCAAGACGACA	GI362927	H

Catalog No.	Description	Vector
TG305552	VAMP8 - Human, 4 unique 29mer shRNA constructs in retroviral GFP vector (Gene ID = 8673). 5μg purified plasmid DNA per construct	pGFP-V-RS
TR30007	HuSH shRNA GFP cloning vector (pGFP-V-RS)	
TR30013	Non-effective 29-mer scrambled shRNA cassette in pGFP-V-RS Vector	

Figure. 2.17

VAMP-8 shRNA sequences

Figure taken from OriGene HuSH shRNA application guide:

http://www.origene.com/assets/Documents/HuSH/AppGuideHuSH29.pdf

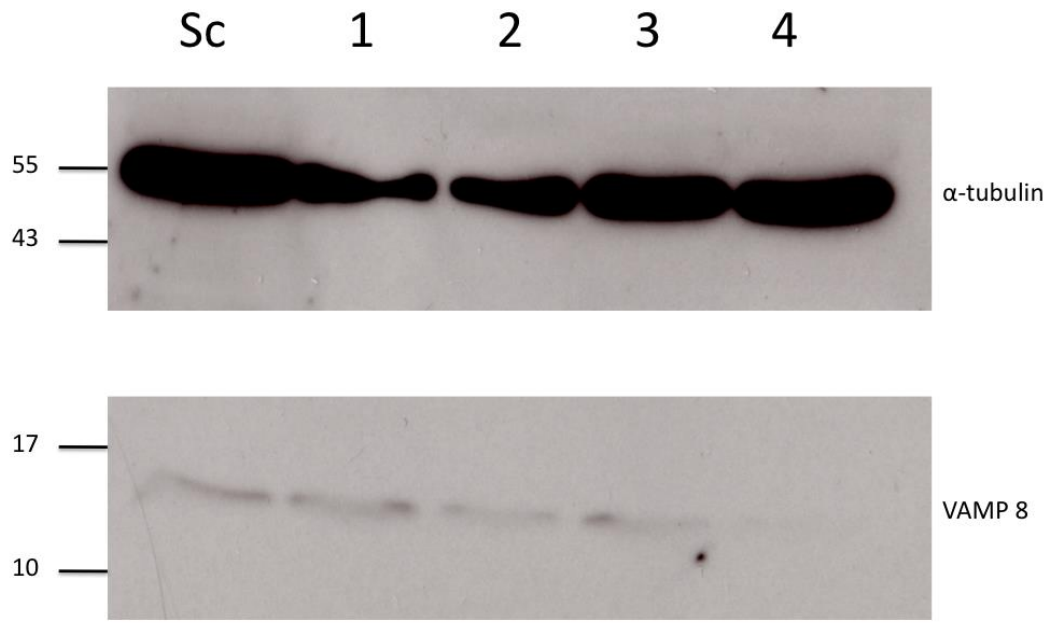

Figure. 2.18

shRNA 4 produces greatest level of knockdown.

LAD 2 cells were transfected with the above shRNA constructs using the neon transfection system. 48 hours post transfection cells were lysed and VAMP-8 expression determined through western blot. α-tubulin used as loading control.

2.19 IL-6 GFP construct

Mast cells have been shown to differentially release IL-6 but the trafficking pathway of release remains elusive [336]. The pathway of release in macrophages is well defined and a fluorescent construct has been generated to assess Il-6 function [183]. The IL-6 GFP construct was purchased from addgene, deposited by Jennifer Stow [183]. The construct contained Mouse Il-6 (genebank number: X54542) within the pEGFP-N1 vector resulting in a C-terminal GFP tag.

2.19.1 IL-6 GFP release assay

LAD 2 cells were transfected with mouse IL-6 GFP using the neon transfection protocol and left to recover for 24 hours. The following day LAD-2 cells were plated in a 96 well V bottomed plate in external solution at 1,000,000 cells/ml. 100,000 per well were used for each condition. Cells were incubated at 37^0C for 10 minutes before addition of agonists. Crosslinking of FcεRI receptor was induced with anti-IgE (Sigma). Cells were then incubated at 37^0C for an additional 6 hours before being centrifuged (550g, 10mins, 4^0C) and the supernatants removed. Supernatants were treated with protease inhibitor cocktail to reduce protease breakdown of IL-6 GFP and stored at -20^0C before use. . Cell pellets were processed as samples in section 2.8 for western blotting and stored at -20^0C in RIPA buffer with protease inhibitor cocktail. Supernatant and lysates were subjected to western blotting using the protocol set out in section 2.8.

Values for release were calculated by normalising band intensity values of IL-6 GFP in the supernatant to cell lysate values.

2.20 BoNT LC constructs

Syntaxin Ltd supplied BoNT light chain constructs used in this study. BoNT LCS were expressed in pcDNA4 Myc/His vectors under the pCMV promotor. Light chains expressed include: BoNT serotypes E, B and the modified form of E (E K224D).

Chapter 3.Defining LAD 2 cells as a mast cell model

3.1 Introduction

Mast cells can be defined through their expression of numerous mast cell associated proteins. For example basophils, cells which closely resemble mast cells, express the high affinity IgE receptor FcεRI but don't express C-kit, the receptor for SCF [337]. Mast cells express both and so by monitoring the cells expression of many of these markers a definitive picture of the cell type can be built. The main mechanism of activation in mast cells is through the interaction of antigen with IgE bound to FcεRI. The FcεRI receptor consists of three subunits α, β and γ [338] with the a subunit binding IgE and the β γ subunits mediating downstream signalling, through the interaction of their associated enzymes, the src kinases [339]. The src family kinases are essential for functional coupling of FcεRI signalling [340, 341]. Numerous src kinase family members are present in mast cells and have differing signalling functions [342-345].

Alongside the expression of mast cell associated receptors, mature mast cells express a number of pre-formed mediators stored within their granules. These include a number of proteases such as tryptase and MC-CPA, histamine and β-hexosaminidase and are discussed in detail in section 1.1.2 [60]. Traditional assays for measuring pre-formed mediator release in mast cells, for example ß-hexosaminidase release assays, are performed on populations of cells and don't permit visualisation of individual cell responses and therefore are inappropriate for potential diagnostic screens where cell numbers are limited. Finding an assay that is affordable, quantitative and can be used for real-time measurements even at the single cell level would be highly advantageous for elucidating the mechanisms and variations of pre-formed mediator release in mast cells. FFN511 is a fluorescent false neurotransmitter. FFN511 was originally developed to quantify exocytosis in dopaminergic terminals [346]. This fluorescent-based probe is similar in structure to monoamines such as dopamine and serotonin, acts as a substrate for the Vesicular Monoamine Transporters (VMATs) that transport monoamines from the

cytoplasm into SVs which enables loading of the dye into SVs [33]. There is evidence that human skin mast cells express VMAT 2 [38], suggesting that FFN511 may also be used to monitor mast cell degranulation. Using FFN511 in mast cells would allow the elucidation of single cell responses and enable detailed characterisation of their responses to stimulation.

LAD 2 cells represent a well differentiated human mast cell model cell line, and have been shown to express mast cell specific proteins [88]. However, some studies have questioned their usefulness as a model and whether they truly represent mast cells [90]. Experiments in this chapter set out to define and assess the suitability of using LAD 2 cells as a mast cell model for studies on exocytosis. Using data obtained through gene microarray, LAD 2 cells were assessed for the expression of relevant mast cell associated receptors and mediators and compared to results obtained at the same time by microarray from mRNA isolated from a single HLMC donor. LAD 2 response to FcεRI stimulation were also determined by calcium imaging and compared to HMLCs. To assess mast cell degranulation, a novel fluorescent-based assay using FFN511 was developed and characterised to investigate and comparisons were made between LAD 2 and HLMC responses to FcεRI mediated degranulation.

3.02 Results

3.2.1 Expression of mast cell associated receptors and mediators in LAD 2 cells

To determine how closely LAD 2 cells resemble primary HMLCs, and thereby evaluate how useful a model they are, microarray data obtained from LAD 2 cell mRNA was used to assess the levels of expression of mast cell associated receptors and mediators. These results were then compared to levels of mRNA expression of the same receptors and mediators in the HMLCs. Due to constraints of the microarray chip, tissue availability and expense, the HLMC data constitutes a single donor and so although informative, the data would need to be repeated to confirm results. However, it still provides a useful comparison and starting point to establish the similarity between LAD 2 cells and HLMCs.

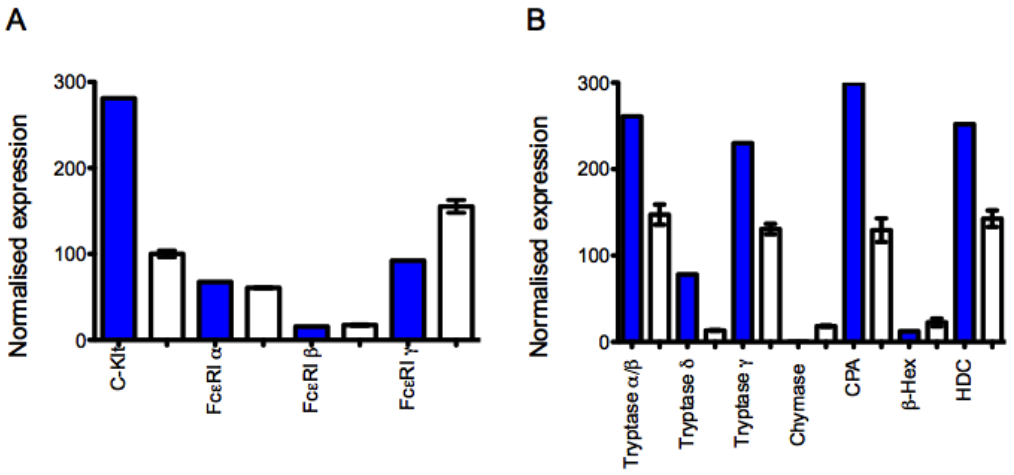

Figure 3.1

LAD 2 cells express mast cell associated genes

Microarray analysis was performed on LAD 2 and HLMC to determine the expression pattern of mast cell associated genes. **A**. LAD 2 cells express mast cell associated receptors C-kit and FcεRI. **B**. LAD 2 and HLMC expression of mast cell associated mediators. Clear bars represent LAD 2 mRNA expression from three independent RNA extractions ±SEM. Blue bars represent mRNA expression from one HLMC donor. CPA is carboxypeptidase and HDC is histidine decarboxylase.

The most logical starting point in characterising the LAD 2 cell line was to assess the expression of mast cell associated receptors. LAD 2 cells have been shown to respond to SCF through expression of C-kit and have functional FcεRI receptors [88]. Using the microarray data mRNA expression of C-kit was confirmed at very high levels in the HMLCs and to a lesser extent in LAD 2 cells (Figure 3.1). As with C-kit, LAD 2 cells expressed all subunits of the FCεRI receptor in a similar manner to that of HMLCs. The β subunit had much lower expression levels than the other subunits α and γ.

After assessing receptor expression, the expression of a number of mast cell mediators such as tryptase were determined and compared to HMLCs (Figure 3.1). LAD 2 cells expressed all the granule associated mediators tested. In addition LAD 2 cells expressed small levels of the serine protease chymase, which was not expressed in HMLCs.

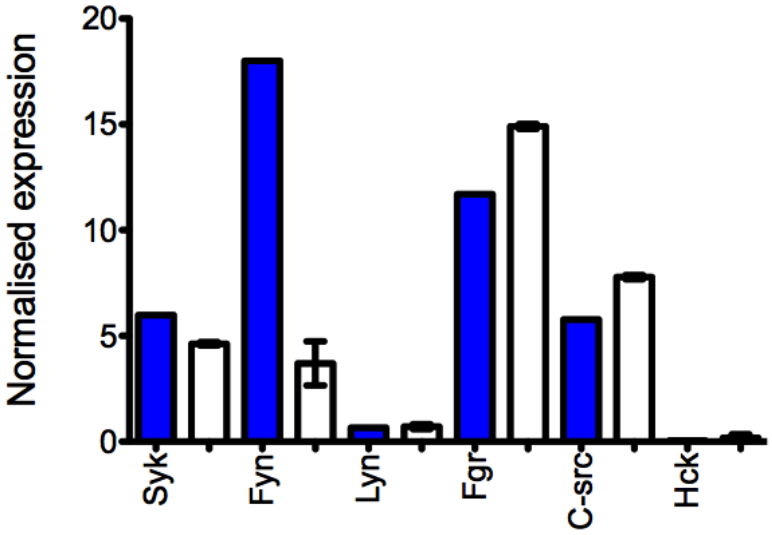

Figure 3.2

Mast cell expression of src family kinases

Microarray analysis of LAD 2 and HLMC src kinase expression. Clear bars represent LAD 2 mRNA expression from three independent RNA extractions ±SEM. Blue bars represent mRNA expression from one HLMC donor.

Microarray data was used to determine expression levels of the src family kinases in LAD 2 and HMLCs. In LAD 2 cells a number of src kinases were expressed in a pattern similar to the HLMC donor (Figure 3.2). The only difference was seen in Fyn kinase expression, LAD 2 cells expressed much lower amounts when compared to the HLMC donor. Further HLMC donors would be needed to determine whether this difference is significant as N only equals one.

3.2.2 Calcium response of LAD 2 cells to FCεRI crosslinking

Stimulation of mast cells through FcεRI and activation of src family kinases leads to downstream signalling events that give rise to large increases in intracellular calcium (see section 1.2.1). From the microarray data it is clear that LAD 2 cells express the mRNA for all subunits of FcεRI and previous studies have shown that LAD 2 cells respond to FcεRI crosslinking [88]. Calcium imaging was performed on LAD 2 cells to confirm they were able to respond to FCεRI stimulation and to compare the responses to HMLCs. There was a clear response upon crosslinking of the FcεRI receptor, almost all cells responded to stimulation (Figure 3.3). The majority of HMLCs responded to FCεRI stimulation but had a much larger response

size compared to LAD 2 cells ($P<0.001$). Upon activation calcium release is induced from the ER through the action of IP_3, this release of calcium induces the activation of CRAC and the influx of extracellular calcium. Experiments were performed in the absence of extracellular calcium to isolate calcium release of intracellular stores from the extracellular influx. Again response sizes were significantly larger in HLMCs than LAD 2 cells ($P<0.001$).

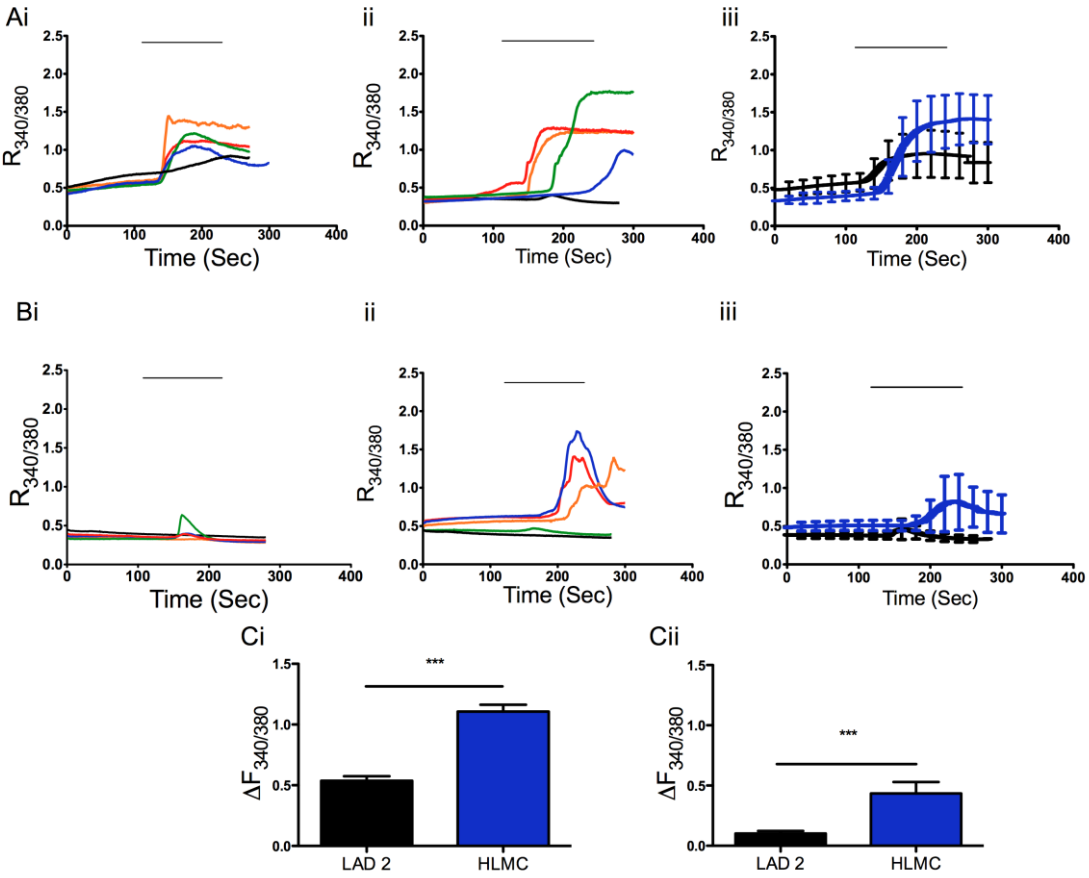

Figure 3.3

IgE-induced calcium signals in LAD 2 cells and HMLCs

Fura 2-loaded cells sensitised overnight with 300ng/ml IgE were stimulated with 3.3µg/ml anti-IgE, which was bath applied as indicated by the horizontal bars. a: IgE-mediated calcium entry in LAD 2 cells, monitored at 340nm and 380nm, in the presence **A.** or absence **B.** of 2mM extracellular calcium. **A**. Traces in **(i)** show representative individual LAD 2 responses **(ii)** show representative individual HLMC responses. Part **(iii)** shows mean ± SEM in LAD 2 (black trace; n=75 cells, N=3 individual experiments, 96% of cell responded) or HLMC (Blue trace, n=33 N=4 donors. 100% cells responded). **B.** Experiments were carried out without the presence of extracellular calcium. **(i)** Shows representative individual LAD 2 and **(ii)** shows representative individual HLMC responses. **(iii)** Shows mean ± SEM in LAD 2 (Black trace, n=33 cells N=3, 81% of cells responded) or HLMCs (Blue trace, n=16 cells N=3, 88% of cells responded) in the absence of extracellular calcium. Results are representative of 2 separate donors. **C** shows mean calcium response size **(i)** in the presence or **(ii)** in the absence of extracellular calcium. *** Denotes significance of P<0.001. unpaired students' T-test. Experiments were carried out by Claire Tree-Brooker

3.2.3 Loading of FFN511 in human mast cells

To determine whether LAD 2 cells could be loaded with FFN511, cells were initially incubated with 1μM FFN511 for 15 minutes. Cells became loaded with the dye and showed a granular staining pattern (Figure 3.4). The dye was excited at 400nm and has a maximum emission of 501nm in 100mM sodium phosphate pH 7 buffer [299].

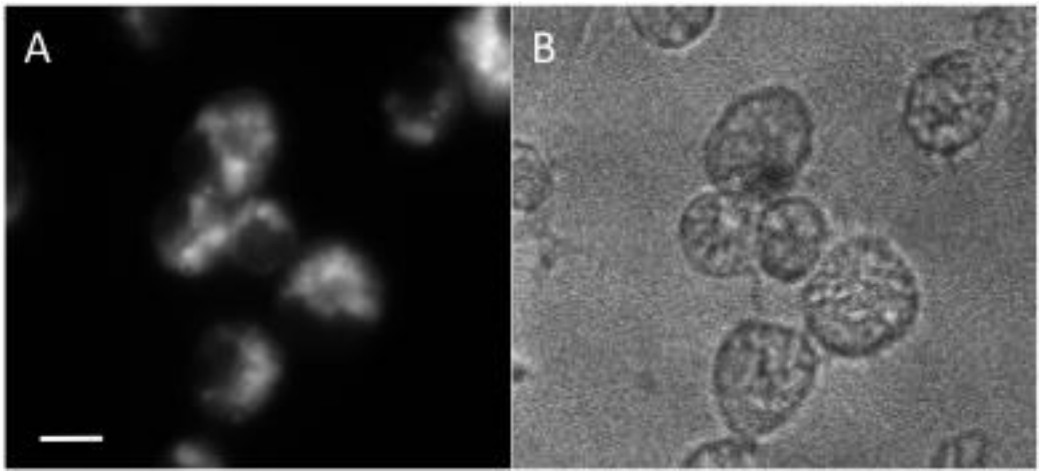

Figure 3.4

FFN511 is loaded into mast cells

Image of LAD 2 cells loaded with FFN511. LAD 2 cells were incubated with 1μM FFN511 and imaged at **A,** excitation l of 400nm, **B**. Bright field image. Scale bar represents 10μm.

Upon initial application of FFN511 and sequent washing of LAD 2 cells there was considerable loss of dye in resting cells. Initially, it was thought to be due to photo bleaching. However, the levels of fluorescence of individual cells was varied for each coverslip and plotting the rate of decay of fluorescence of individual cells over starting fluorescence showed that the higher the levels of fluorescence, the greater the rate of decay (Figure 3.5.).

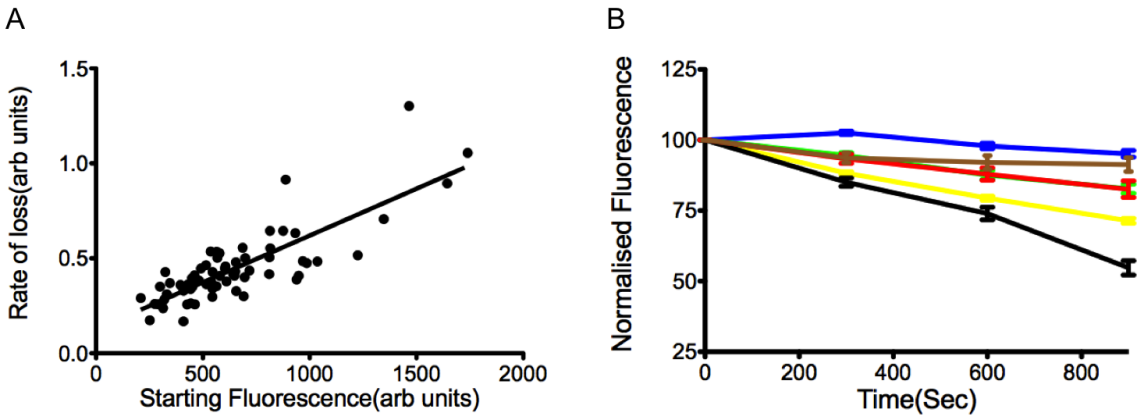

Figure 3.5

FFN511 dye loss in LAD 2 cells

A. There is a significant positive relationship between the starting fluorescence (1μM dye loading) and the rate of loss of fluorescence. n=65 cells from 2 coverslips (y=0.126+0.0004937x, F=122.3,d.f=1,63, P<0.0001). Linear regression fit, R square value = 0.6601. **B.** Effect of concentration and incubation time on dye loss. LAD 2 cells were imaged every 5 minutes at the concentrations and incubation times shown on the graph fluoresence is normalised to starting fluoresence defined as the average of the first five frames data represents mean±SEM. Yellow line 0.01μM 15 mins, Blue 0.01μM 1hr, Green 0.1μM 1hr, Black 0.1μM 15 mins, Red 1μM 1hr, Brown 1μM overnight.

Varying the intensity of excitatory light to minimize photobleaching by using different neutral density filters decreased but did not abolish the gradual decline in the emitted fluorescence. This suggests that the cells were becoming overloaded with the dye and then releasing the dye over time, or that the dye was not efficiently trapped within vesicular compartments. It should be noted a certain level of baseline release of dye would be expected, for example, in degranulation assays there is often a baseline release of at least 5%.

Figure 3.5 shows how increasing the incubation time and reducing the dye concentration reduced the gradual loss of FFN511 fluorescence in resting cells. Despite 0.01μM showing the least rate of loss of dye, the staining was very weak. A similar level of loss is seen after a one hour incubation with 1 μM and 0.1 μM FFN511. Therefore, due to less loss and staining that looked more punctate, 1μM of FFN511 was used in all future experiments. Overnight incubation resulted in greatly reduced dye loss; therefore experiments were carried out using overnight incubation. Background was measured as release of dye from vehicle perfusion

controls and was subtracted from data to normalise for any dye loss. Figure 3.6 shows uptake of the dye into punctate structures occurring within 150 seconds.

To assess whether dye loss under resting conditions was due to FFN511 inducing premature degranulation of the mast cells, ß-hexosaminidase release assays were performed in cells loaded with FFN511 (Figure 3.7). FFN511 did not affect spontaneous or activated release of ß-hexosaminidase. The results indicate that loss of FFN511 is not through the dye overloading mast cell granules and inducing mast cell degranulation.

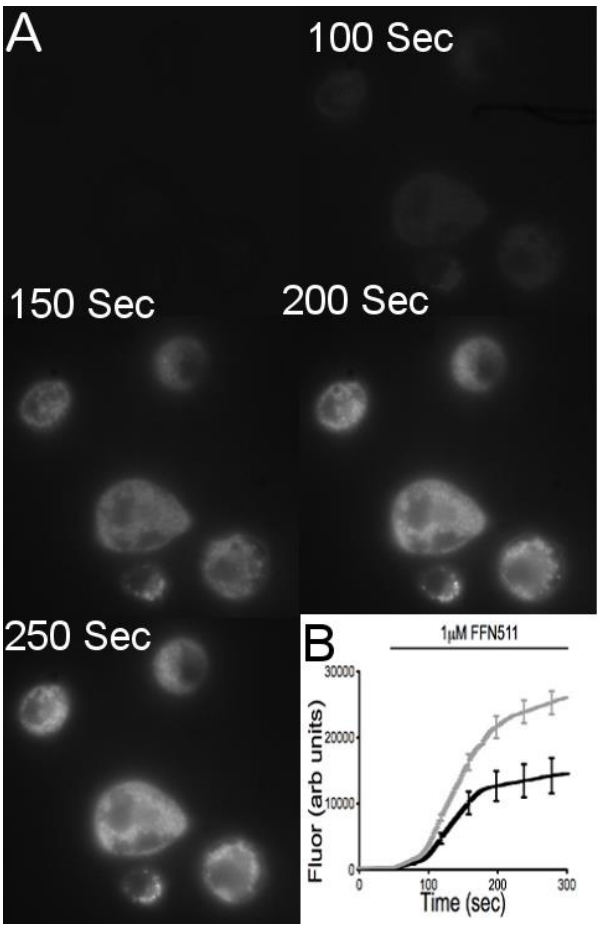

Figure 3.6.

FFN511 is taken up into vesicular structures in LAD 2 cells

LAD-2 cells take up FFN511 into vesicular structures within 150 seconds of FFN511 application. **A.** Images of LAD-2 cells taking up 1μM FFN511 into vesicular structures. **B**. Graph quantifying the uptake of FFN551 into vesicles. Regions of interest were drawn around vesicles (grey) and cytoplasm (black) and intensity values were measured over the stated time period from FFN511 application. Data presented as mean±SEM. Scale bar indicates 20μm. Experiments were performed at 32^{o}C n=7 from 2 passages.

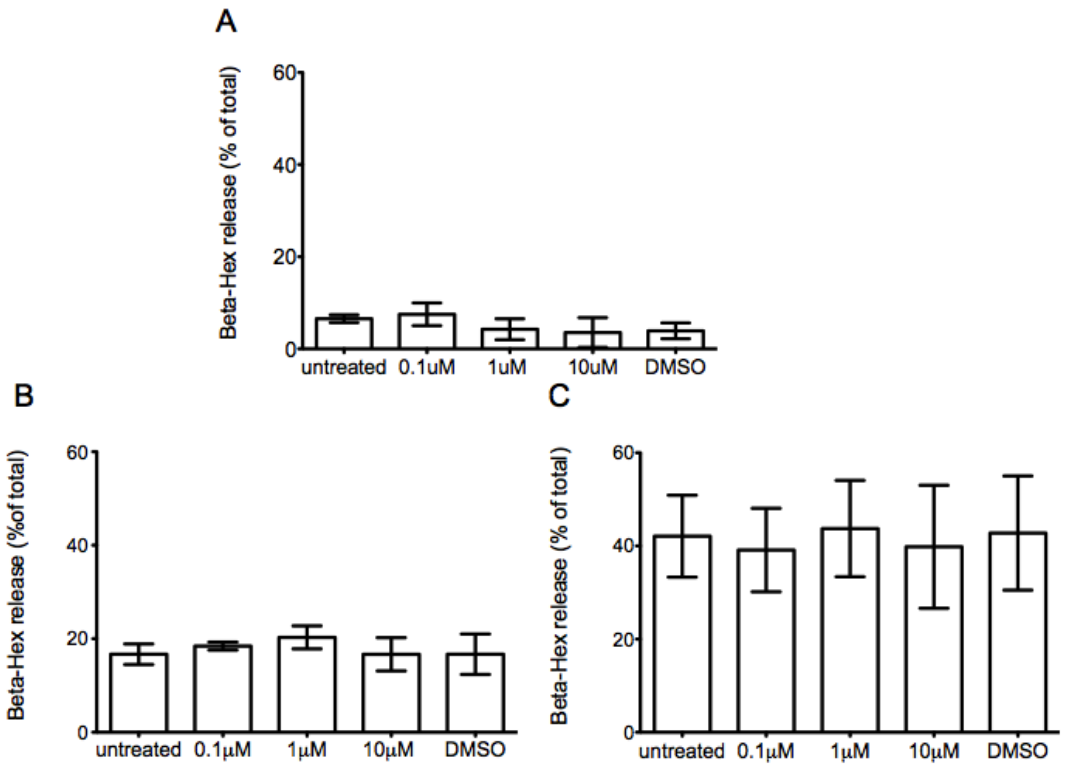

Figure 3.7

FFN511 does not induce degranulation in LAD 2 cells.

No significant difference in β-hexosaminidase release was detected between cells incubated with FFN511 and untreated cells. LAD-2 cells were incubated overnight with varying concentrations (0.1, 1, 10µM) of FFN511 and 300 ng/ml human IgE. The next day cells were stimulated with either **A.** unstimulated **B**. 1µg/ml anti-human IgE or **C.** 10µg/ml anti-human IgE. N=3±SEM. There was no significant difference between cells treated with FFN511 or DMSO control. One way ANOVA post hoc Tukey test, $p>0.05$.

3.2.4 Pharmacological inhibition of FFN511 uptake and expression of VMATS

To define the vesicular localisation of the FFN511, the weak lipophilic base chloroquine was applied to FFN551 loaded cells; this collapses the pH gradient in vesicles [347] (Figure 3.8). Fluorescence was almost completely abolished ($P<0.001$) showing that the FFN511 was localising to acidic organelles, such as SGs.

To assess the mechanism by which LAD 2 cells might transport FFN511 into secretory granules, the expression of VMATS was determined in LAD 2 cells using RT-PCR and microarray data; both methods showed VMAT 2 but not VMAT 1 was expressed (Figure 3.9a and b). To determine whether FFN511 was being loaded

into granules through VMAT 2 we applied the VMAT inhibitor reserpine at 1μM, a concentration used to inhibit FFN uptake in VMAT 2 expressing HEK cell cultures [348], which inhibits the action of VMATS 1 and 2, to LAD 2 cells prior to FFN511 loading (Fig 3.9). There was a significant reduction in total FFN511 uptake ($P<0.0001$), suggesting FFN551 is loaded into mast cell granules through VMAT 2.

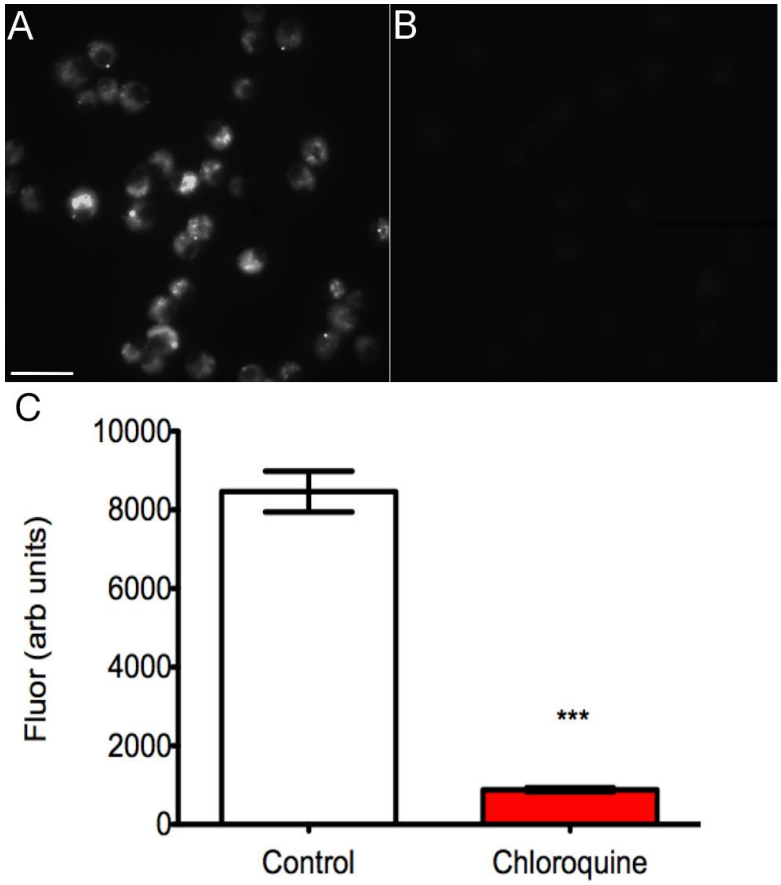

Figure 3.8

Chloroquine abolishes vesicular staining in FFN511 loaded LAD-2 cells.

The addition of the weak lipophilic base chloroquine, which collapses the vesicle pH gradient, abolishes accumulation of FFN511. **A.** Image showing LAD 2 cells untreated and **B.** treated with 300μM Chloroquine (40x Scale bar indicates 40μm.). **C**. LAD 2 cells loaded with 1μM FFN511 were incubated with 300μM of the weak lipophilic base Chloroquine. All data is shown as ±SEM of averaged individual cell fluorescence. Control N=4, n=58 cells, 300μM Chloroquine N= 4. n=70 cells. *** Denotes significance of $P<0.001$. unpaired students' T-test

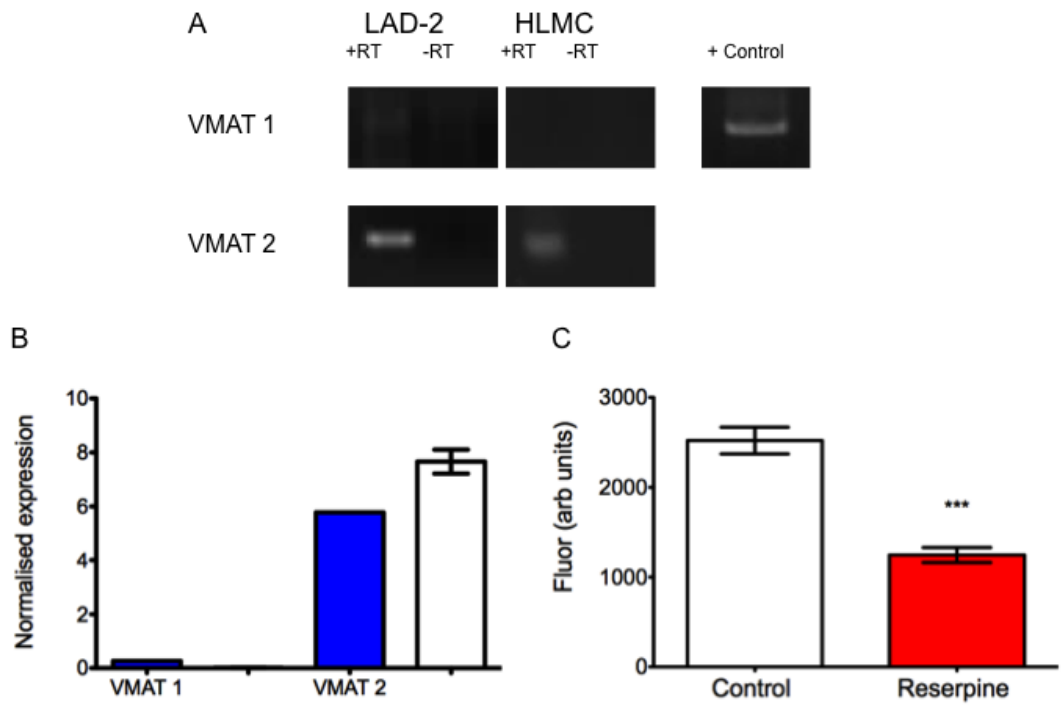

Figure 3.9

FFN511 is loaded into human mast cells granules through VMAT2.

A. RT-PCR analysis of total RNA from LAD 2 and HLMC to determine VMAT expression in human mast cells. A band of the expected size was detected for VMAT 2, while no transcript was detected for VMAT1 in both LAD 2 and HLMC RNA. (+RT) and (-RT) indicated the presence or absence of reverse transcriptase. VMAT1-GFP plasmid was used as a positive control for VMAT1. Data is representative of 3 HLMC donors. **B.** Microarray analysis of VMAT expression in LAD 2 cells and HLMCs produced similar results to that of the RT-PCR. VMAT 2 is the only VMAT expressed in human mast cells LAD 2 mRNA expression from three independent RNA extractions ±SEM. Clear bars represent mRNA expression from one HLMC donor. Blue bars represent LAD 2 mRNA expression from three independent RNA extractions ±SEM. Values are normalised to the 75th percentile. C) Overnight incubation with 1μM reserpine prior to FFN511 loading reduces uptake of FFN511 into LAD 2 cells. LAD 2 cells were incubated overnight with either 1μM reserpine or DMSO as control. Cells were subsequently loaded with FFN511 and fluorescence intensity measured. Data is shown as averaged single cell fluorescence ±SEM. N=3, reserpine n=54 cells, DMSO control n=48 cells. *** Denotes significance of $P<0.001$ unpaired students' T-test.

3.2.5 Stimulation dependent release of FFN511 and characterisation of human mast cell activation

To establish the potential use of FFN511 as an assay for mast cell degranulation and to study LAD 2 secretion, we quantified the effect of known mast cell activators on FFN511 release. 1μM ionomycin, a calcium ionophore widely used to induce mast cell degranulation, was used in addition to the more physiological agonist of the

high affinity FCεRI receptor (Figure. 3.10.). Both stimuli produced a rapid release of dye after application. Ionomycin, known to be a strong activator of mast cells, resulted in 41% stimulated dye loss of FFN511 with 100% of cells responding (N=4, n= 149). FCεRI receptor activation also stimulated rapid dye loss, although as expected, to a lesser degree than that observed with ionomycin, and in fewer cells, with only 33% of cells responding (N=3, n=41 responding cells out of 125 total). No dye loss was observed with either stimulus in nominally calcium free external solution. These experiments indicate that FFN511 is loaded into SGs through VMAT 2 and can subsequently be released through calcium regulated exocytosis.

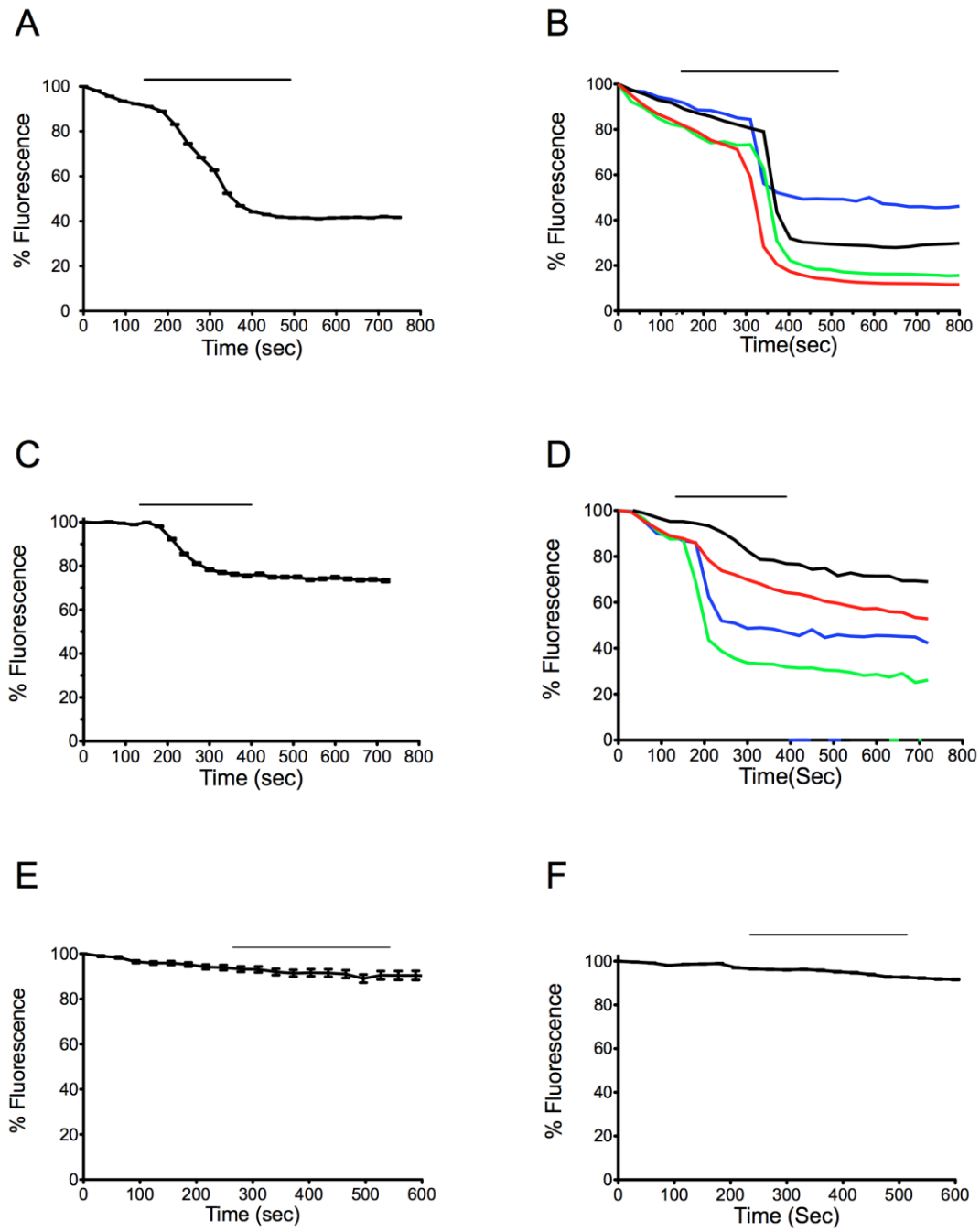

Figure 3.10

Mast cell activators induce FFN511 release from LAD 2 cells.

A. Stimulation with 1µM ionomycin induces a large loss of FFN511 in LAD 2 cells N=4, n= 149. Representative individual cell responses are shown in **B**. **C.** FcεRI induces release of FFN511. LAD 2 cells were sensitised overnight with 300ng/ml of human IgE. FcεRI cross-linking was subsequently induced by perfusion of 10µg/ml anti-IgE N=3 n=41 responding cells (out of a total cell number of 125). Single cell responses to anti-IgE shown in **D**. **E.** Application of ionomycin in calcium free conditions results in no release of FFN511 N=3, n=145. F) FcεRI cross-linking does not induce dye release in calcium free conditions N=3, n=105. Data presented as the mean of % starting fluorescence of individual responding cells ± SEM minus baseline release from an un-stimulated perfusion control normalised to starting fluorescence. All experiments were performed at 32°C.

To compare the activation of LAD 2 cells with a primary cells, FFN511 release following IgE stimulation was also examined in the HLMCs (Figure 3.11). 20% release of dye was induced upon activation with 74% of cells responding, as opposed to 33% of LAD-2 cells (N=3, n=73/104).

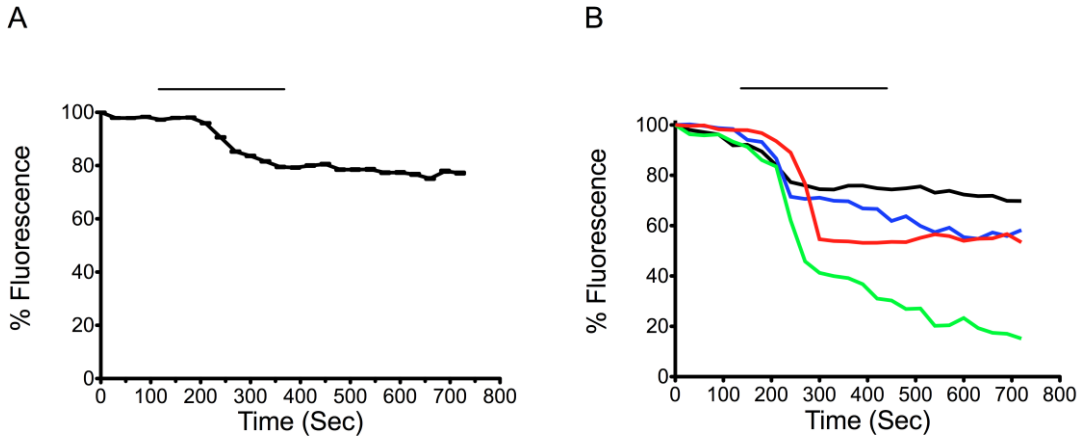

Figure 3.11

HLMC release FFN511 upon FCεRI stimulation.

Release of FFN511 upon FcεRI stimulation was seen in the majority of HLMCs. HLMCs were sensitised overnight with 300ng/ml of human IgE myeloma and cross-linking of FCεRI subsequently induced through the application of anti-IgE. **A**. Grouped and **B** representative single cell responses. N=6 from three separate donors, n=73 responding cells out of 104 total cells. Data presented as mean fluorescence of individual responding cells ± SEM minus baseline release from an unstimulated perfusion control. All experiments were performed at 32°C.

The comparison of LAD 2 and HLMCs FFN511 release in figure 3.12 makes it clear that both LAD 2 cells and HLMCs had a similar level of release of FFN511 when activated but a greater number of HLMCs respond to receptor activation.

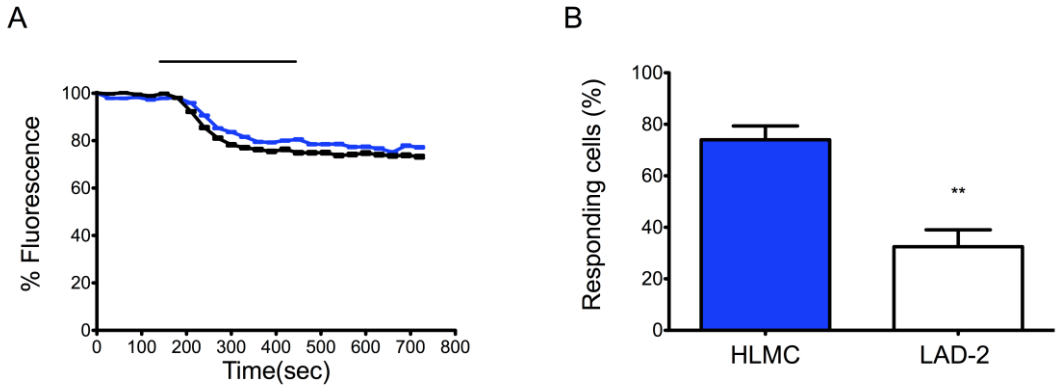

Figure 3.12

Comparison of LAD 2 and HLMC responses to IgE mediated FFN511 release.

A. Overlay of traces show that FFN511 release in LAD-2 cells (black) is similar to release in HLMCs (blue). **B**. A greater proportion of HLMCs (74%) degranulate in response to IgE compared to only 33% of LAD 2 cells. HLMC data represented as the mean ±SEM from 3 separate donors, LAD 2 data represented as mean ±SEM from 3 separate passages. *** Denotes significance of $P<0.001$ unpaired T-test.

3.03 Discussion

The experiments in the current chapter were performed to characterise LAD 2 cells and to determine their suitability as a human mast cell model. To do this mRNA expression levels of mast cell associated receptors and mediators were assessed by microarray and compared to a single HLMC donor. Further assessment of mast cell activation was performed through calcium imaging. Finally, a novel secretion assay using FFN511 was developed and used to assess mast cell degranulation in both LAD 2 cells and HLMCs.

LAD 2 cells were found to express all the relevant mast cell markers tested and compared well with the single HLMC donor. The FCεRI receptor consists of three subunits, all of which were expressed in LAD 2 cells. Interestingly RNA expression of the three subunits was not the same; β was expressed at lower levels than α, while γ had the highest levels of expression. These results are consistent with previous findings [338]. Knockdown of just the γ subunit impairs FCεRI function in BMMCS [349] and the subunit is key for initiation of the downstream signalling events. The FcεRI receptor consists of two γ subunits and one α and β, so it was not a surprise that the γ subunit had the highest expression levels. Low expression levels of the β subunit might be explained by its postulated function as an amplifier of downstream signalling events [350], acting in a supporting role that might have significant redundancy with γ function. The expression of the β subunit might have an additional level of regulation; expression of the subunit mRNA is selectively suppressed through IgE signalling [351], in particular through actions of the src kinases Syk and Fyn, which are expressed at very high levels.

The effects induced by FcεRI are dependent on the Src family kinases, these kinases act at the earliest steps of FcεRI signal transduction. To date several have been shown to be present and functionally important in mast cell signalling, including Syk, Lyn and Fyn [142]. Unlike Fyn and Syk, Lyn expression was low. This was a surprise as it has been heavily implicated in mast cell signal transduction [345]. Lyn associates with the β subunit of the FcεRI receptor, and this association increases upon stimulation [179, 345]. It is interesting to note that the expression of this subunit, almost mirroring that of Lyn expression with the other common mast cell

associated src kinases, was low compared to the expression of the other subunits. Lyn is a key initiator of downstream FcεRI signalling [140]. The relatively low levels of expression of both Lyn and the β subunit of FCεRI might ensure there is no aberrant release of pro-inflammatory mediators, particularly after activation [351].

Alongside FcεRI expression, mast cells are defined by their mast cell granule contents. LAD 2 cells expressed mast cell associated tryptases, MC-CPA, chymase and HDC, the enzyme that catalyses the production of histamine. Both LAD 2 cells and the HLMC donor expressed large amounts of α/β (both are encoded by the *TPSAB1* gene[352]) and γ tryptase mRNA. Of the tryptase subtypes, β-tryptase is the most catalytically active released by mast cells and is thought to exert the majority of effects of mast cell tryptases [353]. Therefore, the high expression levels of α/β seen in the microarray are an expected observation. δ tryptase levels were lower than the other subunits, this subunit has a greatly reduced catalytic activity and might not be as functionally important [354]. γ tryptase is the membrane bound form and its functions are not fully understood, but the high expression levels seen here suggest it might play an important role for mast cells [355]. If γ tryptase remains membrane bound then it might exert pericellular actions, with the diffusible forms acting at more distant sites.

In line with previous studies, LAD 2 cells were found to have mRNA expression of a small amount of chymase [88], and so they represent a MC^{TC} type mast cell. This is opposed to the HLMC donor, where no expression was seen. Chymase expression in HLMCs is not ubiquitous in the lung and can vary significantly depending on their tissue location, with subpopulations of MC^{TC} and MC^{T} existing in specific sites within the lung [356, 357]. The results obtained from the single donor in this study suggest these cells are MC^{T} and most probably from bronchi or bronchioles, where MC^{T} are known to be enriched and are the predominant mast cell type in the lung [357]. What this highlights is the limited comparison of LAD 2 cells with HLMCs that can be drawn from a single HLMC donor where additional experiments would need to be performed on HLMCs to determine whether there is significant variability between HLMC donors and cells extracted from different regions of the lung. Protein expression can differ from mRNA expression and so further experiments assessing protein levels would give a more complete picture of expression levels.

However, from the microarray data and functional data shown in this study it is clear that LAD 2 cells express many mast cell associated factors that correlate well with primary human mast cells. Previous microarrays in human mast cells have provided useful insights and starting points that have subsequently been confirmed by determining protein expression levels. For example Sayama et al found Il-11 up regulation in stimulated cord blood-derived mast cells that was confirmed with an ELISA [358].

This study is the first to explore usage of FFN511 to monitor degranulation in mast cells. FFN511 was able to be loaded into human mast cells and actively released upon stimulation by either ionomycin or FCεRI crosslinking in a calcium-dependent manner. No dye loss was observed with either stimulus in nominally calcium free external solution, indicating that the release of FFN511 is dependent on calcium influx and that the dye is released via calcium-regulated exocytosis, consistent with its accumulation in secretory granules.

FFN511 had a concentration dependent loss of dye that was not due to overloading of the granules (Figure 3.5). FFN511 is lypophilc enough to pass through the PM and so this loss might be from free dye present in the cytoplasm being transported out of the cell. This loss was compensated for in the results by the subtraction of a perfusion control from the data. Both LAD 2 cells and HLMCs expressed VMAT 2 but not VMAT 1. These results are in agreement with previous work identifying VMAT 2 as the vesicle monoamine transporter present in human skin mast cells [38]. The loading and subsequent loss of dye from LAD 2 cells could be the result of a dynamic equilibrium between the extracellular environment, the cytosol and granules involving the vesicle monoamine transporter VMAT 2 and passive transport through the plasma membrane. The fact that the VMAT inhibitor reserpine inhibited uptake of FFN511 supports this view. Only one concentration of reserpine was used, one that has shown to inhibit the uptake of FFNS in PC-12 cell cultures and peritoneal macrophages [348, 359]. A greater inhibition would have most probably been seen if a full dose response to reserpine was performed. The fact that less loss of fluorescence was seen upon overnight storage might be explained by the granular catecholamine storage mechanisms in mast cells. Histamine and serotonin storage in BMMC is dependent on serglycin proteoglycan;

storage of them, as well as proteases, is impaired in serglycin knockout mice but mRNA levels are normal suggesting storage not expression is affected [30, 360]. Also, mast cells lacking the heparan-synthesizing enzyme, N-deacetylase/N-sulfotransferase–2 have reduced histamine content [361]. Storage might occur through a direct interaction with a granule matrix consisting of serglycin proteoglycan, where histamine can directly interact electrostatically with heparin, a glycosaminoglycan that might be attached to the serglycin core present in mast cells [30]. It is possible the positively charged ammonium group in FFN511 interacts with the negatively charged glycosaminoglycan group to hold FFN511 in the granule and overnight incubation increases this association with the granule matrix resulting in less dye loss. Serglycan and the heparan synthesizing enzyme, N-deacetylase/N-sulfotransferase–2 were expressed at high levels in both LAD 2 cells and HLMCS in the microarray data (Appendix figures 5-8)

In this study similar levels of FFN511 release were seen in individual HLMCs compared to LAD 2 cells but a larger proportion of HLMCs underwent degranulation (74% compared to 33%). Previous work has shown that LAD 2 cells exhibit a lower level of mediator release upon FCεRI stimulation than primary skin mast cells [90]. The results shown here suggest that greater release seen with primary mast cells is due to a greater proportion of cells undergoing degranulation. This observation implies that individual LAD 2 cells show heterogeneity in their ability to degranulate in response to FCεRI crosslinking. Phenotypic heterogeneity within *in vitro* cell cultures is common [362] and is likely to arise through differences within a culture of cell cycle stage and length, degree of cell death and concentration gradients of growth factors/nutrients. One would expect these to be more pronounced within a cell line population showing a faster growth rate and longer duration in culture than its primary counterparts. Variation can also be seen in the release of FFN511 in individual responding cells within a culture. Populations of both LAD 2 cells and HLMCs responded to IgE stimulation to varying degrees (Figure 3.6D and 3.7B). This variation in release is not seen to such a great extent in the non-receptor mediated release induced by ionomycin, suggesting that the majority of cells are capable of releasing mediators to the same extent, but variations in receptor and the downstream signalling pathways as well as factors described above contribute to the diversity in response to physiological stimuli.

Hints as to how the difference in release might occur can be drawn from the microarray data. Similar levels of FCεRI subunit expression were seen in the LAD 2 cells and HLMCs; either all individual LAD 2 cells and HLMCs express similar amount of the FCεRI receptor, or some LAD 2 cells might express very high levels while others within the same culture express very low amounts leading to an overall similar levels of expression. The functional data obtained from the FFN511 assay shows a much greater heterogeneity in the ability of LAD 2 cells to degranulate in response to receptor mediated stimulation. The calcium imaging results show that the majority of LAD 2 cells produce a calcium response to FCεRI crosslinking, proving nearly all LAD 2 cells are expressing functional FCεRI to some extent. Unfortunately it wasn't possible to perform dual FFN511 and Fura 2 calcium imaging, due to significant overlap of the excitation and emission spectra. This would have answered the question of whether there is a correlation of the size of the calcium rise to the level of release.

Fyn kinase acts through a signalling pathway complementary to that of Lyn and Syk,[343]. Fyn deficiency, although impairing degranulation, does not affect Lyn downstream signalling or intracellular calcium release in mast cells (Parravicini et al., 2002[363]. Fyn might connect IgE stimulation of FCεRI to the trafficking of TRPC channels to the plasma membrane to permit full extracellular calcium entry, and mediate microtubule-dependant translocation of granules to the plasma membrane [344, 364]. Fyn was expressed at much lower levels in the LAD 2 cells and this might explain why the majority of LAD 2 cells have a calcium response to FCεRI activation but at levels lower than that of HLMCs, and why they do not have such high levels of release of FFN511 as HLMCs. LAD 2 cells expressed the majority of factors associated with granule matrix proteoglycans involved in storage of histamine and proteases that were expressed in the HLMC donor (Appendix figures A5-A8) and so at least at the mRNA level LAD 2 cells express mature granule markers and should be capable of storing granule mediators.

One caveat to conclusions drawn from the FFN511 experiments is that both LAD 2 and HLMCs were actively loaded with FFN511, and if both cells transport the dye through the same mechanism then it might be expected that they would release the

same amount of dye upon activation, as both could load the same amount of dye into their granules. The data in the microarray suggest that granule mediators might be present at lower levels in LAD 2 cells, so this artificial system might be obscuring the fact that individual LAD 2 cells do release fewer amounts of granule mediators as well as having a reduced response. The most likely explanation is a combination of both leading to a response that is lower than that of primary mast cells.

To conclude, the above results show that LAD 2 cells express all the relevant mast cell markers and can respond to antigen stimulation, but there are some potential differences that need to be taken into consideration when interpreting results. For example the FFN511 assay showed lower numbers of LAD 2 cells are able to undergo degranulation in response to FceRI receptor crosslinking and data from the microarray suggests they have potentially lower expression levels of mediators.

Chapter 4: Identification of SNARE proteins in human mast cells

4.1 Introduction

SNARE proteins are key in driving the fusion of two opposing membranes. Work in animal models has made it clear that SNARE proteins are important in the fusion of SGs with the plasma membrane in mast cells [234, 235, 238]. Only two studies have assessed SNARE proteins involved in inflammatory mediator release in human mast cells, using only HGMCs [239, 240]. No attempt has been made to define the SNARE proteins present in other human mast cells, including LAD 2 cells and HLMCS.

The aim of the current set of experiments was to identify the SNARE and SNARE interacting proteins present in human mast cells, with particular focus on VsPs. A microarray was performed on LAD 2 cells and RNA from a single HLMC donor to determine expression of all SNAREs and SNARE interacting proteins. Expression of 4 VAMP isoforms expressed at the highest levels in LAD 2 cells were then confirmed through qPCR. Finally, protein expression and localisation with mediators and organelle markers were examined using western blotting and immunostaining.

4.2 Results

4.2.1 Assessment of SNARE protein expression in HEK and LAD 2 mast cells through RT-PCR

Initial experiments set out to determine SNARE protein mRNA expression in mast cells using RT-PCR. VAMP-2, -3, -7 and -8, SNAP-23 and -25 and syntaxin 1-6 have been implicated in exocytosis in a number of secretory cell types, including mast cells [239, 365] and so this provided a logical starting point in determining SNARE expression in LAD 2 cells. In order to identify SNARE proteins whose expression is less ubiquitous and therefore more likely to be important in regulated secretion of mast cell SGs, data obtained from mast cells was compared with that from HEK cells, a non-haematopoietic endothelial derived cell line. Both cell lines showed expression for the majority SNAREs examined with bands at the expected molecular weight markers (Figure 4.1 and 4.2). One result that was expected was the lack of expression of the neuronal SNAP-25 in LAD 2 cells, present in the human brain control cDNA (Figure 4.1 and 4.2). Syntaxin 1a mRNA had a different band size in HEK and LAD 2 cells than in the human brain control cells, having a higher molecular weight than that for the human brain control. This might represent the alternative spice variant of syntaxin, known as syntaxin 1c [366], as the syntaxin 1a primers used in this study do not differentiate between the two. For syntaxin 1b in both LAD 2 cells and HEK cells a faint band was present in the –RT control. This makes it hard to draw any conclusions for the expression of syntaxin 1b using this data as it is possible there was contamination of that particular well. Overall, these results did not give much insight on any potential mast cell specific SNAREs as expression was similar for HEK and LAD 2 cells.

RT-PCR for the 4 VAMPs, SNAP-23 and SNAP-25 was also performed on HLMC mRNA to compare with the cell line data. Unlike LAD 2 cells, no VAMP-2 was expressed, while other SNAREs had a similar pattern of expression; SNAP-25 could not be detected and VAMPs-3, -7 and -8 and SNAP-23 were present (Fig.4.3). Bands appeared fainter than in LAD 2 or HEK cells but the same amount of RNA was used for all experiments (1μg) and so this was not due to the amount of RNA present. There were also variations in intensity's of different SNAREs within samples but

this technique is not quantitative and so it is impossible to draw conclusions from this.

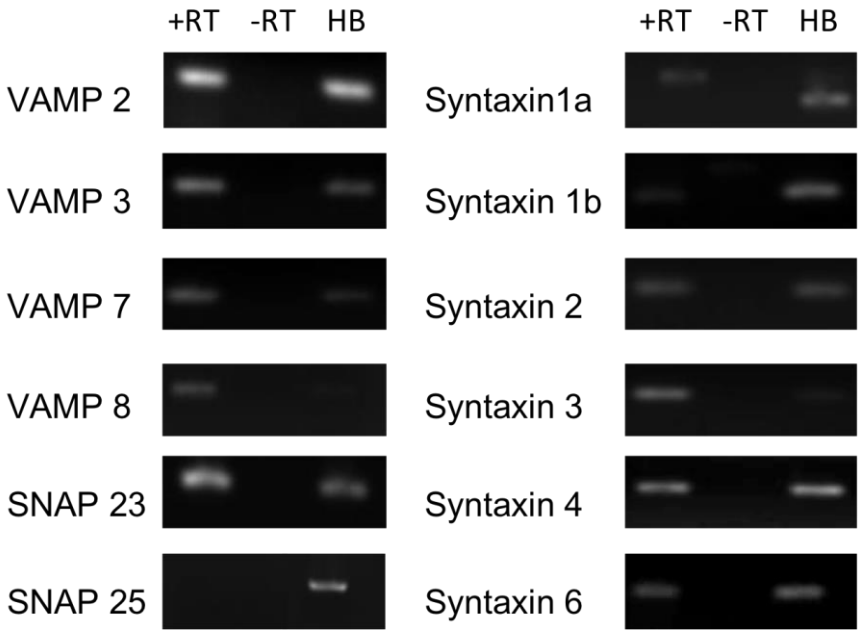

Figure. 4.1

SNARE mRNA expression in LAD 2 human mast cell line.

Non-quantitative RT-PCR of 12 of the 36 mammalian SNAREs present shows that the mRNA of all tested SNAREs apart from the neuronal SNAP-25 are present in the LAD 2 cell line. RT = Reverse transcriptase. HB = Human brain cDNA control. N=3.

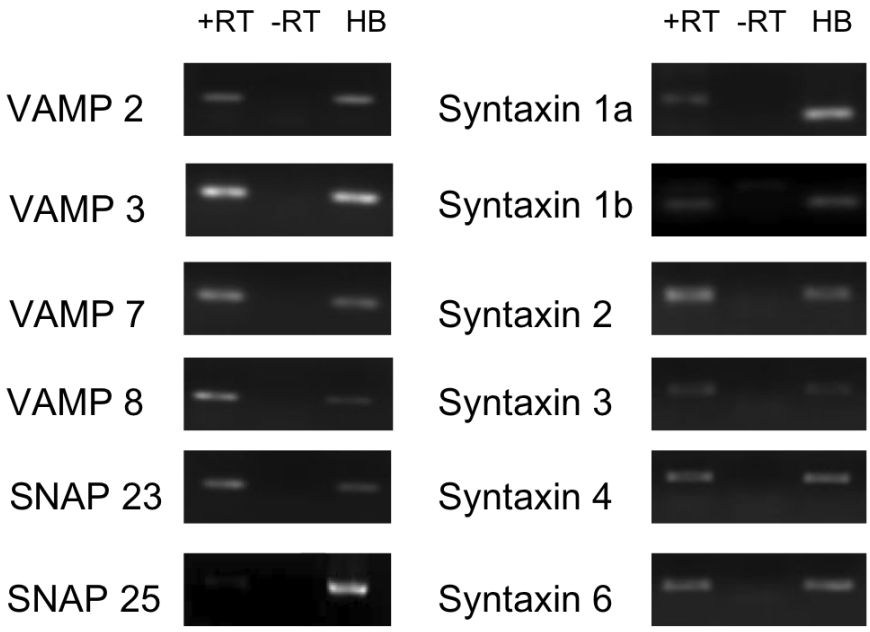

Figure. 4.2

SNARE mRNA expression in HEK293 cells.

Non-quantitative RT-PCR of 12 of the 36 mammalian SNAREs present shows that the mRNA of all tested SNAREs apart from the neuronal SNAP-25 are present in the HEK cell line. RT = Reverse transcriptase. HB = Human brain cDNA control. N=3

Figure. 4.3

SNARE mRNA expression in HLMCS.

Non-quantitative RT-PCR of 4 VAMPs and the two plasma membrane residing Qbc SNAREs SNAP-23 and 25 shows that the mRNA of all tested SNARE apart from the neuronal VAMP-2 and SNAP-25 are present. RT = Reverse transcriptase. Data representative of 3 HLMsdonors.

4.2.2 Microarray identification and comparison of SNARE protein expression in human mast cells.

The results obtained from RT-PCR alone do not faithfully represent relative levels of expression of these genes, just that they are transcribed to some extent. Furthermore, there are many more SNAREs that might be expressed that were not tested through RT-PCR. Therefore, to identify the expression pattern of all SNAREs, a microarray analysis was performed to assess gene expression levels of the syntaxins, SNAPS and VAMPs in LAD 2 cells and in a single HLMC donor.

Syntaxin expression in LAD 2 cells and the HLMC donor correlated well with each other. In LAD 2 cells syntaxins 3 and 4 were the predominant syntaxins, as they were in the HLMC donor, although there were not expressed to such a great extent (figure 4.4). A number of other syntaxins showed an intermediate level of expression, including syntaxins 8, 10 and 16 in both LAD 2 cells and HLMCs (figure 4.4). The neuronal syntaxin 1a was expressed in both mast cells but at higher levels in the HLMC donor, while syntaxin 1b was not expressed. This does not match up with the RT-PCR data showing syntaxin 1b expression but the possible contamination of the sample, as seen by a faint band in the –RT control, might explain this discrepancy. Further work was not performed on syntaxin expression in this study but western blot of protein levels would give a more definitive answer.

Of the Qbc SNARE, surprisingly, SNAP-23 was not expressed at very high levels in either LAD 2 cells or HLMCS (figure 4.5)s. It has been heavily implicated in mast cell exocytosis in studies on HGMCs [239], and in RBL-2H3 cells qPCR has shown SNAP-23 mRNA levels to be high [365]. The neuronal isoform, SNAP-25, had very low levels of expression in two out of the three RNA extractions for LAD 2 cells, but was expressed at higher levels in one sample (this can be seen in the larger error bars) resulting in an overall similar expression level to SNAP-23. In HLMCs it was the lowest expressed Qbc SNARE, which was similar to the two LAD 2 extractions and suggests that the single extraction in LAD 2 cells producing the higher expression of SNAP-25 was an anomaly. This does highlight the need for further repeats of the HLMC donor for future experiments to produce a more reliable result. The RT-PCR data showed no SNAP-25 mRNA expression suggesting that SNAP 25 does not have an important role in mast cells, and the differences in the resuts might be due to a

greater sensitivity of the microarray. Out of all the Qbc SNAREs, SNAP-47 had by far the greatest levels of expression. It does not have a defined role in mast cells and very little is known about its function, but given the high expression levels it might have an important role, possibly in channel trafficking, which is discussed in detail in section 4.3.

VAMPs are present on vesicles, such as those containing inflammatory mediators and so were of particular interest. VAMPs showing high levels of expression might define these vesicles. VAMP-8 had the greatest levels of expression of all SNAREs monitored whilst VAMPs-2, -3 and -7 were expressed at intermediate levels. As with SNAP-25, VAMP-2 was not detected in RT-PCR in HLMCs but was in the microarray. Similarly to SNAP-25 this could be due to a greater sensitivity of the microarray. The neuronal VAMP-1 was not expressed in either cell and highlights the limited expression of neuronal SNAREs in mast cells. The more ubiquitously expressed VAMP-4 and the VAMP mostly enriched in muscle, VAMP-5, had low expression levels in LAD 2 cells. However, in HLMCS, VAMP-5 was expressed at a much higher level. This might be due to a small amount of contaminating cells expressing VAMP-5 at very high levels. The samples contained over 99% HLMCs (section 2.3), so there would still be a small amount of contaminating cells, VAMP-5 has an identified role in myogenesis [367] and possibly with only a few contaminating cells, if it is highly expressed, it might result in expression on the microarray. Despite this difference the expression pattern of the other VAMPs was similar between LAD 2 cells and HLMCS.

To summarise, the microarray data suggests that human mast cells express, at the mRNA level, a number of SNARE isoforms. Syntaxins 3 and 4 are expressed to greatest extent out of all syntaxins, while VAMP-8 is the predominantly expressed VAMP. Finally, results in the LAD 2 cells mirror closely the expression patterns of SNAREs in the HLMC donor.

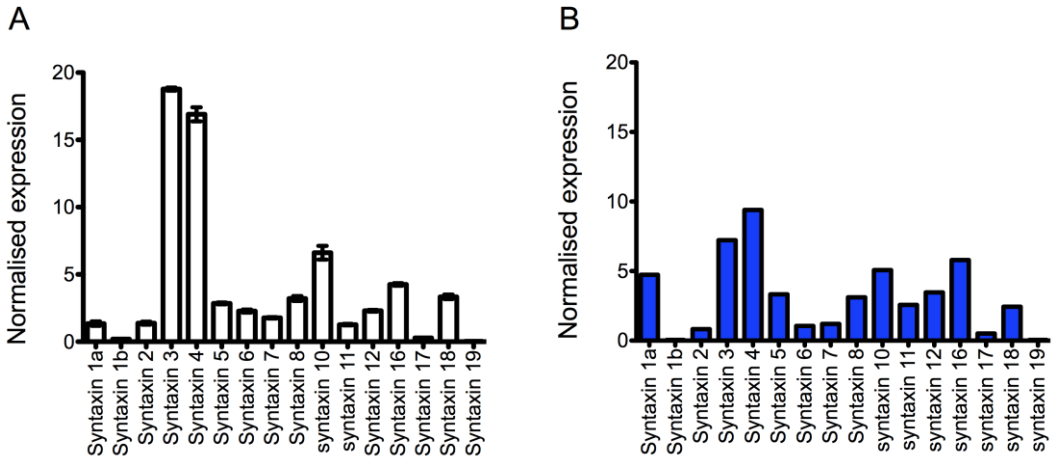

Figure. 4.4

Human mast cells express multiple syntaxins

Syntaxin 3 and 4 are expressed at much greater levels than other syntaxins in LAD 2 cells and are also have the greatest expression in HLMCS. Gene expression values were normalized to the 75th percentile according to Agilent instructions. **A**. Clear bars represent LAD 2 mRNA expression from three independent RNA extractions ±SEM**. B**. Blue bars represent mRNA expression from one HLMC donor

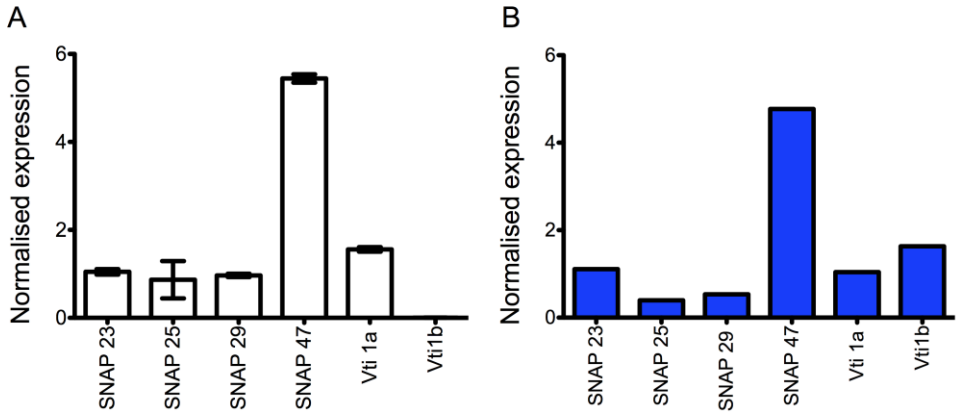

Figure. 4.5 Qb and bc SNARE expression in LAD 2 cells.

SNAP-47 has the highest levels of expression. Gene expression values were normalized to the 75th percentile according to Agilent instructions. **A**. Clear bars represent LAD 2 mRNA expression from three independent RNA extractions ±SEM. **B**. Blue bars represent mRNA expression from one HLMC donor

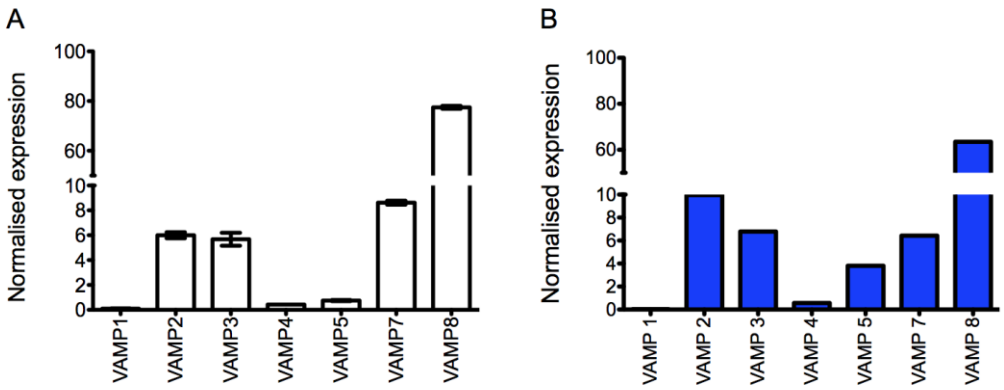

Figure. 4.6

VAMP mRNA expression

VAMP-8 was expressed at the greatest extent out of all SNAREs monitored. Gene expression values were normalized to the 75th percentile according to Agilent instructions**. A.** Clear bars represent LAD 2 mRNA expression from three independent RNA extractions ±SEM. **B**. Blue bars represent mRNA expression from one HLMC donor

4.2.3 QPCR characterization of VAMP-2, 3, 7 and 8

Experiments in this section set out to confirm microarray and RT-PCR results and further define VAMP mRNA expression in LAD 2 cells using qPCR. Results of the microarray experiment identified VAMPs-2, -3, -7 and -8 as the main VAMPs present in LAD 2 human mast cells. These SNARE were alsso expressed at high levels in HLMCs. To validate the results obtained from the microarray qPCR was performed to determine relative levels of VAMPs-2, 3, 7 and 8 in LAD 2 and HEK cell lines. HEK cells were used as a comparison as they are non-haematopoietic and have limited regulated exocytosis but a developed constitutive secretory pathway. Any VAMP expressed at much greater levels in the LAD 2 cells could give clues as to any VAMP important in SG release and VAMPs with similar levels of expression might be important in constitutive trafficking. VAMP-5 was expressed at levels similar to VAMP-7 in the HLMC donor, but given the low expression levels in LAD 2 cells and the identified functional role of VAMP-5 in myogenesis [367] further work concentrated on VAMPs-2, -3, -7 and -8.

Results showed that VAMP-8 mRNA is present at considerably higher levels in LAD 2 cells compared to HEK, as well as being expressed at much higher levels than any other VAMP tested in the LAD 2 cell line (Figure 4.7). This result mirrors the

microarray data and the literature identifying this SNARE as a key component of SGs in human mast cells [239]. VAMP-3, as in the microarray, was expressed at intermediate levels and was expressed at the highest levels out of all four VAMPs in HEK cells. The expression of VAMPs-2 and -7 were similar to VAMP-3, although they had slightly lower levels of expression.

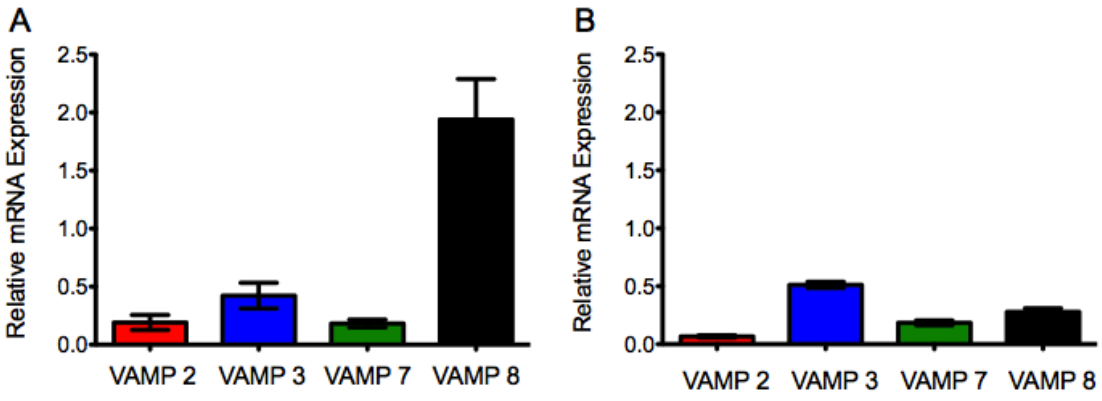

Figure. 4.7

Relative QPCR of VAMPs in LAD 2 and HEK cells.

A. Relative expression levels of VAMPs in LAD 2 cells: VAMP-8 is expressed at very high levels compared to any other VAMP measured. **B**. Relative expression levels of VAMPs in HEK cells: VAMP-3 is expressed at a much higher levels than any other VAMP. mRNA levels were normalized to U1 snRNA to obtain relative expression levels. Data is presented as ±SEM from 3 separate RNA extractions.

Having determined the levels of mRNA expression of VAMPs-2, -3, -7 and -8 through qPCR further experiments were performed to assess whether VAMP expression changes when mast cells become activated. Upon mast cell FcεRI activation numerous genes associated with the inflammatory response become up-regulated [368]. To evaluate possible activation regulated VAMP mRNA expression, VAMP mRNA was measured at specific time points following FcεRI stimulation of LAD 2 cells (figure 4.8a). After two hours all mRNA expression increased in the four VAMPs, although VAMP-2 expression increase was minimal. VAMP-7 levels increased 4-fold, the most out of the four, while VAMP-3 and -8 increased 2 and 3 fold respectively. At 6 hours post stimulation expression started to return to resting levels. Further analysis of FcεRI SNARE regulation was assessed using the microarray data. LAD 2 cells and cells from the same HLMC donor were stimulated fby FcεRI crosslinking for the time point (two hours) which produced the largest increase in VAMP expresssion in qPCR. Changes in VAMP expression were less

prominant, only small changes in VAMP-7 and VAMP-8 were apparant in both LAD 2 cells and the HLMC donor. However, SNAP-23 expression increased 4 fold in stimulated HLMCs and a number of syntaxins also increased in expression, including syntaxins 2, 8 and 9.

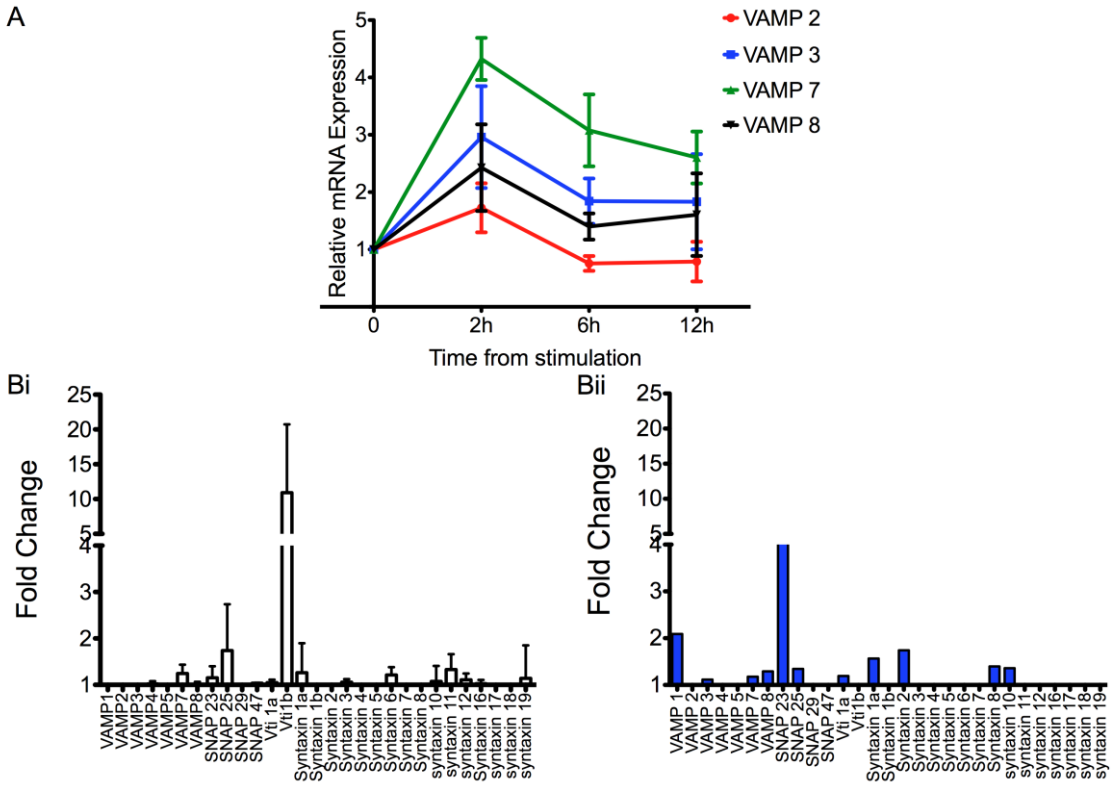

Figure. 4.8

mRNA expression of VAMPs increases after stimulation through IgE receptor crosslinking.

A. LAD 2 cells were incubated overnight with 300ng IgE. Receptor crosslinking was induced through the application of anti-IgE and RNA extracted at the stated time points post stimulation. Data is presented as ± SEM from 3 separate RNA extractions. mRNA levels were normalized to U1 snRNA to obtain relative expression levels. Values at the time points shown were normalised to time point 0.

B.i. LAD 2 cells and, **ii**, single HLMC donor were stimulated for two hours by FcεRI crosslinking, the time at which VAMP expression reached its maximum in A, and mRNA harvested. mRNA levels of SNARE proteins assessed using microarray analysis. Values represent fold change of stimulated cells compared to non-stimulated cells of same passage number (LAD 2 cells N=2) or same donor (HLMC N=1).

These set of results confirm that VAMP-8 is the predominant VAMP in human mast cells and its high level of expression is not replicated in a non-haematopoietic immune cell. VAMP-3 is expressed at intermediate levels in LAD 2 cells and in HEK cells and so might represent a VAMP isoform important for constitutive secretion, given the expression levels in a cell with high metabolic activity. In addition VAMPs

show stimulation dependent increases in expression when activated through the FCεRI receptor.

4.2.4 Protein expression of VAMPs-2, -3, -7 and -8

In the above experiments, expression of SNARE proteins had only been assessed at the mRNA level. mRNA expression does not always correlate well with protein expression and so to determine protein expression of VAMPs-2, -3, -7 and -8 western blotting was used (Figure 4.9). No expression was seen for VAMP-2 in either LAD 2 cells or HLMCS, but clear bands were seen for VAMPs-3, -7 and -8 at the expected molecular weights, although in LAD 2 cells there was an additional band using the VAMP-8 antibody. The size of the band (below 26kda) is similar to double the molecular weight of the native protein (11.5kda) and might be a VAMP-8 dimer or VAMP chaperone protein. This was not present in HLMCs, this discrepancy might be due to higher turnover of LAD 2 cells, a dividing cell line. Although confirming findings in previous studies showing no VAMP-2 protein expression, this result does not correlate with the microarray results showing VAMP-2 mRNA expression. The possible reasons for this are described in section 4.3.

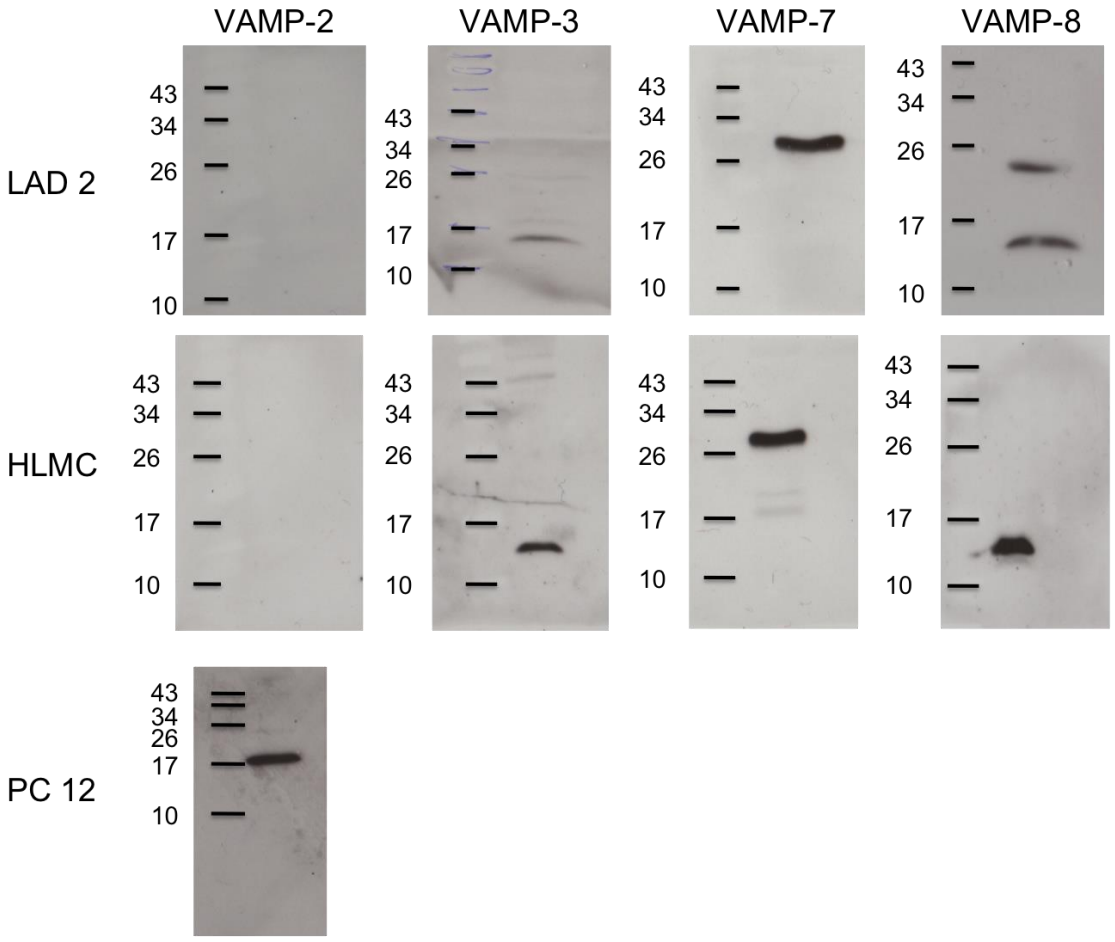

Figure. 4.9

Western blot of VAMPs-2, 3 and 8 in LAD 2 cells and HLMCS

Western blotting confirmed LAD 2 cell and HLMCS express VAMP-3, -7 and VAMP-8 but do not express VAMP-2 protein. PC12 cells are a neuronal cell line, the lysate used as a positive control for the VAMP-2 antibody. Positions of marker proteins run parallel are given.

4.2.5 Localisation and trafficking of VAMPs

Having confirmed expression of VAMPs-3, -7 and -8 through western blotting and mRNA analysis the next set of experiments set out to determine the localisation of these VAMPs within the mast cell. VAMP-2 was not assessed as no protein was detected in western blot despite mRNA being present.

Mast cells contain large amounts of tryptase within their SGs and so this is commonly used to identify SGs in co-immunostaining studies [369]. Immunostaining of VAMPs-3, -7 and -8 with tryptase was performed to identify the VAMP localising to SGs. In LAD 2 cells VAMP-8 colocalised with tryptase while small amounts of VAMP-7 colocalised. VAMP-3 was observed in vesicular structures but did not colocalise with tryptase (Figures 4.10 and 4.11).

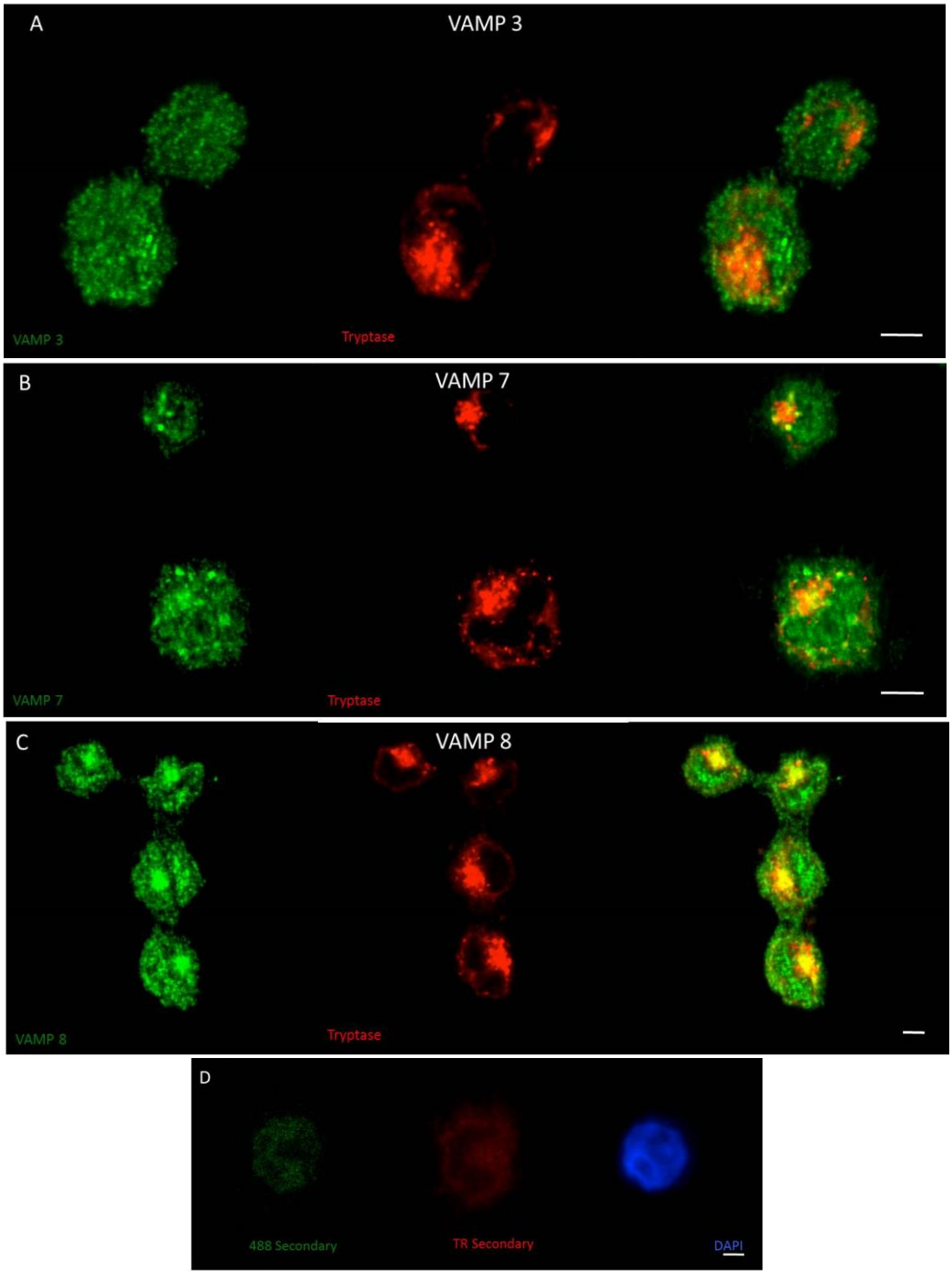

Figure. 4.10

VAMP-8 and VAMP-7 colocalise to the mast cell granule marker tryptase.

LAD 2 cells were labelled using antibodies to VAMP-3, -7 and -8 (Green) and co-stained with anti-tryptase (Red). **A**. VAMP-3 and tryptase. **B**. VAMP-7 and tryptase. **C**. VAMP-8 and tryptase in LAD 2 cells. **D**. Cells incubated with secondary antibodies alone and imaged using the same acquisition settings, excited at 488 and 568nm. Scale bars represent 5μm.

VAMPs present on vesicles whose contents will be released upon stimulation would be expected to translocate to the plasma membrane following fusion. Previous

studies have shown VAMP-8 trafficking to the plasma membrane in ionomycin activated HGMCs but not VAMP-3 [239]. To identify whether this was also the case in LAD 2 cells, cells were stimulated with either the calcium ionophore, ionomycin, or through FcεRI crosslinking and then fixed and processed for immunostaining. Intensity values across cells were measured to determine the distribution of each VAMP (figure 4.11 Aii and Bii). Ionomycin is known to produce high levels of granule mediator release in mast cells and it was clear that this secretagogue also stimulated translocation of VAMP-8 to the periphery of the cell upon stimulation. Intensity values peaked at the edge of cells compared to a more even distribution in un-stimulated cells. VAMP-3 also distributed to the membrane, again seen by the measured intensity values across the cell. Stimulation through FceRI did not produce such pronounced trafficking and the results were inconclusive (Figure 4.11).

To determine whether VAMP trafficking was similar in HLMCS, HLMCS were co-stained with VAMP-3 or VAMP-8 and tryptase. As with LAD 2 cells, VAMP-8 co-localised with tryptase, VAMP3 did not (Figure 4.12). In HLMCS a much clearer response was seen in the trafficking of VAMP-3 and VAMP-8 in stimulated cells, with both VAMP-3 and VAMP-8 vesicles trafficking to the plasma membrane following stimulation with either ionomycin or FcεRI crosslinking in the majority of cells (Figure 4.13.). In HLMCs VAMP-3 positive vesicles were larger and more punctate than VAMP-8. This was not the case in LAD 2 cells and might be indicative of the cell line representing a less mature cell that its primary counterpart, not containing fully developed compartments.

The time course of 20 minutes was chosento monitor trafficking of VAMPs involved in regulated release as upon stimulation mast cells secrete preformed mediators for up to 20 minutes post stimulation and recycling of SGs can take hours [370]. Any VAMP involved in this pathway would have reached and remained at the plasma membrane in this time. What these results do not show is the trafficking of any SNAREs mediating the fusion of vesicles carrying newly synthesised mediators, or any compartments possibily storing pre-formed cytokines that might undergo more rapid fusion and endocytosis. A time course post stimulation covering a shorter and longer time period might enable visualisation of these.

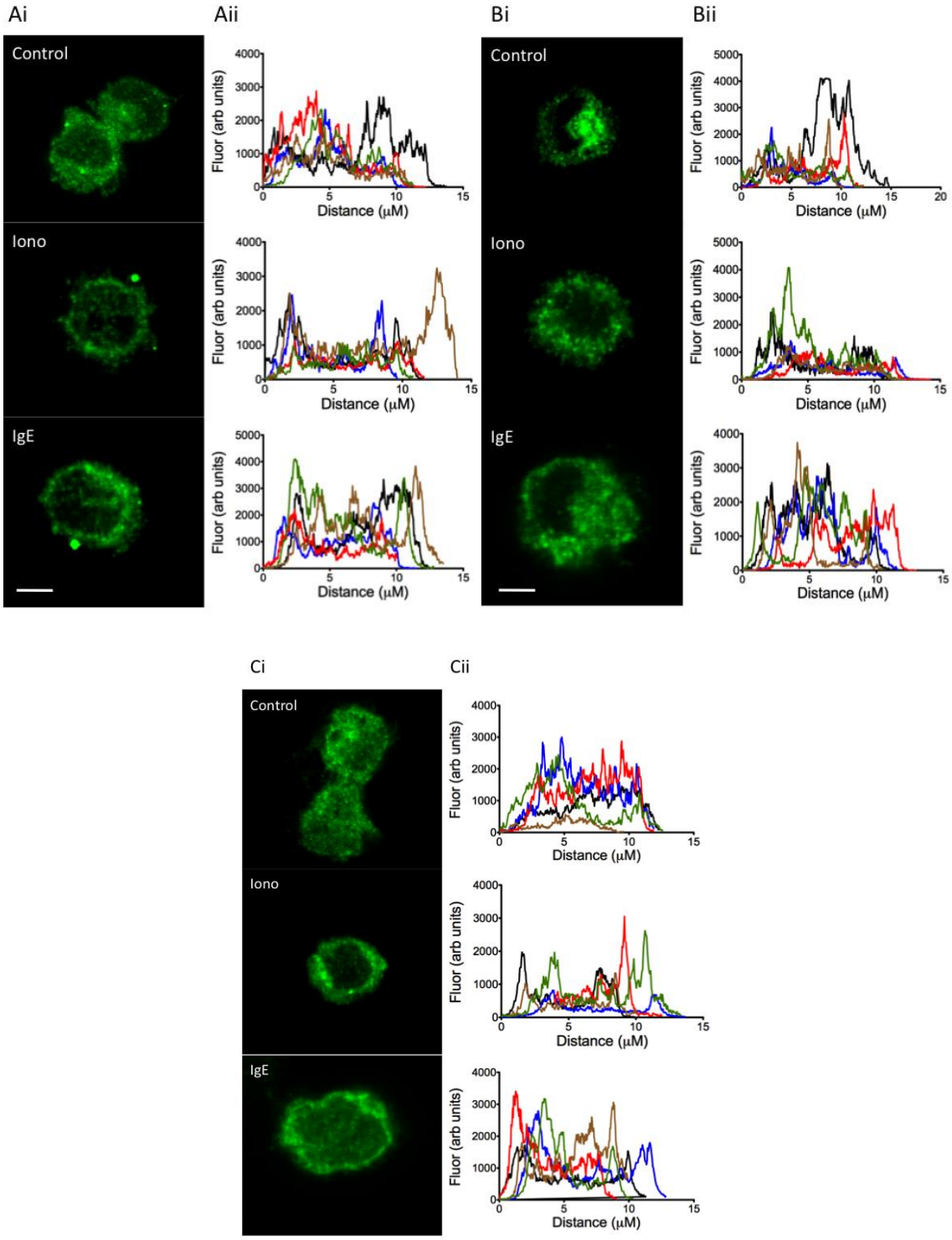

Figure. 4.11

VAMP-3 and VAMP-8 traffic to the membrane upon stimulation in LAD 2 cells

LAD 2 cells were stimulated with either 1μM ionomycin or 10μg/ml Anti-IgE for 20mins then fixed and stained for either **A**. VAMP-3, **B**. VAMP-7 or **C** VAMP-8 to assess trafficking of these SNAREs to the plasma membrane. Figures **Ai, Bi** and **Ci** are representative of experiments performed 3 times. Figures **Aii, Bii** and **Cii** show superimposed, intensity values cross-sections from multiple cells. Scale bars represent 5μm. Cells were selected at random.

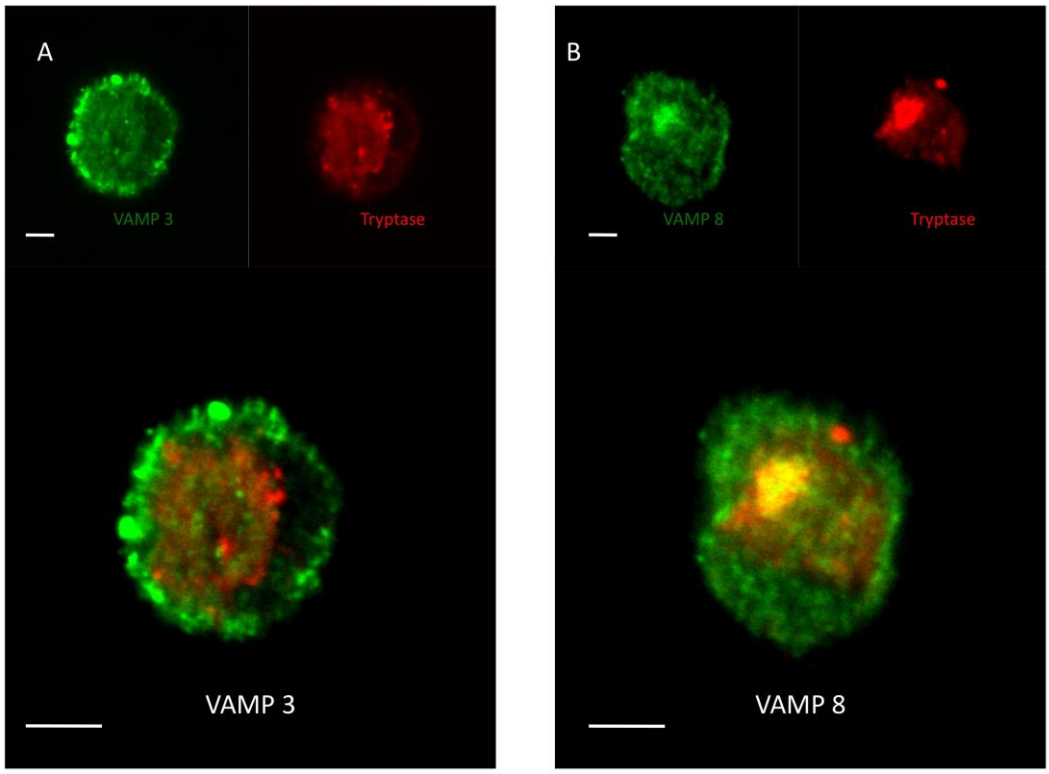

Figure. 4.12

VAMP-8 colocalises to the mast cell granule marker tryptase in HLMCs.

HLMCS were labelled using antibodies to VAMP-3 and -8 and co-stained with anti-tryptase. **A.** Expression of VAMP-3 and tryptase. **B.** Expression of VAMP-8 and tryptase. Scale bars represent 5μm. Data representative of 3 donors.

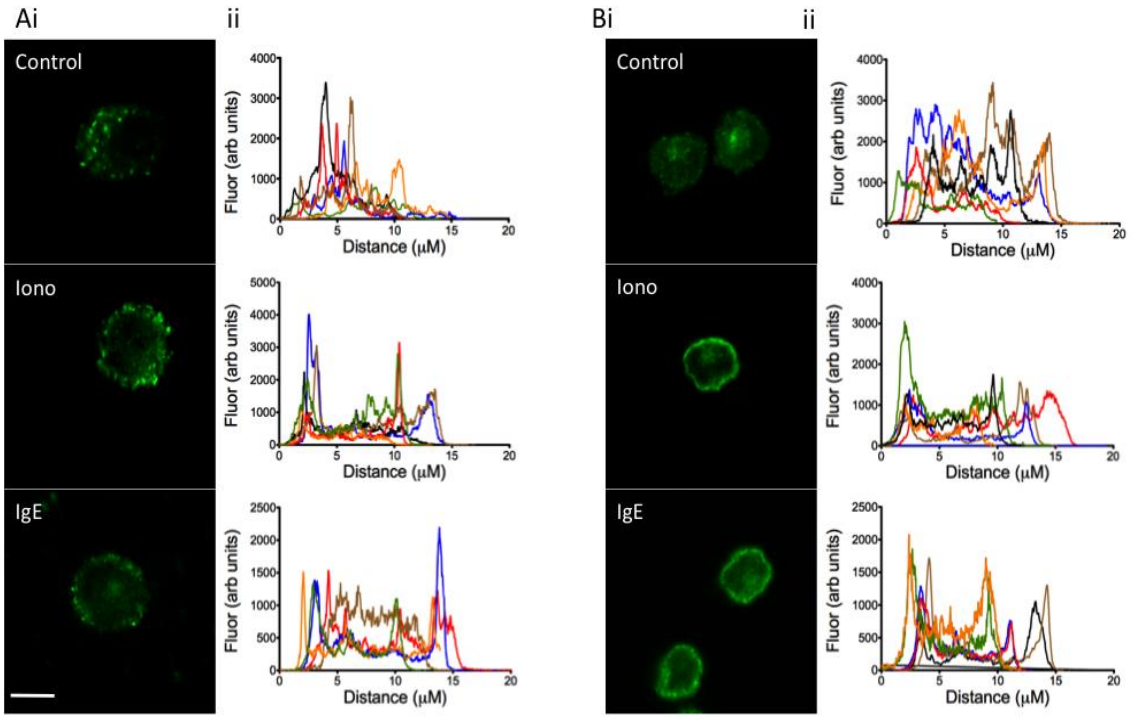

Figure. 4.13

VAMP-3 and VAMP-8 traffic to the membrane upon stimulation in HLMCS

HLMCS were stimulated with either 1μM ionomycin or 10μg/ml Anti-IgE for 20mins then fixed and stained for either **A**. VAMP-3 or **B**. VAMP-8 to assess trafficking of these SNAREs to the plasma membrane. Figures of HLMCS in **Ai** and **Bi** are representative cells of experiments performed in 2 donors. Figures **Aii** and **Bii** show superimposed intensity values across multiple cells. Scale bars represent 5μm.

Although present in mast cells, the above experiments show that VAMP-3 does not localise to tryptase. VAMP-3 resides in the recycling endosomal compartment in macrophages, Il-6 and TNF-α have been shown to reside within [182, 371] and the release of these mediators is directed through this compartment. In mast cells a similar system might be present by which mast cells release certain cytokines. Therefore, to assess potential localisation of VAMP-3 to the recycling endosomal compartment in mast cells, localisation of VAMP-3 with rab11, a recycling endosome marker [372], was examined in LAD 2 cells.

Imaging of fixed cells, indicate VAMP-3 does co-localise to some extent with rab11 while VAMP-8, previously shown to localise to tryptase-positive granules, did not

(Figure 4.14). LAD 2 cells were subsequently transfected with a chimera of IL-6 and GFP to determine whether this modified cytokine also localises to recycling endosomes labelled with rab11. A representative image from a transfected cell is shown in Figure 4.15, as can be seen the GFP tagged IL-6 co-localizes with rab11 positive structures but not with mast cell granules labelled with anti-tryptase. It was not possible to perform dual staining of IL-6 GFP and VAMP-3 due to antibodies of the two being of that same species. Future experiments using another set of antibodies will provide more conclusive evidence as to whether VAMP-3 colcalises with Il-6. However, these results suggest VAMP-3 localises to the same subcellular compartment as IL-6, defined by rab11.

The results show VAMP-8 and to some extent VAMP-7 colocalise with the mast cell granule marker tryptase, while VAMP-3 does not but localises to a rab11 positive compartment, as does an overexpressed IL-6 construct. In LAD 2 cells VAMP-3 and VAMP-8 vesicles traffic to the plasma membrane upon stimulation with ionomycin but VAMP-7 does not, while trafficking of VAMPs upon stimulation of the FcεRI receptor is inconclusive, possibility due to LAD 2 cells producing a small degranulation response to FcεRI crosslinking (see FFN511 results in chapter 3). However, in HLMCs both VAMP-3 and VAMP-8 traffic to the plasma membrane upon stimulation with either ionomycin or FcεRI.

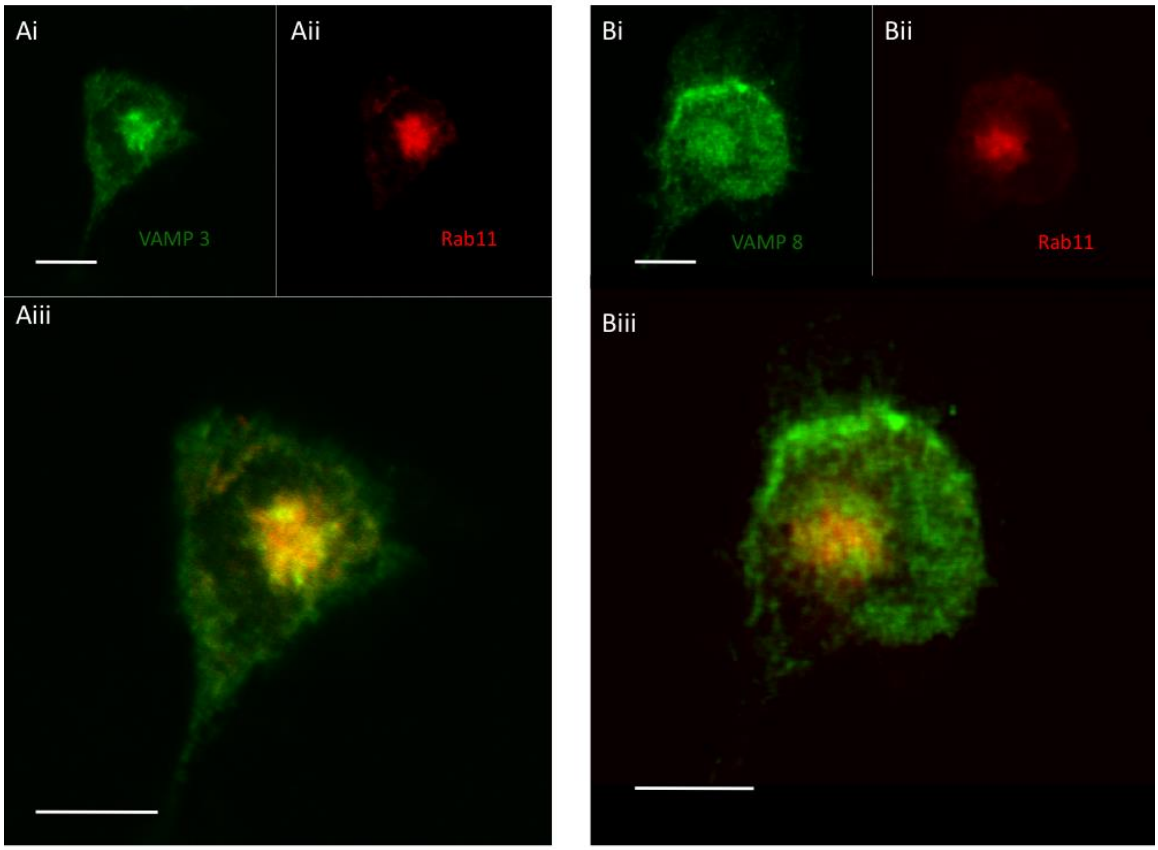

Figure 4.14

VAMP-3 colocalises to recycling endosomes in LAD 2 cells

LAD 2 cells were labelled using antibodies to VAMP-3 and VAMP-8 (green) and co-stained with anti-rab11 (red). **A**. VAMP-3 labelled cells, **i**, VAMP-3, **ii**, rab11 and **iii** overlaid image. **B**. VAMP- labelled cells, **i,** VAMP-8, **ii**, rab11 and iii overlaid image. Scale bars represent 5μm.

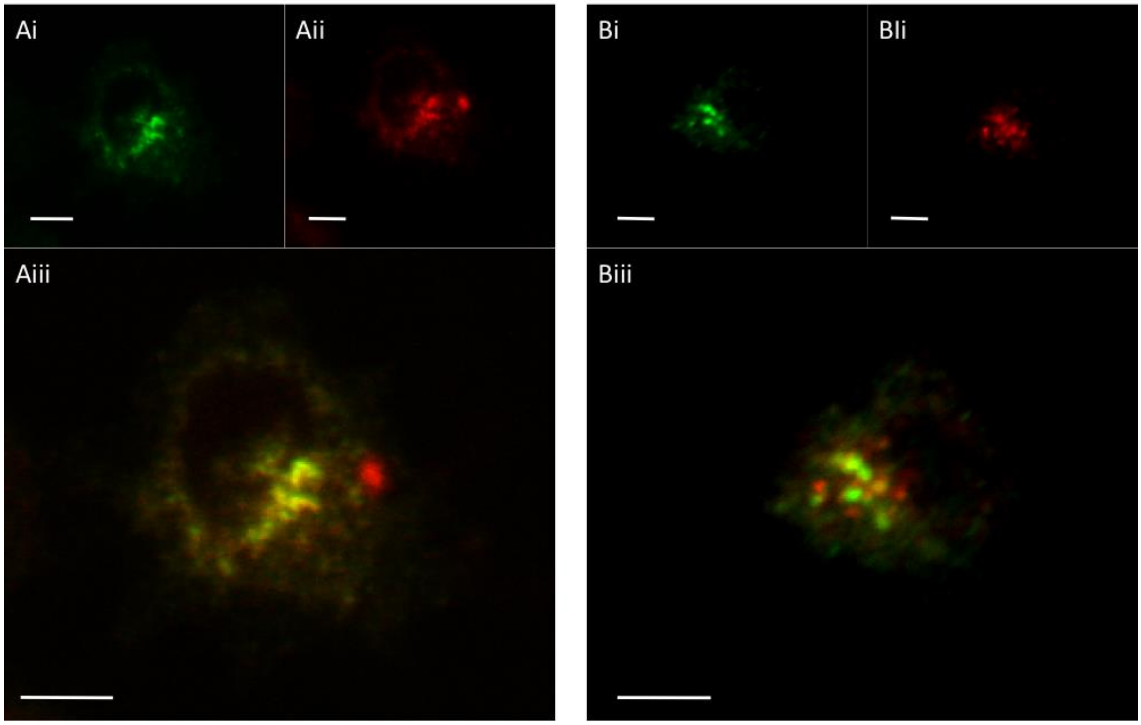

Figure 4.15

Il-6 GFP colocalises to recycling endosomes

LAD 2 cells were transfected with IL-6 GFP, fixed and probed using and Anti-GFP antibody and co-stained with Anti-rab11 orAnti-tryptase. **A** IL-6 GFP and rab11 staining, **i**, Il-6, **ii** rab11 and **iii** overlaid image. **B** Il-6 and tryptase staining. **i**,Il-6, **ii,** tryptase and iii overlaid image. Scale bars represent 5μm.

4.2.6 Expression of plasma membrane Qbc SNAREs

Vesicles require interactions with SNAREs present on target membranes to undergo fusion. At the plasma membrane, syntaxins and the Qbc family of SNAREs form complexes with VAMPs present on vesicles to form the SNARE bundle that drives membrane fusion. The Qbc family of SNARE proteins lack transmembrane domains and contain two SNARE motifs [373]. Four members exist, SNAP-23, -25, -29 and -47. SNAP-29 and -47 are not known to be enriched at the plasma membrane and lack membrane anchors [241]. SNAP-23 and -25 are the Qbc SNARE implicated in exocytosis in non-neuronal and neuronal cells, respectively [215]. Previous studies have identified SNAP-23 as nesessary for fusion of mast cell granules at the plasma membrane [233, 365, 374, 375].

PCR and Microarray data suggested that multiple Qbc SNAREs are expressed in LAD 2 and HLMCS (Figure. 4.5). Furthermore, SNAP-23 expression increased four fold in stimulated HLMCs (figure 4.8bii). Therefore experiments were performed to assess protein expression of SNAP 23 and SNAP 25 in LAD 2 and HLMCS using western blotting and to determine localisation in mast cells by immunostaining. As predicted SNAP-23 protein was expressed (Figure. 4.16) and SNAP-23 localised to the plasma membrane of both LAD 2 and HLMCS (Figure. 4.17). However, the neuonal Qbc SNARE SNAP-25 was not present in LAD 2 or HLMCs, showing the neuronal SNARE has no role in human mast cells. This data is in agreement with previous studies showing mast cells do not expressed neuronal SNAREs and that SNAP-23 is highly expressed on the plasma membrane of mast cells.

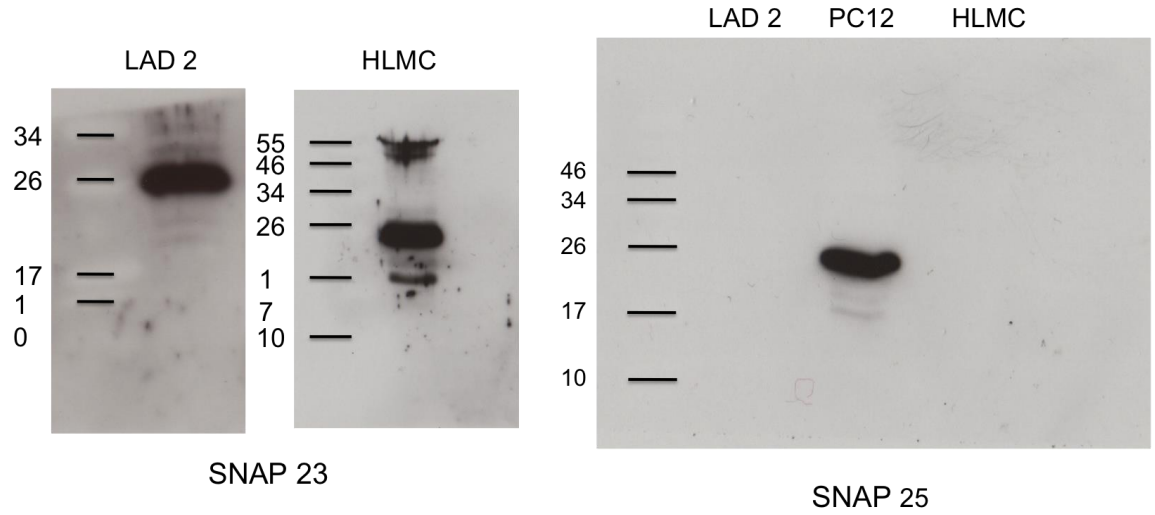

Figure. 4.16

LAD 2 and HLMCS express SNAP-23 but not SNAP-25

Western blotting of LAD 2 and HLMCS lysates of the plasma membrane Qbc SNAREs SNAP-25 and SNAP-23 show that human mast cells express SNAP-23 but not SNAP-25. PC12 neuronal cell line lysate used as positive control for SNAP-25 antibody.

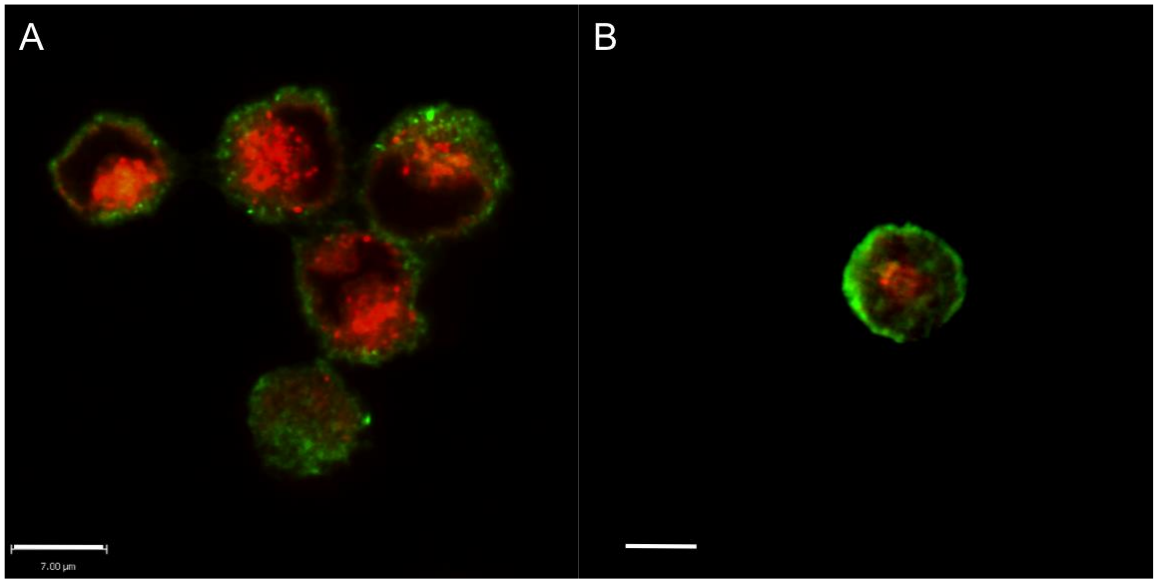

Figure. 4.17

SNAP-23 resides on the membrane of human mast cells

LAD 2 and HLMCS co-stained with tryptase (red) and SNAP-23 (green) show SNAP-23 around the plasma membrane. **A.** LAD 2, **B.** HLMC. Scale bar represents 10µm

4.2.7 SNARE regulator expression

A large number of proteins act either directly or indirectly with SNARE proteins to help the cell exert tight control over membrane fusion (Discussed in detail in section 1.3.5). Complexins, Munc13s and Munc18s have well defined roles in neuronal exocytosis, and putative roles in murine mast cell secretion [282, 284, 376].

The expression pattern of these regulators in LAD 2 cells and mRNA isolated from the HLMC donor, as determind by microarray analysis, is shown in figure 4.18. The data indicates that human mast cells express significant levels of the non-neuronal SNARE regulatory proteins, Munc18-3 and Munc 13-4 compared with the neuronal isforms, and that with the possibile exception of complexin II, complexins are not expressed in these cells. Taken together this data agrees with the lack of expression of neuronal SNARE proteins found in human mast cells consistant with their haematopoetic origins and consolidates the view that some of the specialisations required for fast synaptic vesicular release in neurotransmission are not present in mast cells.

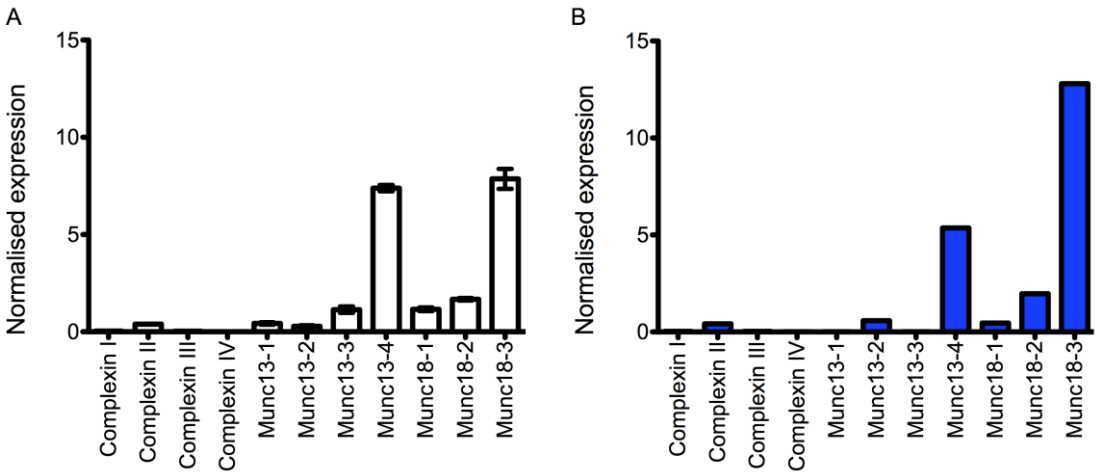

Figure. 4.18.

LAD 2 and HLMCS express high levels of non-neuronal Munc13 and Munc18 isoforms and low expression of complexin II

Gene expression values were normalized to the 75th percentile according to Agilent instructions. **A.** Clear bars represent LAD 2 mRNA expression from three independent RNA extractions ±SEM. **B**. Blue bars represent mRNA expression from one HLMC donor

However, like in neurons and endocrine cells, calcium is still a critical regulator of exocytosis. The calcium dependent nature of mast cell degranulation suggests that a calcium sensor may be recruited to vesicles. Tandem C2 domain-containing proteins that contain C2A and C2B domains are involved in vesicle trafficking and impart calcium sensitivity to vesicles [377, 378]. There are four groups of tandem C2 domain-containing proteins: syts, rabphilin-3 (RPH), doc2 and syt-like proteins (SLP) [379]. Numerous studies have identified the expression of syts and the expression of doc2 proteins in murine mast cells [260, 261, 380, 381]. However, no studies have assessed C2 domain-containing protein expression in human mast cells. Analysis of our microarray data shows that LAD 2 cells and HLMCs express mRNA for syt III, XI and XV. Slps, in particular slp2, showed high expression levels in either LAD 2 cells or HLMCs. Doc2α and β and RPH however, were not expressed to any great extent.

Previous studies in murine mast cells provided functional evidence for a role of syt II in regulating degranulation. Suprisingly, as can be seen in figure 4.18, the apparant expression of this isoform in human mast cells is very low. Suggesting that one of the other calcium sensing isoforms of syt, possibly syt III may fullfill the role

of calcium sensor for degranulation in LAD 2 and HLMCs. It is equally plausable another set of tandem C2 domain containing proteins might fullfill this role, especially considering slp expression in both LAD 2 cells and HLMC was much higher than syt expression levels (Figure 4.19 C and D). Given the low levels of syt II, mRNA from stimulated cells was analysed to look for any changes in syt expression to see if any syt implicated in murine mast cell exocytosis becomes upregulated in human mast cells (figure 4.20). Changes were very varied and inconclusive in the two LAD 2 cell samples. In the HLMC donor the non-calcium binding isoforms syt IV and XII had increases in expression, but in both LAD 2 cells and HLMCs syt II, heavily implicated in murine mast cell exocytosis, was not upregulated. This result, taken together with figure 4.19, suggests that the syt associated with murine mast cell SG exocytosis is not involved in human mast cell exocytosis and another C2 domain containing protein, a syt or slp, is invovled in this process.

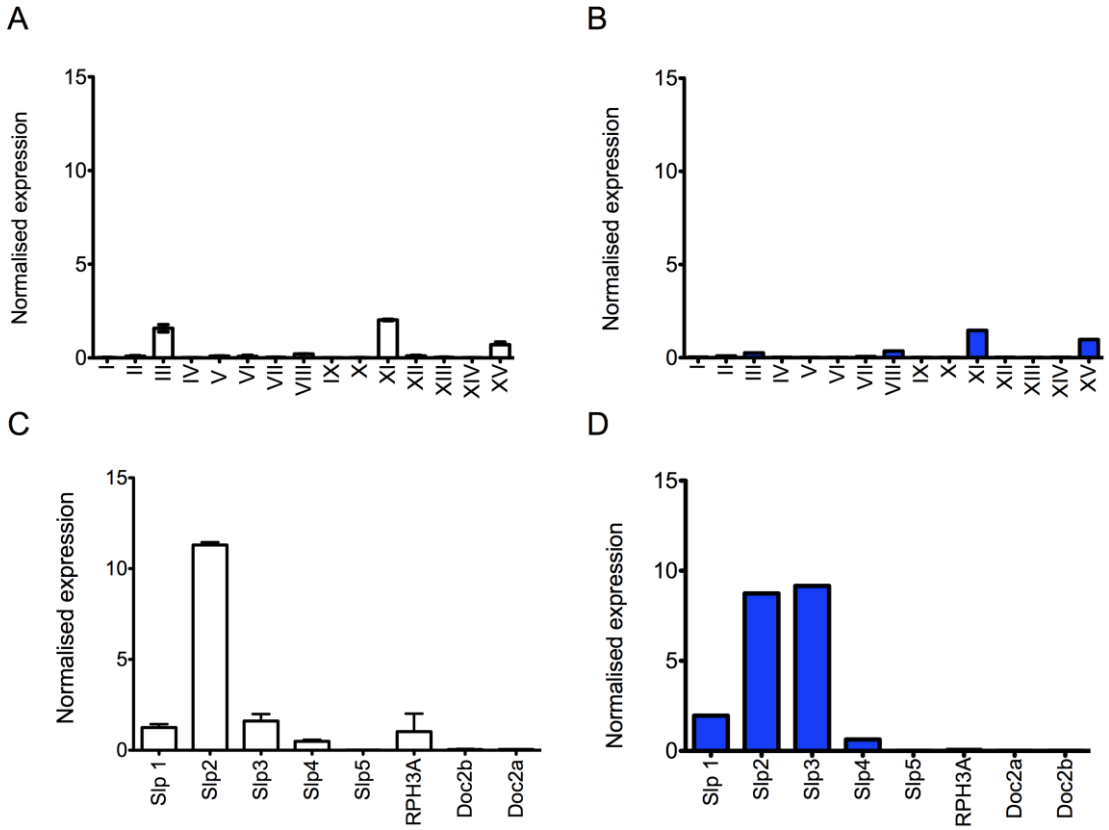

Figure. 4.19.

LAD 2 and HLMC calcium sensor expression

Microarray data was analysed to detemine calcium sensor expression in human mast cells. **A** LAD 2 syt expression. **B** HLMC syt expression. **C** and **D** show LAD 2 and HLMC slp expression. Human mast cells express syt III XI and XV and express a number of slps. slp2 had the highest expression of all Tandem C2 domain-containing proteins. Gene expression values were normalized to the 75th percentile according to Agilent instructions. Clear bars represent LAD 2 mRNA expression from three independent RNA extractions ±SEM. Blue bars represent mRNA expression from one HLMC donor

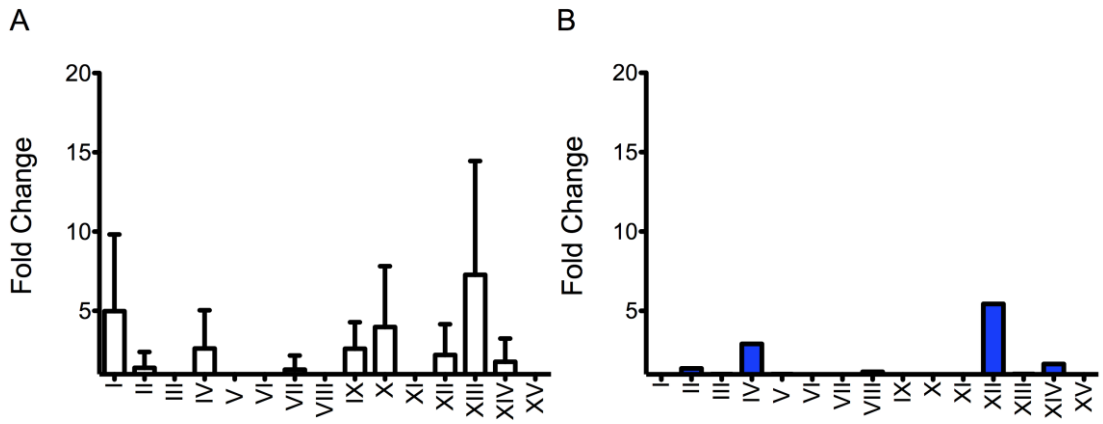

Figure 4.20

FceRI crosslinking induces changes in syt expression

A. LAD 2 cells and, **B**, single HLMC donor were stimulated for two hours by FceRI crosslinking, the time at which VAMP expression reached its maximum in qPCR experiments, and mRNA harvested. mRNA levels of syts were assessed by analysis of microarray data. Values represent fold change of stimulated cells compared to non-stimulated cells of same passage number (LAD 2 cells N=2) or same donor (HLMC N=1).

4.3 Discussion

Results in this chapter have identified the expression of numerous SNARE proteins in LAD 2 cells and HLMCs at the mRNA level through microarray analysis and PCR. Additional experiments determining protein expression and localisation have been confirmed. From these results two VAMPs, VAMP-3 and VAMP-8 have been identified as potential candidate SNAREs residing on vesicles mediating the release of inflammatory mediators. Additional analysis of microarray data has also determined the level of mRNA expression of a number of SNARE regulators. This has highlighted potential differences in expression, particularly with syts, from murine mast cells.

Analysis of the microarray data shows that mRNA for syntaxins 3 and 4 are highly expressed in LAD 2 cells, more so than any other syntaxin. Previous studies have implicated syntaxins 3 and 4 in mast cell exocytosis [233, 239]. Immunostainging has shown syntaxin 4 localises to the plasma membrane in both murine and HGMCs, and experiments inhibiting function in RBL-2H3 cells through siRNA and HGMCs using inhibitory antibodies result in reduced histamine and β-hexosaminidase release [232, 233, 239, 365]. Further evidence exists in other cell types of a role in regulated exocytosis; syntaxin 4 knockout mice have reduced insulin release from pancreatic β-cells that can be restored by the addition of recombinant syntaxin 4 [382.]. Whilst in another immune cell, neutrophils, syntaxin 4 has been shown to mediate fusion of tertiary and azurophilic granules with the plasma membrane [383]. For syntaxin 3 contradictory evidence exists as to its role in mast cells. Immunostaining of an overexpressed syntaxin 3 construct in RBL-2H3 cells was found on SGs and in unstimulated BMMCs partial colocalisation with serotonin is seen. However, in stimulated BMMC syntaxin 3 localises to the plasma membrane [235, 277] and in HGMCs, immunostaining has found syntaxin 3 to localise exclusively to the plasma membrane in unstimulated cells [240]. Further evidence of a role of syntaxin 3 in HGMCs has also been shown; CCL2, 3 and 4 secretion was found to be inhibited by the use of syntaxin 3 targeting antibodies [240]. RBL-2H3 cells are not a reliable mast cell model (section 1) and overexpression of syntaxin might have lead to miss targeting to SG. Furthermore, BMMCs are differentiated in culture and so are a more artifical system and serotonin is not expressed to any

great extent in human mast cells so the relevance of these studies to human mast cells is limited. HGMCs are primary cells derived directly from human patients and represent the most similar cell type to those used in this study and so findings from these cells are most likely to be replicated in LAD 2 and HLMCs.

Given the prominent expression in LAD 2 cells and HLMCS of both syntaxin 4 and syntaxin 3 mRNA found in this study, it is likely that they have prominant functions in LAD 2 and HLMCs, with roles similar to that in HGMCs. Syntaxin 4 mediating SG fusion, syntaxin 3 possibily having a role in cytokine secretion. Further experiments using immunostaining and mediator release assays in cells with knocked down expression of these syntaxins would give a more definitive answer as to their role in exocytosis.

Many other isoforms of syntaxins were also expressed in LAD 2 and HLMCs, including syntaxin 10 and 16, which had the third and fourth highest expression levels. Syntaxin 10 has been reported to function in retrograde transport from the late endosome to Golgi and siRNA deletion and expression of a soluble form of syntaxin 10 leads to hyper-secretion of hexosaminidase in HeLa and HEK293 cells [384]. Given these findings, in mast cells, syntaxin 10 might have a role in retrograde transport from SGs and regulate SG contents. Knockdown of syntaxin 10 might lead to enlargement of SGs and the miss targeting of proteins to them. Syntaxin 16 on the other hand has been reported to have an ubiqtious role in early endosome to Golgi trafficking [385]. However, there is a reported tissue specific role in adipocytes, whereby syntaxin 16 is involved in the intracellular sequestering of GLUT4 in the abscence of insulin [386]. It is possible that syntaxin 16 might have a similar sequestering role in mast cells that could act as a store for pre-formed cytokines allowing rapid release after stimulation.

The wide expression of syntaxins is not surprising given the diverse trafficking pathways that exist within a cell. Further experiments determining syntaxin localisation and functional studies were beyond the scope of this study but the results show the expression of multiple syntaxins, and there is the possibility of a number of syntaxins mediating the regulated release of inflammatory mediators in human mast cells.

SNAP-23 protein was found to be abundantly present in this study and localized to the plasma membrane. SNAP-23 has been identified as the plasma membrane Qbc SNARE in that mediates the fusion of exocytotic vesicles in non-neuronal secretory cells. In mast cells it is present at the plasma membrane and numerous studies have shown it is vital in mediating release of mast cell mediators, through the use of siRNA and inhibitory antibodies [240, 387, 388]. RBL-2H3 cells have high levels of mRNA expression of SNAP-23 mRNA [365]. However, the mRNA levels of SNAP-23 in this study were not very high when compared to other SNAREs implicated in mast cell exocytosis, such as VAMP-8 and syntaxin 4 [365], although a four fold increase was seen in mRNA expression in stimulated HLMCs. A possible explanation is that the SNAP-23 protein could have a very low turnover and high half-life in human mast cells. Housekeeping proteins are often longer lived and have a greater protein to mRNA ratio [389]. This might explain the apparent discrepancy from mRNA to protein levels. However, although SNAP-23 is expressed in all non-neuronal tissues, it has been reported not be essential for constitutive exocytosis in HeLa cells [390]. This study used siRNA knockdown and a dominant negative mutant SNAP-23. There might have been possibile compensatory effects by other SNAPS, or just that another SNAP mediates constituitive traffic. SNAP 25 wasn't expressed but SNAP-29 or -47, not normally residing on the plasma membrane, might be able to participate in the final fusion steps of constituitive release. This argument is particularly relevant given a recent siRNA screen has implicated SNAP-29 in constituitive exocytosis in C1 cells [391] and adds further evidence for a limited role of SNAP-23 in constituitive exocytosis. Alternatively, as 10% of SNAP-23 protein remained upon knockdown in the former study, small amounts of SNAP-23 might be sufficient to support exocytosis. Also, Gorden et al showed a number of SNAREs involved in constitutive traffic. Multiple constitutive pathways might exist, some of which were not detected in the two studies, which might utilise SNAP-23 and so SNAP-23 might mediate the fusion of both regulated and constitutive traffic. Alternatively, given the findings of both studies, it is possible that SNAP-23 is only important for regulated secretion. In highly specialised secretory cells that use SNAP-23 for regulated secretion, a high level of regulation of expression levels might be required. As a result, in unstimulated cells, mRNA levels remain low and a high level of mRNA expression is only required upon stimulation.

SNAP-25 protein was not expressed in either LAD 2 or HLMCS, confirming previous studies in HGMCs and murine mast cells showing no expression of SNAP-25 protein [239].

The Qbc SNARE with by far the highest expression levels is SNAP-47. SNAP-47 is ubiquitously expressed SNARE that has been shown to be present in unidentified intracellular compartment, not on the plasma membrane and enriched in SV fractions [241]. In neurons it has been reported to mediate trafficking of AMPAR regulated exocytosis in Long-Term Potentiation (LTP) with syntaxin 3, but is not required for synaptic transmission [392]. The apparent lack of a membrane anchor to SNAP-47 might allow more transient trafficking in SNAP-47 to the plasma membrane. It would be interesting to identify where SNAP-47 is localizing to in resting and activated mast cells and determine whether it has a role in receptor trafficking or mediator secretion in immune cells. This might form part of the process by which other channels or receptors are trafficked to the plasma membrane in activated cells, such as TRP channels, which are through to be important in the development of sustained calcium rises in activated mast cells[393]. The fact that syntaxin 3 was also expressed at relatively high levels and has been shown to interact with SNAP-47 in AMPAR trafficking suggests a potentially similar mechanism of receptor trafficking could exist in mast cells. Further focused functional studies are needed to assess the protein expression of SNAP-47 along with other Qbc SNAREs to address the role of distinct syntaxin and SNAP protein isoforms in mast cell biology.

Results in this chapter have identified the expression of VAMPs-3, -7 and -8 in LAD 2 cells and HLMCs. VAMP-1 was not expressed in mast cells. VAMP-2, although expressed at relatively high levels in the microarray and qPCR, wasn't found in western blotting. Interestingly the single previous study assessing mRNA and protein expression of VAMP-2 in human mast cells had a similar observation; VAMP-2 was expressed in PCR but not through western blot [239] and this is not due to problems with antibody detection as strong staining was observed in PC12 cells. In embryonic rat hippocampal neurons VAMP-2 mRNA is synthesised at a constant rate throughout neuronal development but levels of protein increase

steadily, suggesting that for VAMP-2 in neurons there is a high level of post-translational control of expression and that mRNA levels don't correlate to protein levels [394]. VAMP-2 protein might have a short half-life in mast cells, resulting in the relatively high levels of mRNA with no protein expression. Given no SNAP-25 protein was expressed either, these results confirm that human mast cells, although expressing some neuronal SNAREs at the mRNA level, are not likely to utilize neuronal SNAREs for regulated exocytosis of inflammatory mediators.

Of other non-neuronal associated VAMPs, microarray data identified VAMP-8 as the most highly expressed in LAD 2 cells and HLMCs. This was confirmed with qPCR and the non-haematopoetic secretory cell line, HEK 294, did not have such high levels of expression. Immunostaining showed VAMP-8 localised with the mast cell granule marker tryptase and translocated to the membrane upon stimulation. These observations point to VAMP-8 having a key role in mast cell SG release. This would agree with current evidence, whereby inhibition of VAMP-8 function in HGMCs with inhibitory antibodies or knockdown in murine mast cells leads to reduced histamine release [235, 239]. Although a large amount of VAMP-8 colocalised with tryptase a large portion of VAMP-8 did not. The tryptase negative proportion that didn't might represent an immature SG pool or non-secretory lysosomes. In murine mast cells three types of granules have been reported; type I containing lysosomal markers, and type III containing serotonin and type II containing both. Type I and II might represent immature granules or type I normal lysosomes [178]. VAMP-8 might be present on both type I and II but not type III representing a pool that does not colocalise to mast cell granule markers. Whether they are immature granules or non-secretory lysosomes remains to be determined. Further colocalisation analysis using lysosomal markers such as the LAMPS could be performed to determine whether the large non-tryptase localising pool is present in lysosomes. Another explanation is that tryptase positive granules might only represent a subpopulation of granules, a more detailed proteomic analysis of SG isolated from mast cells is needed to identify the nature of possible function of these VAMP-8 positive granules. What is clear from the results in this study is that VAMP-8 is the predominant VAMP in human mast cells and most probably mediates the fusion of SG with the plasma membrane. Functional studies in chapter 5 address this role in greater detail.

Like VAMP-8, VAMP-7 has also been reported to mediate the release of mast cell granule mediators [240]. In this study the microarray data identified a high level of VAMP-7 mRNA expression when compared to the majority of other VAMPs (Figure. 4.6). All VAMPs increased mRNA expression within 2 hours of stimulation. VAMP-7 expression increased 4 fold, the most out of all SNAREs tested. VAMP-7, as with VAMP-8, colocalised with tryptase. Previous reports have shown both VAMP-8 and VAMP-7 colocalise with SG markers and inhibition of function through inhibitory antibodies attenuates secretion of histamine [239, 395]. In this study, only a small proportion of VAMP-7 colocalised with tryptase and VAMP-7 exhibited minimal trafficking to the plasma membrane upon stimulation in LAD 2 cells. In other cell types, such as HeLa cells, VAMP-7 has been shown to mediate the trafficking from the late endosome to the lysosome [237]. VAMP-7 might regulate a trafficking vesicle that is important for maturation of granules. siRNA knockdown of VAMP-7 in RBL-2H3 cells results in reduced granular release but VAMP-7 does not significantly colocalise with serotonin containing granules and does not co-precipitate with SNAP-23, while VAMP-8 does [365, 396]. The large increase in expression might indicate a role in replenishing granules, where there would be a greater need for VAMP-7 after stimulation to aid recovery and refilling of granules. This process takes hours [397] and this time course could indicate changes at the transcriptional level as shown here. The reduction in mediator release could be explained by an inability of the cell to form fully mature granules. Further experiments determining whether inhibition of VAMP-7 results in immature granules and the accumulation of SG associated factors might help to provide this evidence. This could be done by using high resolution imaging to follow vesicle synthesis and maturation with VAMP-7 and VAMP-8 GFP and RFP-tryptase constructs. Assessment of granule morpholgy could also be performed using electron microscopy.

In my study VAMP-3 was expressed at intermediate levels in mast cells and was clearly present in pools distinct to VAMP-8. Furthermore, there were clear differences in VAMP3 and VAMP-8 vesicle size in HLMCS, VAMP-3 being present on much larger vesicles or clusters of small ones, the resolution of the images is not high enough to differentiate. LAD 2 cells did not show such as stark variation in the size of the two sets of vesicles. LAD 2 cells are described as a well-differentiated

mast cell model, and data in chapter 3 is suggestive of this. However, the variation seen might be indicative of the cell line not representing a fully differentiated model. Another observation leading to a similar conclusion is the fact that VAMP-3 or VAMP-8 showed little trafficking to the plasma membrane in LAD 2 cells stimulated through FcεRI crosslinking, but clear trafficking with ionomycin stimulation. This discrepancy might be explained by results in chapter 3. Stimulation by ionomycin results in release of large amounts of FFN511 release in all mast cells, whilst less than half of LAD 2 cells respond to FcεRI crosslinking and so changes to the distributions of SNAREs in LAD 2 cells stimulated in this manner might be too small to identify using immunostaining. In contrast VAMP-3 and VAMP-8 both trafficked to the plasma membrane upon ionomycin and FcεRI mediated stimulation in HLMCs. The FFN511 data in chapter 3 shows many more HLMCs produce a degranuation response to FcεRI crosslinkning and so changes in distribution of VAMPs might be more prominant.

Previous studies in human mast cells found VAMP-8 vesicles translocating to the membrane but not VAMP-3, and VAMP-3 to not be important in mediator release [239]. The translocation of VAMP-3 seen upon stimulation in my studies suggests that at least a proportion of these vesicles undergo stimulus dependent translocation to the plasma membrane. Differences in the observations made between the stimulus dependent translocation of VAMP-3 to the plasma membrane in the study by Biscoff et al and myself could result from phenotypic differences between mast cell populations in the gut and lung. For example intestinal mast cells can be phenotypically altered in culture by exposing the culture to Il-4, producing Th2-type response [398]. The differing cocktail of factors mast cells are exposed to at different tissue locations results in phenotypical differences, discussed in detail in section 1.1. Some evidence suggests that cytokine expression also varies in cells differentially expressing proteases. MC_T cells express IL-5 and IL-6 while only a very small number MC_{TC} do in the lung [20]. In cells releasing differential sets of mediators, it is possible that the release of these might be controlled by a different combination of SNAREs that vary in mast cell subpopulations. Another explanation might lie in the types of experiments performed in each study. In the study of Frank et al only the release of histamine and four chemokines were assessed. Within the four chemokines, differences were observed in the effect of VAMP immobilisation.

For example anti-VAMP-8 inhibited CXCL8 release but not CCL4, CCL4 release was not inhibited by either VAMP-3, -7 or -8 immobilisation. The effectivness of the antibody technique was not verfied with any other approaches. Cytokine release was not measured and considering different combinations of SNAREs were found to mediate the release of just four chemokines, mast cells might utilize other SNARE combinations to control the release of different cytokines and chemokines. Previous studies in macrophages have identified a secretory pathway within which TNF-α and Il-6 are trafficked from the Golgi to the plasma membrane through the recycling endosome, with VAMP-3 mediating the release from the plasma membrane [182, 183]. In murine mast cells, VAMP-3 has been shown to reside in a pool distinct to that of VAMP-8 that colocalises with TNF-α [235]. Moreover VAMP-3 was found to complex with SNAP-23 and syntaxin 4 [399]. In agreement with these studies, VAMP-3 colocalised to recycling endosomes, as did Il-6. The IL-6 monitored was overexpressed and so it is possible that there was some miss-targeting as a result of overexpression but minimal amounts were present in SGs, supporting the notion that VAMP-3 is involved in IL-6 secretion and that VAMP-3 recycles through the rab11 positive recyling endosome.

What is clear from the findings in my study is that mast cells express a number of VAMPs that localise to different mast cell compartments. VAMP-8 is the best candidate for mediating the fusion of SG with the plasma membrane whilst VAMP-7 could have a role in granule maturation. VAMP-3, as of yet having no defined role in mast cells, is present in significant quantities and might well represent a vesicle subset that mediates the release of cytokines. Given more time further analysis of colocalisation would have been performed. Determining the colocalisation with other subcellular markers would have enabled a better picture of VAMP localisation to be built. Furthermore in this study no colocalisation analysis was performed. Using analysis such as pearsons coefficient to quantify the levels of colocalisation would give a more definitive evidence of the findings described above. Also, this study has not provided conclusive evidence that the antibodies used for immunostaining are specific. Further experiments showing a loss of staining after knockdown of a particular VAMP would give some evidence for specificity. Despite these drawbacks, the results described here give a great starting point and insights for the functional studies performed in chapter 5.

Complexins are small α helical containing proteins that mediate rapid fusion of exocytotic vesicles in neurons [271]. Mast cells do not undergo such rapid fusion and, despite reports suggesting the importance of complexin II in mast cell exocytosis [400], very little mRNA expression was seen in mast cells in this study. Murine models have been used in the majority of studies assessing the exocytotic machinery in mast cells, including complexin. Many of the proteins expressed in these cells have clearly defined roles in neuronal exocytosis, including: Munc18-1 and 2, VAMP-2 and SNAP-25 [233, 235, 376, 401]. In the single study performed in HGMCs and data shown here in LAD 2 and HLMCS makes it clear human mast cells do not express SNAP-25 or VAMP-2 protein [239]. Differences of expression of other exocytotic components were also found in the microarray data.

Munc13-1-3 are isoforms of Munc13 predominantly found in neuronal systems and were not expressed to any great extent in LAD 2 cells or the HLMC donor. Munc13-4 was expressed at much higher levels. These results do mirror work performed in murine models, where Munc13-4 is expressed at high levels and is thought to mediate the docking and tethering of mast cell granules to the plasma membrane [282].

Syt XI had the greatest expression out of all syts. Little is known of the function of syt XI in mast cells but in macrophages it is reported to regulate phagocytosis and cytokine secretion[402]. Syt XI and IV belong to a group of syts that have an altered C2 domain that renders them insensitive to calcium binding [403]. Syt XI acts as a negative regulator of cytokine secretion; it localises to recycling endosomes and lysosomes, over expression inhibits TNF and Il-6 release and knockdown increases it [402]. Syt XI might add an additional level of control to cytokine secretion preventing the aberrant release of cytokines. Syt XI is expressed at high levels when compared to other syts in mast cells and could possess a similar function in mast cells as in macrophages. Very little is known of syt XV. It is not expressed in neurons but is more ubiquitously expressed in non-neuronal tissue and is also postulated to be calcium insensitive [404].
Syt II is expressed at high levels in murine mast cells, localises to SGs and mediates the release of preformed mediators [255, 260]. Surprisingly, little expression was

seen in the microarray. All the work characterising syts in mast cells has been performed using murine mast cells. As discussed in the previous paragraphs, they possess high levels of many proteins of the neuronal exocytotic machinery. Syt II is highly expressed in neurons and so, as with complexin, the functional relevance in human mast cells might be limited. Syt I, II and IX have high sequence similarity within their two C2 domains and have been termed Class A syts [405]. They are differentially expressed in neurons and all act as fast calcium sensors, the only syts able to rescue fast synchronous release [406] and have the lowest affinity to calcium and so allow cells to respond to high calcium concentrations (~10μM) at the active zone [253]. Exocytosis in mast cells occurs within minutes rather than milliseconds [397] and lack the voltage gated calcium channels that give rise to large local calcium concentrations. So the ability to respond as rapidly is not required and might explain the lack of expression of these isoforms.

Syt III has been termed a class B syt [405] and was expressed at levels similar to syt XI in LAD 2 cells. Syt III has a higher affinity to calcium than the class A syts [253]. Previous studies have shown syt III localises to the Early Endosome and SGs and report a putative role in the formation of the ERC and delivery of material from the EE to the ERC and SGs rather than a direct role in exocytosis [261].

The apparent lack of expression of a calcium sensitive syt isoform mediating the release of SGs might be explained by the expression of other tandem C2 domain-containing proteins. Slps have been implicated in exocytosis in numerous cell types including platelets and pancreatic β cells [407-409]. They contain two c-terminal C2 domains but no transmembrane sequences [410]. Slp1-3 can interact with rab27a and b, and slp 2 had been shown to mediate the peripheral trafficking of melansomes in melanocytes [411]. Murine mast cells express rab27a and b on SGs, assisting in docking and tethering granules to the plasma membrane in interaction with Munc13-4 and doc2α [284, 412]. High levels of expression of rab27b and Munc 13-4 were seen in both LAD 2 cells and HLMCS but not rab27a or Doc2α (an expression table of rabs can be seen in the appendix. Slp 2 was expressed at the highest levels of all tandem C2 domain-containing proteins in LAD 2 cells and HLMCS. Slp2 might have a role in granule docking and tethering in human mast cells and act as calcium sensors for exocytosis in mast cells. A calcium insensitive syt

isoform might act with an slp to bend the plasma membrane, a critical step in calcium-dependent exocytosis [413].

In conclusion using the microarray data it has been possible to determine the expression of SNARE regulators in human mast cells. Finding suggest that mast cells express large amounts of the non-neuronal isoforms of Muncs, while express relatively little syts but express at high levels other tandem C2 domain proteins, the slps.

Chapter 5: Functional characterisation of VAMP-3 and VAMP-8 in human mast cells

5.1 Introduction

pHluorins are variants of GFP rendered sensitive to pH through a cluster of mutations [295]. The fluorescence of ecliptic forms is quenched at acidic pHs (pH<6), conditions encountered in secretory vesicles, and shows peak fluorescence at neutral pHs. Vesicular SNARE proteins can be tagged with pHluorin on their C-termini, resulting in an intra-vesicular tag that becomes unquenched upon vesicle fusion with the plasma membrane as the pHluorin is exposed to the more alkaline extracellular environment. In Chapter 4, the predominant vesicular SNARE proteins present in human mast cells likely to contribute to inflammatory mediator secretion were identified as VAMP-3 and VAMP-8. Here I describe the results from functional experiments that were performed to further elucidate the roles these two v-SNARE play in mast cell exocytosis. VAMP-3 and VAMP-8, each tagged with pHluorin, were stransfected into LAD 2 cells to monitor vesicle fusion in living cells before and after stimulation. Dual imaging experiments combining measurements of fluorescence emission from pHluorin with ratiometric measurements of intracellular calcium, as assessed with Fura-2, were performed to examine the relationship between VAMP-3 vesicle fusion or VAMP-8 vesicle fusion and calcium signalling. Targeting of VAMP-3 with BoNT/B or VAMP-8 with shRNA was used to identify the functional role each plays in mast cell mediator secretion. The results of these experiments provide insight as to the feasibility of controlling the release of cytokines from human mast cells through BoNTs, which could be exploited as a novel treatment for chronic inflammatory diseases.

5.2 Results

5.2.1 VAMP-pHluorins as tools to monitor exocytosis

Given the reported role of VAMP-8 in mast cell granule exocytosis and VAMP-3 in cytokine secretion in other immune cells [182, 183], the decision was made to

produce VAMP-3 and VAMP-8 ecliptic pHluorin constructs to monitor vesicle fusion in human mast cells. A diagram depicting the pHluorin constructs and their pH sensitive nature is in Figure 5.1

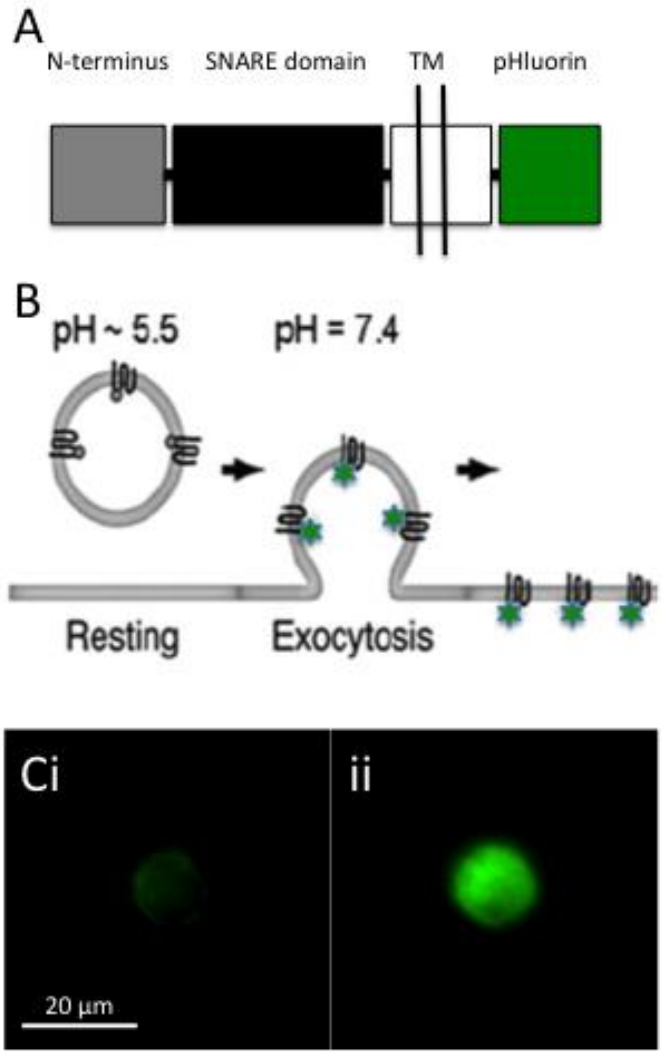

Figure. 5.1

VAMP pHluorin constructs.

A. Diagram of SNARE-pHluorin fusion proteins, the pHluorin tag is present on the C-terminal end of VAMP. **B.** Diagram depicting the pH sensitive nature of the VAMP-pHluorin constructs. Upon stimulation acidic secretory vesicles fuse with the plasma membrane and become alkalised as they are exposed to the more neutral extracellular environment. pHluorin, intravesicularly tagged to a membrane protein, is initially quenched in the acidic conditions of resting vesicles. After the vesicle undergoes membrane fusion the tag becomes de-quenched and this increase in fluorescence can be monitored (adapted from Dreosti et al Exp Physiol 2011[414]. **C**. Live cell image of LAD 2 cell transfected with VAMP-8-pHluorin i) before and ii) following stimulation with 10µg/ml of anti-IgE for 3 minutes.

The VAMP-3 and VAMP-8-pHluorin constructs were transfected in to LAD 2 cells using the neon transfection system, the protocol is described in detail in section 2.16. Over-expression of proteins can result in miss targeting to cellular compartments. Therefore initial experiments using the pHluorin constructs sought to determine whether the pHluorin constructs were localising to similar intracellular compartments as the endogenous VAMPs. To do this immunostaining was performed on LAD 2 cells expressing the pHluorin constructs. Cells were co-stained using anti-GFP, to detect pHluorin and anti-tryptase, where endogenous VAMP-8 colocalised to, or with or anti-rab11, the compartment to which endogenous VAMP-3 localised. Representative images of fixed, transfected cells are shown in Figure 5.2. As can be seen VAMP-8 pHluorin colocalised with tryptase but very little colocalised to rab11, while VAMP-3-pHluorin colocalised with rab11 but did not colocalised to tryptase, indicating that the tagged VAMPs trafficked to the same intracellular compartments as their endogenous counterparts (see also chapter 4, figure 4.15).

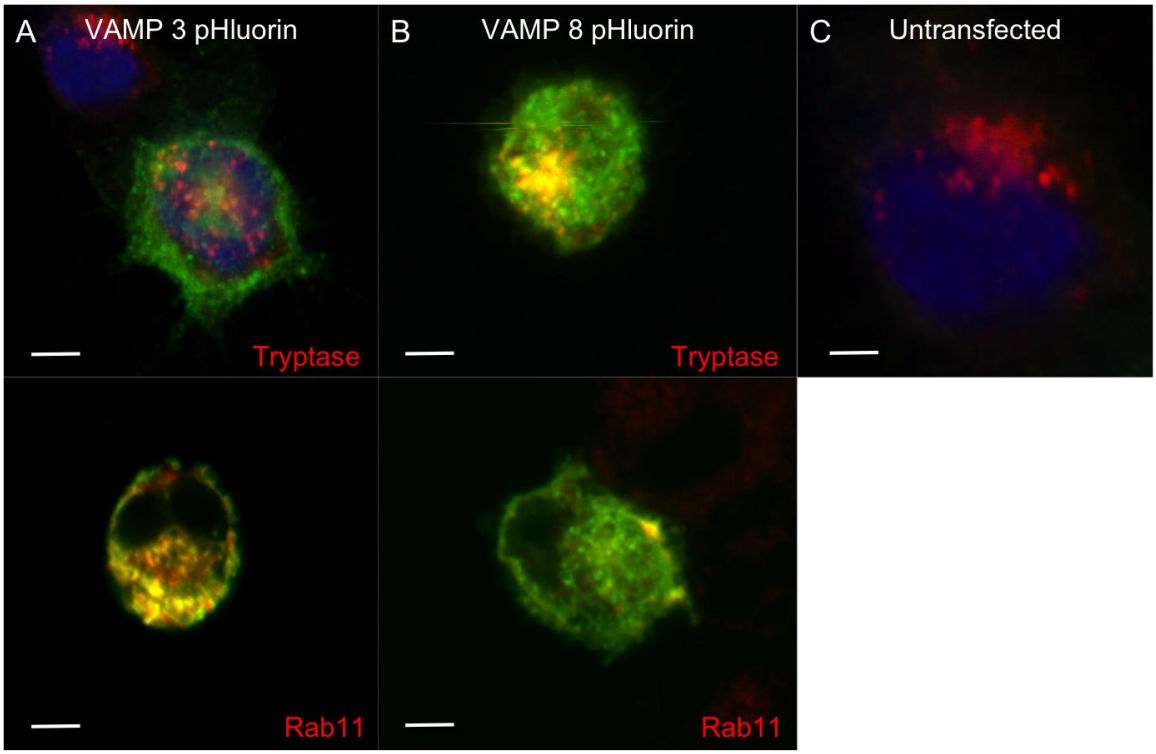

Figure. 5.2

VAMP-8 pHluorin and VAMP-3 pHluorin localise to different cellular compartments

LAD 2 cells were transfected with either VAMP-3 or VAMP-8-pHluorin for 24 hours and then, fixed and co-stained with anti-GFP (green) and anti-tryptase or rab11 (red), as indicated below each image. Colocalistion can be seen as yellow in the overlaid figures. **A**. VAMP-3 does not colocalise with mast cell granules marker tryptase but does with rab11**. B**. VAMP-8-pHluorin colocalising with tryptase, the mast cell granule marker .C No staining for GFP is seen in un-transfected cells, only tryptase staining can be seen (Red). Scale bar represents 5μm. Representative images from two transfections.

To identify the cellular distribution of the VAMP-pHluorins an acid wash experiment was performed in resting cells expressing either VAMP 3 or VAMP 8 pHluorin. Ecliptic forms of pHluorin are non-fluorescent at pH<6[295], these conditions are encountered in resting vesicles and so in resting cells only pHluorin present on the cell surface will fluoresce if tagged intra-vesicularly. A small amount of background fluorescence from pHluorin may also come through pHluorin present in the Golgi (pH 6.2) and ER (pH7.0)[415]. The proportion of VAMP-pHluorin on the cell surface was calculated in non-stimulated cells by washing the cells in a pH 5.6 external solution to quench cell surface fluorescence. Cells were subsequently washed in 50mM ammonium chloride (NH_4Cl) external solution to determine intracellular fluorescence. NH_4Cl is a weak lypophilic base, whereby the neutral NH_3 can cross cellular membranes and bind free intracellular protons resulting in

alkalisation and subsequent de-quenching of the pHluorin contained within [415, 416]. The proportion of cell surface to intracellular VAMP-pHluorin can be estimated from these two values (details in chapter 2 section 2.17.2). Upon application of the pH 5.6 external solution, clear decreases in fluorescence were produced indicative of quenching of cell surface pHluorin (figure 5.3 A and B) Application of NH_4CL resulted in large rises in pHluorin fluorescence as intracellular pHluorin became de-quenched. From the resulting traces, the proportion of cell surface to intracellular pHluorin was calculated (figures 5.3 C and D) (details in section 2.17.2). A significantly greater proportion of VAMP-8 pHluorin was intracellular (>60%, $P<0.0001$) compared to the amount present at the cell surface (figure 5.2 B and D). VAMP-3-pHluorin was evenly distributed between the cell surface and intracellular compartments with no significant difference being measured between the distribution of the two compartments ($P=0.97$). These results highlight that VAMP-3 and VAMP-8-pHluorin have differing distributions within the cells. And that VAMP-3 may be cycling between the plasma membrane and an intracellular compartment in 'resting' cells, while VAMP-8 remains largely trapped in an intracellular compartment until the cells are activated.

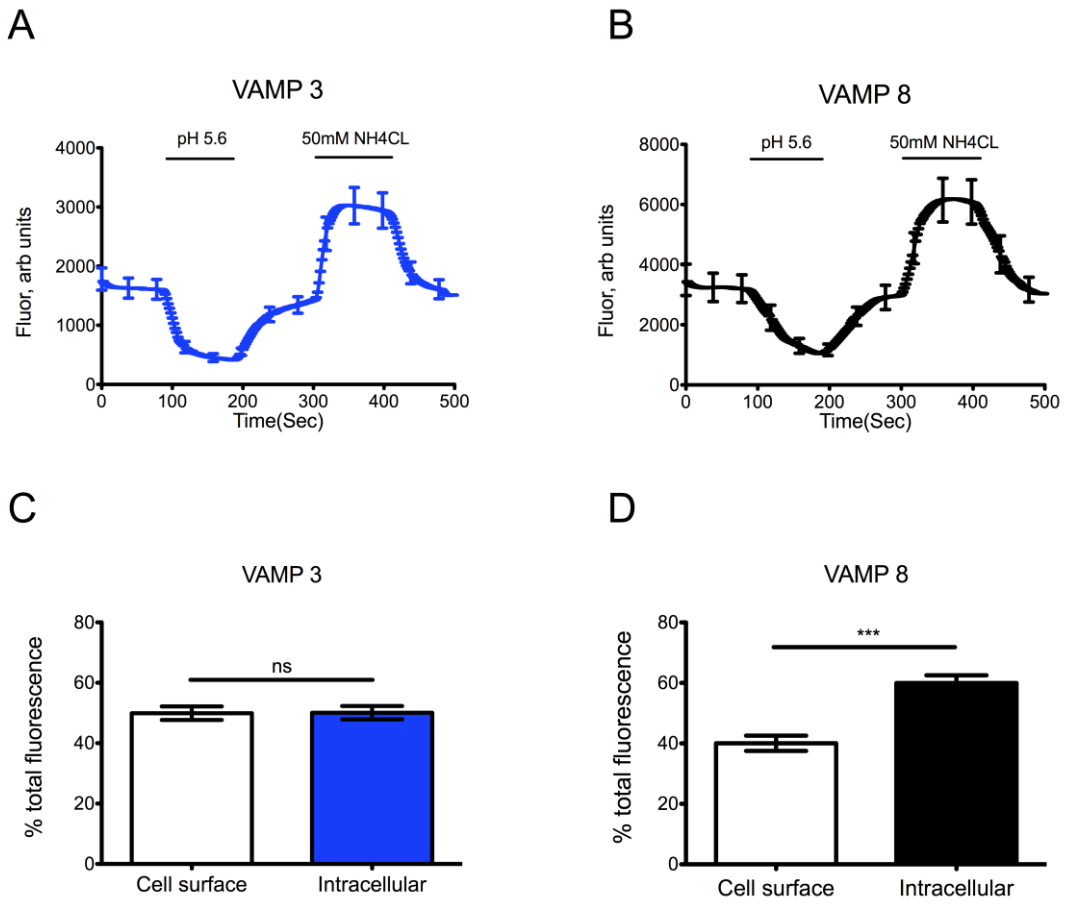

Figure. 5.3

VAMP-3 and VAMP-8 pHluorins have distinct cell surface and intracellular distributions

A. Plot of mean total cellular fluorescence over time during the superfusion of external solution with the application of an adjusted pH external solution or NH_4CL indicated above the traces. A greater proportion of VAMP-3 is present at the cell surface compared to VAMP-8, which shows a more intracellular distribution. Blue line indicates VAMP-3-pHluorin fluorescence, black line VAMP-8-pHluorin fluorescence. C and D show calculated percentage distribution of VAMP-3 and VAMP-8 pHluorins calculated from the cellular fluorescent values shown in figures A and B (details of calculation in section2.17.2) VAMP-8-pHluorin n=58 cells ± SEM. **B**. VAMP-3-pHluorin n=88 cells ± SEM. *** denotes P<0.0001 unpaired students T-test. Data from three separate transfections of LAD 2 cells at three different passage numbers.

As described in chapter 4, and others have shown that VAMPs reported to be present on secretory vesicles in mast cells and other secretory cell types translocate to the membrane upon stimulation [239]. To ascertain whether VAMP-3 and VAMP-8 vesicles not only translocate, but also undergo fusion with the plasma membrane in a stimulus dependent manner VAMP-3 and VAMP-8 pHluorin expressing LAD 2 cells were activated by FCεRI crosslinking and whole cell fluorescence monitored over time. Cells were loaded with the calcium dye Fura-2AM and calcium levels and

pHluorin fluorescence monitored at the same time. Both VAMP-3-pHluorin and VAMP-8-pHluorin transfected cells showed pronounced increases in pHluorin fluorescence within seconds of application of anti-IgE, showing that both VAMP-3 and VAMP-8 pHluorin vesicles undergo fusion with the plasma membrane upon stimulation (Figure 5.4). There was however, cell to cell variability. n=33/57 of VAMP-8-pHluorin and 28/53 of VAMP-3-pHluorin cells monitored showed stimulus-dependent increases in fluorescence. Furthermore, within the cohort of responding cells there were variations in the size of responses, as can be seen in example individual cell traces (figure 5.4 D and F). These results mirror the FFN511 findings in chapter 3, where individual mast cells have a varied degranulation response to FCεRI activation.

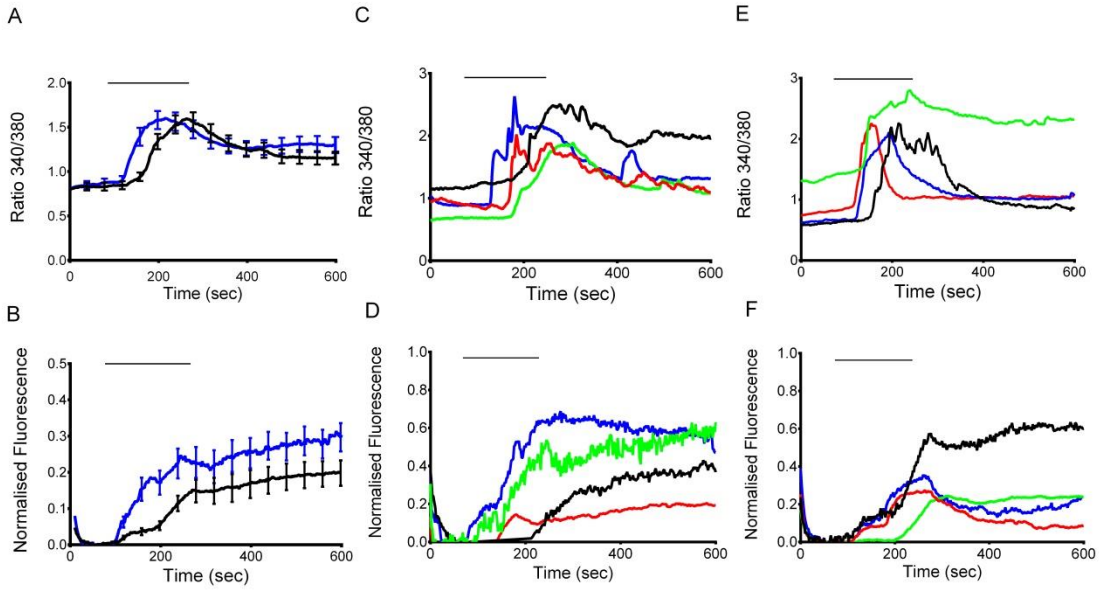

Figure. 5.4

VAMP-3 and VAMP-8-pHluorin cells undergo membrane fusion upon FcεRI cross-linking.

LAD 2 cells were transfected with either VAMP-8 or VAMP-3 pHluorin, sensitised overnight with 300ng/ml of human IgE. The next day cells were loaded with 1μM fura-2AM.and FCεRI cross-linking was subsequently induced by perfusion of 10μg/ml anti-IgE shown by horizontal bars above graphs. **A**. Mean $R_{340/380}$ values representing calcium responses and **B.** Mean normalised pHluorin fluorescence over time from individual responding cells. Blue lines represent data obtained from VAMP-3 pHluorin expressing LAD2 cells, black lines represent data obtained from VAMP-8 pHluorin expressing cells. VAMP-8 n=33/57±SEM. VAMP-3 n=28/53±SEM. **C** Calcium and **D** Changes pHluorin emission fluorescence measured in representative individual cells expressing VAMP-3 pHluorin before and after cell stimulation (indicated by the bar above the traces). **E**. Calcium and F. pHluorin representative individual cell responses of VAMP-8 pHluorin expressing cells. Data from three transfections. pHluorin values are given as normalized fluorescence values, normalized to total fluorescence determined by fluorescence resulting from NH_4CL wash which is superfused at the end of each experiment (details can be found in section 2.17.2 in chapter 2)

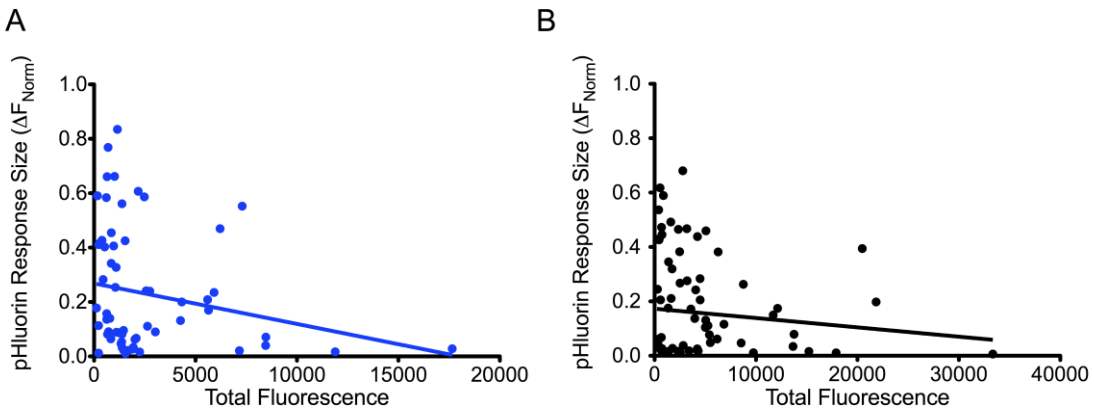

Figure. 5.5

pHluorin expression does not determine the VAMP-pHluorin response size

Data from the same cohort of cells used in figure 5.4 was analysed to determine whether there was a significant correlation of the amount of pHluorin expressed in individual cells to the maximum response size. Response size is the maximum change in fluorescence following stimulation, total fluorescence is determined by NH_4CL wash at the end of each experiment. No significant correlation was seen between the response size and the total amount of pHluorin present in mast cells. For either VAMP-3 (**B**) or VAMP-8. **(A)** VAMP-8 r=-0.057 P =0.63 VAMP-3 r=-0.206 P=0.11.

The ability of a cell to produce an increase in fluorescence following stimulation and the response elicited might be dependent on the amount of pHluorin expressed in the cell. If this was the case then differences in the size of pHluorin responses might be artifactual and caused by differences in the amount of pHluorin expressed in each cell, rather than differences in the level of receptor signalling evoked upon stimulation. To assess whether this was the case, correlation analysis was performed on cells stimulated with anti-IgE to determine whether response size correlated with the total fluorescence (determined by NH_4Cl wash, Figure. 5.5). No significant correlation was seen for either VAMP-3-pHluorin or VAMP-8-pHlourin expressing cells (P=0.63, P=0.11), meaning that differences in the size of VAMP-pHluorin responses are not due to the amount of pHluorin expressed, but more likely due to cell to cell variability in receptor signalling.

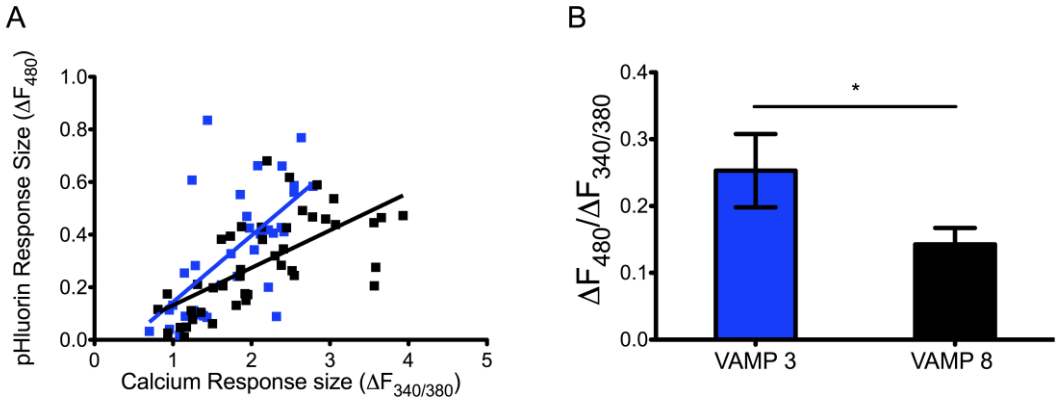

Figure. 5.6

VAMP-3 vesicles have greater calcium sensitivity than VAMP-8 vesicles.

Data from the same cohort of cells used in figure 5.4 was analysed to determine whether VAMP-3 and VAMP-8 vesicles differed in their sensitivity to calcium. **A**, Shows a scatter plot of the maximum pHluorin (y axis) and calcium (x axis) response sizes of individual cells. Blue dots represent VAMP-3 pHluorin expressing cells and blue line shows linear regression (best fit) line, Black dots VAMP-8 pHluorin expressing cells. And black line shows linear regression line. Both VAMP-3 and VAMP-8 vesicles had sensitivity to calcium, where pHluorin response sizes significantly correlated to calcium response sizes, determined by linear regression analysis $P<0.0001$. **B**. VAMP-3 vesicles had a greater sensitivity to calcium than VAMP-8. Graph shows the slope values of linear regression lines shown in A calculated using Graphpad Prism software, blue bar represent VAMP-3, black VAMP-8. , Significance was determined through ANCOVA. VAMP-3 slope value: 0.25±SEM, VAMP-8 slope value 0.14±SEM, * denotes significance between groups of $P<0.05$.

The release of mast cell mediators such as Il- 6, TNF-α and VEGF have been reported to be independent from degranulation and without the need for extracellular calcium [60] suggesting a distinct population of vesicles containing these mediators could exist, and that the fusion of these vesicles is regulated independently of calcium, or is sensitive to calcium signals ensuing from an intracellular store. To examine the calcium sensitivity of VAMP-3 and VAMP-8 vesicle fusion, calcium levels (Ratio $_{340/380}$) were monitored at the same time as pHluorin fluorescence before and after cell activation and correlation analysis performed. Both VAMP-3 and VAMP-8 ($P<0.0001$) pHluorin response size had a significant correlation to the size of the calcium signal (figure 5.6). This suggests that exocytosis of VAMP-3 and VAMP-8 vesicles are regulated by calcium. However, VAMP-3-pHluorin and VAMP-8-pHluorin vesicles displayed differing calcium dependencies. Analysis of figure 5.6 was fitted by linear regression and analysis of covariance (ANCOVA) shows there was a significant difference ($P=0.04954$) in the

co-dependence of exocytosis of VAMP-3 and VAMP-8 pHluorin expressing vesicles. The higher slope value of VAMP-3 (0.2529±0.055) to VAMP-8 (0.1425±0.025) identified VAMP-3 vesicles as having a greater sensitivity to calcium, whereby a greater pHluorin response size would be produced from the same concentration of calcium.

Given VAMP-3-pHluorin vesicles seemingly have different calcium dependencies to VAMP-8-pHluorin vesicles, one might expect that stimulation with the same ligand (Anti-IgE) would result in different distributions of pHluorin response sizes between VAMP-3 and VAMP-8-pHluorins. This is hinted at in the traces of figure5.4 B where the normalised VAMP-3-pHluorin fluorescence trace is larger than VAMP-8-pHluorin trace. To assess this the individual cell maximum pHluorin responses were calculated and the number of cells classed as high responders (ΔpHluorin between 0.5-1), mid responders (0.25-0.5) and low responders (0.25-0) were plotted (figure 5.7) VAMP-3 responses had a more even distribution in their response size than VAMP-8; there were equal numbers of low, mid and high responders, whereas in VAMP-8 pHluorin cells the majority of cells were low responders (Figure. 5.7). This difference was not due to differences in the overall calcium responses as the average size of responses in VAMP-8-pHluorin cells were higher than in VAMP-3, although not significantly (Figure. 5.7c). These results again point to VAMP-3-pHluorin vesicles having differing calcium dependences as, for the same intracellular calcium rise, a greater response is elicited in VAMP-3-pHluorin vesicles. From this data it is not possible to differentiate whether the larger responses of VAMP-3 pHluorin vesicles constitute more vesicles undergoing exocytosis, more vesicles with a higher amount of pHluorin per vesicle undergoing exocytosis or whether there is more full fusion and less kiss and run exocytosis. TIRF microscopy would give a definitive answer as the technique used here measured whole cell fluorescence and cannot differentiate single vesicles.

From the graph in Figure 5.4 it looked as though VAMP-3-pHluorin expressing cells displayed a more rapid rise in cytosolic calcium to FCεRI crosslinking that VAMP-8-pHluorin expressing cells. To determine whether this observation was significant the Ratio $_{340/380}$ was measured at time points of 0, 120 and 240 seconds post stimulation and compared for both sets of cells. At resting conditions there was no

significant difference in the Ratio $_{340/380}$ between VAMP-3-pHluorin and VAMP-8-pHluorin transfected cells, showing that pHluorin expression does not affect basal calcium concentrations. However, at 120 seconds VAMP-3-pHluorin cells had a significantly larger Ratio $_{340/380}$ than VAMP-8-pHluorin cells, showing that there was a greater increase of cytosolic calcium at this time point. After this time at 240 seconds the VAMP 8-pHluorin Ratio $_{340/380}$ caught up to reach the same level as VAMP-3-pHluorin expressing cells. Therefore the overall calcium response sizes are the same but VAMP-3-pHluorin calcium rises occur more rapidly, suggesting that overexpression of VAMP-3-pHluorin results in a more rapid calcium influx after FCεRI crosslinking. This could be due to an increase in the rate of calcium channel trafficking to the plasma membrane, possibly TRP channels. Due to time constraints this hypothesis was not tested further.

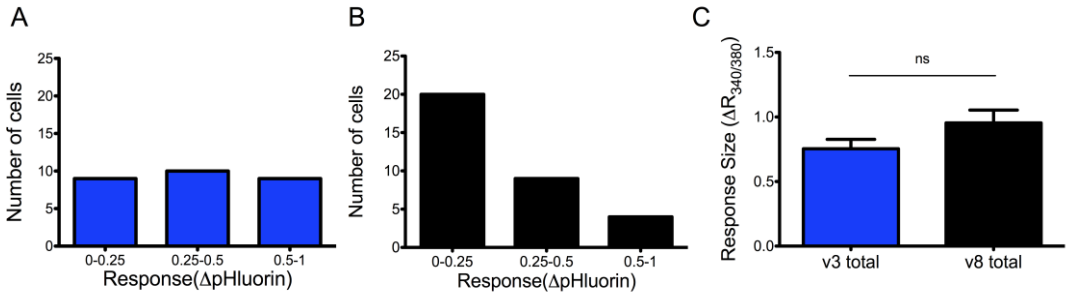

Figure. 5.7

pHluorin response sizes in VAMP-3-pHluorin transfected cells are more evenly distributed than VAMP-8

The maximum increases in normalised pHluorin fluorescence from data in figure 5.4 were grouped as either low (-0.25) med (0.25-0.5) or high (0.5-1) responders to determine the distribution of pHluorin response sizes. **A.**VAMP-3-pHluorin response sizes grouped as low med or determined by subtracting the baseline fluorescence (average of the last 5 frames before stimulation) from the maximum fluorescence (average 5 frames of frame with maximum response). **B**. VAMP-8-pHluorin response sizes grouped as low (-0.25) med (0.25-0.5) or high (0.5-1). **C**. Average calcium response sizes (Δ Ratio$_{340/380}$) in VAMP-3-pHluorin (blue) and VAMP-8-pHluorin (black) transfected cells were not significantly different. Data was from the same cohort of cells used in figure 5.4, data presented as mean± SEM from individual cells. Data Unpaired students T-test P=0.11.

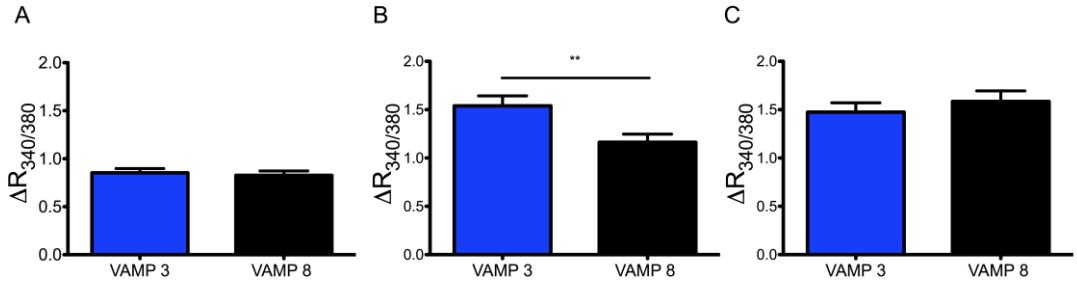

Figure 5.8

VAMP-3-pHluorin cells have a faster calcium rise in response to FCεRI crosslinking than VAMP-8-pHluorin cells

Fura-2AM ratios were monitored at A. 0 sec, B. 120 sec and C. 240 sec post stimulation with FCεRI crosslinking to assess differences in the time course of FCεRI crosslinking induced calcium rises. Data presented as mean± SEM from individual cells, data was from the same cohort of cells used in figure 5.4. **denotes $P<0.01$, unpaired students T-test.

Results so far in this study have highlighted the possibility that VAMP-3 vesicles have a greater sensitivity to cytosolic calcium concentrations than VAMP-8 vesicles. The higher sensitivity to calcium of VAMP-3 vesicles suggests that the sensor(s) regulating fusion of these vesicles could detect calcium which has diffused from entry at the plasma membrane or to calcium release from intracellular stores. The release of calcium from intracellular stores could form a microdomain of calcium, defined by a localised rise/plume of calcium within a particular part of the cell, and microdomains of calcium can lead to regulation of specific cellular events [417]. In this instance this localised increase in calcium concentration might be large enough to lead to selective release of VAMP-3 vesicles that could possibly localise near to calcium stores, while VAMP-8 exocytosis requires global increases in calcium, independent of the need for microdomains, or localised increases of calcium at the plasma membrane.

To gather further evidence of differing calcium sensitivities, VAMP-pHluorin responses to FCεRI stimulation in a nominally calcium free external solution were assessed to determine whether stimulation in the presence of no external calcium influx could still induce VAMP-3 vesicle exocytosis.

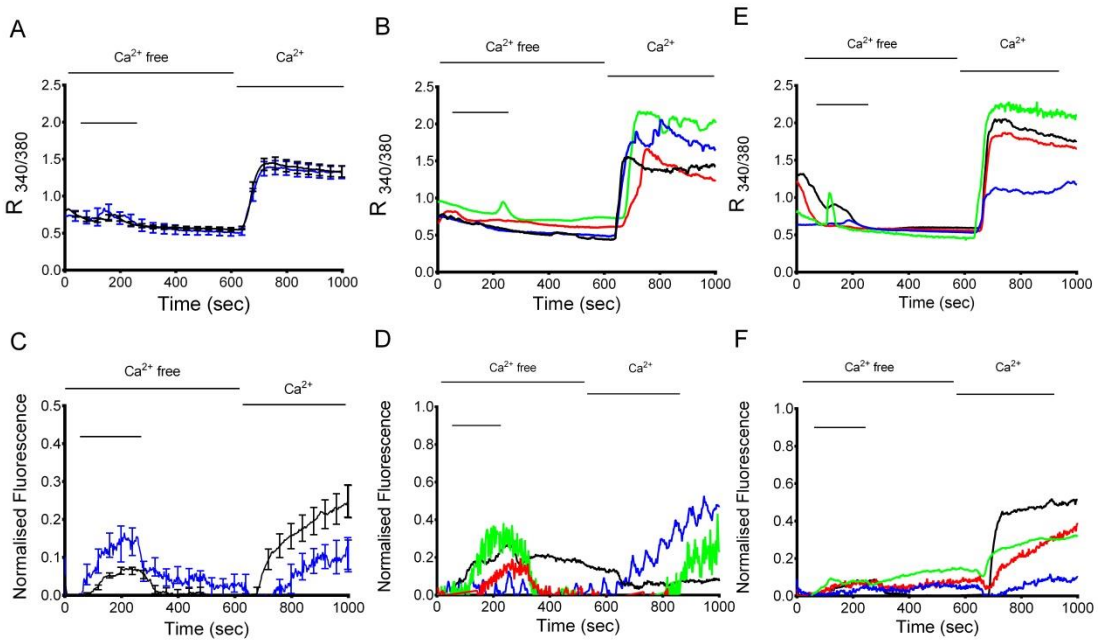

Figure. 5.9

VAMP-8 and VAMP-3 vesicles show distinct calcium sensitivities

LAD 2 cells transfected with either VAMP-8 or VAMP-3 pHluorin were sensitised overnight with 300ng/ml of human IgE. The next day cells were loaded with fura-2am and FCεRI cross-linking was subsequently induced by perfusion of 10µg/ml anti-IgE in nominally calcium free external solution (as indicated by the bar above each trace**). A.** Mean individual cell traces, $R_{340/380}$, representing calcium responses and **B**. Mean individual traces of normalised pHluorin fluorescence. Blue lines represent data measured in VAMP-3-pHluorin transfected cells, black lines represent data measured in VAMP-8-pHluorin transfected cells. **C** Calcium and **D** pHluorin representative individual cell responses of VAMP-3 pHluorin expressing cells. **E**. Calcium and **F**. pHluorin representative individual cell responses of VAMP-8 pHluorin expressing cells. VAMP-8-pHluorin n=33± SEM, VAMP-3-pHluorin n=49± SEM. Data from three transfections.

As expected, VAMP-8 vesicles underwent minimal exocytosis in calcium free conditions in comparison to their responses when external calcium was added back into the external solution (figure 5.9). This confirms that exocytosis of VAMP-8 positive vesicles is highly regulated by calcium influx or plasmalemmal calcium channels and may well be triggered by local calcium microdomains acting on a low affinity calcium sensor. VAMP-3 vesicles showed similar sized responses with or without the presence of external calcium. From this data it is clear that VAMP-3-pHluorin vesicles do not require extracellular calcium influx, and release from intracellular stores could be sufficient to induce exocytosis. What is not clear from these experiments is whether VAMP-3-pHluorin vesicles require calcium at all. However, given the results in figure 5.6 showing a significant correlation between

the pHluorin and calcium response sizes of VAMP-3 vesicles, the results would be consistent with the view that VAMP-3 vesicles are sensitive to smaller concentrations in intracellular calcium concentrations than VAMP-8 containing vesicles. Alternatively, there might be no difference in the sensitivity of each vesicle to calcium, just that VAMP-3 localises near to intracellular stores and gets exposed to high localised calcium concentrations present near IP3 receptors. Further studies to identify the calcium sensors regulating exocytosis of VAMP-3 and VAMP-8 containing vesicles are required to distinguish between these possibilities.

5.2.5 Retargeted BoNT/E to target mast cell degranulation

Mast cells have been implicated in a number of allergic diseases, including asthma and IBD [2]. Targeting the release of inflammatory mediators through inhibition of SNARE mediated membrane fusion could provide a novel therapy for inflammatory disease. BoNTs cleave SNARE proteins (section 1.5) and so might provide a way of targeting mast cell mediator release. One BoNT serotype, BoNT/E, cleaves the neuronal plasma membrane SNARE SNAP-25, which is not expressed in human mast cells (figure 4.16) However, a modified form of BoNT/E has been developed that, with a single point mutation to the LC (K224D), has been successfully retargeted to SNAP-23, referred to as BoNT/E(K224D) [323]. This SNARE is present in mast cells (figure 4.16) and is essential for degranulation [239, 365, 388]. Therefore using this toxin it might be possible to target release of VAMP-8 vesicles indirectly by cleaving SNAP-23 and thus stopping VAMP-8 fusion with the plasma membrane. Western blot of SNAP-23 in BoNT/E (K224D) LC transfected LAD-2 cells showed a reduced band size and lower KD band compared to native BoNT/E LC transfected cells, suggesting the toxin was cleaving SNAP-23 (Figure 5.10). To determine whether this construct could inhibit VAMP-8 vesicle exocytosis, LAD 2 cells were transfected with VAMP-8-pHluorin along with either BoNT/E LC or the SNAP-23 cleaving BoNT/E (K224D) LC in a dual transfection. Cells expressing BoNT/E(K224D) LC showed a reduced level of exocytosis compared to BoNT/E LC in FCεRI stimulated cells as measured by increases in pHluorin fluorescence (Figure 5.11). However, the calcium response to anti-IgE was also reduced suggesting effects on receptor signalling. No difference in exocytosis

was seen following stimulation with the calcium ionophore ionomycin (Figure 5.12).

Taken together these results suggest the toxin is affecting cell signalling, either by inhibiting the trafficking of calcium channels to the plasma membrane or affecting the trafficking of the FceRI to the cell surface directly. It is not directly inhibiting VAMP-8-pHluorin exocytosis. Results from the ionomycin experiments, suggests it is not. Whether in the absence of SNAP-23 another Qbc SNARE (SNAP-29,-47) regulates exocytosis in mast cells remains to be determined. Or as a result of incomplete cleavage, the remaining SNAP-23 might be enough to mediate ionomycin induced exocytosis (figure 5.10). As a result of these observations there was no point in continuing using this mutant construct. Alternative methods for inhibiting the release of mast cell mediators were sought.

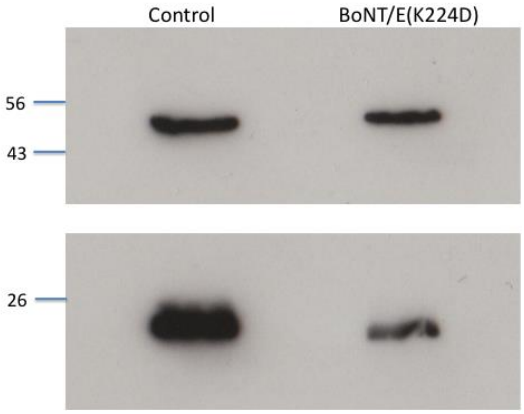

Figure. 5.10

BoNT/E(K224D) cleavage of SNAP-23 in LAD 2 cells

Western blot of SNAP-23 in BoNT/E and BoNT/E(K224) LC expressing cells. Figure representative of 3 transfections. Top bands represent α-tubulin expression, bottom SNAP-23.

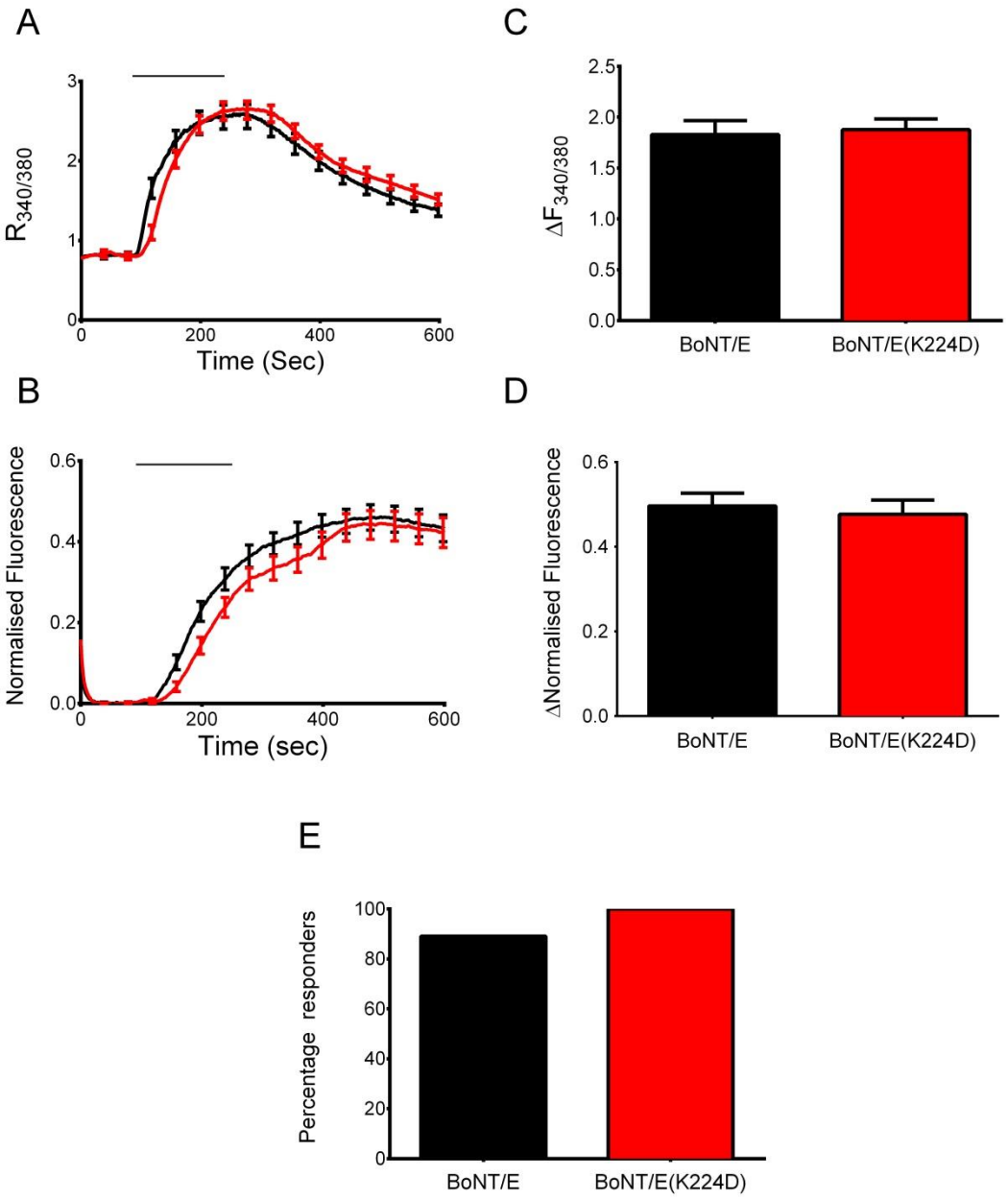

Figure. 5.11

BoNT/E(K224D) LC has no effect on ionomycin induced exocytosis of VAMP-8-pHluorin.

LAD2 cells were transfected with VAMP-8-pHuorin and either BoNT/E LC or BoNT/E(K224D) LC. Cells were then sensitised overnight with 300ng/ml of human IgE myeloma. The next day cells were loaded with Fura2 calcium dye and imaged at 340,380 and 480nM. Cells were stimulated through the perfusion of 1µM ionomycin as indicated in bars above trace. **A**. Grouped single cell fluorescence shows calcium responses of BoNT/E(K224D) (red) and BoNT/E LC (Black) responding to the non-receptor mediated stimulation of ionomycin. **B**. Grouped single cell pHluorin responses in the same cells as in A. **C**. Calcium response sizes. **D**. pHluorin response sizes. **E**. Percentage of responding cells. BoNT/E n=43± SEM, BoNT(K224d) n=44± SEM. Data from 3 transfections.

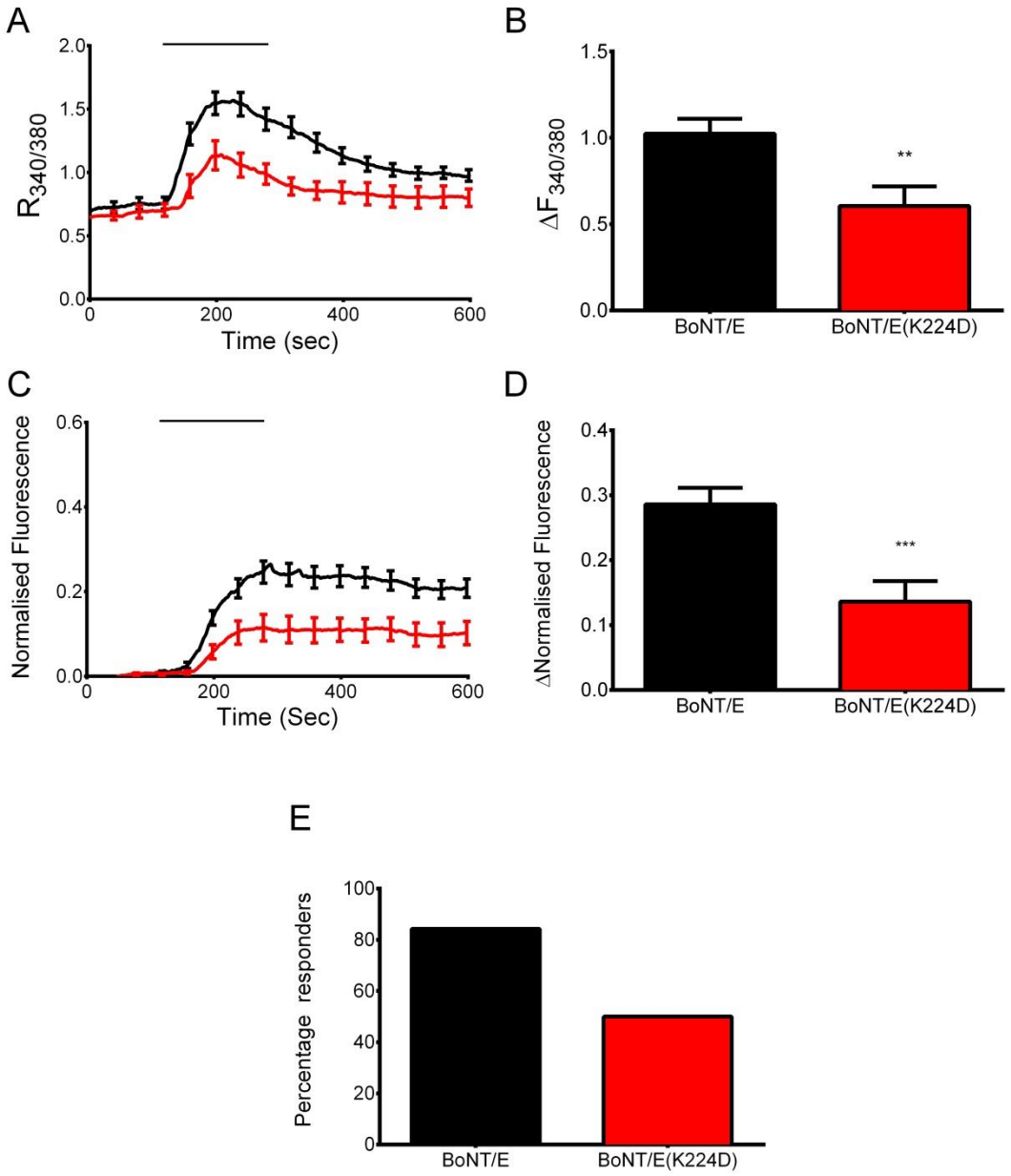

Figure. 5.12

BoNT/E(K224D) LC inhibits FCεRI induced exocytosis of VAMP-8-pHluorin.

LAD 2 cells were transfected with VAMP-8-pHuorin and either BoNT/E LC or BoNT/E(K224D) LC. Cells were then sensitised overnight with 300ng/ml of human IgE myeloma. The next day cells were loaded with Fura2 calcium dye and imaged at 340,380 and 480nM. Cross-linking of FCεRI subsequently induced through the application of 10µg/ml anti-IgE as indicated in bars above traces. **A**. Grouped single cell fluorescence shows calcium responses of BoNT/E(K224D) (red) and BoNT/E LC (Black) responding to the non-receptor mediated stimulation of Ionomycin.. **B.** Grouped single cell pHluorin responses in the same cells as in A. **C**. Calcium response sizes. **D**. pHluorin response sizes. **E**. Percentage of responding cells BoNT/E n=42/51± SEM, BoNT(K224d) n=22/44± SEM. Data from 3 transfections. ** denotes P<0.01 *** denotes p<0.001, unpaired students T-test.

5.2.2 Selective targeting of VAMP-3 vesicles by BoNT/B

The data presented in this chapter and in chapter 4 identifies VAMP-3 positive vesicles that undergo plasma membrane fusion upon mast cell activation. BoNT/B cleaves VAMPs- 1, 2 and 3 [418]. Work in chapter 4 confirmed human mast cells do not express VAMP-1 and 2 and so VAMP-3 is the only BoNT/B targetable SNARE expressed in LAD 2 cells. Therefore, it is possible to assess the functional role of VAMP-3 in mast cells by using BoNT/B to cleave and therefore inhibit VAMP-3 dependent fusion. To do this LAD 2 cells were transfected with the LC of BoNT/B. Western blot was performed on BoNT/B LC transfected cells to confirm BoNT cleavage of VAMP-3 (as shown in figure 5.13). Cells transfected with the BoNT/B LC construct had significantly reduced VAMP-3 protein compared to a non-transfected control, showing that the construct could cleave VAMP-3 in LAD 2 cells and could be useful in subsequent functional studies.

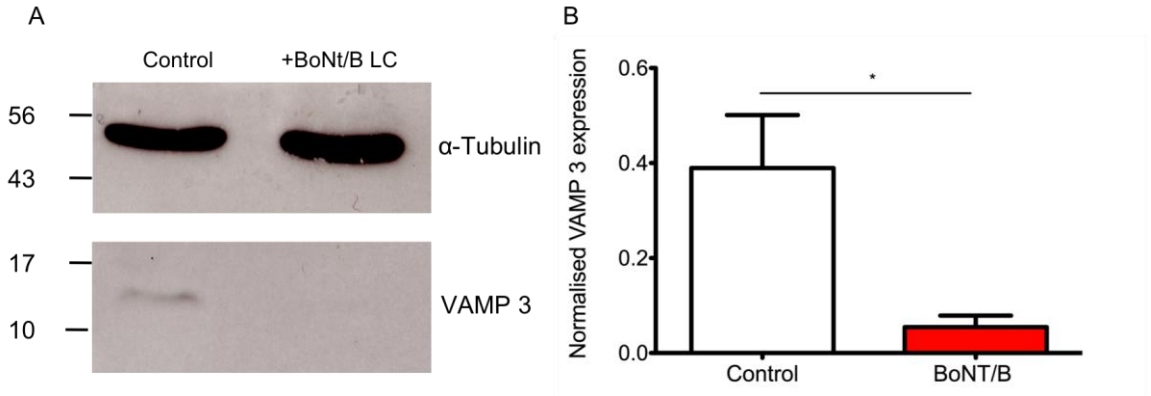

Figure. 5.13

BoNT/B cleaves VAMP-3 in LAD 2 cells

LAD 2 cells were transfected with a BoNT/B LC expressing plasmid. After 48 hours cells were lysed and protein levels of VAMP-3 were compares to an untransfected cell lysate control through western blot. **A**. Western blot confirms cleavage of VAMP-3 by BoNT/B LC,, above bands show α-tubulin loading control expression, below bands indicate VAMP-3 expression. **B**. Band intensity values of VAMP-3 in figure A were normalised to α-tubulin loading control, Intensity values measured using Image J software. Mean data from three separate BoNT/B LC transfections ± SEM.

5.2.3 VAMP-8-shRNA knockdown

VAMP-8 is insensitive to BoNTs (section 1.5.1). Therefore, to assess the functional role VAMP-8 has in mast cell mediator release knockdown of VAMP-8 was performed through the use of shRNA. Four mammalian expression plasmids containing unique 29mer shRNA constructs were tested alongside a scramble

control for their ability to knockdown VAMP-8 gene expression (data presented in section 2.18). shRNA 4 produced the highest level of knockdown and was used in all future shRNA experiments. The experiment was repeated with shRNA 4 to confirm the knockdown (figure 5.14) and levels of VAMP-8 compared to LAD 2 cells transfected with a scramble control, normalised to α-tubulin. VAMP-8 protein levels were reduced when compared to the scramble control. There was also a reduction in the band intensity of the higher molecular weight band, although less pronounced. This suggests this could be a VAMP chaperone or VAMP-8 dimer.

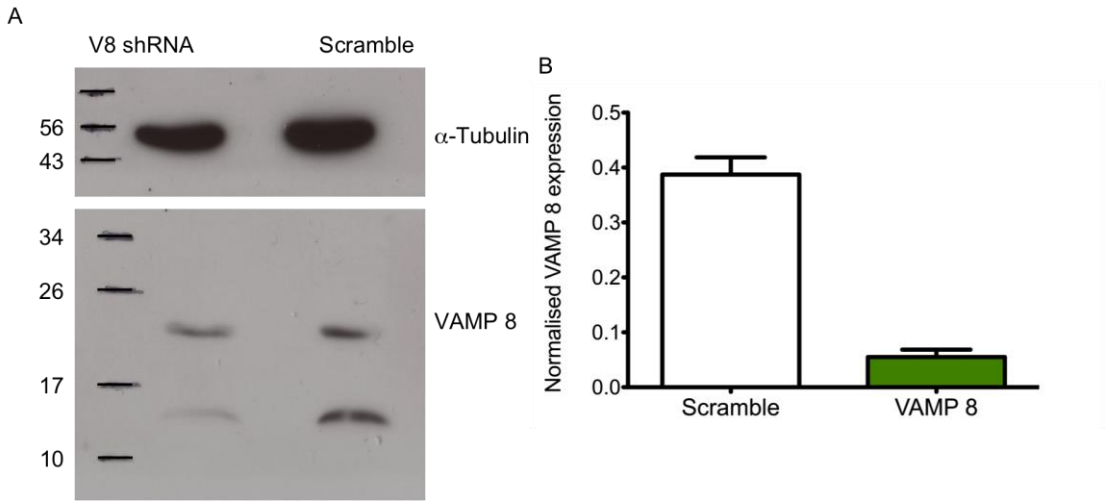

Figure. 5.14

VAMP-8 shRNA knocks down the expression of VAMP-8 protein in LAD 2 cells

LAD 2 cells were transfected with either a VAMP-8 shRNA plasmid or a scramble control. After 48 hours cells were lysed and expression levels of VAMP-8 monitored through western blotting. **A**. Western blot of VAMP-8 shRNA expressing cells above bands show α-tubulin loading control expression, below bands indicate VAMP-8 expression. **B**. Band intensity values of VAMP-8 normalised to α-tubulin loading control. Intensity values measured using Image J software. Mean data from two separate shRNA transfections ± SEM.

5.2.4 Targeting VAMP-3 and VAMP-8 mediated exocytosis

Having developed independent methods to knockdown VAMP-8 and VAMP-3 in human mast cells, functional experiments were performed to determine whether these SNAREs regulate the release of mast cell mediators. Previous studies have implicated VAMP-8 in mast cell granule release but found no role for VAMP-3 [239, 395]. β-hexosaminidase release from LAD 2 cells following FcεRI stimulation was monitored and compared in BoNT/B LC and VAMP-8 shRNA transfected cells to assess the role of VAMP-3 and 8 in mast cell granule release. β-hexosaminidase is a

granule constituent that is regularly used to monitor degranulation in mast cells (section 1.1.2). β-hexosaminidase release in cells transfected with either a scrambled shRNA construct, VAMP-8 shRNA or BoNT/B LC was normalised to release from un-transfected cells. (figure 5.15). Knockdown of VAMP-8 inhibited release of β-hexosaminidase while BoNT/B LC or the scramble control had no significant effect. Combined with data from chapter 3 showing VAMP-8 colocalising with tryptase, a SG marker, the results here confirm that VAMP-8 regulates SG release in human mast cells, whilst VAMP-3 does not.

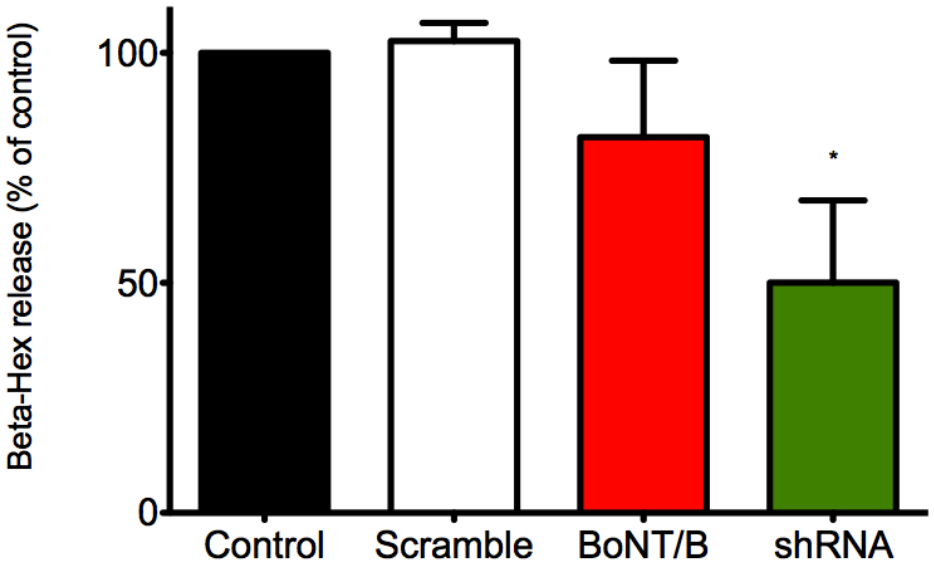

Figure. 5.15

Knockdown of VAMP-8 in LAD 2 cells inhibits mast cell degranulation

LAD 2 cells were transfected with either VAMP-8 shRNA,(green bar) a scramble control (white bar) or with BoNT/B LC (red bar) and after 48 hours were stimulated through the addition of 10µg/ml anti-IgE to induced FCεRI crosslinking for 20 minutes. Cells expressing VAMP-8 shRNA had a reduced degranulation response compared to scramble control cells and cells transfected with the VAMP-3 targeting BoNT/B LC. β-Hexosaminidase release is expressed as percentage release from untransfected mast cells. N=4 transfections ±SEM *denotes $P<0.05$, one way ANOVA post hoc Tukey test.

From the β-hexosaminidase assay it was clear that BoNT/B treatment had no significant effect on degranulation in human mast cells. To test whether BoNT/B could selectively inhibit VAMP-3 exocytosis, VAMP-3-pHluorin and VAMP-8-pHluorin assays were performed in cells transfected with the BoNT/B LC. In ionomycin-stimulated cells, BoNT/B LC inhibited VAMP-3-pHluorin exocytosis (Figure 5.17) but had no effect on VAMP-8-pHluorin exocytosis (Figure 5.16).

However, Figure 5.17 C shows that BoNT/B LC expression only leads to a small reduction in the number of VAMP-3-pHluorin cells responding. This suggests not all VAMP-3-pHluorin is cleaved in each cell but that the reduction is sufficient to see a reduction in the size of the VAMP-3-pHluorin response. The calcium responses of both VAMP-3-pHluorin and VAMP-8-pHluorin cells were unaffected by BoNT/B LC expression, showing inhibition of VAMP-3-pHluorin vesicle exocytosis is due to direct cleavage of VAMP-3 and not the result in any off target effects on signalling pathways, as was the case with the modified BoNT/E toxin, E(K224D).

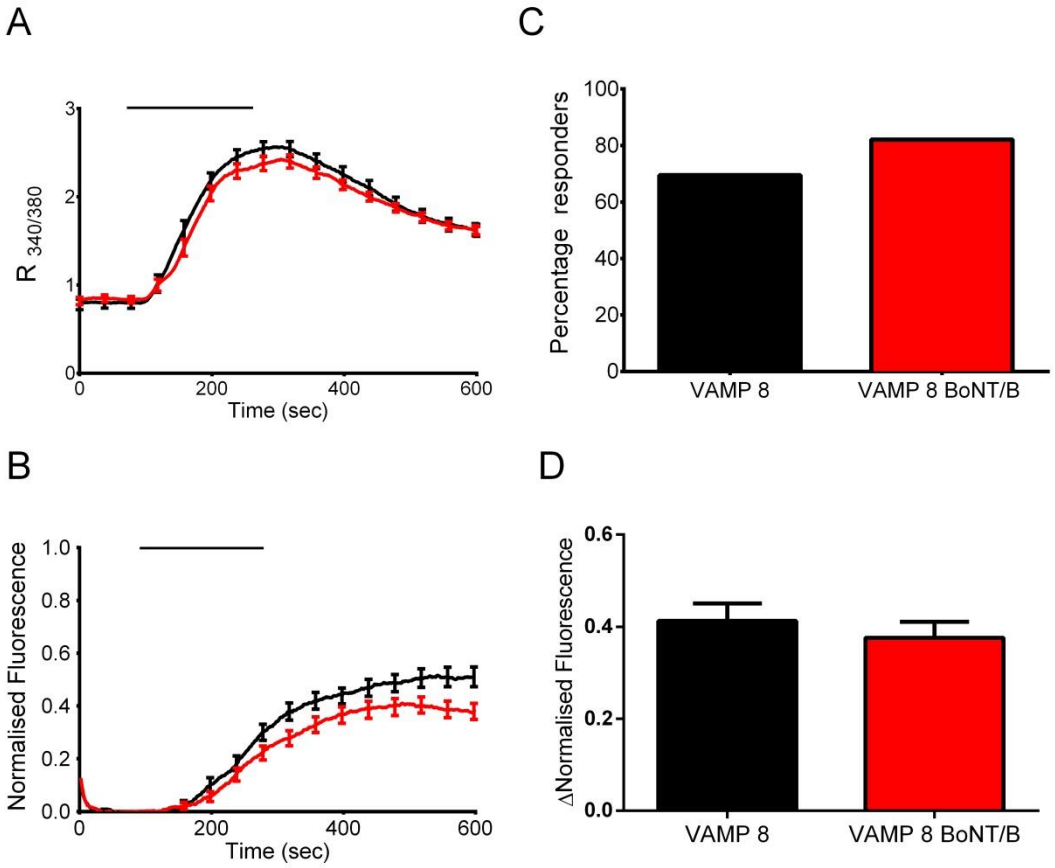

Figure. 5.16

BoNT/B LC does not significantly inhibit ionomycin-induced exocytosis of VAMP-8-pHluorin. LAD 2 cells were transfected with either VAMP-8 pHluorin or VAMP-8 pHluorin and BoNT/B LC, sensitized overnight with 300ng/ml of human IgE and subsequently stimulated by perfusion of 1µM ionomycin, shown by horizontal bars above graphs. **A**. Calcium response in VAMP-8 pHluorin transfected cells. **B**. VAMP-8 pHluorin responses. **C** shows percentage responding cells for VAMP-8 coverslips. D. Size of VAMP-8 pHluorin responses. Black lines and bar represent VAMP-8 pHluorin and red lines and bar represent dual pHluorin and BoNT/B transfected cells. Data represented as mean data from individual cells. VAMP-8 n=58± SEM, VAMP-8 BoNT/B LC n=54± SEM. Data from 3 transfections.

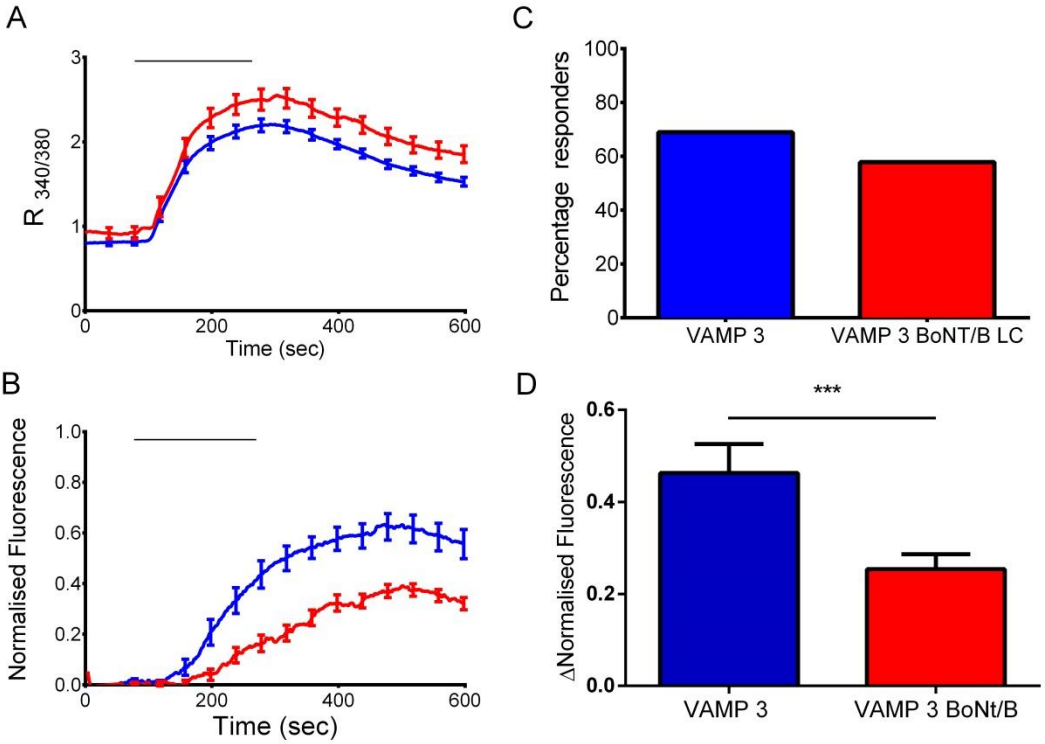

Figure. 5.17

BoNT/B LC inhibits exocytosis of ionomycin stimulated VAMP-3-pHluroin vesicles

LAD 2 cells were transfected with either VAMP-3 pHluorin or VAMP-3 pHluorin and BoNT/B LC, sensitized overnight with 300ng/ml of human IgE and subsequently stimulated by perfusion of 1μM ionomycin, shown by horizontal bars above graphs. **A.** Fura2 ratio increase in VAMP-3 pHluorin transfected cells. **B.** VAMP-3 pHluorin responses. **C**. Percentage responding cells for VAMP-3 coverslips. **D.** VAMP-3 pHluorin response sizes. Blue lines and bar represent VAMP-3 pHluorin and red lines represent dual pHluorin and BoNT/B LC transfected cells. Data represented as mean data from single cells. VAMP-3 n=34± SEM VAMP-3 BoNt/B LC n=45± SEM. *** denotes P<0.0001 unpaired students T-test. Data from 3 transfections.

Ionomycin is not a physiological stimulus and the results in figure 5.11 highlight how different results can be obtained by activation of mast cells through different stimuli. Therefore, BoNT/B LC experiments were repeated using the more physiological stimulus of FcεRI crosslinking. As with ionomycin, there was no inhibition of VAMP-8-pHluorin exocytosis (figure 5.18). In VAMP-3 pHluorin cells there was only a small reduction in the percentage of cells showing a pHluorin response (53 to 45) (figure 5.19 C) and there was no significant difference in the pHluorin response size of cells that did respond to receptor activation (figure 5.19). However, examination of the diary plots of the pHluorin fluorescence for non-responding BoNT/B LC expressing VAMP-3-pHluorin cells, a negative change of fluorescence is detected, not seen in VAMP-3 pHluorin cells not expressing the toxin

construct or VAMP-8-pHluorin BoNT/B LC expressing cells (figure 5.19 E and F). This could indicate that following FCeRI crosslinking the balance between VAMP-3 pHluorin exocytosis and endocytosis is altered in such a way that endocytosis predominates. The fact that this was not observed following ionomycin stimulation suggests that signalling molecules other than calcium are responsible for this receptor induced endocytosis.

Results in figure 5.8 showed VAMP-3-pHluorin expressing cells have a more rapid calcium rise than VAMP-8-pHluorin cells in response to FCεRI crosslinking. This process might be reversed in cells expressing the BoNT/B LC. To determine whether this was the case, $Ratio_{340/380}$ values were monitored at the same time points post stimulation (0,120 and 240 seconds) as in figure 5.8. In BoNT/B LC VAMP-3-pHluorin expressing cells the faster rise in intracellular calcium to FCεRI crosslinking is reversed, as VAMP-3 is cleaved, nullifying the effects of overexpression (figure 5.20)

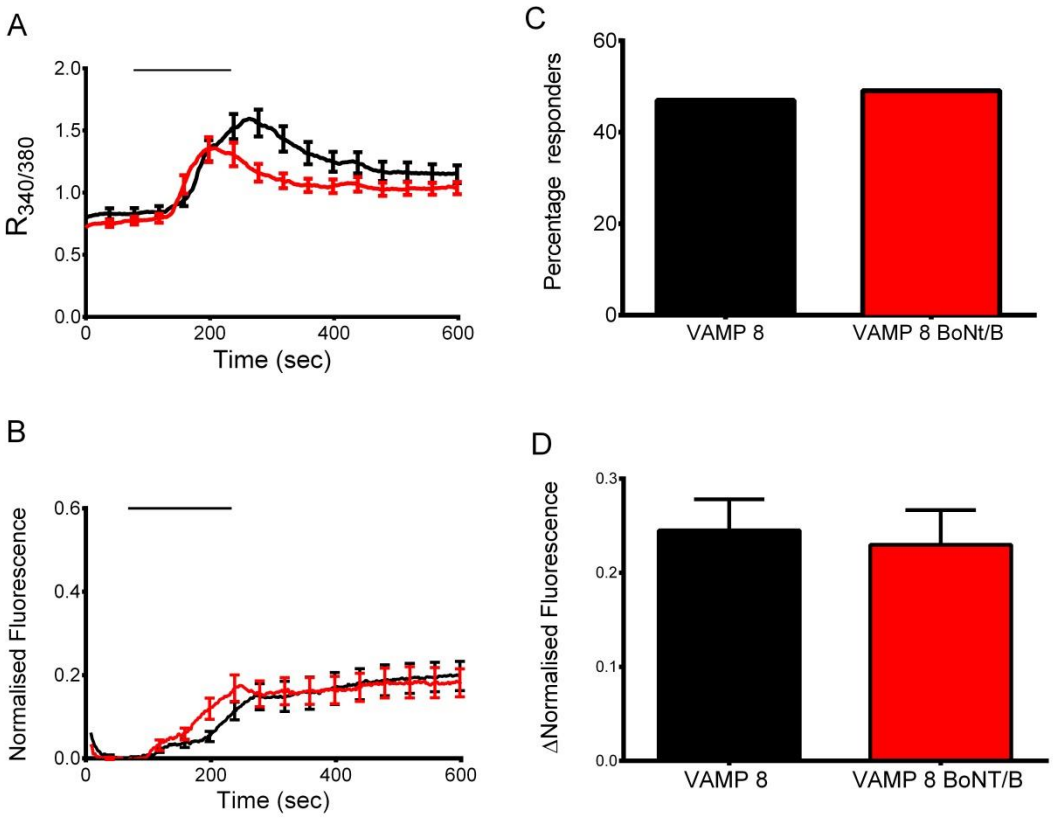

Figure. 5.18

BoNT/B LC does not significantly inhibit exocytosis of FcεRI VAMP-8 pHluorin vesicles

LAD 2 cells were transfected with either VAMP-8 pHluorin or VAMP-8 pHluorin and BoNT/B LC and sensitized overnight with 300ng/ml of human IgE. The next day cells were loaded with Fura2AM calcium dye and imaged at 340,380 and 480nM. Cross-linking of FCεRI subsequently induced through the application of 10μg/ml anti-IgE. **A.** Calcium response in VAMP-8 and VAMP-8 BoNT/B LC pHluorin cells. **B**. VAMP-8 and VAMP-8 BoNT/B LC pHluorin responses**. C.** Percentage responding cells for VAMP-8 coverslips. **D**. Size of VAMP-8 pHluorin responses Black lines and bar represent VAMP-8 pHluorin and red lines represent dual pHluorin and BoNT/B transfected cells. Data represented as mean data from single cells. VAMP-8 n=±33 SEM, VAMP-8 BoNT/B LC n=30±SEM. Data from 3 transfections.

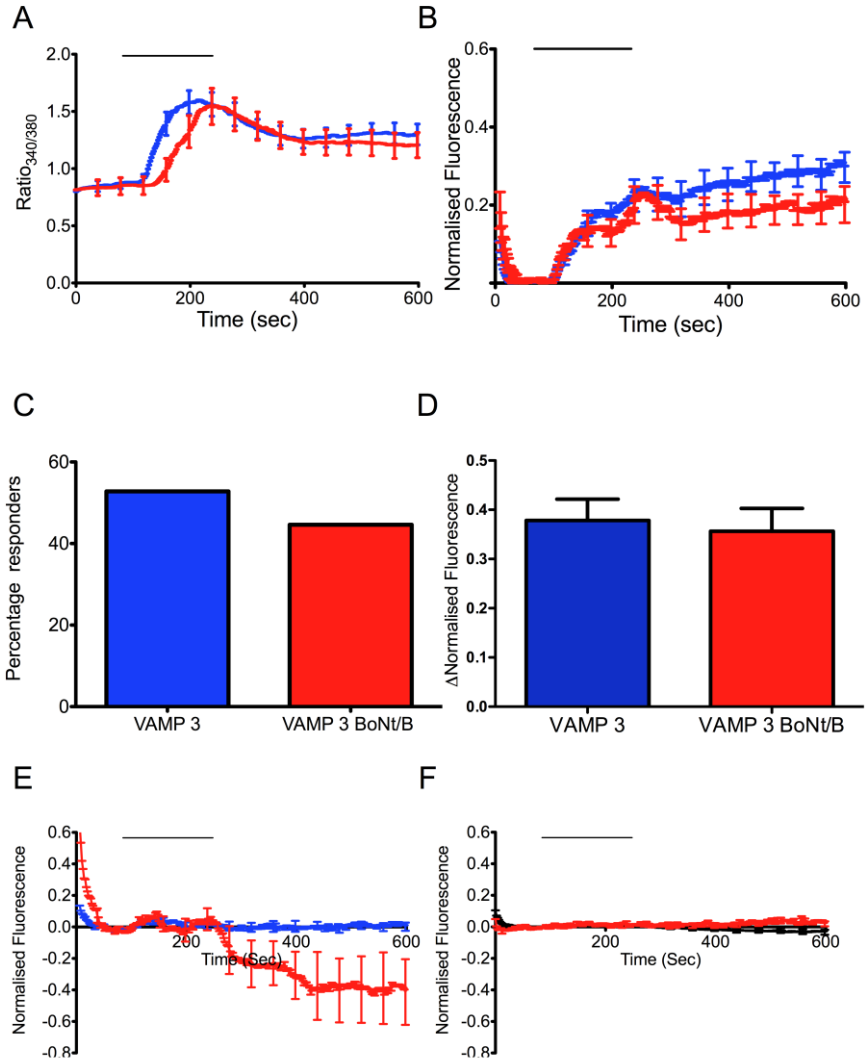

Figure. 5.19

BoNT/B LC inhibits exocytosis of FCεRI stimulated VAMP-3 pHluroin vesicles

LAD 2 cells were transfected with either VAMP-3 pHluorin or VAMP-3 pHluorin and BoNT/B LC, sensitized overnight with 300ng/ml of human IgE, The next day cells were loaded with Fura2 calcium dye and imaged at 340, 380 and 480nM. Cross-linking of FcεRI subsequently induced through the application of 10µg/ml anti-IgE, shown by horizontal bars above graphs. **A.** Calcium response in VAMP-3 pHluorin transfected cells. **B.** VAMP-3 and VAMP-3 BoNT/B LC pHluorin responses. **C**. Percentage responding cells for VAMP-3 coverslips. **D**. Size of VAMP-3 pHluorin responses. Blue lines and bar represent VAMP-3 pHluorin and red lines represent dual pHluorin and BoNT/B transfected cells. Data represented as mean data from single cells. VAMP-3 n=±34 SEM VAMP-3 BoNT/B LC n=±27 SEM, E shows pHluorin responses from non-responding VAMP-3 pHluorin cells. Blue lines represent VAMP-3 pHluorin and red lines represent dual pHluorin and BoNT/B transfected cells. VAMP-3 non-responders n=26±SEM VAMP-3 BoNT/B LC non responders n=27±SEM, F shows pHluorin responses from non-responding VAMP-8 pHluorin cells. Black lines represent VAMP-8 pHluorin and red lines represent dual pHluorin and BoNT/B transfected cells. VAMP-8 non-responders n=23±SEM, VAMP-8 BoNT/B LC non-responders n=13±SEM. Data from 3 transfections.

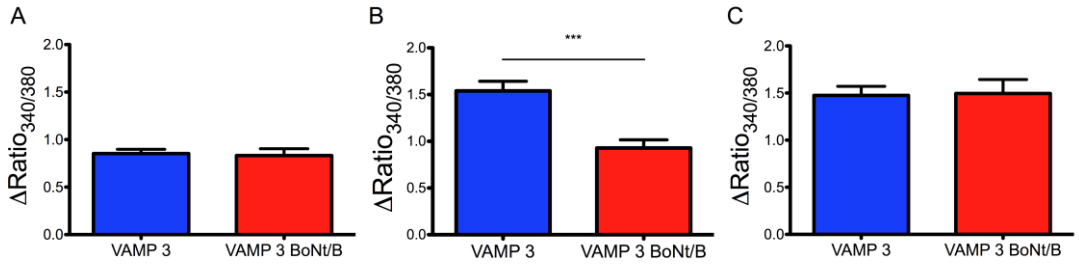

Figure. 5.20

BoNT/B reverses VAMP-3-pHluorin induced fast calcium response to FCεRI crosslinking

340nm/380nm ratios were monitored at **A**. 0 sec, **B**. 120 sec and **C**. 240 sec post stimulation to assess differences in the time course of FCεRI crosslinking induced calcium rises between VAMP-3-pHluorin and VAMP-3-pHLuorin and BoNT/LC expressing cells. Data represented as mean data from single cells. VAMP-3 n=34±SEM VAMP-3 BoNt/B LC n=27±SEM, *** denotes $p<0.001$, unpaired students T-test.

To gather a better understanding of the potential physiological effects of BoNT/B cleavage of VAMP-3 on secretion in mast cells, the effects of BoNT/B expression on IL-6 release was measured. Experiments in chapter 4 identified VAMP-3 vesicles and IL-6 GFP, colocalising to rab11, a recycling endosomal marker and studies in macrophages have identified a role of VAMP-3 in Il-6 release (Section 1.3.2). To evaluate the role of VAMP-3 in regulating IL-6 secretion from human mast cells, LAD 2 cells were transfected with IL-6 GFP and BoNT/B LC, and stimulated through FcεRI crosslinking. Secretion of IL-6 was monitored by western blotting and normalising the band intensity values of IL-6 GFP released in the cell supernatant by the cell lysate. As shown in figure 5.21, expression of BoNT/B significantly inhibited IL-6 secretion from stimulated LAD 2 cells. In contrast, knocking down VAMP-8 expression through shRNA did not attenuate IL-6 GFP secretion in similarly stimulated cells. This is the opposite of what was found with β-hexosaminidase release (figure 5.15) where knockdown of VAMP-8, but not VAMP-3, resulted in reduced degranulation and suggests shows that VAMP-3 and VAMP-8 mediate the fusion of vesicles containing different types of mediators in mast cells.

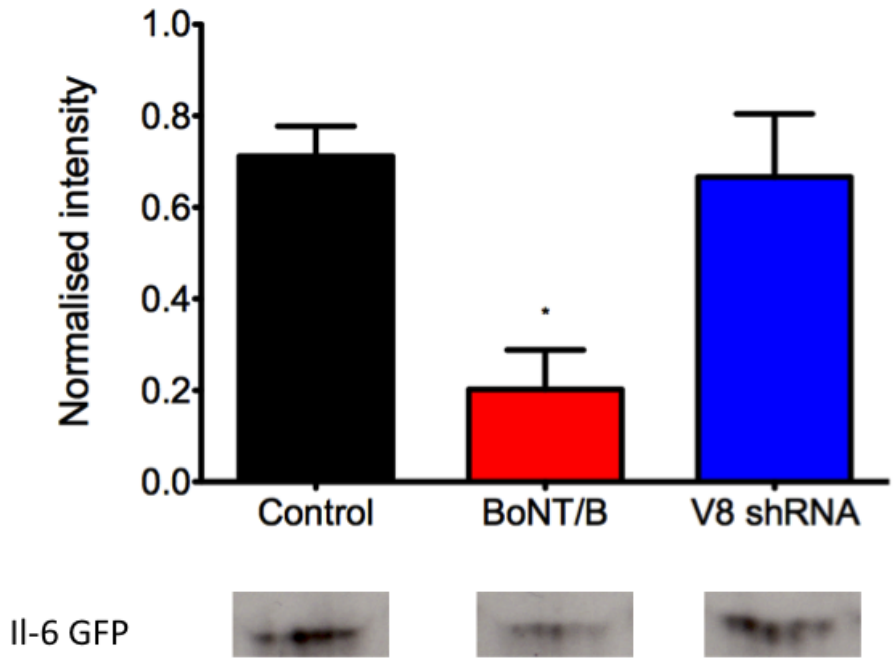

Figure. 5.21

BoNT/B inhibits IL-6 GFP release

LAD 2 cells were transfected with IL-6 GFP and Il-6 GFP + BoNT/B LC or V8 shRNA. Cells were stimulated by FCεRI crosslinking and the cell supernatant collected after 6 hours and subjected to western blot using an anti-GFP antibody. Values represent supernatant band intensity values normalised to cell lysate band intensities. Red bar indicates normalised Il-6 release in BoNT/B expressing cells, while blue bar shows release in VAMP-8 shRNA expressing cells. Black shows release in control cells expressing the IL-6 GFP construct. N=3± SEM. One way ANOVA post hoc Tukey test, $p<0.05$).

The results shown here identify two distinct pools of vesicles, defined in part by the expression of VAMP-3 or VAMP-8, mediating the release of inflammatory mediators from mast cells. One pool is characterised by the expression of VAMP-8 and mediates the fusion of SGs whose exocytosis is dependent on the influx of extracellular calcium. Another pool express VAMP-3 and mediate the secretion release of Il-6 and can be selectively targeted by BoNT/B. VAMP-3 vesicles display differing sensitivities to the levels and/or source of calcium to VAMP-8 vesicles. VAMP-3 vesicles are able to undergo fusion with the plasma membrane without the presence of extracellular calcium while VAMP-8 vesicle exocytosis under these conditions is minimal. These results highlight the differential control of secretory pathways in mast cells that can be defined, in part, by VAMP-3 and VAMP-8 expression.

5.3 Discussion

Using pHluorin tagged VAMP-3 and VAMP-8 has allowed further analysis of their function in mast cells. Results in chapter 4 identified these two VAMPs as possible mediators of fusion of vesicles containing inflammatory mediators. In this chapter using the pHluorin tagged forms of VAMP-3 and -8 it is clear both VAMP-3 and VAMP-8 vesicles traffic and fuse to the plasma membrane but display distinct calcium sensitivities. Furthermore utilising shRNA targeted to VAMP-8 it has been possible to inhibit the release of β-hexosaminidase. It has been possible to selectively target VAMP-3 vesicles by BoNT/B and in doing so inhibit the release of IL-6 GFP. Finally preliminary experiments suggest it might also be possible to target the release of mast cell mediators by the use of BoNT/E(K224D) although this would result in significant off target effects.

A greater proportion of VAMP-8 was present in intracellular compartments than VAMP-3, which has a significantly greater cell surface distribution. This observation might be explained by the roles each VAMP has in membrane trafficking and the mast cell. With VAMP-8 residing on mast cell granules, released in regulated exocytosis, one might expect the greatest proportion of the protein in resting conditions to reside within pre-formed granules awaiting a trigger to undergo exocytosis. VAMP-3, potentially mediating traffic of a more constitutive nature, might have a more dynamic distribution as there would be greater recycling to and from the membrane. One note of caution is that in both pHluorins the proportion of vesicles that were present at the membrane was high (50% VAMP-3, 40% VAMP-8). It is possible that with overexpression excess VAMP is trafficked out onto the plasma membrane as the pathways that are defined by each VAMP become saturated. However, the fact that there are still significant differences highlights the different distributions of VAMP-3-pHluorin and VAMP-8-pHluorin in LAD 2 cells.

VAMP-8 was confirmed as the SNARE responsible for mediating granule fusion and the release of preformed granule mediators in human mast cells. VAMP-8-pHluorin vesicles fuse with the plasma membrane in a calcium-dependent manner and shRNA knockdown of VAMP-8 function inhibited the release of granule β-hexosaminidase. This augments the evidence in chapter 4 showing colocalisation of VAMP-8 with tryptase and trafficking of the endogenous protein to the plasma

membrane. These results are in agreement with previous studies in both murine and human mast cells that have found knockdown or inhibition of VAMP-8 to inhibit histamine release [235, 239]. The incomplete ablation of β-hexosaminidase secretion in VAMP-8 shRNA transfected cells is likely due to limited transfection efficiency (see section 2.16). With this efficiency it would be impossible to completely inhibit release. Also one has to consider the possibility of compensation of other VAMPs; upon knockdown of VAMP-8 in murine mast cells VAMP-3 increases its association with other SNAREs such as SNAP-23 [238], this possibility has not been ruled out in this study. Furthermore, given a small amount of VAMP-7 colocalised to tryptase, there might be a proportion of granules whose exocytosis is mediated by this SNARE and not VAMP-8. Knockdown of a SNARE of the exocytotic machinery can result in compensatory expression of another SNARE protein. In this study expression levels of other SNARE and SNARsE regulators upon VAMP-8 knockdown was not assessed and so it is not possible to rule out the possibility of compensatory SNARE expression. Functional data including IL-6 GFP release and β-hexosaminidase release showed that inhibiting the function of VAMP-3 and VAMP-8 did result in different functional effects. Comparing protein level or mRNA levels of the exocytotic machinery in shRNA expressing cells would give a more definitive answer as to whether certain SNAREs or SNARE regulators become overexpressed upon VAMP-8 knockdown. Further experiments could also be performed using dominant negative constructs to complement the knockdown experiments. Overall these results still give strong evidence that VAMP-8 is present on SGs and mediates their release, but whether VAMP-8 is the sole VAMP responsible for mast cell degranulation requires further study.

Release of preformed mediators contained within SGs requires large increases in cytosolic calcium [419]. VAMP-3 and VAMP-8 vesicle showed differences in their dependencies on calcium. Both VAMP-3 and VAMP-8 vesicles fused to the membrane upon stimulation and upon further analysis differences in the sensitivity to calcium were found. VAMP-3-pHluorin responses were greater than VAMP-8; the distribution of pHluorin response sizes was more equal between low, mid and high responders, while the majority of VAMP-8-pHluorin cells were low responders. These differences were not a result of VAMP-3-pHluorin cells producing larger intracellular calcium rises as the average calcium responses in both sets of cells was

not significantly different. By monitoring the relationship between pHluorin response size and calcium response size through ANCOVA, there is some evidence VAMP-3 vesicles have a significantly greater sensitivity to calcium than VAMP-8 (VAMP-3 (0.25±0.055) (0.14±0.025)). Further analyses of VAMP-pHluorin responses in a nominally calcium free solution confirmed that VAMP-3 vesicle responses in the absence of calcium influx into the cell were similar to responses once calcium was added back, while VAMP-8 responses were blocked and it was only upon addition of external calcium that fusion could proceed.

Explanations into how possible differing calcium sensitivities are conferred onto vesicles arise from the microarray data presented in chapter 4. Numerous calcium sensors were expressed in mast cells including slps 1,2 and 3 and syts III and XI. Studies have highlighted the differing calcium sensitivities of syt isoforms [253, 420] and differential expression of isoforms has been shown to alter the calcium dependency of vesicles [421]. Less is known of slp calcium sensitivities but it is not a great leap of faith to suggest that these will also have differing sensitivities to calcium. No other studies have currently determined slp expression in mast cells but with human mast cell possessing a number of these, at least at the mRNA level, differential expression on VAMP-3 and VAMP-8 vesicle populations might lead to differing sensitivities to calcium. Alternatively, VAMP-3 and VAMP-8 vesicles could have similar calcium sensitivities and the different responses in the presence of no external calcium could arise from the location of calcium microdomains. Microdomains can lead to localised high concentrations of calcium [417]. VAMP-3 vesicles might localise close to internal calcium stores with release from these stores controlling the secretion of cytokines, stored in VAMP-3 positive vesicles. VAMP-8 vesicles undergoing fusion on the other hand may be localised away from these stores and require a global cytosolic calcium rise to undergo exocytosis. To determine whether the fusion of VAMP-3 vesicles is dependent on calcium, pHluorin experiments in the presence of no external calcium could be performed with the addition of Bapta-AM, an intracellular calcium chelator. If VAMP-3 vesicles still fuse with Bapta-AM present then this would show they undergo fusion in a calcium independent manner.

Work in chapter 4 identified the expression of VAMP-3 but not VAMPs-1 or -2 and its colocalisation to a rab11 compartment, as with Il-6 GFP. Here, using VAMP targeting BoNT/B LC, it was possible to selectively target VAMP-3 vesicles and inhibit release of IL-6 GFP. The responses of VAMPs 3 and 8-pHluorins confirmed BoNT/B could selectively target VAMP-3 vesicle exocytosis; ionomycin VAMP-8-pHluorin responses remained intact in the presence of BoNT/B LC but VAMP-3 exocytosis was inhibited. With the IgE responses this was not as clear and in responding cells there was no significant difference in the response sizes. However, when analysing the pHluorin traces of non-responding cells there was a clear drop in fluorescence after application of anti-IgE. This could be the result of either endocytosis removing VAMP-3-pHluorin from the plasma membrane or degradation. In activated cells VAMP-3 might become more exposed to the toxin resulting in a more rapid rate of cleavage resulting in the subsequent loss of pHluorin fluorescence. It is known that the levels of cleavage of SNAREs by BoNT toxins is increased in stimulated cells, but this is currently thought to be due to a larger presentation of cell surface receptors on the plasma membrane that allows greater toxin entry [422]. Activation might also lead to intracellular changes that allows the toxin better access to its target SNARE. Thiss could occur through greater delivery of the LC of the toxin to regions near the plasma membrane as a result of activation of endosomal recycling pathways brought about by the need for receptor trafficking and recycling. This might be an artefact of expressing the BoNT/B LC rather than using native protein, whereby the pathway of delivery does not require uptake of the toxin through endocytosis on the plasma membrane. This might also explain the mild phenotype whereby without the translocation domain the delivery of the light chain into the cytosol might be much less efficient. Alternatively cleavage of VAMP-3 by BoNT/B could disrupt the balance between exocytosis and endocytosis. Where VAMP-3 vesicles are no longer able to fuse with the plasma membrane they might be more rapidly recycled resulting in an increases in endocytosis and removal from the plasma membrane. It would be interesting to see whether endocytic inhibitors, such as the dynamin inhibitor Dyngo 4a [423] could reverse this loss. Finally, one cannot rule out the possibility that for some reason for this set of experiments the BoNT/B LC construct was not efficiently expressed and so only a minimal affect could be seen. This toxin did not have a fluorescent tag and so it was not possible to select only toxin expressing cells, however, given the

western blot data showing a loss of VAMP-3 and ionomycin pHluorin data showing an inhibition of exocytosis it seems unlikely. Despite the minimal effect on inhibiting VAMP-3 pHluorin exocyotsis in FCεRI stimulated cells, BoNT/LC was still able to inhibit the release of IL-6 GFP in FCεRI stimulated cells. The time points of these experiments were different (6 hours for IL-6 GFP release, minutes for pHluorin responses) over a longer period of stimulation a greater effect might be seen. Also it is worth bearing in mind that for this set of experiments the toxin was only targeting native VAMP-3 while in pHluorin expressing cells VAMP-3 was greatly overexpressed giving the toxin much more VAMP-3 to cleave, which might have resulted in more uncleaved VAMP-3 being present compensating for the effects of the toxin. What was clear was that BoNT/B LC could significantly inhibit the release of Il-6-GFP and highlights a previously undefined pathway in mast cells, whereby vesicles defined by VAMP-3 control the release of IL-6. VAMP-3 colocalised with rab11. A dominant negative rab11 construct, one of which has already been used to disseminate trafficking pathways [424], could be used to functionally determine whether rab11 plays a part in Il-6 trafficking and it would be interesting to see whether the use of this dominant negative construct could inhibit VAMP-3-pHluorin exocytosis.

Cytokine secretion in this study was assessed by the use of an overexpressed fluorescent construct. This is not ideal given potential miss-targeting of overexpressed proteins. Further experiments assessing the effect of BoNT/B on endogenous cytokines using ELISA and cytokine arrays would be needed to confirm the results shown here and also determine whether other cytokines could be targeted. Also, greater assessment of IL-6 GFP secretion would allow a more extensive elucidation of the mechanisms of secretion. For example determining release at different time points, in particular when determining pre-formed over de novo synthesised and assessing the effect of BoNT/B on release at these different time points. Given VAMP-3 exhibits considerable trafficking with no external calcium it would be interesting to see if IL-6 GFP is still secreted in these conditions and whether BoNT/B could target this release or whether preformed cytokine secretion utilises a different pathway. The fact that BoNT/B LC did not convincingly inhibit FCεRI mediated VAMP-3-pHluorin exocytosis, which most likely represents a pre-stored pool, suggests this might be the case. What these results do show is the

first evidence of VAMP-3 mediating the release of a cytokine in human mast cells and given this was achieved with BoNT/B this highlights the possibility of a novel way of therapeutically targeting inflammatory mediator release in human mast cells for the treatment of chronic inflammatory diseases.

Overexpression of VAMP-3 surprisingly brought about a change in the rate of calcium influx into the cell and is suggestive of another role in mast cells. Cells expressing VAMP-3-pHluorin had a faster calcium rise in response to FCεRI crosslinking than in VAMP-8-pHluorin expressing cells. Furthermore, in BoNT/B LC transfected cells, where VAMP-3 would be cleaved, this faster response was reversed. Taken together these results suggest VAMP-3 might be playing a role in channel trafficking. TRP channels traffic to the plasma membrane upon stimulation in numerous cell types [425]. They are widely expressed in mast cells and are thought to contribute to calcium influx from the plasma membrane [393]. For example, knockdown of TRPC1 in murine mast cells results in impaired calcium influx and impaired degranulation [363]. TRP channel insertion into the plasma membrane requires SNARE proteins and in HEK293 cells, TRPC3 insertion is tetanus toxin sensitive [426]. Rab11 has also been implicated in TRP channel trafficking, reportedly having a role in TRPV5 and 6 trafficking to the plasma membrane in epithelial cells [427]. TRP channels might be present in a residual pool of the recycling endosome, that traffic to the membrane upon stimulation. In other systems, for example glucose transporter 4 (GLUT4) channel trafficking in adipocytes, overexpression of VAMP-3 decreases the amount of protein translocating to the plasma membrane [428]. The fact that in resting cells a greater proportion of VAMP-3-pHluorin is present on the plasma membrane than VAMP-8-pHluorin might mean that a greater proportion of channels that VAMP-3 is important in trafficking, such as TRP channels, are also delivered to the plasma membrane so that upon stimulation the cell is able to produce a more rapid response. This effect is not seen in ionomycin stimulated cells which is not surprising given this is an ionophore and so transports calcium ions across the plasma membrane without relying on the subsequent trafficking of addition channels to the plasma membrane. These results highlight potential multiple roles of VAMP-3 in the mast cell, which through the recycling endosome mediates the

trafficking of cytokines and possibly calcium channels to the plasma membrane, contributing to mast cell activation and release of mast cell mediators.

BoNT/B can only target a subset of vesicles in mast cells and the VAMP-8 vesicle pathway, governing SG release, remained intact. To look at the potential for targeting this vesicle pool, cells were transfected with the modified form of BoNT/E consisting of a single point mutation at amino acid position 224 that is reported to target SNAP-23. Cells expressing BoNT/E(K224D) LC showed reduced VAMP-8-pHluroin exocytosis compared to BoNT/E LC, this shows the modified toxin can inhibit exocytosis in mast cells. The calcium response to IgE was also reduced but no difference in exocytosis was seen through activation with the non-receptor mediated calcium ionophore ionomycin. These results would suggest that the toxin could be affecting other trafficking pathways, for example trafficking of ion channels or even the FCεRI receptor to the plasma membrane, rather than the fusion of secretory vesicles. BoNTs cannot cleave, or show greatly reduced cleavage, of SNAREs in the assembled fusion complex [429]. The lack of inhibition of exocytosis seen with stimulation through ionomycin might have been a result of fusion of some SGs still docked with the plasma membrane and so the SNAREs are already in complex. Where ionomycin stimulation might differ from FCεRI is by the induction of greater amounts of compound degranulation, where vesicles undergo fusion with each other as well as the plasma membrane [196]. SNAP-23 is only present on the membrane, therefore a different set of SNAREs might mediate this vesicle to vesicle fusion and may be unaffected by BoNT cleavage, or SNAP-23 not at the plasma membrane might not be cleaved by BoNTs. Ionomycin induces greater release of SG mediators in mast cells and induces a larger and more artificial rise in calcium than IgE induced crosslinking, and might result in a great propensity for compound exocytosis. If there was still a large proportion of uncleaved SNAP-23 remaining, and if vesicles are undergoing compound fusion and fusing to the protected “pre-docked” vesicles already present on the plasma membrane, then this would still lead to acidification of the vesicles and hence increase in pHluorin fluorescence. This could couple with the fact that ionomycin bypasses the need of ion channels, and hence even if ion channels such as TRP channels could not fuse to the plasma membrane this wouldn’t affect the ionomycin response. Another possibility is compensation by other SNAREs in ionomycin-stimulated cells. SNAP-47 was

expressed at very high levels in LAD 2 cells but most probably does not possess a membrane anchor. Stimulation with ionomycin it might be more likely for compensation to occur by a means that would not occur under physiological conditions. The results shown here are only exploratory and much more work would be needed to determine the effectiveness of BoNT/E (K224D) in inhibition of mast cell degranulation and possible cytokine secretion. Repeats of the same experiments performed in BoNT/B LC transfected cells in this study would need to be performed, where one would expect both IL-6 and β–hexosaminidase release to be inhibited given the prominent role SNAP-23 is reported to play in mast cell exocytosis. Given the problems encountered in this study with some obvious inhibition of signalling pathways by the modified construct the potential use of this construct, either as a tool to monitor SNAP-23 in exocytosis, or as a potential therapy is limited.

In conclusion the results shown here identify two distinct pools of vesicles in human mast cells that are defined, in part, by VAMP-3 and VAMP-8. They display distinct calcium sensitivities and control the release of different sets of mediators, with the VAMP-3 pathway being able to be selectively targeted by BoNT/B, and regulates secretion of IL-6. VAMP-8 mediates the fusion of SGs and therefore the release of preformed mediators such as β-hexosaminidase. Disruption of VAMP3-mediated vesicle fusion could provide a novel means of inhibiting the release of pro-inflammatory cytokines. Together these experiments provide evidence for the possibility of new therapeutic strategies for the treatment of mast cell related disease

Chapter 6: Discussion and future directions

This study demonstrates for the first time the SNAREs expressed in LAD and HLMCs. Of the SNAREs detected, a previously undescribed role for VAMP-3 has been shown. Looking at endogenous VAMPs and using VAMPs tagged with pHluorins, this study has assessed the cellular distribution of VAMP-3 and VAMP-8 containing vesicles, and their behaviour upon IgE stimulation in live cells. In unstimulated cells, VAMPs 3 and 8 were found to have distinct cellular distributions. Upon IgE stimulation both VAMP-3 and VAMP-8 containing vesicles translocate to the membrane and undergo membrane fusion, consistent with roles in exocytosis. However, their responses show distinct time courses and calcium dependences. Inhibition of VAMP-3 by BoNT/B inhibited the release of IL-6 GFP, while knockdown of VAMP-8 inhibited SG release. The data presented here supports the notion that distinct vesicle pools, defined in part by expression of VAMP-3 and VAMP-8, regulate the release of inflammatory mediators from mast cells.

The notion of different pools of mediators, defined in part by different SNAREs, has only recently been described. In neuronal cells it is becoming accepted that multiple pools of vesicles exist that consist of different molecular constituents. The standard view of SV fusion being mediated solely by VAMP-2 positive vesicles is increasingly becoming dated and it is clear multiple SNAREs define different pools of vesicles. Vesicles that give rise to spontaneous release have been reported to be defined through the expression of Vti1a, a non-canonical SNARE that was not originally associated with exocytosis [298]. Further observations have found differences in the molecular makeup of the vesicle pools that govern synchronous and asynchronous release; the later defined through the expression of VAMP-4 [430]. With a picture starting to emmerge in neuronal cells of different pools of vesicles defined by unique molecular constituents, the question arises of whether other cells types might contain differential pools. Mast cells have long been known to differentially release cytokine and growth factors selectively without degranulation by activation of a number of stimuli; for example stimulation by Il-1 and CRH can induce the selective release of IL-6 and VEGF respectively [87, 431]

Many of these cytokines are both present in pre-stored pools and are de novo synthesised, TNF-α, VEGF and IL-6 have all been found in resting cells either present in a small number of SGs or in separate small vesicles [87, 432]. The SNAREs that control the release of these mediators are not well defined and much work has been focussed on identifying the molecular makeup of SGs membrane fusion proteins, of which VAMP-7 and 8, syntaxin 4 and SNAP-23 are heavily implicated and VAMP-8s role in SG release was confirmed in this study. The fact that inhibiting VAMP-7 or 8 function has no effect on the release of many cytokines or growth factors makes it clear a different set of SNAREs are mediating the release of these mediators [235]. Only very recent studies have started to identify what these might be and interestingly a number of SNAREs have been implicated. In assessing the release of just four chemokines Frank et al 2013 implicated syntaxin 3 and 6, VAMP-7 and 8 (previously thought to only mediate SG release) and SNAP-23. Another recent study found VEGF release in murine mast cells to be tetanus toxin sensitive [248] and it is becoming clear that a number of combinations of SNAREs exist in mast cells on vesicles possessing different mediators.

This is the first study to directly identify a role for VAMP-3 in mediator release in human mast cells. It is not clear whether this just represents de-novo synthesised or includes preformed mediators. Only an artificial system has been used as direct evidence for VAMP-3 involvement in cytokine release in this study, through the use of an IL-6 GFP construct. These results would need to be confirmed by determining the effects of the BoNT/B LC on endogenous cytokine release as overexpressed proteins can be miss-targeted and result in misleading observations. To differentiate whether VAMP-3 mediates preformed or de-novo synthesised cytokine release, release of endogenous cytokines at different time points could be monitored. Monitoring release after 10 minutes would measure only preformed release and so studying the effect of toxin treatment at this time point would determine if VAMP-3 pools represent pre-stored pools. Also, immunostaining of endogenous cytokines in resting cells with VAMP-3 might give an insight as to whether VAMP-3 localises to pre-stored cytokine pools.
Given the findings in this study a putative picture of one possible pathway of VAMP-3 mediated cytokine release can be built involving storage of cytokines within an

adapted endosomal pathway. VAMP-3 was seen to traffic to the plasma membrane within minutes of stimulation and colocalised to recycling endosomes. In macrophages a pathway exists whereby trafficking of IL-6 and TNF-α involves trafficking through the recycling endosome before being transported to the plasma membrane in a VAMP-3 positive pathway[182]. It is possible that small amounts of cytokines and growth factors are stored preformed in this compartment ready to be released upon stimulation and this might represent the initial fusion of VAMP-3 vesicles with the plasma membrane seen in this study. One mechanism that has parallels to this and is well defined is the GLUT4 transport mechanism in adipocytes. GLUT4 resides in specialised storage reservoirs sequestered away from normal endosomal compartments by the action of the endosomal sorting complex [185, 428]. This store can limit the amount of GLUT4 at the plasma membrane and then be readily delivered to the plasma membrane. Preformed cytokines in mast cells could similarly be stored, in a rab11 positive compartment, and released rapidly upon stimulation.

Syts and other calcium sensors such as the slps might provide a level of control in the release of cytokines. Recently a potential control mechanism has been found in macrophages whereby syt XI, localising to recycling endosomes, negatively regulates IL-6 and TNF-α release and syt XI was a syt that had the greatest expression in LAD2 and HLMCS in the microarray in this study. Release of cytokines and growth factors are independent of extracellular calcium and in this study VAMP-3-pHluorin vesicles were found to have greater sensitivity to calcium than VAMP-8-pHluorin, a SNARE that mediates SG plasma membrane fusion. Different isoforms of syts have differing calcium sensitivities and can be broadly classed into three groups: Low calcium affinity (syt I II V), high calcium affinity (syt III and VII) and syts that do not bind SNAREs or phospholipids in a calcium-dependent manner, including IV and XI. As with SNARE expression differential syt expression on vesicles has been shown in neurons. Importantly, given the differences in calcium sensitivities, this differential expression can confer functional differences in the propensity of vesicles to undergo fusion. PC12 cells express numerous syts and the differential expression of these on dense core vesicles results in differences the propensity to undergo fusion and the type of fusion that occurs [254]. Syt I, which has a low calcium affinity, confers onto them a greater tendency to undergo kiss and

run fusion rather than full fusion. Vesicles expressing IX or VII isoforms show intermediate or low propensity respectively to undergo kiss and run fusion. This highlights how the expression of different calcium sensors might result in differential release, where they can modify a vesicles ability to respond to calcium signals. Furthermore each of these vesicles varied in their sensitivity to being inhibited to undergo fusion by syt IV, which lacks calcium binding and has been shown to negatively modulate Brain derived neurotrophic factor (BDNF) release in hippocampal neurons [433]. Syt XI is similar in structure to syt IV and given its role in regulating cytokine release in macrophages mirroring that of syt IV in BDNF release and it being the predominant syts in mast cells, it is possible that the differential expression of syts or other calcium sensors such as slps on mast cell vesicles might confer different calcium sensitivities. One could imagine expression of syt XI on vesicles modifying the calcium dependences by co-expression with another syt that is calcium sensitive and mast cells containing vesicles expressing different calcium sensors with different calcium sensitivities.

This is the first time that the expression of such a wide range of calcium sensors has been determined in mast cells and it is interesting to note the low levels of syts compared to other calcium sensors such as slps. It is possible that rather than syts, slps have a greater role in mast cell exocytosis but this remains to be determined. Determining protein expression and localisation as well as functional studies assessing calcium sensitivities will be vital in elucidating the role if any these proteins have in mast cell exocytosis. To address these possibilities determination of the expression of calcium sensor proteins through western blot and immunostaining to determine localization in human mast cells would be the most important starting point. This would confirm or disprove the microarray data in this study and murine cell data of previous studies [256, 260]. Once expression of the particular calcium sensors in confirmed, functional studies would then allow dissemination of their functions. Using the pHluorin assays with knockdown of particular sensors would enable assessment of any changes in calcium sensitivities and using mediator release assays allow determination of any roles in mediator release. The calcium sensors themselves could also be tagged with pHluorins to assess their presence on vesicles undergoing fusion with the plasma membrane.

In this study the main focus was on the four highest expressed VAMPs. From the microarray data it is clear than many other SNAREs are present including many syntaxins and Qb SNAREs whose function in mast cells has not be defined. How and whether these SNAREs and SNARE regulators control mast cell mediator release and how calcium sensitivities are differentially imparted onto vesicles are questions that are sure to be answered in the coming years.

Chronic inflammatory disease is characterised by the aberrant release of cytokines over a prolonged period of time by mast cells and other immune cells. Il-6 has been shown to pivotal in many chronic inflammatory diseases such as rheumatoid arthritis, asthma and inflammatory bowel disease. It has also been implicated in cancer and Tocilizumab, a IL-6 receptor antibody, is effective in the treatment of rheumatoid arthritis [434]. The pathway for IL-6 release in mast cells, as with many other cytokines, had not previously been defined. Given the data in this study showing BoNT/B can target Il-6 release and moreover given the toxin did not affect normal granular release, BoNTs might provide a novel means of selectively targeting the release of chronic inflammatory mediators without affecting SG release. This study has shown that VAMP-3 is the most likely candidate SNARE for its release, and BoNT/B can target its release by cleaving this SNARE. Until recently the therapeutic use of BoNT was limited to neuronal cells due to the highly specific binding of the toxins to their target receptor. The work of Foster et al 2006 opened up the therapeutic potential of BoNTs by retargeting the toxin to non-neuronal cells. A modified form of BoNT/C was created whereby the Hc receptor binding domain was replaced with EGF domain and this was able to be taken up into epithelial cells, cleave syntaxin I and inhibit mucin secretion [435]. Much more recent work has highlighted the therapeutic potential of this strategy. Using a recombinant protein consisting of growth hormone releasing hormone and the Hn/LC domains of BoNT/D Somm et al showed this could selectively enter into pituitary somatotroph cells and target the release of growth hormone by cleavage of VAMP-2 and this proved a novel treatment strategy for acromegaly [436]. This strategy could be used in targeting mast cells for treatment of chronic inflammatory disease, although there are a number of challenges particularly when regarding mast cell specific targeting.

In targeting the toxin to mast cell, a suitable peptide receptor for toxin uptake would need to be found. When deciding on a suitable receptor target a number of considerations would need to be made. It is important the receptor is mast cell specific, or at least not widely expressed in other cell types as this would lead to off target effects. Another consideration is to ensure the peptide does not induce mast cell degranulation. This would produce an acute response when activating its receptor on mast cells and as only a subset of mediators would be targeted and SG release would remain intact, activation would lead to mast cells releasing factors such as proteases and histamine potentially inducing an early phase allergic response. Unfortunately this means that targeting mast cells through the FceRI receptor is not possible, which otherwise could have been a useful target receptor. From the microarray two peptide receptors expressed at the highest levels in both LAD 2 cells and the HLMC donor were galanin 3 and urotensin 2 receptors (appendix figure 3 and 4), but these receptors have fairly ubiquitous expression and so would not be ideal for selective targeting. One potential receptor that might provide a target for mast cell toxin entry is the melanocortin 1 receptor. Although the receptor is highly expressed in melanocytes the melanosomes present in them are lysosomal related organelles and so most likely utilise endosomal SNAREs for exocytosis such as VAMP-8 that are not affected by the toxin [437]. VAMP-3 does not seem to have a predominant role in these cells; a siRNA screen found knocking down VAMP-3 not to affect pigment production, however, VAMP-2 co-immunoprecipitates with SNAP-23 from purified cell membranes [438]. Of course further off target effects might be seen in melanocytes depending on the role of VAMP-3 in these cells and also the receptor has not been defined in mast cells and so it is not known whether activation of the receptor induces degranulation. Also, as other studies have recently shown, numerous SNAREs seem to control the release of multiple cytokines. This method of targeting release might be too specific. Cleaving VAMP-3 might not 'hit' the release of enough mediators to have a physiological effect, if the mast cell can still release a wide number of inflammatory mediators then there might be minimal physiological effects.

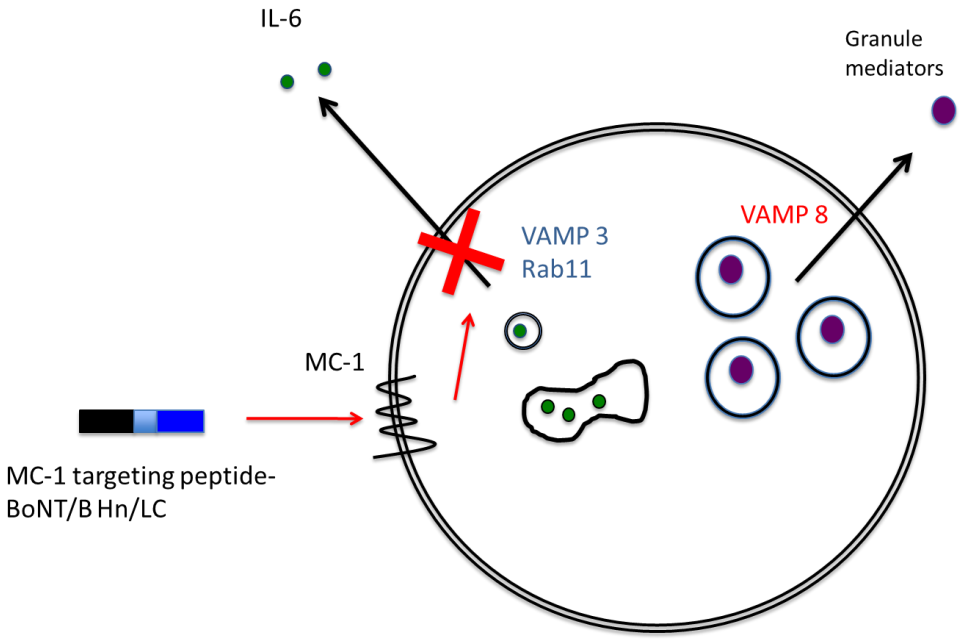

Figure 6.1

Targeting of mast cell cytokine release using modified BoNTs.

Using an MC-1 liganded targeting domain of BoNT/B it might be possible to target mast cell cytokine release whilst having minimal side effects.

Future experiments should firstly focus on defining in more detail expression of suitable receptors in human mast cells, and whether there are significant differences between mast cell populations that might limit the effectiveness of any particular treatment. After finding a suitable target receptor, testing of cell entry of these modified toxins and determining their ability to cleave and inhibit cytokine release using the assays described in this study should take place. In using calcium imaging, pHluorin and mediator release assays many steps along the secretory pathway could be monitored which would be important, particularly if looking for off target effects. For example the VAMP-8-pHluorin assay could be used to ensure specific targeting of the cytokine release pathway and calcium imaging to ensure the cells signalling pathways remain intact. Despite the potential pitfalls, the use of this 'magic bullet' approach to treatment is appealing and could provide a highly effective way of treating chronic inflammatory diseases.

Bibliography

1. **Galli, S.J. and M. Tsai, *Mast cells in allergy and infection: versatile effector and regulatory cells in innate and adaptive immunity.* Eur J Immunol. 40(7): p. 1843-51.**

2. **Brown, J.M., T.M. Wilson, and D.D. Metcalfe, *The mast cell and allergic diseases: role in pathogenesis and implications for therapy.* Clin Exp Allergy, 2008. 38(1): p. 4-18.**

3. **Theoharides, T.C. and D. Kalogeromitros, *The critical role of mast cells in allergy and inflammation.* Ann N Y Acad Sci, 2006. 1088: p. 78-99.**

4. **Di Girolamo, N. and D. Wakefield, *In vitro and in vivo expression of interstitial collagenase/MMP-1 by human mast cells.* Dev Immunol, 2000. 7(2-4): p. 131-42.**

5. **Brownell, E., et al., *Immunolocalization of stromelysin-related protein in murine mast cell granules.* Int Arch Allergy Immunol, 1995. 107(1-3): p. 333-5.**

6. **Galli, S.J., S. Nakae, and M. Tsai, *Mast cells in the development of adaptive immune responses.* Nat Immunol, 2005. 6(2): p. 135-42.**

7. **Theoharides, T.C., et al., *Differential release of mast cell mediators and the pathogenesis of inflammation.* Immunol Rev, 2007. 217: p. 65-78.**

8. **Bischoff, S.C., *Physiological and pathophysiological functions of intestinal mast cells.* Semin Immunopathol, 2009. 31(2): p. 185-205.**

9. **Rao, K.N. and M.A. Brown, *Mast cells: multifaceted immune cells with diverse roles in health and disease.* Ann N Y Acad Sci, 2008. 1143: p. 83-104.**

10. **Rodewald, H.R., et al., *Identification of a committed precursor for the mast cell lineage.* Science, 1996. 271(5250): p. 818-22.**

11. **Arinobu, Y., H. Iwasaki, and K. Akashi, *Origin of basophils and mast cells.* Allergol Int, 2009. 58(1): p. 21-8.**

12. **Chen, C.C., et al., *Identification of mast cell progenitors in adult mice.* Proc Natl Acad Sci U S A, 2005. 102(32): p. 11408-13.**

13. **Arinobu, Y., et al., *Developmental checkpoints of the basophil/mast cell lineages in adult murine hematopoiesis.* Proc Natl Acad Sci U S A, 2005. 102(50): p. 18105-10.**

14. **Zola, H., et al., *CD molecules 2005: human cell differentiation molecules.* Blood, 2005. 106(9): p. 3123-3126.**

15. **Bischoff, S.C. and S. Kr‰mer, *Human mast cells, bacteria, and intestinal immunity.* Immunological Reviews, 2007. 217(1): p. 329-337.**

16. **Okayama, Y. and T. Kawakami, *Development, migration, and survival of mast cells.* Immunol Res, 2006. 34(2): p. 97-115.**

17. **Chabot, B., et al., *The proto-oncogene c-kit encoding a transmembrane tyrosine kinase receptor maps to the mouse W locus.* Nature, 1988. 335(6185): p. 88-89.**

18. **Copeland, N.G., et al., *Mast cell growth factor maps near the steel locus on mouse chromosome 10 and is deleted in a number of steel alleles.* Cell, 1990. 63(1): p. 175-183.**

19. **Andersson, C.K., et al., *Novel site-specific mast cell subpopulations in the human lung.* Thorax, 2009. 64(4): p. 297-305.**

20. **Bradding, P., et al., *Heterogeneity of human mast cells based on cytokine content.* J Immunol, 1995. 155(1): p. 297-307.**

21. **Shanahan, F., et al., *Mast cell heterogeneity: effects of neuroenteric peptides on histamine release.* J Immunol, 1985. 135(2): p. 1331-7.**

22. **Ferry, X., et al., *G protein-dependent activation of mast cell by peptides and basic secretagogues.* Peptides, 2002. 23(8): p. 1507-15.**

23. **Fureder, W., et al., *Differential expression of complement receptors on human basophils and mast cells. Evidence for mast cell heterogeneity and CD88/C5aR expression on skin mast cells.* J Immunol, 1995. 155(6): p. 3152-60.**

24. **Matsushima, H., et al., *TLR3-, TLR7-, and TLR9-mediated production of proinflammatory cytokines and chemokines from murine connective tissue type skin-derived mast cells but not from bone marrow-derived mast cells.* J Immunol, 2004. 173(1): p. 531-41.**

25. **Saluja, R., et al., *FcepsilonR1-mediated mast cell reactivity is amplified through prolonged Toll-like receptor-ligand treatment.* PLoS One, 2012. 7(8): p. e43547.**

26. **Kulka, M. and D.D. Metcalfe, *TLR3 activation inhibits human mast cell attachment to fibronectin and vitronectin.* Mol Immunol, 2006. 43(10): p. 1579-86.**

27. **Gordon, J.R. and S.J. Galli, *Mast cells as a source of both preformed and immunologically inducible TNF-alpha/cachectin.* Nature, 1990. 346(6281): p. 274-6.**

28. R√∂hlich, P.l., P. Anderson, and B.r. Uvn√§s, *ELECTRON MICROSCOPE OBSERVATIONS ON COMPOUND 48/80-INDUCED DEGRANULATION IN RAT MAST CELLS: Evidence for Sequential Exocytosis of Storage Granules.* The Journal of Cell Biology, 1971. 51(2): p. 465-483.

29. Jeong, H.J., et al., *Activation of hypoxia-inducible factor-1 regulates human histidine decarboxylase expression.* Cell Mol Life Sci, 2009. 66(7): p. 1309-19.

30. Ringvall, M., et al., *Serotonin and histamine storage in mast cell secretory granules is dependent on serglycin proteoglycan.* Journal of Allergy and Clinical Immunology, 2008. 121(4): p. 1020-1026.

31. Benditt, E.P., et al., *5-Hydroxytryptamine in mast cells.* Proc Soc Exp Biol Med, 1955. 90(1): p. 303-4.

32. Kushnir-Sukhov, N.M., et al., *Human mast cells are capable of serotonin synthesis and release.* J Allergy Clin Immunol, 2007. 119(2): p. 498-9.

33. Wimalasena, K., *Vesicular monoamine transporters: structure-function, pharmacology, and medicinal chemistry.* Med Res Rev, 2011. 31(4): p. 483-519.

34. Schuldiner, S., A. Shirvan, and M. Linial, *Vesicular neurotransmitter transporters: from bacteria to humans.* Physiol Rev, 1995. 75(2): p. 369-92.

35. Henry, J.P., et al., *Molecular pharmacology of the vesicular monoamine transporter.* Adv Pharmacol, 1998. 42: p. 236-9.

36. Knoth, J., M. Zallakian, and D. Njus, *Stoichiometry of H+-linked dopamine transport in chromaffin granule ghosts.* Biochemistry, 1981. 20(23): p. 6625-9.

37. Kanner, B.I. and A. Bendahan, *Transport of 5-hydroxytryptamine in membrane vesicles from rat basophilic leukemia cells.* Biochim Biophys Acta, 1985. 816(2): p. 403-10.

38. Anlauf, M., et al., *The vesicular monoamine transporter 2 (VMAT2) is expressed by normal and tumor cutaneous mast cells and Langerhans cells of the skin but is absent from Langerhans cell histiocytosis.* J Histochem Cytochem, 2004. 52(6): p. 779-88.

39. Di Girolamo, N., et al., *Human mast cell-derived gelatinase B (matrix metalloproteinase-9) is regulated by inflammatory cytokines: role in cell migration.* J Immunol, 2006. 177(4): p. 2638-50.

40. Strik, M.C., et al., *Human mast cells produce and release the cytotoxic lymphocyte associated protease granzyme B upon activation.* Mol Immunol, 2007. 44(14): p. 3462-72.

41. Humphries, D.E., et al., *Heparin is essential for the storage of specific granule proteases in mast cells.* Nature, 1999. 400(6746): p. 769-772.

42. Pejler, G., M. Åbrink, and S. Wernersson, *Serglycin proteoglycan: Regulating the storage and activities of hematopoietic proteases.* BioFactors, 2009. 35(1): p. 61-68.

43. Pereira, P.J.B., et al., *Human [beta]-tryptase is a ring-like tetramer with active sites facing a central pore.* Nature, 1998. 392(6673): p. 306-311.

44. Henningsson, F., et al., *A role for serglycin proteoglycan in granular retention and processing of mast cell secretory granule components.* FEBS Journal, 2006. 273(21): p. 4901-4912.

45. Sommerhoff, C.P., S.J. Ruoss, and G.H. Caughey, *Mast cell proteoglycans modulate the secretagogue, proteoglycanase, and amidolytic activities of dog mast cell chymase.* The Journal of Immunology, 1992. 148(9): p. 2859-66.

46. Stevens, R.L. and R. Adachi, *Protease-proteoglycan complexes of mouse and human mast cells and importance of their beta-tryptase-heparin complexes in inflammation and innate immunity.* Immunol Rev, 2007. 217: p. 155-67.

47. Caughey, G.H., et al., *Characterization of human gamma-tryptases, novel members of the chromosome 16p mast cell tryptase and prostasin gene families.* J Immunol, 2000. 164(12): p. 6566-75.

48. Caughey, G.H., *Mast cell tryptases and chymases in inflammation and host defense.* Immunol Rev, 2007. 217: p. 141-54.

49. Reed, D.E., et al., *Mast cell tryptase and proteinase-activated receptor 2 induce hyperexcitability of guinea-pig submucosal neurons.* J Physiol, 2003. 547(Pt 2): p. 531-42.

50. Dai, Y., et al., *Sensitization of TRPA1 by PAR2 contributes to the sensation of inflammatory pain.* J Clin Invest, 2007. 117(7): p. 1979-87.

51. Ruoss, S.J., T. Hartmann, and G.H. Caughey, *Mast cell tryptase is a mitogen for cultured fibroblasts.* The Journal of Clinical Investigation, 1991. 88(2): p. 493-499.

52. Akers, I.A., et al., *Mast cell tryptase stimulates human lung fibroblast proliferation via protease-activated receptor-2.* American Journal of Physiology - Lung Cellular and Molecular Physiology, 2000. 278(1): p. L193-L201.

53. Huang, C., et al., *The tryptase, mouse mast cell protease 7, exhibits anticoagulant activity in vivo and in vitro due to its ability to degrade fibrinogen in the presence of the diverse array of protease inhibitors in plasma.* J Biol Chem, 1997. 272(50): p. 31885-93.

54. Samoszuk, M., M. Corwin, and S.L. Hazen, *Effects of human mast cell tryptase on the kinetics of blood clotting.* Thromb Res, 2003. 109(2-3): p. 153-6.

55. Caughey, G.H., *New developments in the genetics and activation of mast cell proteases.* Mol Immunol, 2002. 38(16-18): p. 1353-7.

56. Akahoshi, M., et al., *Mast cell chymase reduces the toxicity of Gila monster venom, scorpion venom, and vasoactive intestinal polypeptide in mice.* J Clin Invest, 2011

121(10): p. 4180-91.

57. Tchougounova, E., G. Pejler, and M. √Öbrink, *The Chymase, Mouse Mast Cell Protease 4, Constitutes the Major Chymotrypsin-like Activity in Peritoneum and Ear Tissue. A Role for Mouse Mast Cell Protease 4 in Thrombin Regulation and Fibronectin Turnover.* The Journal of Experimental Medicine, 2003. 198(3): p. 423-431.

58. Pejler, G., et al., *Mast cell proteases- multifaceted regulators of inflammatory disease.* Blood, 2010

p. blood-2010-01-257287.

59. Schneider, L.A., et al., *Molecular mechanism of mast cell mediated innate defense against endothelin and snake venom sarafotoxin.* J Exp Med, 2007. 204(11): p. 2629-39.

60. Theoharides, T.C., et al., *Differential release of mast cell mediators and the pathogenesis of inflammation.* Immunological Reviews, 2007. 217(1): p. 65-78.

61. Lundequist, A. and G. Pejler, *Biological implications of preformed mast cell mediators.* Cell Mol Life Sci, 2011. 68(6): p. 965-75.

62. Dragonetti, A., et al., *The lysosomal protease cathepsin D is efficiently sorted to and secreted from regulated secretory compartments in the rat basophilic/mast cell line RBL.* J Cell Sci, 2000. 113 (Pt 18): p. 3289-98.

63. Turk, V., B. Turk, and D. Turk, *Lysosomal cysteine proteases: facts and opportunities.* EMBO J, 2001. 20(17): p. 4629-33.

64. Wendeler, M. and K. Sandhoff, *Hexosaminidase assays.* Glycoconj J, 2009. 26(8): p. 945-52.

65. McLachlan, J.B., et al., *Mast cell-derived tumor necrosis factor induces hypertrophy of draining lymph nodes during infection.* Nat Immunol, 2003. 4(12): p. 1199-205.

66. Grutzkau, A., et al., *Synthesis, storage, and release of vascular endothelial growth factor/vascular permeability factor (VEGF/VPF) by*

human mast cells: implications for the biological significance of VEGF206. **Mol Biol Cell, 1998. 9(4): p. 875-84.**

67. Boesiger, J., et al., *Mast cells can secrete vascular permeability factor/ vascular endothelial cell growth factor and exhibit enhanced release after immunoglobulin E-dependent upregulation of fc epsilon receptor I expression.* J Exp Med, 1998. 188(6): p. 1135-45.

68. Wilson, et al., *Localization of interleukin (IL) -4 but not IL-5 to human mast cell secretory granules by immunoelectron microscopy.* Clinical & Experimental Allergy, 2000. 30(4): p. 493-500.

69. Bozza, P.T., et al., *Lipid body function in eicosanoid synthesis: An update.* Prostaglandins, Leukotrienes and Essential Fatty Acids, 2011. 85(5): p. 205-213.

70. Dichlberger, A., et al., *Lipid body formation during maturation of human mast cells.* Journal of Lipid Research.

71. Funk, C.D., *Prostaglandins and Leukotrienes: Advances in Eicosanoid Biology.* Science, 2001. 294(5548): p. 1871-1875.

72. Dinarello, C.A., *Historical insights into cytokines.* European Journal of Immunology, 2007. 37(S1): p. S34-S45.

73. Katsanos, G.S., et al., *Mast cells and chemokines.* J Biol Regul Homeost Agents, 2008. 22(3): p. 145-51.

74. Charo, I.F. and R.M. Ransohoff, *The Many Roles of Chemokines and Chemokine Receptors in Inflammation.* New England Journal of Medicine, 2006. 354(6): p. 610-621.

75. Baggiolini, M. and C.A. Dahinden, *CC chemokines in allergic inflammation.* Immunol Today, 1994. 15(3): p. 127-33.

76. Leonard, B.J., et al., *Basophilic leukemia in the rat induced by a -chlorethylamine--ICI 42464.* J Pathol, 1971. 103(2): p. Pxv.

77. Carson, D.A. and H. Metzger, *Interaction of IgE with rat basophilic leukemia cells. IV. Antibody-induced redistribution of IgE receptors.* J Immunol, 1974. 113(4): p. 1271-7.

78. Barsumian, E.L., et al., *IgE-induced histamine release from rat basophilic leukemia cell lines: isolation of releasing and nonreleasing clones.* Eur J Immunol, 1981. 11(4): p. 317-23.

79. Butterfield, J.H., et al., *Establishment of an immature mast cell line from a patient with mast cell leukemia.* Leukemia Research, 1988. 12(4): p. 345-355.

80. Tsujimura, T., et al., *Substitution of an aspartic acid results in constitutive activation of c-kit receptor tyrosine kinase in a rat tumor mast cell line RBL-2H3.* Int Arch Allergy Immunol, 1995. 106(4): p. 377-85.

81. Passante, E., et al., *Toll-like receptors and RBL-2H3 mast cells.* Inflamm Res, 2009. 58 Suppl 1: p. 11-2.

82. Passante, E. and N. Frankish, *The RBL-2H3 cell line: its provenance and suitability as a model for the mast cell.* Inflammation Research, 2009. 58(11): p. 737-745.

83. Froese, A., et al., *Comparison of the receptors for IgE of various rat basophilic leukaemia cell lines. II. Studies with different anti-receptor antisera.* Immunology, 1982. 46(1): p. 117-23.

84. Nilsson, G., et al., *Phenotypic characterization of the human mast-cell line HMC-1.* Scand J Immunol, 1994. 39(5): p. 489-98.

85. Wierecky, J., et al., *Cytokine release from a human mast cell line (HMC-1) in response to stimulation with anti-IgE and other secretagogues.* Inflamm Res, 2000. 49 Suppl 1: p. S7-8.

86. Lorentz, A., et al., *Human intestinal mast cells are capable of producing different cytokine profiles: role of IgE receptor cross-linking and IL-4.* J Immunol, 2000. 164(1): p. 43-8.

87. Kandere-Grzybowska, K., et al., *IL-1 Induces Vesicular Secretion of IL-6 without Degranulation from Human Mast Cells.* J Immunol, 2003. 171(9): p. 4830-4836.

88. Kirshenbaum, A.S., et al., *Characterization of novel stem cell factor responsive human mast cell lines LAD 1 and 2 established from a patient with mast cell sarcoma/leukemia; activation following aggregation of FcepsilonRI or FcgammaRI.* Leuk Res, 2003. 27(8): p. 677-82.

89. Kulka, M., et al., *Neuropeptides activate human mast cell degranulation and chemokine production.* Immunology, 2008. 123(3): p. 398-410.

90. Guhl, S., et al., *Mast cell lines HMC-1 and LAD2 in comparison with mature human skin mast cells – drastically reduced levels of tryptase and chymase in mast cell lines.* Experimental Dermatology, 2010. 19(9): p. 845-847.

91. Laidlaw, T.M., et al., *Characterization of a novel human mast cell line that responds to stem cell factor and expresses functional FcŒµRI.* Journal of Allergy and Clinical Immunology, 2011. 127(3): p. 815-822.e5.

92. Kumar, V. and A. Sharma, *Mast cells: Emerging sentinel innate immune cells with diverse role in immunity.* Molecular Immunology, 2010

48(1,Äì3): p. 14-25.

93. Marshall, J.S. and D.M. Jawdat, *Mast cells in innate immunity.* Journal of Allergy and Clinical Immunology, 2004. 114(1): p. 21-27.

94. Velin, D., et al., *Mast cells are critical mediators of vaccine-induced Helicobacter clearance in the mouse model.* Gastroenterology, 2005. 129(1): p. 142-55.

95. Wei, O.L., et al., *Mast cells limit systemic bacterial dissemination but not colitis in response to Citrobacter rodentium.* Infect Immun, 2005. 73(4): p. 1978-85.

96. Metz, M. and M. Maurer, *Mast cells--key effector cells in immune responses.* Trends Immunol, 2007. 28(5): p. 234-41.

97. Malaviya, R., et al., *Mast cells process bacterial Ags through a phagocytic route for class I MHC presentation to T cells.* J Immunol, 1996. 156(4): p. 1490-6.

98. Di Nardo, A., A. Vitiello, and R.L. Gallo, *Cutting edge: mast cell antimicrobial activity is mediated by expression of cathelicidin antimicrobial peptide.* J Immunol, 2003. 170(5): p. 2274-8.

99. Woodbury, R.G., et al., *Mucosal mast cells are functionally active during spontaneous expulsion of intestinal nematode infections in rat.* Nature, 1984. 312(5993): p. 450-2.

100. Knight, P.A., et al., *Delayed expulsion of the nematode Trichinella spiralis in mice lacking the mucosal mast cell-specific granule chymase, mouse mast cell protease-1.* J Exp Med, 2000. 192(12): p. 1849-56.

101. Kulka, M., et al., *Activation of mast cells by double-stranded RNA: evidence for activation through Toll-like receptor 3.* J Allergy Clin Immunol, 2004. 114(1): p. 174-82.

102. Burke, S.M., et al., *Human mast cell activation with virus-associated stimuli leads to the selective chemotaxis of natural killer cells by a CXCL8-dependent mechanism.* Blood, 2008. 111(12): p. 5467-5476.

103. Castleman, W.L., et al., *Viral bronchiolitis during early life induces increased numbers of bronchiolar mast cells and airway hyperresponsiveness.* Am J Pathol, 1990. 137(4): p. 821-31.

104. Mekori, Y.A. and D.D. Metcalfe, *Mast cell-T cell interactions.* J Allergy Clin Immunol, 1999. 104(3 Pt 1): p. 517-23.

105. Frandji, P., et al., *Exogenous and endogenous antigens are differentially presented by mast cells to CD4+ T lymphocytes.* Eur J Immunol, 1996. 26(10): p. 2517-28.

106. Leon, A., et al., *Mast cells synthesize, store, and release nerve growth factor.* Proceedings of the National Academy of Sciences, 1994. 91(9): p. 3739-3743.

107. Gr√ºtzkau, A., et al., *Synthesis, Storage, and Release of Vascular Endothelial Growth Factor/Vascular Permeability Factor (VEGF/VPF) by Human Mast Cells: Implications for the Biological Significance of VEGF206.* Molecular Biology of the Cell, 1998. 9(4): p. 875-884.

108. Artuc, M., U.M. Steckelings, and B.M. Henz, *Mast Cell-Fibroblast Interactions: Human Mast Cells as Source and Inducers of Fibroblast and Epithelial Growth Factors.* 2002. 118(3): p. 391-395.

109. Noli, C. and A. Miolo, *The mast cell in wound healing.* Veterinary Dermatology, 2001. 12(6): p. 303-313.

110. Weller, K., et al., *Mast cells are required for normal healing of skin wounds in mice.* The FASEB Journal, 2006. 20(13): p. 2366-2368.

111. Grimbaldeston, M.A., et al., *Mast Cell-Deficient W-sash c-kit Mutant KitW-sh/W-sh Mice as a Model for Investigating Mast Cell Biology in Vivo.* The American Journal of Pathology, 2005. 167(3): p. 835-848.

112. Nigrovic, P.A., et al., *Genetic inversion in mast cell-deficient (Wsh) mice interrupts corin and manifests as hematopoietic and cardiac aberrancy.* Am J Pathol, 2008. 173(6): p. 1693-701.

113. Ring, J. and H. Behrendt, *Anaphylaxis and anaphylactoid reactions.* Clinical Reviews in Allergy & Immunology, 1999. 17(4): p. 387-399.

114. Beaven, M.A., *Our perception of the mast cell from Paul Ehrlich to now.* European Journal of Immunology, 2009. 39(1): p. 11-25.

115. Silverstein, A.M., *Clemens Freiherr von Pirquet: explaining immune complex disease in 1906.* Nat Immunol, 2000. 1(6): p. 453-5.

116. Ishizaka, K. and T. Ishizaka, *Identification of gamma-E-antibodies as a carrier of reaginic activity.* J Immunol, 1967. 99(6): p. 1187-98.

117. Emanuel, M.B., *Histamine and the antiallergic antihistamines: a history of their discoveries.* Clin Exp Allergy, 1999. 29 Suppl 3: p. 1-11; discussion 12.

118. Dale, H.H. and P.P. Laidlaw, *The physiological action of Œ≤-iminazolylethylamine.* The Journal of Physiology, 1910. 41(5): p. 318-344.

119. Riley, J.F. and G.B. West, *The presence of histamine in tissue mast cells.* The Journal of Physiology, 1953. 120(4): p. 528-537.

120. Galli, S.J. and M. Tsai, *Mast cells in allergy and infection: versatile effector and regulatory cells in innate and adaptive immunity.* Eur J Immunol, 2010. 40(7): p. 1843-51.

121. Edwards, A., *The mast cell and allergic diseases: role in pathogenesis and implications for therapy.* Clin Exp Allergy, 2008. 38(6): p. 1063-4; author reply 1064-5.

122. Samoszuk, M., E. Kanakubo, and J.K. Chan, *Degranulating mast cells in fibrotic regions of human tumors and evidence that mast cell heparin interferes with the growth of tumor cells through a mechanism involving fibroblasts.* BMC Cancer, 2005. 5: p. 121.

123. Conti, P., et al., *Role of Mast Cells in Tumor Growth.* Ann Clin Lab Sci, 2007. 37(4): p. 315-322.

124. Theoharides, T.C. and P. Conti, *Mast cells: the JEKYLL and HYDE of tumor growth.* Trends in Immunology, 2004. 25(5): p. 235-241.

125. Molin, D., et al., *Mast cell infiltration correlates with poor prognosis in Hodgkin's lymphoma.* British Journal of Haematology, 2002. 119(1): p. 122-124.

126. Soucek, L., et al., *Mast cells are required for angiogenesis and macroscopic expansion of Myc-induced pancreatic islet tumors.* Nat Med, 2007. 13(10): p. 1211-8.

127. Yuan, A., et al., *The role of interleukin-8 in cancer cells and microenvironment interaction.* Front Biosci, 2005. 10: p. 853-65.

128. Hicklin, D.J. and L.M. Ellis, *Role of the vascular endothelial growth factor pathway in tumor growth and angiogenesis.* J Clin Oncol, 2005. 23(5): p. 1011-27.

129. Garc√≠a-Rom√°n, J., et al., *VEGF secretion during hypoxia depends on free radicals-induced Fyn kinase activity in mast cells.* Biochemical and Biophysical Research Communications, 2010. 401(2): p. 262-267.

130. Schafer, Z.T. and J.S. Brugge, *IL-6 involvement in epithelial cancers.* The Journal of Clinical Investigation, 2007. 117(12): p. 3660-3663.

131. Bromberg, J. and T.C. Wang, *Inflammation and Cancer: IL-6 and STAT3 Complete the Link.* Cancer Cell, 2009. 15(2): p. 79-80.

132. Wei, J.J., et al., *SCF and TLR4 ligand cooperate to augment the tumor-promoting potential of mast cells.* Cancer Immunol Immunother, 2012. 61(3): p. 303-12.

133. Maltby, S., K. Khazaie, and K.M. McNagny, *Mast cells in tumor growth: angiogenesis, tissue remodelling and immune-modulation.* Biochim Biophys Acta, 2009. 1796(1): p. 19-26.

134. Ribatti, D. and E. Crivellato, *Mast cells, angiogenesis, and tumour growth.* Biochim Biophys Acta, 2012. 1822(1): p. 2-8.

135. Imada, A., et al., *Mast cells correlate with angiogenesis and poor outcome in stage I lung adenocarcinoma.* European Respiratory Journal, 2000. 15(6): p. 1087-1093.

136. Ribatti, D., et al., *Tumor vascularity and tryptase-positive mast cells correlate with a poor prognosis in melanoma.* Eur J Clin Invest, 2003. 33(5): p. 420-5.

137. Elpek, G.O., et al., *The prognostic relevance of angiogenesis and mast cells in squamous cell carcinoma of the oesophagus.* J Clin Pathol, 2001. 54(12): p. 940-4.

138. Coussens, L.M. and Z. Werb, *Matrix metalloproteinases and the development of cancer.* Chem Biol, 1996. 3(11): p. 895-904.

139. Wu, L.C., *Immunoglobulin E receptor signaling and asthma.* J Biol Chem, 2011

286(38): p. 32891-7.

140. Pribluda, V.S., C. Pribluda, and H. Metzger, *Transphosphorylation as the mechanism by which the high-affinity receptor for IgE is phosphorylated upon aggregation.* Proc Natl Acad Sci U S A, 1994. 91(23): p. 11246-50.

141. Siraganian, R.P., et al., *Protein tyrosine kinase Syk in mast cell signaling.* Mol Immunol, 2002. 38(16-18): p. 1229-33.

142. MacGlashan, D., Jr., *IgE receptor and signal transduction in mast cells and basophils.* Curr Opin Immunol, 2008. 20(6): p. 717-23.

143. Liou, J., et al., *Live-cell imaging reveals sequential oligomerization and local plasma membrane targeting of stromal interaction molecule 1 after Ca2+ store depletion.* Proc Natl Acad Sci U S A, 2007. 104(22): p. 9301-6.

144. Calloway, N., D. Holowka, and B. Baird, *A basic sequence in STIM1 promotes Ca2+ influx by interacting with the C-terminal acidic coiled coil of Orai1.* Biochemistry, 2010

49(6): p. 1067-71.

145. Gross, S.A., et al., *Murine ORAI2 splice variants form functional Ca2+ release-activated Ca2+ (CRAC) channels.* J Biol Chem, 2007. 282(27): p. 19375-84.

146. Ma, H.T., et al., *Canonical transient receptor potential 5 channel in conjunction with Orai1 and STIM1 allows Sr2+ entry, optimal influx of Ca2+, and degranulation in a rat mast cell line.* J Immunol, 2008. 180(4): p. 2233-9.

147. Freichel, M., J. Almering, and V. Tsvilovskyy, *The Role of TRP Proteins in Mast Cells.* Front Immunol, 2012

3: p. 150.

148. Metcalfe, D.D., *Mast cells and mastocytosis.* Blood, 2008. 112(4): p. 946-56.

149. Iemura, A., et al., *The c-kit ligand, stem cell factor, promotes mast cell survival by suppressing apoptosis.* Am J Pathol, 1994. 144: p. 321 - 328.

150. Kirshenbaum, A., et al., *Thrombopoietin alone or in the presence of stem cell factor supports the growth of KIT(CD117)low/MPL(CD110)+ human mast cells from hematopoietic progenitor cells.* Exp Hematol, 2005. 33: p. 413 - 21.

151. el-Lati, S.G., C.A. Dahinden, and M.K. Church, *Complement peptides C3a- and C5a-induced mediator release from dissociated human skin mast cells.* J Invest Dermatol, 1994. 102(5): p. 803-6.

152. Fureder, W., et al., *Differential response of human basophils and mast cells to recombinant chemokines.* Ann Hematol, 1995. 70(5): p. 251-8.

153. Schulman, E.S., et al., *Differential effects of the complement peptides, C5a and C5a des Arg on human basophil and lung mast cell histamine release.* J Clin Invest, 1988. 81(3): p. 918-23.

154. Venkatesha, R.T., et al., *Distinct regulation of C3a-induced MCP-1/CCL2 and RANTES/CCL5 production in human mast cells by extracellular signal regulated kinase and PI3 kinase.* Mol Immunol, 2005. 42(5): p. 581-7.

155. Ali, H., et al., *Chemokine production by G protein-coupled receptor activation in a human mast cell line: roles of extracellular signal-regulated kinase and NFAT.* J Immunol, 2000. 165(12): p. 7215-23.

156. Nilsson, G., et al., *C3a and C5a are chemotaxins for human mast cells and act through distinct receptors via a pertussis toxin-sensitive signal transduction pathway.* J Immunol, 1996. 157(4): p. 1693-8.

157. Marquardt, D.L., J.L. Alongi, and L.L. Walker, *The phosphatidylinositol 3-kinase inhibitor wortmannin blocks mast cell exocytosis but not IL-6 production.* The Journal of Immunology, 1996. 156(5): p. 1942-5.

158. Leal-Berumen, I., P. Conlon, and J.S. Marshall, *IL-6 production by rat peritoneal mast cells is not necessarily preceded by histamine release and can be induced by bacterial lipopolysaccharide.* The Journal of Immunology, 1994. 152(11): p. 5468-76.

159. Moresco, E.M.Y., D. LaVine, and B. Beutler, *Toll-like receptors.* Current Biology, 2011. 21(13): p. R488-R493.

160. Akira, S., S. Uematsu, and O. Takeuchi, *Pathogen Recognition and Innate Immunity.* Cell, 2006. 124(4): p. 783-801.

161. Sandig, H. and S. Bulfone-Paus, *TLR signaling in mast cells: common and unique features.* Frontiers in Immunology, 2012. 3.

162. Varadaradjalou, S., et al., *Toll-like receptor 2 (TLR2) and TLR4 differentially activate human mast cells.* Eur J Immunol, 2003. 33: p. 899 - 906.

163. Supajatura, V., et al., *Differential responses of mast cell Toll-like receptors 2 and 4 in allergy and innate immunity.* J Clin Invest, 2002. 109(10): p. 1351-9.

164. Moresco, E.M., D. LaVine, and B. Beutler, *Toll-like receptors.* Curr Biol. 21(13): p. R488-93.

165. Bienenstock, J., et al., *Mast cell/nerve interactions in vitro and in vivo.* Am Rev Respir Dis, 1991. 143(3 Pt 2): p. S55-8.

166. Benyon, R.C., C. Robinson, and M.K. Church, *Differential release of histamine and eicosanoids from human skin mast cells activated by IgE-dependent and non-immunological stimuli.* Br J Pharmacol, 1989. 97(3): p. 898-904.

167. Bischoff, S.C., et al., *Substance P and other neuropeptides do not induce mediator release in isolated human intestinal mast cells.* Neurogastroenterol Motil, 2004. 16(2): p. 185-93.

168. Nakayama, T., et al., *Prostaglandin E2 promotes degranulation-independent release of MCP-1 from mast cells.* J Leukoc Biol, 2006. 79(1): p. 95-104.

169. Abdel-Majid, R.M. and J.S. Marshall, *Prostaglandin E2 induces degranulation-independent production of vascular endothelial growth factor by human mast cells.* J Immunol, 2004. 172(2): p. 1227-36.

170. Kandere-Grzybowska, K., et al., *IL-1 induces vesicular secretion of IL-6 without degranulation from human mast cells.* J Immunol, 2003. 171(9): p. 4830-6.

171. Griffiths, G.M., *Secretory lysosomes - a special mechanism of regulated secretion in haemopoietic cells.* Trends Cell Biol, 1996. 6(9): p. 329-32.

172. Schwartz, L.B. and K.F. Austen, *Enzymes of the Mast Cell Granule.* J Investig Dermatol, 1980. 74(5): p. 349-353.

173. Sagi-Eisenberg, R., *The mast cell: where endocytosis and regulated exocytosis meet.* Immunol Rev, 2007. 217: p. 292-303.

174. Benado, A., Y. Nasagi-Atiya, and R. Sagi-Eisenberg, *Protein trafficking in immune cells.* Immunobiology, 2009. 214(6): p. 403-21.

175. Rodriguez, A., et al., *Lysosomes behave as Ca2+-regulated exocytic vesicles in fibroblasts and epithelial cells.* J Cell Biol, 1997. 137(1): p. 93-104.

176. Settembre, C., et al., *Signals from the lysosome: a control centre for cellular clearance and energy metabolism.* Nat Rev Mol Cell Biol, 2013. 14(5): p. 283-96.

177. Blott, E.J. and G.M. Griffiths, *Secretory lysosomes.* Nat Rev Mol Cell Biol, 2002. 3(2): p. 122-31.

178. Raposo, G., et al., *Accumulation of major histocompatibility complex class II molecules in mast cell secretory granules and their release upon degranulation.* Mol Biol Cell, 1997. 8(12): p. 2631-45.

179. Eiseman, E. and J.B. Bolen, *Engagement of the high-affinity IgE receptor activates src protein-related tyrosine kinases.* Nature, 1992. 355(6355): p. 78-80.

180. Kaur, J. and D.F. Cutler, *P-selectin targeting to secretory lysosomes of Rbl-2H3 cells.* J Biol Chem, 2002. 277(12): p. 10498-505.

181. Blott, E.J., et al., *Fas ligand is targeted to secretory lysosomes via a proline-rich domain in its cytoplasmic tail.* Journal of Cell Science, 2001. 114(13): p. 2405-2416.

182. Murray, R.Z., et al., *A Role for the Phagosome in Cytokine Secretion.* Science, 2005. 310(5753): p. 1492-1495.

183. Manderson, A.P., et al., *Subcompartments of the macrophage recycling endosome direct the differential secretion of IL-6 and TNFalpha.* J Cell Biol, 2007. 178(1): p. 57-69.

184. Martin, S., et al., *The glucose transporter (GLUT-4) and vesicle-associated membrane protein-2 (VAMP-2) are segregated from recycling endosomes in insulin-sensitive cells.* The Journal of Cell Biology, 1996. 134(3): p. 625-635.

185. Bryant, N.J. and G.W. Gould, *SNARE Proteins Underpin Insulin-Regulated GLUT4 Traffic.* Traffic, 2011. 12(6): p. 657-664.

186. Williams, D. and J.E. Pessin, *Mapping of R-SNARE function at distinct intracellular GLUT4 trafficking steps in adipocytes.* The Journal of Cell Biology, 2008. 180(2): p. 375-387.

187. Zhu, F.-G., K. Gomi, and J.S. Marshall, *Short-Term and Long-Term Cytokine Release by Mouse Bone Marrow Mast Cells and the*

Differentiated KU-812 Cell Line Are Inhibited by Brefeldin A. **The Journal of Immunology, 1998. 161(5): p. 2541-2551.**

188. Stow, J.L., et al., *Cytokine secretion in macrophages and other cells: pathways and mediators.* Immunobiology, 2009. 214(7): p. 601-12.

189. Dvorak, A., et al., *Piecemeal degranulation of mast cells in the inflammatory eyelid lesions of interleukin-4 transgenic mice. Evidence of mast cell histamine release in vivo by diamine oxidase-gold enzyme-affinity ultrastructural cytochemistry.* Blood, 1994. 83(12): p. 3600-3612.

190. Lacy, P., et al., *Fusion protein vesicle-associated membrane protein 2 is implicated in IFN-gamma-induced piecemeal degranulation in human eosinophils from atopic individuals.* J Allergy Clin Immunol, 2001. 107(4): p. 671-8.

191. Melo, R.C.N., et al., *Human Eosinophils Secrete Preformed, Granule-Stored Interleukin-4 Through Distinct Vesicular Compartments.* Traffic, 2005. 6(11): p. 1047-1057.

192. Melo, R.C., et al., *Human eosinophils secrete preformed, granule-stored interleukin-4 through distinct vesicular compartments.* Traffic, 2005. 6(11): p. 1047-57.

193. Melo, R.C., et al., *Intragranular vesiculotubular compartments are involved in piecemeal degranulation by activated human eosinophils.* Traffic, 2005. 6(10): p. 866-79.

194. Blank, U., *The mechanisms of exocytosis in mast cells.* Adv Exp Med Biol, 2011. 716: p. 107-22.

195. Alvarez de Toledo, G. and J.M. Fernandez, *Compound versus multigranular exocytosis in peritoneal mast cells.* J Gen Physiol, 1990. 95(3): p. 397-409.

196. Pickett, J.A. and J.M. Edwardson, *Compound exocytosis: mechanisms and functional significance.* Traffic, 2006. 7(2): p. 109-16.

197. Cohen, R., et al., *Spatiotemporal resolution of mast cell granule exocytosis reveals correlation with Ca2+ wave initiation.* J Cell Sci, 2012. 125(Pt 12): p. 2986-94.

198. Baumert, M., et al., *Synaptobrevin: an integral membrane protein of 18,000 daltons present in small synaptic vesicles of rat brain.* EMBO J, 1989. 8(2): p. 379-84.

199. Trimble, W.S., D.M. Cowan, and R.H. Scheller, *VAMP-1: a synaptic vesicle-associated integral membrane protein.* Proc Natl Acad Sci U S A, 1988. 85(12): p. 4538-42.

200. Inoue, A., K. Obata, and K. Akagawa, *Cloning and sequence analysis of cDNA for a neuronal cell membrane antigen, HPC-1.* Journal of Biological Chemistry, 1992. 267(15): p. 10613-10619.

201. Bennett, M.K., N. Calakos, and R.H. Scheller, *Syntaxin: a synaptic protein implicated in docking of synaptic vesicles at presynaptic active zones.* Science, 1992. 257: p. 255-259.

202. Oyler, G.A., et al., *The identification of a novel synaptosomal-associated protein, SNAP-25, differentially expressed by neuronal subpopulations.* J Cell Biol, 1989. 109(6 Pt 1): p. 3039-52.

203. Sudhof, T.C., et al., *A synaptic vesicle membrane protein is conserved from mammals to Drosophila.* Neuron, 1989. 2(5): p. 1475-81.

204. Chin, G.J. and S.A. Goldman, *Purification of squid synaptic vesicles and characterization of the vesicle-associated proteins synaptobrevin and Rab3A.* Brain Research, 1992. 571(1): p. 89-96.

205. Risinger, C., et al., *Evolutionary conservation of synaptosome-associated protein 25 kDa (SNAP-25) shown by Drosophila and Torpedo cDNA clones.* J Biol Chem, 1993. 268(32): p. 24408-14.

206. Schiavo, G.G., et al., *Tetanus and botulinum-B neurotoxins block neurotransmitter release by proteolytic cleavage of synaptobrevin.* Nature, 1992. 359(6398): p. 832-835.

207. Link, E., et al., *Tetanus toxin action: Inhibition of neurotransmitter release linked to synaptobrevin proteolysis.* Biochemical and Biophysical Research Communications, 1992. 189(2): p. 1017-1023.

208. Schiavo, G., et al., *Botulinum neurotoxin serotype F is a zinc endopeptidase specific for VAMP/synaptobrevin.* Journal of Biological Chemistry, 1993. 268(16): p. 11516-11519.

209. Blasi, J., et al., *Botulinum neurotoxin C1 blocks neurotransmitter release by means of cleaving HPC-1/syntaxin.* EMBO J, 1993. 12(12): p. 4821-8.

210. Blasi, J., et al., *Botulinum neurotoxin A selectively cleaves the synaptic protein SNAP-25.* Nature, 1993. 365(6442): p. 160-163.

211. Horikawa, H.P.M., et al., *A complex of rab3A, SNAP-25, VAMP/synaptobrevin-2 and syntaxins in brain presynaptic terminals.* FEBS Letters, 1993. 330(2): p. 236-240.

212. McMahon, H.T., et al., *Cellubrevin is a ubiquitous tetanus-toxin substrate homologous to a putative synaptic vesicle fusion protein.* Nature, 1993. 364(6435): p. 346-349.

213. Ralston, E., S. Beushausen, and T. Ploug, *Expression of the synaptic vesicle proteins VAMPs/synaptobrevins 1 and 2 in non-neural tissues.* Journal of Biological Chemistry, 1994. 269(22): p. 15403-15406.

214. Ravichandran, V., A. Chawla, and P.A. Roche, *Identification of a Novel Syntaxin- and Synaptobrevin/VAMP-binding Protein, SNAP-23, Expressed in Non-neuronal Tissues.* Journal of Biological Chemistry, 1996. 271(23): p. 13300-13303.

215. Jahn, R. and R.H. Scheller, *SNAREs [mdash] engines for membrane fusion.* Nat Rev Mol Cell Biol, 2006. 7(9): p. 631-643.

216. Sutton, R.B., et al., *Crystal structure of a SNARE complex involved in synaptic exocytosis at 2.4[thinsp]A resolution.* Nature, 1998. 395(6700): p. 347-353.

217. Perin, M.S., et al., *Phospholipid binding by a synaptic vesicle protein homologous to the regulatory region of protein kinase C.* Nature, 1990. 345(6272): p. 260-3.

218. Weber, T., et al., *SNAREpins: Minimal Machinery for Membrane Fusion.* Cell, 1998. 92(6): p. 759-772.

219. Shukla, A., et al., *Regulated exocytosis in immune function: are SNARE-proteins involved?* Respir Med, 2000. 94(1): p. 10-7.

220. Hanson, P.I., et al., *Structure and conformational changes in NSF and its membrane receptor complexes visualized by quick-freeze/deep-etch electron microscopy.* Cell, 1997. 90(3): p. 523-35.

221. Furst, J., et al., *Electron cryomicroscopy structure of N-ethyl maleimide sensitive factor at 11 A resolution.* EMBO J, 2003. 22(17): p. 4365-74.

222. Marz, K.E., J.M. Lauer, and P.I. Hanson, *Defining the SNARE complex binding surface of alpha-SNAP: implications for SNARE complex disassembly.* J Biol Chem, 2003. 278(29): p. 27000-8.

223. Fernandez, I., et al., *Three-Dimensional Structure of an Evolutionarily Conserved N-Terminal Domain of Syntaxin 1A.* Cell, 1998. 94(6): p. 841-849.

224. Lerman, J.C., et al., *Structural Analysis of the Neuronal SNARE Protein Syntaxin-1A,Ä†„Ä°.* Biochemistry, 2000. 39(29): p. 8470-8479.

225. Hata, Y., C.A. Slaughter, and T.C. Sudhof, *Synaptic vesicle fusion complex contains unc-18 homologue bound to syntaxin.* Nature, 1993. 366(6453): p. 347-51.

226. Ma, C., et al., *Reconstitution of the Vital Functions of Munc18 and Munc13 in Neurotransmitter Release.* Science, 2013

339(6118): p. 421-425.

227. Verhage, M., et al., *Synaptic Assembly of the Brain in the Absence of Neurotransmitter Secretion.* Science, 2000. 287(5454): p. 864-869.

228. Rossi, V., et al., *Longins and their longin domains: regulated SNAREs and multifunctional SNARE regulators.* Trends Biochem Sci, 2004. 29(12): p. 682-8.

229. Kent, H.M., et al., *Structural basis of the intracellular sorting of the SNARE VAMP7 by the AP3 adaptor complex.* Dev Cell, 2012. 22(5): p. 979-88.

230. Chaineau, M., L. Danglot, and T. Galli, *Multiple roles of the vesicular-SNARE TI-VAMP in post-Golgi and endosomal trafficking.* FEBS Lett, 2009. 583(23): p. 3817-26.

231. Martinez-Arca, S., et al., *A dual mechanism controlling the localization and function of exocytic v-SNAREs.* Proc Natl Acad Sci U S A, 2003. 100(15): p. 9011-6.

232. Hibi, T., N. Hirashima, and M. Nakanishi, *Rat Basophilic Leukemia Cells Express Syntaxin-3 and VAMP-7 in Granule Membranes.* Biochemical and Biophysical Research Communications, 2000. 271(1): p. 36-41.

233. Paumet, F., et al., *Soluble NSF attachment protein receptors (SNAREs) in RBL-2H3 mast cells: functional role of syntaxin 4 in exocytosis and identification of a vesicle-associated membrane protein 8-containing secretory compartment.* J Immunol, 2000. 164(11): p. 5850-7.

234. Puri, N. and P.A. Roche, *Mast cells possess distinct secretory granule subsets whose exocytosis is regulated by different SNARE isoforms.* Proc Natl Acad Sci U S A, 2008. 105(7): p. 2580-5.

235. Tiwari, N., et al., *VAMP-8 segregates mast cell-preformed mediator exocytosis from cytokine trafficking pathways.* Blood, 2008. 111(7): p. 3665-3674.

236. Woska Jr, J.R. and M.E. Gillespie, *Small-Interfering RNA-Mediated Identification and Regulation of the Ternary SNARE Complex Mediating RBL-2H3 Mast Cell Degranulation.* Scandinavian Journal of Immunology, 2011. 73(1): p. 8-17.

237. Advani, R.J., et al., *VAMP-7 mediates vesicular transport from endosomes to lysosomes.* J Cell Biol, 1999. 146(4): p. 765-76.

238. Tiwari, N., et al., *Increased formation of VAMP-3-containing SNARE complexes in mast cells from VAMP-8 deficient cells. appetite.* Inflamm Res, 2009. 58 Suppl 1: p. 13-4.

239. Sander, L.E., et al., *Vesicle associated membrane protein (VAMP)-7 and VAMP-8, but not VAMP-2 or VAMP-3, are required for activation-induced degranulation of mature human mast cells.* European Journal of Immunology, 2008. 38(3): p. 855-863.

240. Frank, S.P., et al., *SNAP-23 and syntaxin-3 are required for chemokine release by mature human mast cells.* Mol Immunol, 2011. 49(1-2): p. 353-8.

241. Holt, M., et al., *Identification of SNAP-47, a novel Qbc-SNARE with ubiquitous expression.* J Biol Chem, 2006. 281(25): p. 17076-83.

242. Su, Q., et al., *SNAP-29: a general SNARE protein that inhibits SNARE disassembly and is implicated in synaptic transmission.* Proc Natl Acad Sci U S A, 2001. 98(24): p. 14038-43.

243. Steegmaier, M., et al., *Three novel proteins of the syntaxin/SNAP-25 family.* J Biol Chem, 1998. 273(51): p. 34171-9.

244. Rapaport, D., et al., *Loss of SNAP29 Impairs Endocytic Recycling and Cell Motility.* PLoS ONE, 2010. 5(3): p. e9759.

245. dos Santos, L.D., et al., *Proteomic profiling of the molecular targets of interactions of the mastoparan peptide Protopolybia MP-III at the level of endosomal membranes from rat mast cells.* Proteomics, 2012. 12(17): p. 2682-93.

246. Wesolowski, J., V. Caldwell, and F. Paumet, *A Novel Function for SNAP29 (Synaptosomal-Associated Protein of 29 kDa) in Mast Cell Phagocytosis.* PLoS ONE, 2012. 7(11): p. e49886.

247. Yamamori, S., et al., *Differential expression of SNAP-25 family proteins in the mouse brain.* J Comp Neurol, 2011. 519(5): p. 916-32.

248. GarcÌa-Rom·n, J., et al., *VEGF secretion during hypoxia depends on free radicals-induced Fyn kinase activity in mast cells.* Biochemical and Biophysical Research Communications, 2010. In Press, Accepted Manuscript.

249. Chapman, E.R., *How does synaptotagmin trigger neurotransmitter release?* Annu Rev Biochem, 2008. 77: p. 615-41.

250. Kochubey, O., X. Lou, and R. Schneggenburger, *Regulation of transmitter release by Ca(2+) and synaptotagmin: insights from a large CNS synapse.* Trends Neurosci, 2011. 34(5): p. 237-46.

251. Hui, E., et al., *Three distinct kinetic groupings of the synaptotagmin family: Candidate sensors for rapid and delayed exocytosis.* Proceedings of the National Academy of Sciences of the United States of America, 2005. 102(14): p. 5210-5214.

252. Bhalla, A., W.C. Tucker, and E.R. Chapman, *Synaptotagmin isoforms couple distinct ranges of Ca2+, Ba2+, and Sr2+ concentration to SNARE-mediated membrane fusion.* Mol Biol Cell, 2005. 16(10): p. 4755-64.

253. Sugita, S., et al., *Synaptotagmins form a hierarchy of exocytotic Ca(2+) sensors with distinct Ca(2+) affinities.* EMBO J, 2002. 21(3): p. 270-80.

254. Zhang, Z., et al., *Release mode of large and small dense-core vesicles specified by different synaptotagmin isoforms in PC12 cells.* Mol Biol Cell, 2011. 22(13): p. 2324-36.

255. Baram, D., et al., *Synaptotagmin II Negatively Regulates Ca2+-triggered Exocytosis of Lysosomes in Mast Cells.* J. Exp. Med., 1999. 189(10): p. 1649-1658.

256. Haberman, Y., et al., *Synaptotagmin (Syt) IX is an essential determinant for protein sorting to secretory granules in mast cells.* Blood, 2007. 109(8): p. 3385-92.

257. Haberman, Y., et al., *Classical protein kinase C(s) regulates targeting of synaptotagmin IX to the endocytic recycling compartment.* J Cell Sci, 2005. 118(Pt 8): p. 1641-9.

258. Haberman, Y., et al., *Synaptotagmin IX, a possible linker between the perinuclear endocytic recycling compartment and the microtubules.* J Cell Sci, 2003. 116(Pt 21): p. 4307-18.

259. Baram, D., et al., *Ca2+-dependent exocytosis in mast cells is stimulated by the Ca2+ sensor, synaptotagmin I.* J Immunol, 1998. 161(10): p. 5120-3.

260. Melicoff, E., et al., *Synaptotagmin-2 controls regulated exocytosis but not other secretory responses of mast cells.* J Biol Chem, 2009. 284(29): p. 19445-51.

261. Grimberg, E., et al., *Synaptotagmin III is a critical factor for the formation of the perinuclear endocytic recycling compartment and determination of secretory granules size.* J Cell Sci, 2003. 116(Pt 1): p. 145-54.

262. Brunger, A.T., *Structure and function of SNARE and SNARE-interacting proteins.* Q Rev Biophys, 2005. 38(1): p. 1-47.

263. Giraudo, C.G., et al., *A clamping mechanism involved in SNARE-dependent exocytosis.* Science, 2006. 313: p. 676-680.

264. Giraudo, C.G., et al., *Distinct domains of complexins bind SNARE complexes and clamp fusion in vitro.* J Biol Chem, 2008. 283(30): p. 21211-9.

265. Lu, B., S. Song, and Y.K. Shin, *Accessory alpha-helix of complexin I can displace VAMP2 locally in the complexin-SNARE quaternary complex.* J Mol Biol, 2009. 396(3): p. 602-9.

266. K√ºmmel, D., et al., *Complexin cross-links prefusion SNAREs into a zigzag array.* Nat Struct Mol Biol, 2011. 18(8): p. 927-933.

267. Sudhof, T.C. and J.E. Rothman, *Membrane fusion: grappling with SNARE and SM proteins.* Science, 2009. 323(5913): p. 474-7.

268. Reim, K., et al., *Structurally and functionally unique complexins at retinal ribbon synapses.* The Journal of Cell Biology, 2005. 169(4): p. 669-680.

269. Tadokoro, S., M. Nakanishi, and N. Hirashima, *Complexin II facilitates exocytotic release in mast cells by enhancing Ca2+ sensitivity of the fusion process.* J Cell Sci, 2005. 118(Pt 10): p. 2239-46.

270. Tadokoro, S., M. Nakanishi, and N. Hirashima, *Complexin II regulates degranulation in RBL-2H3 cells by interacting with SNARE complex containing syntaxin-3.* Cell Immunol, 2009. 261(1): p. 51-6.

271. Malsam, J., et al., *Complexin arrests a pool of docked vesicles for fast Ca2+-dependent release.* EMBO J, 2012. 31(15): p. 3270-81.

272. Lorentz, A., et al., *The SNARE Machinery in Mast Cell Secretion.* Front Immunol, 2012. 3: p. 143.

273. Verhage, M., et al., *Synaptic assembly of the brain in the absence of neurotransmitter secretion.* Science, 2000. 287(5454): p. 864-9.

274. Rathore, S.S., et al., *Syntaxin N-terminal peptide motif is an initiation factor for the assembly of the SNAREâ€"Sec1/Munc18 membrane fusion complex.* Proceedings of the National Academy of Sciences, 2010. 107(52): p. 22399-22406.

275. Zhou, P., et al., *Syntaxin□1 N peptide and Habc□domain perform distinct essential functions in synaptic vesicle fusion.* The EMBO Journal, 2013. 32(1): p. 159-171.

276. Nigam, R., et al., *Expression and transcriptional regulation of Munc18 isoforms in mast cells.* Biochimica et Biophysica Acta (BBA) - Gene Structure and Expression, 2005. 1728(1-2): p. 77-83.

277. Martin-Verdeaux, S., et al., *Evidence of a role for Munc18-2 and microtubules in mast cell granule exocytosis.* J Cell Sci, 2003. 116(Pt 2): p. 325-34.

278. Tadokoro, S., et al., *Munc18-2 regulates exocytotic membrane fusion positively interacting with syntaxin-3 in RBL-2H3 cells.* Molecular Immunology, 2007. 44(13): p. 3427-3433.

279. Bin, N.R., et al., *Crucial role of the hydrophobic pocket region of Munc18 protein in mast cell degranulation.* Proc Natl Acad Sci U S A, 2012.

280. Neeft, M., et al., *Munc13-4 Is an Effector of Rab27a and Controls Secretion of Lysosomes in Hematopoietic Cells.* Molecular Biology of the Cell, 2005. 16(2): p. 731-741.

281. van der Sluijs, P., et al., *Methods for Analysis of rab27a/munc13,Äê4 in Secretory Lysosome Release in Hematopoietic Cells*, in *Methods in Enzymology*. 2008, Academic Press. p. 185-201.

282. Elstak, E.D., et al., *The munc13-4,Äìrab27 complex is specifically required for tethering secretory lysosomes at the plasma membrane.* Blood, 2011. 118(6): p. 1570-1578.

283. Neeft, M., et al., *Munc13-4 Is an Effector of Rab27a and Controls Secretion of Lysosomes in Hematopoietic Cells.* Mol. Biol. Cell, 2005. 16(2): p. 731-741.

284. Higashio, H., et al., *Doc2{alpha} and Munc13-4 Regulate Ca2+-Dependent Secretory Lysosome Exocytosis in Mast Cells.* J Immunol, 2008. 180(7): p. 4774-4784.

285. Singh, R.K., et al., *Distinct and opposing roles for Rab27a/Mlph/MyoVa and Rab27b/Munc13-4 in mast cell secretion.* FEBS Journal, 2013. 280(3): p. 892-903.

286. Stenmark, H., *Rab GTPases as coordinators of vesicle traffic.* Nat Rev Mol Cell Biol, 2009. 10(8): p. 513-25.

287. Hutagalung, A.H. and P.J. Novick, *Role of Rab GTPases in membrane traffic and cell physiology.* Physiol Rev, 2011. 91(1): p. 119-49.

288. Goishi, K., et al., *Involvement of Rab27 in antigen-induced histamine release from rat basophilic leukemia 2H3 cells.* Biochem Biophys Res Commun, 2004. 324(1): p. 294-301.

289. Kageyama-Yahara, N., et al., *Rab5a regulates surface expression of FcepsilonRI and functional activation in mast cells.* Biol Pharm Bull, 2011. 34(5): p. 760-3.

290. Betz, W.J., F. Mao, and C.B. Smith, *Imaging exocytosis and endocytosis.* Curr Opin Neurobiol, 1996. 6(3): p. 365-71.

291. Cochilla, A.J., J.K. Angleson, and W.J. Betz, *Monitoring secretory membrane with FM1-43 fluorescence.* Annu Rev Neurosci, 1999. 22: p. 1-10.

292. Chiarini-Garcia, H.l., et al., *Using the Fluorescent Styryl Dye FM1-43 to Visualize Synaptic Vesicles Exocytosis and Endocytosis in Motor Nerve Terminals*, in *Light Microscopy*. 2011, Humana Press. p. 137-148.

293. Williams, R.M. and W.W. Webb, *Single granule pH cycling in antigen-induced mast cell secretion.* J Cell Sci, 2000. 113 Pt 21: p. 3839-50.

294. Curtis, T., et al., *Development of a mast cell-based biosensor.* Biosens Bioelectron, 2008. 23(7): p. 1024-31.

295. Miesenbock, G., D.A. De Angelis, and J.E. Rothman, *Visualizing secretion and synaptic transmission with pH-sensitive green fluorescent proteins.* Nature, 1998. 394(6689): p. 192-195.

296. Mahon, M.J., *pHluorin2: an enhanced, ratiometric, pH-sensitive green florescent protein.* Adv Biosci Biotechnol, 2011. 2(3): p. 132-137.

297. Shaner, N.C., et al., *Improved monomeric red, orange and yellow fluorescent proteins derived from Discosoma sp. red fluorescent protein.* Nat Biotech, 2004. 22(12): p. 1567-1572.

298. Ramirez, D.M.O., et al., *Vti1a Identifies a Vesicle Pool that Preferentially Recycles at Rest and Maintains Spontaneous Neurotransmission.* Neuron, 2012. 73(1): p. 121-134.

299. Gubernator, N.G., et al., *Fluorescent False Neurotransmitters Visualize Dopamine Release from Individual Presynaptic Terminals.* Science, 2009. 324(5933): p. 1441-1444.

300. Lee, M., et al., *Development of pH-Responsive Fluorescent False Neurotransmitters.* Journal of the American Chemical Society, 2010. 132(26): p. 8828-8830.

301. Schiavo, G., M. Matteoli, and C. Montecucco, *Neurotoxins Affecting Neuroexocytosis.* Physiol. Rev., 2000. 80(2): p. 717-766.

302. Pellizzari, R., et al., *Tetanus and botulinum neurotoxins: mechanism of action and therapeutic uses.* Philos Trans R Soc Lond B Biol Sci, 1999. 354(1381): p. 259-68.

303. Brunger, A.T. and A. Rummel, *Receptor and substrate interactions of clostridial neurotoxins.* Toxicon, 2009. 54(5): p. 550-60.

304. Dong, M., et al., *SV2 Is the Protein Receptor for Botulinum Neurotoxin A.* Science, 2006. 312(5773): p. 592-596.

305. Dong, M., et al., *Glycosylated SV2A and SV2B mediate the entry of botulinum neurotoxin E into neurons.* Mol Biol Cell, 2008. 19(12): p. 5226-37.

306. Yamamoto, H., et al., *Specificity of botulinum protease for human VAMP family proteins.* Microbiol Immunol, 2012. 56(4): p. 245-53.

307. Humeau, Y., et al., *How botulinum and tetanus neurotoxins block neurotransmitter release.* Biochimie, 2000. 82(5): p. 427-46.

308. Meunier, F.r.d.r.A., et al., *Dynamics of motor nerve terminal remodeling unveiled using SNARE-cleaving botulinum toxins: the extent and duration are dictated by the sites of SNAP-25 truncation.* Molecular and Cellular Neuroscience, 2003. 22(4): p. 454-466.

309. Dolly, O., *Synaptic transmission: inhibition of neurotransmitter release by botulinum toxins.* Headache, 2003. 43 Suppl 1: p. S16-24.

310. Fernández-Salas, E., et al., *Is the light chain subcellular localization an important factor in botulinum toxin duration of action?* Movement Disorders, 2004. 19(S8): p. S23-S34.

311. Smith, T.J., et al., *Sequence Variation within Botulinum Neurotoxin Serotypes Impacts Antibody Binding and Neutralization.* Infection and Immunity, 2005. 73(9): p. 5450-5457.

312. Arndt, J.W., et al., *A Structural Perspective of the Sequence Variability Within Botulinum Neurotoxin Subtypes A1-A4.* Journal of Molecular Biology, 2006. 362(4): p. 733-742.

313. Chen, Y., et al., *Sequencing the Botulinum Neurotoxin Gene and Related Genes in Clostridium botulinum Type E Strains Reveals orfx3 and a Novel Type E Neurotoxin Subtype.* Journal of Bacteriology, 2007. 189(23): p. 8643-8650.

314. Raphael, B.H., et al., *Sequence Diversity of Genes Encoding Botulinum Neurotoxin Type F.* Applied and Environmental Microbiology, 2010. 76(14): p. 4805-4812.

315. Kalb, S.R., et al., *De novo subtype and strain identification of botulinum neurotoxin type B through toxin proteomics.* Anal Bioanal Chem, 2012. 403(1): p. 215-26.

316. Shone, C.C., P. Hambleton, and J. Melling, *A 50-kDa fragment from the NH2-terminus of the heavy subunit of Clostridium botulinum type A neurotoxin forms channels in lipid vesicles.* Eur J Biochem, 1987. 167(1): p. 175-80.

317. Chaddock, J.A., et al., *Expression and purification of catalytically active, non-toxic endopeptidase derivatives of Clostridium botulinum toxin type A.* Protein Expr Purif, 2002. 25(2): p. 219-28.

318. Duggan, M.J., et al., *Inhibition of release of neurotransmitters from rat dorsal root ganglia by a novel conjugate of a Clostridium botulinum toxin A endopeptidase fragment and Erythrina cristagalli lectin.* J Biol Chem, 2002. 277(38): p. 34846-52.

319. Meng, J., et al., *Activation of TRPV1 Mediates Calcitonin Gene-Related Peptide Release, Which Excites Trigeminal Sensory Neurons and Is Attenuated by a Retargeted Botulinum Toxin with Anti-Nociceptive Potential.* The Journal of Neuroscience, 2009. 29(15): p. 4981-4992.

320. Dolly, J.O., et al., *Neuro-exocytosis: botulinum toxins as inhibitory probes and versatile therapeutics.* Curr Opin Pharmacol, 2009. 9(3): p. 326-35.

321. Wang, J., et al., *Novel chimeras of botulinum neurotoxins A and E unveil contributions from the binding, translocation, and protease domains to their functional characteristics.* J Biol Chem, 2008. 283(25): p. 16993-7002.

322. Foster, K.A., et al., *Re-engineering the target specificity of Clostridial neurotoxins - a route to novel therapeutics.* Neurotox Res, 2006. 9(2-3): p. 101-7.

323. Chen, S. and J.T. Barbieri, *Engineering botulinum neurotoxin to extend therapeutic intervention.* Proc Natl Acad Sci U S A, 2009. 106(23): p. 9180-4.

324. Binz, T., S. Sikorra, and S. Mahrhold, *Clostridial neurotoxins: mechanism of SNARE cleavage and outlook on potential substrate specificity reengineering.* Toxins (Basel), 2010. 2(4): p. 665-82.

325. Graff, L., et al., *Expression of vesicular monoamine transporters, synaptosomal-associated protein 25 and syntaxin1: a signature of human small cell lung carcinoma.* Cancer Res, 2001. 61(5): p. 2138-44.

326. Galiveti, C.R., et al., *Application of housekeeping npcRNAs for quantitative expression analysis of human transcriptome by real-time PCR.* RNA, 2009

16(2): p. 450-61.

327. Takahashi, A., et al., *Measurement of intracellular calcium.* Physiol Rev, 1999. 79(4): p. 1089-125.

328. Grynkiewicz, G., M. Poenie, and R.Y. Tsien, *A new generation of Ca2+ indicators with greatly improved fluorescence properties.* Journal of Biological Chemistry, 1985. 260(6): p. 3440-3450.

329. Keighron, J.D., A.G. Ewing, and A.-S. Cans, *Analytical tools to monitor exocytosis: a focus on new fluorescent probes and methods.* Analyst, 2012. 137(8): p. 1755-1763.

330. Liew, C.-G., et al., *Transient and Stable Transgene Expression in Human Embryonic Stem Cells.* STEM CELLS, 2007. 25(6): p. 1521-1528.

331. Bansal, G., et al., *RGS13 Controls G Protein-Coupled Receptor-Evoked Responses of Human Mast Cells.* The Journal of Immunology, 2008. 181(11): p. 7882-7890.

332. Kim, J.A., et al., *A novel electroporation method using a capillary and wire-type electrode.* Biosens Bioelectron, 2008. 23(9): p. 1353-60.

333. Anderson, R.G. and L. Orci, *A view of acidic intracellular compartments.* J Cell Biol, 1988. 106(3): p. 539-43.

334. Sankaranarayanan, S., et al., *The Use of pHluorins for Optical Measurements of Presynaptic Activity.* Biophysical Journal, 2000. 79(4): p. 2199-2208.

335. Sliva, K. and B.S. Schnierle, *Selective gene silencing by viral delivery of short hairpin RNA.* Virol J, 2010. 7: p. 248.

336. Gagari, E., et al., *Differential release of mast cell interleukin-6 via c-kit.* Blood, 1997. 89(8): p. 2654-63.

337. Wedemeyer, J., M. Tsai, and S.J. Galli, *Roles of mast cells and basophils in innate and acquired immunity.* Curr Opin Immunol, 2000. 12(6): p. 624-31.

338. Kinet, J.P., *The high-affinity IgE receptor (Fc epsilon RI): from physiology to pathology.* Annu Rev Immunol, 1999. 17: p. 931-72.

339. Siraganian, R.P., *Mast cell signal transduction from the high-affinity IgE receptor.* Curr Opin Immunol, 2003. 15(6): p. 639-46.

340. Kalesnikoff, J. and S.J. Galli, *New developments in mast cell biology.* Nat Immunol, 2008. 9(11): p. 1215-23.

341. Marc, B. and B. Ulrich, *Stimulus-secretion coupling by high-affinity IgE receptor: New developments.* FEBS Letters, 2010.

342. Siraganian, R.P., et al., *Mast cell signaling: the role of protein tyrosine kinase Syk, its activation and screening methods for new pathway participants.* FEBS Lett, 2010. 584(24): p. 4933-40.

343. Parravicini, V., et al., *Fyn kinase initiates complementary signals required for IgE-dependent mast cell degranulation.* Nat Immunol, 2002. 3(8): p. 741-8.

344. Sanchez-Miranda, E., A. Ibarra-Sanchez, and C. Gonzalez-Espinosa, *Fyn kinase controls FcepsilonRI receptor-operated calcium entry necessary for full degranulation in mast cells.* Biochem Biophys Res Commun, 2010. 391(4): p. 1714-20.

345. Xiao, W., et al., *Positive and negative regulation of mast cell activation by Lyn via the FcepsilonRI.* J Immunol, 2005. 175(10): p. 6885-92.

346. Gubernator, N.G., et al., *Fluorescent false neurotransmitters visualize dopamine release from individual presynaptic terminals.* Science, 2009. 324(5933): p. 1441-4.

347. Sulzer, D. and S. Rayport, *Amphetamine and other psychostimulants reduce pH gradients in midbrain dopaminergic neurons and chromaffin granules: a mechanism of action.* Neuron, 1990. 5(6): p. 797-808.

348. Lee, M., et al., *Development of pH-responsive fluorescent false neurotransmitters.* J Am Chem Soc, 2011. 132(26): p. 8828-30.

349. Ryan, J.J., C.A. Kinzer, and W.E. Paul, *Mast cells lacking the high affinity immunoglobulin E receptor are deficient in Fc epsilon RI gamma messenger RNA.* The Journal of Experimental Medicine, 1995. 182(2): p. 567-574.

350. Lin, S., et al., *The FcŒµRIŒ≤ Subunit Functions as an Amplifier of FcŒµRIŒ≥-Mediated Cell Activation Signals.* Cell, 1996. 85(7): p. 985-995.

351. Brenzovich, J., et al., *IgE signaling suppresses FcepsilonRIbeta expression.* J Leukoc Biol, 2009. 86(6): p. 1351-8.

352. Pallaoro, M., et al., *Characterization of Genes Encoding Known and Novel Human Mast Cell Tryptases on Chromosome 16p13.3.* Journal of Biological Chemistry, 1999. 274(6): p. 3355-3362.

353. Hallgren, J. and G. Pejler, *Biology of mast cell tryptase.* FEBS Journal, 2006. 273(9): p. 1871-1895.

354. Trivedi, N.N., W.W. Raymond, and G.H. Caughey, *Chimerism, point mutation, and truncation dramatically transformed mast cell delta-tryptases during primate evolution.* J Allergy Clin Immunol, 2008. 121(5): p. 1262-8.

355. Wong, G., et al., *Biochemical and functional characterization of human transmembrane tryptase (TMT)/tryptase gamma. TMT is an exocytosed mast cell protease that induces airway hyperresponsiveness in vivo via an interleukin-13/interleukin-4 receptor alpha/signal transducer and activator of transcription (STAT) 6-dependent pathway.* J Biol Chem, 2002. 277: p. 41906 - 15.

356. Matin, R., et al., *Distribution of chymase-containing mast cells in human bronchi.* J Histochem Cytochem, 1992. 40(6): p. 781-6.

357. Andersson, C.K., et al., *Novel site-specific mast cell subpopulations in the human lung.* Thorax, 2009. 64(4): p. 297-305.

358. Sayama, K., et al., *Transcriptional response of human mast cells stimulated via the Fc(epsilon)RI and identification of mast cells as a source of IL-11.* BMC Immunol, 2002. 3: p. 5.

359. Rudd, M.L., et al., *Peritoneal macrophages express the serotonin transporter.* Journal of Neuroimmunology, 2005. 159(1,Äì2): p. 113-118.

360. √Öbrink, M., M. Grujic, and G. Pejler, *Serglycin Is Essential for Maturation of Mast Cell Secretory Granule.* Journal of Biological Chemistry, 2004. 279(39): p. 40897-40905.

361. Forsberg, E., et al., *Abnormal mast cells in mice deficient in a heparin-synthesizing enzyme.* Nature, 1999. 400(6746): p. 773-6.

362. Stockholm, D., et al., *The Origin of Phenotypic Heterogeneity in a Clonal Cell Population In Vitro.* PLoS ONE, 2007. 2(4): p. e394.

363. Suzuki, R., et al., *Loss of TRPC1-mediated Ca2+ influx contributes to impaired degranulation in Fyn-deficient mouse bone marrow-derived mast cells.* J Leukoc Biol, 2010. 88(5): p. 863-75.

364. Nishida, K., et al., *Fc{epsilon}RI-mediated mast cell degranulation requires calcium-independent microtubule-dependent translocation of granules to the plasma membrane.* J Cell Biol, 2005. 170(1): p. 115-26.

365. Woska, J.R., Jr. and M.E. Gillespie, *Small-interfering RNA-mediated identification and regulation of the ternary SNARE complex mediating RBL-2H3 mast cell degranulation.* Scand J Immunol, 2010. 73(1): p. 8-17.

366. Nakayama, T., et al., *Expression of syntaxin 1C, an alternative splice variant of HPC-1/syntaxin 1A, is enhanced by phorbol-ester stimulation in astroglioma: participation of the PKC signaling pathway.* FEBS Letters, 2003. 536(1,Äì3): p. 209-214.

367. Zeng, Q., et al., *A novel synaptobrevin/VAMP homologous protein (VAMP5) is increased during in vitro myogenesis and present in the plasma membrane.* Mol Biol Cell, 1998. 9(9): p. 2423-37.

368. Jayapal, M., et al., *Genome-wide gene expression profiling of human mast cells stimulated by IgE or FcepsilonRI-aggregation reveals a complex network of genes involved in inflammatory responses.* BMC Genomics, 2006. 7: p. 210.

369. Olszewski, M.B., et al., *TNF Trafficking to Human Mast Cell Granules: Mature Chain-Dependent Endocytosis.* J Immunol, 2007. 178(9): p. 5701-5709.

370. Burwen, S.J., *Recycling of mast cells following degranulation in vitro: An ultrastructural study.* Tissue and Cell, 1982. 14(1): p. 125-134.

371. Daro, E., et al., *Rab4 and cellubrevin define different early endosome populations on the pathway of transferrin receptor recycling.* Proceedings of the National Academy of Sciences, 1996. 93(18): p. 9559-9564.

372. Ullrich, O., et al., *Rab11 regulates recycling through the pericentriolar recycling endosome.* The Journal of Cell Biology, 1996. 135(4): p. 913-924.

373. Hong, W., *SNAREs and traffic.* Biochim Biophys Acta, 2005. 1744(3): p. 493-517.

374. Behrendorff, N., et al., *Vesicle-associated membrane protein 8 (VAMP8) is a SNARE (soluble N-ethylmaleimide-sensitive factor attachment protein receptor) selectively required for sequential granule-to-granule fusion.* J Biol Chem. 286(34): p. 29627-34.

375. Sakiyama, H., et al., *Membrane fusion between liposomes containing SNARE proteins involved in mast cell exocytosis.* Inflammation Research, 2009. 58(3): p. 139-142.

376. Bin, N.R., et al., *Crucial role of the hydrophobic pocket region of Munc18 protein in mast cell degranulation.* Proc Natl Acad Sci U S A, 2012. 110(12): p. 4610-5.

377. Tsuboi, T., *Molecular mechanism of docking of dense-core vesicles to the plasma membrane in neuroendocrine cells.* Med Mol Morphol, 2008. 41(2): p. 68-75.

378. Kasai, H., N. Takahashi, and H. Tokumaru, *Distinct Initial SNARE Configurations Underlying the Diversity of Exocytosis.* Physiological Reviews, 2012. 92(4): p. 1915-1964.

379. Kuroda, T.S., et al., *The Slp Homology Domain of Synaptotagmin-like Proteins 1,Äì4 and Slac2 Functions as a Novel Rab27A Binding Domain.* Journal of Biological Chemistry, 2002. 277(11): p. 9212-9218.

380. Kimura, N., et al., *Synaptotagmin I Expression in Mast Cells of Normal Human Tissues, Systemic Mast Cell Disease, and a Human Mast Cell Leukemia Cell Line.* J. Histochem. Cytochem., 2001. 49(3): p. 341-346.

381. Tuvim, M.J., et al., *Synaptotagmin 2 couples mucin granule exocytosis to Ca2+ signaling from endoplasmic reticulum.* J Biol Chem, 2009. 284(15): p. 9781-7.

382. Spurlin, B.A. and D.C. Thurmond, *Syntaxin 4 Facilitates Biphasic Glucose-Stimulated Insulin Secretion from Pancreatic β-Cells.* Molecular Endocrinology, 2006. 20(1): p. 183-193.

383. Mollinedo, F., et al., *Combinatorial SNARE Complexes Modulate the Secretion of Cytoplasmic Granules in Human Neutrophils.* The Journal of Immunology, 2006. 177(5): p. 2831-2841.

384. Ganley, I.G., E. Espinosa, and S.R. Pfeffer, *A syntaxin 10-SNARE complex distinguishes two distinct transport routes from endosomes to the trans-Golgi in human cells.* J Cell Biol, 2008. 180(1): p. 159-72.

385. Mallard, F., et al., *Early/recycling endosomes-to-TGN transport involves two SNARE complexes and a Rab6 isoform.* J Cell Biol, 2002. 156(4): p. 653-64.

386. Proctor, K.M., et al., *Syntaxin 16 controls the intracellular sequestration of GLUT4 in 3T3-L1 adipocytes.* Biochemical and Biophysical Research Communications, 2006. 347(2): p. 433-438.

387. Hepp, R., *Phosphorylation of SNAP-23 regulates exocytosis from mast cells.* J. Biol. Chem., 2005. 280: p. 6610-6620.

388. Castle, J.D., Z. Guo, and L. Liu, *Function of the t-SNARE SNAP-23 and secretory carrier membrane proteins (SCAMPs) in exocytosis in mast cells.* Mol Immunol, 2002. 38(16-18): p. 1337-40.

389. Vogel, C. and E.M. Marcotte, *Insights into the regulation of protein abundance from proteomic and transcriptomic analyses.* Nat Rev Genet, 2012. 13(4): p. 227-32.

390. Okayama, M., et al., *SNAP-23 is not essential for constitutive exocytosis in HeLa cells.* FEBS Lett, 2007. 581(24): p. 4583-8.

391. Gordon, D.E., et al., *A targeted siRNA screen to identify SNAREs required for constitutive secretion in mammalian cells.* Traffic, 2010. 9999(999A).

392. Jurado, S., et al., *LTP requires a unique postsynaptic SNARE fusion machinery.* Neuron, 2013. 77(3): p. 542-58.

393. Freichel, M., J. Almering, and V. Tsvilovskyy, *The role of TRP proteins in mast cells.* Frontiers in Immunology, 2012. 3.

394. Daly, C. and E.B. Ziff, *Post-transcriptional regulation of synaptic vesicle protein expression and the developmental control of synaptic vesicle formation.* J Neurosci, 1997. 17(7): p. 2365-75.

395. Lippert, U., D.M. Ferrari, and R. Jahn, *Endobrevin/VAMP8 mediates exocytotic release of hexosaminidase from rat basophilic leukaemia cells.* FEBS Lett, 2007. 581(18): p. 3479-84.

396. Paumet, F., et al., *Soluble NSF Attachment Protein Receptors (SNAREs) in RBL-2H3 Mast Cells: Functional Role of Syntaxin 4 in Exocytosis and Identification of a Vesicle-Associated Membrane Protein 8-Containing Secretory Compartment.* The Journal of Immunology, 2000. 164(11): p. 5850-5857.

397. Blank, U. and J. Rivera, *The ins and outs of IgE-dependent mast-cell exocytosis.* Trends Immunol, 2004. 25(5): p. 266-73.

398. Bischoff, S.C., et al., *Interleukin-4 induces a switch of human intestinal mast cells from proinflammatory cells to Th2-type cells.* Int Arch Allergy Immunol, 2001. 124(1-3): p. 151-4.

399. Paumet, F., *Soluble NSF attachment protein receptors (SNAREs) in RBL-2H3 mast cells: functional role of syntaxin 4 in exocytosis and*

identification of a vesicle-associated membrane protein 8-containing secretory compartment. **J. Immunol., 2000. 164: p. 5850-5857.**

400. Tadokoro, S., M. Nakanishi, and N. Hirashima, *Complexin II regulates degranulation in RBL-2H3 cells by interacting with SNARE complex containing syntaxin-3.* Cell Immunol, 2009.

401. Salinas, E., et al., *Presence of SNAP-25 in rat mast cells.* Immunol Lett, 2004. 95(1): p. 105-8.

402. Arango Duque, G., M. Fukuda, and A. Descoteaux, *Synaptotagmin XI Regulates Phagocytosis and Cytokine Secretion in Macrophages.* The Journal of Immunology, 2013. 190(4): p. 1737-1745.

403. von Poser, C., et al., *The evolutionary pressure to inactivate. A subclass of synaptotagmins with an amino acid substitution that abolishes Ca2+ binding.* J Biol Chem, 1997. 272(22): p. 14314-9.

404. Fukuda, M., *Molecular cloning and characterization of human, rat, and mouse synaptotagmin XV.* Biochem Biophys Res Commun, 2003. 306(1): p. 64-71.

405. Rickman, C., et al., *Comparative analysis of tandem C2 domains from the mammalian synaptotagmin family.* Biochem J, 2004. 378(Pt 2): p. 681-6.

406. Xu, J., T. Mashimo, and T.C. S√ºdhof, *Synaptotagmin-1, -2, and -9: Ca2+ Sensors for Fast Release that Specify Distinct Presynaptic Properties in Subsets of Neurons.* Neuron, 2007. 54(4): p. 567-581.

407. Hampson, A., A. O'Connor, and A. Smolenski, *Synaptotagmin-like protein 4 and Rab8 interact and increase dense granule release in platelets.* J Thromb Haemost, 2013. 11(1): p. 161-8.

408. Neumuller, O., et al., *Synaptotagmin-like protein 1 interacts with the GTPase-activating protein Rap1GAP2 and regulates dense granule secretion in platelets.* Blood, 2009. 114(7): p. 1396-404.

409. Coppola, T., et al., *Pancreatic beta-cell protein granuphilin binds Rab3 and Munc-18 and controls exocytosis.* Mol Biol Cell, 2002. 13(6): p. 1906-15.

410. Pang, Z.P. and T.C. Sudhof, *Cell biology of Ca2+-triggered exocytosis.* Curr Opin Cell Biol, 2010. 22(4): p. 496-505.

411. Kuroda, T.S. and M. Fukuda, *Rab27A-binding protein Slp2-a is required for peripheral melanosome distribution and elongated cell shape in melanocytes.* Nat Cell Biol, 2004. 6(12): p. 1195-1203.

412. Mizuno, K., et al., *Rab27b regulates mast cell granule dynamics and secretion.* Traffic, 2007. 8(7): p. 883-92.

413. Hui, E., et al., *Synaptotagmin-mediated bending of the target membrane is a critical step in Ca(2+)-regulated fusion.* Cell, 2009. 138(4): p. 709-21.

414. Dreosti, E. and L. Lagnado, *Optical reporters of synaptic activity in neural circuits.* Experimental Physiology, 2011. 96(1): p. 4-12.

415. Ashby, M.C., K. Ibaraki, and J.M. Henley, *It's green outside: tracking cell surface proteins with pH-sensitive GFP.* Trends Neurosci, 2004. 27(5): p. 257-61.

416. Sankaranarayanan, S., et al., *The use of pHluorins for optical measurements of presynaptic activity.* Biophys J, 2000. 79(4): p. 2199-208.

417. Berridge, M.J., *Calcium microdomains: organization and function.* Cell Calcium, 2006. 40(5-6): p. 405-12.

418. Brunger, A.T. and A. Rummel, *Receptor and substrate interactions of clostridial neurotoxins.* Toxicon, 2009. 54(5): p. 550-560.

419. Ma, H.-T., et al., *Canonical Transient Receptor Potential 5 Channel in Conjunction with Orai1 and STIM1 Allows Sr2+ Entry, Optimal Influx of Ca2+, and Degranulation in a Rat Mast Cell Line.* The Journal of Immunology, 2008. 180(4): p. 2233-2239.

420. Xu, J., T. Mashimo, and T.C. Sudhof, *Synaptotagmin-1, -2, and -9: Ca(2+) sensors for fast release that specify distinct presynaptic properties in subsets of neurons.* Neuron, 2007. 54(4): p. 567-81.

421. Johnson, S.L., et al., *Synaptotagmin IV determines the linear Ca2+ dependence of vesicle fusion at auditory ribbon synapses.* Nat Neurosci, 2010. 13(1): p. 45-52.

422. Keller, J.E., F. Cai, and E.A. Neale, *Uptake of Botulinum Neurotoxin into Cultured Neurons.* Biochemistry, 2003. 43(2): p. 526-532.

423. Nguyen, T.H., et al., *Actin- and Dynamin-Dependent Maturation of Bulk Endocytosis Restores Neurotransmission following Synaptic Depletion.* PLoS ONE, 2012. 7(5): p. e36913.

424. Choudhury, A., et al., *Rab proteins mediate Golgi transport of caveola-internalized glycosphingolipids and correct lipid trafficking in Niemann-Pick C cells.* The Journal of Clinical Investigation, 2002. 109(12): p. 1541-1550.

425. Cayouette, S. and G. Boulay, *Intracellular trafficking of TRP channels.* Cell Calcium, 2007. 42(2): p. 225-232.

426. Singh, B.B., et al., *VAMP2-Dependent Exocytosis Regulates Plasma Membrane Insertion of TRPC3 Channels and Contributes to Agonist-Stimulated Ca2+ Influx.* Molecular Cell, 2004. 15(4): p. 635-646.

427. van de Graaf, S.F.J., et al., *Direct Interaction with Rab11a Targets the Epithelial Ca2+ Channels TRPV5 and TRPV6 to the Plasma Membrane.* Molecular and Cellular Biology, 2006. 26(1): p. 303-312.

428. Schwenk, R.W., et al., *Overexpression of Vesicle-associated Membrane Protein (VAMP) 3, but Not VAMP2, Protects Glucose Transporter (GLUT) 4 Protein Translocation in an in Vitro Model of Cardiac Insulin Resistance.* Journal of Biological Chemistry, 2012. 287(44): p. 37530-37539.

429. Hayashi, T., et al., *Synaptic vesicle membrane fusion complex: action of clostridial neurotoxins on assembly.* EMBO J, 1994. 13(21): p. 5051-61.

430. Raingo, J., et al., *VAMP4 directs synaptic vesicles to a pool that selectively maintains asynchronous neurotransmission.* Nat Neurosci, 2012. 15(5): p. 738-45.

431. Cao, J., C.L. Cetrulo, and T.C. Theoharides, *Corticotropin-Releasing Hormone Induces Vascular Endothelial Growth Factor Release from Human Mast Cells via the cAMP/Protein Kinase A/p38 Mitogen-Activated Protein Kinase Pathway.* Molecular Pharmacology, 2006. 69(3): p. 998-1006.

432. Grutzkau, A., et al., *Synthesis, Storage, and Release of Vascular Endothelial Growth Factor/Vascular Permeability Factor (VEGF/VPF) by Human Mast Cells: Implications for the Biological Significance of VEGF206.* Mol. Biol. Cell, 1998. 9(4): p. 875-884.

433. Dean, C., et al., *Synaptotagmin-IV modulates synaptic function and long-term potentiation by regulating BDNF release.* Nat Neurosci, 2009. 12(6): p. 767-76.

434. Hashizume, M. and M. Mihara, *The roles of interleukin-6 in the pathogenesis of rheumatoid arthritis.* Arthritis, 2011. 2011: p. 765624.

435. Chaddock, J.A. and P.M. Marks, *Clostridial neurotoxins: structure-function led design of new therapeutics.* Cell Mol Life Sci, 2006. 63(5): p. 540-51.

436. Somm, E., et al., *A botulinum toxin-derived targeted secretion inhibitor downregulates the GH/IGF1 axis.* J Clin Invest, 2012. 122(9): p. 3295-306.

437. Wasmeier, C., et al., *Melanosomes at a glance.* Journal of Cell Science, 2008. 121(24): p. 3995-3999.

438. Scott, G. and Q. Zhao, *Rab3a and SNARE Proteins: Potential Regulators of Melanosome Movement.* 2001. 116(2): p. 296-304.

Appendix

Rab	Expression (Mean)	SEM
RAB7A	42.14667035	1.308287815
RAB27B	36.17365014	2.093663277
RAB37	31.45506754	2.087959186
RAB32	17.68610334	0.875649345
RAB10	16.04888679	0.334028198
RAB6C	16.31109601	0.646533978
RAB33A	13.47740037	0.263877042
RAB1B	13.30413589	1.188275804
RAB8A	10.43748348	0.172411297
RAB2A	9.157260148	0.815967544
RAB24	5.774752969	0.560692685
RAB21	6.418816732	0.088507341
RAB5A	5.994184157	0.116135986
RAB9A	5.714308915	0.022169397
RAB12	2.659264928	0.205055335
RAB4B	3.004315924	0.072659741
RAB28	2.829078036	0.09225224
RAB2B	2.821418544	0.185165216
RAB43	2.40032222	0.059472876
RAB20	2.283782334	0.221721455
RAB18	2.161102068	0.116759293
RAB18	2.161102068	0.116759293
RAB11A	2.173492017	0.110817002
RAB5C	1.6552309	0.304197576
RAB7	1.986772428	0.073162634
RAB1A	2.202052896	0.168183476
RAB26	1.506396149	0.139979742
RAB22A	1.656229199	0.089072208
RAB5B	1.65377153	0.0987161
RAB13	1.510316467	0.148266898
RAB40B	1.015395551	0.032004321
RAB8B	1.091681268	0.035855547
RAB40C	0.817946642	0.064882336
RAB39B	0.93876375	0.031797218
RAB3A	0.631588841	0.063450024
RAB3D	0.488999849	0.022517014
RAB27A	0.445771641	0.015186177
RAB4A	0.304641212	0.050211932
RAB11B	0.366276239	0.010118863
RAB36	0.312262398	0.006057205
RAB28	0.225755415	0.043793884
RAB40A	0.226315986	0.015267501
RAB14	0.21242869	0.007366978
RAB3C	0.148450591	0.041008244
RAB38	0.086961183	0.01501017
RAB30	0.081460298	0.012418007
RAB15	0.107274683	0.03537951
RAB33B	0.061816661	0.001619518
RAB34	0.02084703	0.016041453
RAB9B	0.01886425	0.014932312
RAB39	0.01713101	0.013347806
RAB3B	0.016683618	0.012494905
RAB31	0.056961414	0.021953543
RAB23	0.038045796	0.002545329
RAB17	0.015397448	0.011348209
RAB19,	0.019447649	0.009085745
RAB42	0.013405251	0.009075574
RAB25	0.008571841	0.005064551
RAB6B	0.010278196	0.001986211
RAB41	0.004149671	0.000587021

Figure 1.
Table of RAB expression in LAD 2 cells in order of expression level
Values are normalised to the 75th percentile

RAB	Expression
RAB7A	36.23697635
RAB27B	29.02574107
RAB37	20.31067975
RAB1B	19.55376983
RAB6C	16.53149453
RAB10	9.521421469
RAB32	7.900656406
RAB8A	7.116957042
RAB21	7.107197412
RAB34	6.521497125
RAB2A	6.462960961
RAB24	6.338150102
RAB5A	5.95604744
RAB9A	4.945232228
RAB13	4.01055582
RAB12	3.368207888
RAB20	3.269982203
RAB28	2.936362097
RAB8B	2.35830127
RAB22A	2.272674838
RAB43	2.223743389
RAB1A	2.200565979
RAB33A	2.119120444
RAB18	1.981589281
RAB5B	1.764286744
RAB4B	1.673162639
RAB5C	1.58134466
RAB2B	1.536627253
RAB11A	1.441909126
RAB7	1.292919675
RAB4A	1.162182064
RAB31	1.097812099
RAB27A	0.781299266
RAB38	0.747644935
RAB40B	0.617187252
RAB40C	0.559932558
RAB-like 5	0.540740781
RAB11B	0.467333521
RAB15	0.411491433
RAB39B	0.374015391
RAB14	0.329232884
RAB3A	0.327922881
RAB36	0.287776217
RAB26	0.252040263
RAB3D	0.236888879
RAB40A	0.212488255
RAB3C	0.170391574
RAB28	0.155533303
RAB23	0.129673382
RAB25	0.12798391
RAB33B	0.100989293
RAB9B	0.082864878
RAB30	0.063520924
RAB42	0.031859633
RAB19	0.017407746
RAB17	0.013912001
RAB6B	0.01085139
RAB3B	0.007678919
RAB41	0.007066033
RAB39	0.006571581

Figure 2.
Table of RAB expression in HLMC donor in order of expression levels
Values are normalised to the 75th percentile

Family	Ligand	Official IUPHAR name	Expression Value	SEM
Galanin receptors	galanin, galanin-like peptide	GAL receptor	54.69256685	7.065002308
Adrenoceptors	(-)-adrenaline, (-)-noradrenaline	&betaadrenoceptor	44.166348	1.404831816
Urotensin receptor	urotensin-II, urotensin-related peptide	UT receptor	41.35329667	5.823774614
Complement peptide recep	C3a, C5a	C3a receptor	22.61178783	0.472432867
Melanocortin receptors	ACTH, α-MSH, β-MSH, γ-MSH	MC receptor	17.86259816	3.533618865
Class A Orphans	(lyso)phospholipid mediators	GPR65	16.17034798	0.436859474
Class A Orphans		MRGPRX2	9.319605777	0.29772196
Dopamine receptors	dopamine	D2 receptor	7.437817132	0.451208191
Adenosine receptors	adenosine	A2B receptor	7.006728757	0.60912472
Prostanoid receptors	PGD2, PGE2, PGF2&alpha, PGI2	EP4 receptor	6.431908945	0.837433757
Lysophospholipid (LPA) re	LPA	LPA5 receptor	6.591318897	0.913346481
Chemokine receptors	CXCL10, CXCL11, CXCL9,	CXCR3	5.689139939	1.258212449
Leukotriene receptors	12R-HETE, 20-hydroxy-LTB4, LTB4	BLT1 receptor	3.586378514	0.331437815
Protease-activated recepto	cathepsin G, thrombin, serine proteases	PAR4	5.00026641	0.42931806
P2Y receptors	UDP-glucose	P2Y14 receptor	4.136231071	0.171872863
Succinate receptor	succinic acid	succinate receptor	3.726046002	0.240980816
Class A Orphans	oleoylethanolamide	GPR119	3.598032174	0.171355259
Class A Orphans		GPR152	3.788701544	0.466267573
Somatostatin receptors	CST-14, CST-17, SRIF-14, SRIF-28	sst3 receptor	3.458637325	0.226030983
Adenosine receptors	adenosine	A3 receptor	2.496328818	0.262812678
Adenosine receptors	adenosine	A2A receptor	3.117497677	0.142880904
Chemokine receptors	CCL19	CCRL2	2.738228811	0.19034067
Class A Orphans		iGPR160	1.939951069	0.044193409
Leukotriene receptors	LTC4, LTD4, LTE4	CysLT1 receptor	1.737661404	0.035218263
Protease-activated recepto	thrombin	PAR1	1.469278835	0.080586299
Class A Orphans		TAAR3	3.602885196	1.344325807
Class A Orphans		TAAR5	3.602885196	1.344325807
Complement peptide recep	C3a, C5a	C5a receptor	1.84706272	0.310084744
Prolactin-releasing peptide	PrRP-20, PrRP-31	PRRP receptor	1.396912597	0.076981703
Chemokine receptors	CCL11, CCL14, CCL16, CCL3, CCL3, CCL4, CCL5, CCL8	CCR5	0.936209942	0.15574454
Adrenoceptors	(-)-adrenaline, (-)-noradrenaline	&alpha2 Aadrenoceptor	0.770150723	0.168721278

Figure 3.
LAD 2 cell GPCR expression
Table lists the top 30 expressed GPCRS in LAD 2 cells. Values are normalised to the 75th percentile

Family	Ligand	Official IUPHAR name	Expression value
Galanin receptors	galanin, galanin-like peptide	GAL3 receptor	89.05199372
Urotensin receptor	urotensin-II, urotensin-related peptide	UT receptor	61.81956393
Adrenoceptors	(-)-adrenaline, (-)-noradrenaline	&beta2adrenoceptor	31.95078034
Platelet-activating factor re	mc-PAF, PAF	PAF receptor	17.97012667
Class A Orphans	oleoylethanolamide	GPR119	16.4915013
Complement peptide recep	C3a, C5a	C3a receptor	12.97323577
Class A Orphans	(lyso)phospholipid mediators	GPR65	8.036884124
Protease-activated recepto	cathepsin G, thrombin, serine proteases	PAR4	7.932529218
P2Y receptors	UDP-glucose	P2Y receptor	6.676566801
Somatostatin receptors	CST-14, CST-17, SRIF-14, SRIF-28	sst3 receptor	6.549212457
Melanocortin receptors	ACTH, α-MSH, β-MSH, γ-MSH	MC1 receptor	6.509046302
Class A Orphans		TAAR3	5.526800254
Class A Orphans		TAAR5	5.526800254
Prostanoid receptors	PGD2, PGE2, PGF2&alpha, PGI2	E4 receptor	5.313212428
Class A Orphans		GPR152	4.924747453
Lysophospholipid (S1P) re	sphingosine 1-phosphate, sphingosyl phosphorylcholine	S1P1 receptor	4.103230873
Leukotriene receptors	5-oxo-C20:3, 5-oxo-ETE, 5S-HETE, 5S-HPETE	OXE receptor	3.459440794
Chemokine receptors	CCL19,	CCRL2	3.11779106
Lysophospholipid (LPA) re	LPA	LPA5 receptor	2.85911151
Adenosine receptors	adenosine	A2B receptor	2.723322958
Protease-activated recepto	thrombin, thrombin, thrombin	PAR1	2.671419307
Leukotriene receptors	LTC4, LTD4, LTE4	CysLT1 receptor	2.090445362
Lysophospholipid (S1P) re	sphingosine 1-phosphate, sphingosyl phosphorylcholine	S1P2 receptor	1.935571311
Prolactin-releasing peptide	PrRP-20, PrRP-20, PrRP-31, PrRP-31	PRRP receptor	1.042730895
Bradykinin receptors	bradykinin, kallidin, T-kinin	B1receptor	1.018262649
Class A Orphans		GPR161	0.818176545
Class A Orphans	(lyso)phospholipid mediators, protons	GPR132	0.800034946
Formylpeptide receptors	humanin, formyl-humanin	FPR3	0.758000086
Class A Orphans		GPR162	0.74661133
P2Y receptors	ADP, ATP	P2Y1receptor	0.739550099
Adenosine receptors	adenosine	A2A receptor	0.686283199

Figure 4.
HLMC donor GPCR expression
Table lists the top 30 expressed GPCRS in HLMCS. Values are normalised to the 75th percentile

Genes of Proteoglycan Core Proteins	Expression (Mean)	SEM
aggrecan	69.38033891	5.359629087
serglycin	89.99153665	5.896686375
glypican 1	2.470812721	0.10294894
syndecan 1	0.139013888	0.002956167
syndecan 4	0.195733859	0.024963564
glypican 3	0.547346842	0.022093883
agrin	0.595325702	0.018457409
syndecan 3	0.166003315	0.026428269
glypican 4	0.052617918	0.003461608
glypican 2	0.205524348	0.005257595
biglycan	0.071945946	0.041191712
amyloid beta (A4) precursor protein	0.036212879	0.031512466
syndecan 3	0.095535268	0.03570296
glypican 3	0.032722289	0.028335733
glypican 6	0.014110381	0.009476772
syndecan 2	0.005516398	0.001518692
glypican 5	0.009276037	0.00555826

Figure 6.
Proteoglycan core protein expression in LAD 2 cells
Values are normalised to the 75th percentile

Genes of Proteoglycan Core Proteins	Expression (Mean)
aggrecan	103.5615984
serglycin	91.72726356
glypican 1	1.816165535
syndecan 1	0.93143905
syndecan 4	0.912933941
glypican 3	0.549387186
agrin	0.421065165
syndecan 3	0.3513443
glypican 4	0.283976374
glypican 2	0.175729829
biglycan	0.110741681
amyloid beta (A4) precursor protein	0.086631216
syndecan 3	0.072490345
glypican 3	0.050576859
glypican 6	0.031506283
syndecan 2	0.00772222
glypican 5	0.00672071

Figure 7.
Proteoglycan core protein expression in HLMCS
Values are normalised to the 75th percentile

Enzymes associated with glycosaiminoglycan synthesis	Expression (Mean)	SEM
heparan sulfate 6-O-sulfotransferase 1	25.27654261	1.1698695
carbohydrate (chondroitin 4) sulfotransferase 13	24.42412341	1.9857086
N-deacetylase/N-sulfotransferase (heparan glucosaminyl) 2	39.14180068	2.8231143
heparan sulfate proteoglycan 2	8.926548923	0.2823991
chondroitin sulfate synthase 1	9.697752621	0.3740241
heparan sulfate (glucosamine) 3-O-sulfotransferase 1	0.021531542	0.0071628
carbohydrate (N-acetylglucosamine-6-O) sulfotransferase 2	3.40780871	0.5650773
N-deacetylase/N-sulfotransferase (heparan glucosaminyl) 2	36.76555152	0.8535488
N-deacetylase/N-sulfotransferase (heparan glucosaminyl) 1	23.19488294	3.2879512
heparan-alpha-glucosaminide N-acetyltransferase	1.055807196	0.1725722
carbohydrate (chondroitin 4) sulfotransferase 12	6.033154307	0.8497229
carbohydrate (N-acetylglucosamine 6-O) sulfotransferase 6	4.176028995	0.1234512
carbohydrate (N-acetylgalactosamine 4-sulfate 6-O) sulfotransferase 15	0.03400655	0.0110026
chondroitin sulfate N-acetylgalactosaminyltransferase 2	1.758639648	0.1562294
heparan sulfate 2-O-sulfotransferase 1	1.820254176	0.1468026
heparan sulfate 2-O-sulfotransferase 1	4.386044621	0.3271173
dermatan sulfate epimerase	0.307028152	0.0662026
chondroitin sulfate glucuronyltransferase	1.864058605	0.0327537
heparan sulfate 2-O-sulfotransferase 1	2.815424651	0.4474627
carbohydrate (chondroitin 4) sulfotransferase 11	1.961417676	0.0339981
galactosamine (N-acetyl)-6-sulfate sulfatase	0.780938188	0.0746645
sulfatase 2	0.055536406	0.0167546
carbohydrate (N-acetylgalactosamine 4-0) sulfotransferase 8	0.412052921	0.0493365
arylsulfatase B	0.129122679	0.014307
carbohydrate (chondroitin 4) sulfotransferase 13	0.167410475	0.0057831
carbohydrate (keratan sulfate Gal-6) sulfotransferase 1	0.004478764	0.0004497
carbohydrate (N-acetylglucosamine 6-O) sulfotransferase 5	0.222388	0.0117011
carbohydrate (N-acetylgalactosamine 4-0) sulfotransferase 14	0.223997619	0.0163352
heparan-alpha-glucosaminide N-acetyltransferase	0.01201386	0.005331
carbohydrate (N-acetylglucosamine 6-O) sulfotransferase 7	0.099662111	0.0158617
carbohydrate (keratan sulfate Gal-6) sulfotransferase 1	0.030042484	0.0040076
carbohydrate (N-acetylglucosamine 6-O) sulfotransferase 4	0.100396893	0.0101881
amyloid beta (A4) precursor protein	0.036212879	0.0315125
chondroitin sulfate proteoglycan 4	0.017356238	0.0132226
heparan sulfate (glucosamine) 3-O-sulfotransferase 3A1	0.003955645	0.0002002
heparan sulfate proteoglycan 2	0.040952602	0.0135128
heparan sulfate (glucosamine) 3-O-sulfotransferase 3B1	0.030570421	0.0092129
heparan sulfate 6-O-sulfotransferase 2	0.003222617	0.000163
chondroitin sulfate N-acetylgalactosaminyltransferase 1	0.027430581	0.0195278
heparan sulfate (glucosamine) 3-O-sulfotransferase 2	3.981651096	0.294253
chondroitin sulfate proteoglycan 5 (neuroglycan C)	0.046460969	0.019882
heparan sulfate 6-O-sulfotransferase 3	0.023706733	0.0195275
chondroitin sulfate synthase 3	0.00819018	0.0040489
heparan sulfate 6-O-sulfotransferase 2	0.035132232	0.0311172
carbohydrate (N-acetylgalactosamine 4-0) sulfotransferase 9	0.004337929	0.0001768
N-deacetylase/N-sulfotransferase (heparan glucosaminyl) 4	0.012982282	0.0085669
N-deacetylase/N-sulfotransferase (heparan glucosaminyl) 3	0.01073681	0.0067041
heparan sulfate (glucosamine) 3-O-sulfotransferase 4	0.003372744	0.0001786
heparan sulfate (glucosamine) 3-O-sulfotransferase 6	0.018577587	0.0136275

Figure 8.
Enzymes associated with glycosaminoglycan synthesis in LAD 2 cells.
Values are normalised to the 75th percentile

Enzymes associated with glycosaiminoglycan synthesis	HLMC
heparan sulfate 6-O-sulfotransferase 1	64.23627023
carbohydrate (chondroitin 4) sulfotransferase 13	52.34879599
N-deacetylase/N-sulfotransferase (heparan glucosaminyl) 2	33.33459427
heparan sulfate proteoglycan 2	18.78510801
chondroitin sulfate synthase 1	18.67651276
heparan sulfate (glucosamine) 3-O-sulfotransferase 1	18.37884225
carbohydrate (N-acetylglucosamine-6-O) sulfotransferase 2	9.730023201
N-deacetylase/N-sulfotransferase (heparan glucosaminyl) 2	8.890021328
N-deacetylase/N-sulfotransferase (heparan glucosaminyl) 1	7.913550358
heparan-alpha-glucosaminide N-acetyltransferase	6.101044053
carbohydrate (chondroitin 4) sulfotransferase 12	5.648044471
carbohydrate (N-acetylglucosamine 6-O) sulfotransferase 6	4.509334515
carbohydrate (N-acetylgalactosamine 4-sulfate 6-O) sulfotransferase 15	3.407630453
chondroitin sulfate N-acetylgalactosaminyltransferase 2	3.170681481
heparan sulfate 2-O-sulfotransferase 1	3.064104809
heparan sulfate 2-O-sulfotransferase 1	2.718166818
dermatan sulfate epimerase	2.257400963
chondroitin sulfate glucuronyltransferase	2.140082573
heparan sulfate 2-O-sulfotransferase 1	1.512045884
carbohydrate (chondroitin 4) sulfotransferase 11	1.509755307
galactosamine (N-acetyl)-6-sulfate sulfatase	0.385849798
sulfatase 2	0.319296651
carbohydrate (N-acetylgalactosamine 4-0) sulfotransferase 8	0.283734166
arylsulfatase B	0.242817323
carbohydrate (chondroitin 4) sulfotransferase 13	0.240091868
carbohydrate (keratan sulfate Gal-6) sulfotransferase 1	0.225555387
carbohydrate (N-acetylglucosamine 6-O) sulfotransferase 5	0.222930339
carbohydrate (N-acetylgalactosamine 4-0) sulfotransferase 14	0.193943337
heparan-alpha-glucosaminide N-acetyltransferase	0.138208069
carbohydrate (N-acetylglucosamine 6-O) sulfotransferase 7	0.118345222
carbohydrate (keratan sulfate Gal-6) sulfotransferase 1	0.103912174
carbohydrate (N-acetylglucosamine 6-O) sulfotransferase 4	0.089274026
amyloid beta (A4) precursor protein	0.086631216
chondroitin sulfate proteoglycan 4	0.057981533
heparan sulfate (glucosamine) 3-O-sulfotransferase 3A1	0.05319618
heparan sulfate proteoglycan 2	0.046820212
heparan sulfate (glucosamine) 3-O-sulfotransferase 3B1	0.034309015
heparan sulfate 6-O-sulfotransferase 2	0.022928808
chondroitin sulfate N-acetylgalactosaminyltransferase 1	0.021279571
heparan sulfate (glucosamine) 3-O-sulfotransferase 2	0.008465234
chondroitin sulfate proteoglycan 5 (neuroglycan C)	0.007784935
heparan sulfate 6-O-sulfotransferase 3	0.007775784
chondroitin sulfate synthase 3	0.007653881
heparan sulfate 6-O-sulfotransferase 2	0.007592772
carbohydrate (N-acetylgalactosamine 4-0) sulfotransferase 9	0.007554941
N-deacetylase/N-sulfotransferase (heparan glucosaminyl) 4	0.007433318
N-deacetylase/N-sulfotransferase (heparan glucosaminyl) 3	0.007125571
heparan sulfate (glucosamine) 3-O-sulfotransferase 4	0.007020582
heparan sulfate (glucosamine) 3-O-sulfotransferase 6	0.006802858

Figure 9.
Enzymes associated with glycosaminoglycan synthesis in HLMCS.
Values are normalised to the 75th percentile